THE SELECTION OF ULTRASONIC TRANSDUCERS FOR INSPECTION OF PIPELINE GIRTH WELDS

PART 1

FINAL REPORT BY:

M.P. FINGERHUT
R.I. COOTE
D. HODGKINSON

WORK ON THIS PROJECT WAS JOINTLY FUNDED BY NOVA, AN ALBERTA CORPORATION AND THE PHYSICAL METALLURGY RESEARCH LABORATORIES, CANADA CENTRE FOR MINERAL AND ENERGY TECHNOLOGY, ENERGY MINES AND RESOURCES CANADA.

DSS FILE NUMBER: 23SQ-23340-2-9027-4

DSS CONTRACT SERIAL NUMBER: 0SQ82-00244

CANMET SCIENTIFIC AUTHORITY: DR. D. K. MAK

DECEMBER, 1986

123 AP

MEF-28

Phase 3

TABLE OF CONTENTS

1.0 SUMMARY

2.0 CONCLUSIONS

3.0 RECOMMENDATIONS

4.0 INTRODUCTION

5.0 PROBLEM DEFINITION AND APPROACH

- 5.1 Sensitivity and Missed Imperfections
- 5.2 False Indications

6.0 INSPECTION DESIGN AND TRANSDUCER SELECTION

- 6.1 Inspection Design
- 6.2 Transducer Selection
- 6.3 Transducer Purchase

7.0 TRANSDUCER PERFORMANCE

- 7.1 Selected Transducers
  - 7.1.1 Beam Width
  - 7.1.2 Working Range
  - 7.1.3 Signal to Noise
  - 7.1.4 Beam Angle
  - 7.1.5 Frequency
  - 7.1.6 Squint Angle
  - 7.1.7 Side Lobes

- 7.2 Conventional Transducers
  - 7.2.1 Beam Width
  - 7.2.2 Working Range
  - 7.2.3 Signal to Noise
  - 7.2.4 Beam Angle
  - 7.2.5 Squint Angle
  - 7.2.6 Side Lobes

8.0 EQUIPMENT AND MATERIALS

- 8.1 Transducer Testing System
- 8.2 Test Plates
  - 8.2.1 Simulated Imperfection Plates
  - 8.2.2 Weld Imperfection Plates

TABLE OF CONTENTS
(continued)

9.0 EXPERIMENTAL PROCEDURE

- 9.1 Inspection Data Recording

10.0 RESULTS AND ANALYSIS

- 10.1 Data Reduction
- 10.2 Performance on Simulated Imperfections
- 10.3 Corner Effects
- 10.4 Performance on Real Weld Imperfections
  - 10.4.1 Sensitivity and Missed Imperfections
  - 10.4.2 False Indications
  - 10.4.3 Detection Threshold

11.0 SUPPLEMENTARY WORK

- 11.1 Pitch-Catch
- 11.2 Creeping Wave

12.0 DISCUSSION

REFERENCES

TABLES

FIGURES

APPENDICES

1.0 SUMMARY

This report describes the work performed to develop an inspection design and procedures for selecting transducers to inspect pipeline girth welds made by the gas metal arc process in on-shore and off-shore pipelines. The methodology used for the design was developed to provide reliable detection of significant weld imperfections and avoid false indications due to variable weld surface geometry.

The design approach using specialized ultrasonic beams chosen to detect specific imperfections in well-defined regions of the weld was evaluated on simulated and real weld imperfections. The results and analysis show the approach was very successful in achieving good performance in the root region of the weld, however, performance in the cap and body regions was less than satisfactory.

Further evaluation of the inspection design on full scale girth welds is recommended, following completion of alternative inspection designs for the body and cap regions of the weld which have been investigated in a preliminary manner during this project.

2.0 CONCLUSIONS

2.1 The inspection design approach using ultrasonic beams oriented to provide near perpendicular incidence on expected imperfections, and control of the beam width was successful in detecting significant real weld imperfections in the root region with a signal to noise level greater than 12 dB. The approach also eliminated the occurrence of false indications from weld geometries most susceptible to the problem.

2.2 The pulse echo technique which performed well in the root region was not totally satisfactory for detection of real weld imperfections in the body and cap regions of the weld where shear wave beams perpendicular to the inspection planes cannot be produced. Preliminary investigation of alternative techniques indicates that a pitch-catch technique is suitable for detection of imperfections in the body of the weld, and a creeping wave technique is suitable for imperfections located close to the outside surface beneath the weld cap.

2.3 The use of test plates to indicate inspection performance can provide a misleading impression of good performance if detection relies on a corner reflection geometry which is not duplicated in real welds. This effect was observed to occur for lack of fusion defects located beneath the weld cap.

3.0 RECOMMENDATIONS

3.1 The plans for developing and demonstrating the suitability of the ultrasonic inspection design approach for field inspection anticipate assembly of a complete inspection design for evaluation on full scale girth welds, manufactured to contain realistic imperfections. The results of the project reported here indicate such full scale testing is appropriate, however, preliminary work is needed to finalize the inspection design and establish that proposed solutions to the observed problems are satisfactory. Therefore it is recommended that a limited amount of experimental work be performed using new weld plates, prepared with well-separated imperfections, to verify that the specific tasks outlined below have been satisfactorily completed.

3.2 Develop the inspection design and transducer selection for using the pitch-catch technique to inspect the body regions of the weld. Consider also, using each transducer of the pitch-catch assembly in the pulse echo mode during testing on welded plates.

3.3 Complete assessment of creeping wave transducer designs and evaluate their performance on weld plates.

3.4 Evaluate the characteristics of conical and/or toroidal focused transducers and if appropriate, include such transducer designs for evaluation of performance on welded plates.

3.5 Consider the sources of noise originating within transducer assemblies and within the weld zone of GMA welds and, in cooperation with transducer suppliers, develop a method to specify and obtain satisfactory signal to noise levels for transducers.

4.0 INTRODUCTION

Non-Destructive Testing is an important part of the pipeline construction process, providing the information used to control girth weld quality according to the appropriate construction specification. Cost-effective pipeline offshore construction demands reliable and rapid inspection and currently depends on the x-ray radiography method.

Mechanized ultrasonics can provide near instantaneous results compared to film radiography which commonly requires that results be interpreted from an incompletely processed film to prevent delays in welding production. In addition, the ultrasonic system is more sensitive to significant planar (lack of fusion) type welding defects than radiography which is sensitive to less significant non-planar (porosity) defects.

Mechanized gas metal arc welding using the CRC system is a high productivity process attractive for offshore work, and has been used extensively for recent large diameter construction onshore in Canada. Previous work by NOVA (1,2,3) to evaluate mechanized ultrasonic inspection system performance on CRC welds showed that ultrasonic inspection was capable of reliably detecting significant planar weld imperfections that are generally undetectable by radiography, but also indicated problems related to missed imperfections and false indications that must be overcome before any of the mechanized systems could be used during construction.

The problems described were experienced with mechanized ultrasonic inspection on wall thicknesses up to 12 mm, typical of onshore pipelines, and it was recognized that additional work to obtain satisfactory performance must include larger wall thicknesses more typical of offshore pipelines. The project described in this report addressed the inspection of two wall thicknesses, 10 mm and 20 mm.

Development of mechanized ultrasonic systems has taken two basically different approaches to covering the girth weld volume. The fixed transducer systems use an array of transducers, located at a fixed distance from the weld centerline, which is moved around the circumference. The transducer elements and detection gates are chosen with the intention of covering the cross section area where imperfections occur while excluding the surface areas in the root and cap which would produce echos unrelated to the presence of imperfections. The moveable probe systems produce a zig-zag or step scanning path and in that respect are similar to manual scanning methods. Such systems are also extremely slow compared to weld production rates and have not been considered in this work.

The mechanical simplicity of the fixed transducer systems which facilitates the rapid inspection, however, results in other complications related primarily to the transducers used. Figure 1 shows a schematic of a weld cross section and conventional transducer arrangement to achieve complete coverage of the weld volume. The inspection design is based on each transducer providing coverage of about 5 mm of the wall, therefore, a minimum of two transducers are used for 10 mm thick material. Also, the index position for all transducers in the array are nearly coincident on the pipe surface so that the transducer array can be conveniently constructed into one housing. The resulting transducer selections provide inspection beams which are necessarily broad and oriented to provide complete coverage of the weld with little regard to the orientation of the expected imperfections.

The detection of weld imperfections with the fixed transducer systems is based on identifying locations which produce an echo response within the detection gate above a threshold level. If the threshold is set too low, large numbers of false indications occur and discredit the inspection. A large signal level for imperfections, relative to the noise level from other weld features is clearly desirable. If the threshold is set too high, significant imperfections will not be detected.

The problems associated with missed imperfections and false indications are considered to be fundamentally related to the characteristics of the ultrasonic beam used, and to the design of the inspection geometry. The objective of this project was to develop and evaluate a logical approach to designing the inspection geometry and selecting transducers specifically for GMA girth welds, in order to minimize the problems of missed imperfections and false indications.

5.0 PROBLEM DEFINITION AND APPROACH

5.1 Sensitivity and Missed Imperfections

The past problems of missed imperfections have arisen due to a lack of sensitivity and a surmised lack of coverage due to positioning of the detection gate.

The lack of sensitivity has arisen because the detection of imperfections was being attempted with beams poorly oriented to the expected imperfections. The poor beam orientation is a result of the inspection angle of the selected transducer and the use of a relatively large beam size which covered regions where several planar weld imperfections were expected to occur with different orientations.

The approach used in this work, to use specialized beams to detect specific imperfections, is intended to largely overcome the problem of variable response from the range of imperfection types and location. The goal is to obtain a large echo signal, relative to the background noise, from specific imperfections in the region being examined by a particular beam.

In order to obtain a large echo response, the ultrasonic beam was selected to be normal to the plane of the expected imperfections in the root region, and as close as practical in other regions of the weld.

The inspection regions are shown in Figure 2 and referred to as inspection planes throughout this report. The goal was a signal to noise ratio greater than 12 dB for all imperfections with a projected depth exceeding 1.0 mm, so that significant imperfections will be detected without the risk of false indications. The value of 1.0 mm for projected depth has been chosen because such imperfections are generally considered tolerable, regardless of length, in any fitness for purpose assessment.

5.2 False Indications

The occurrence of false indications, in past experience, was attributed to echos from the root or cap surface occurring within the gated time zone. Positioning of the detection gate involves a compromise between avoiding such surface echos and providing full coverage of the weld. When wide, diverging beams are used, and the position of the weld centerline is in doubt, a satisfactory compromise was not always possible, particularly when significant Hi-Lo exists. The goal of using a narrow beam whose angle and position are accurately known is to ensure that echos from the weld surfaces will be clearly separated from the imperfection signals and will occur outside the detection gate.

6.0 INSPECTION DESIGN AND TRANSDUCER SELECTION

The design approach used, which is described in this section, considers only the pulse-echo technique, although alternative techniques were explored in a preliminary fashion for the cap and body region of the weld. The alternative techniques are described in Section 11.0.

6.1 Inspection Design

The primary goals of the design for each inspection plane of the weld are to achieve:

(a) An ultrasonic shear wave beam which is perpendicular to the inspection plane.

(b) A 6 dB beam width confined to the inspection plane.

(c) For focused transducers, a beam which results in a working range that includes the inspection plane.

The geometry of the weld preparation determines the required beam angle, transducer location and target path distance for each inspection plane as illustrated for plane C in Figure 3.

In practice, it was necessary to select designs for some regions of the weld which did not exactly meet the goals of perpendicular incidence at the inspection plane. The inspection planes D and E would require the use of 85° refracted beams and enormous target distances; both of which are not feasible, in order to achieve normal beam incidence at the inspection plane. It was therefore necessary to use a beam with a refracted angle of 70° which is considered to be the maximum for practical purposes, and accept the expected effects of reduced sensitivity due to the 15° misorientation between the beam and the inspection plane normal. The difference in target distance for inspection planes D and E is very small so it was not considered necessary to use different transducers for each region, although the surface position of the transducer to inspect each region was different.

The inspection of plane C requires that the beam reflect off the inside surface of the plate, very close to the edge of the root bead reinforcement. In order to minimize the potential for portions of the incident beam to be transmitted into the reinforcement region, where reflections from the weld surface would cause false indications, several design adjustments were made. A 50° beam was used to increase the distance from the edge of the reinforcement to the beam centerline, as illustrated in Figure 4a. The 5° misorientation resulting from this adjustment was considered acceptable because the decrease in sensitivity, relative to that for normal incidence, was expected to be quite small. In addition, the beam focus where the minimum width occurs, was designed to occur at the inside plate surface as shown in Figure 4b and clearly reduces the potential for the edge of the beam being transmitted into the root reinforcement as shown in Figure 4c.

The inspection plane C which is 4 mm wide was divided into two separate inspection planes, C_1 and C_2, each of 2.0 mm. Since the difference in target path distance was very small, the same transducer, located in slightly different positions, was selected for each region.

The design parameters for each inspection plane in the two weld thicknesses are summarized in Table 1.

6.2 Transducer Selection

Once the inspection design parameters were established, transducers were chosen with the appropriate combination of frequency, diameter and focusing to meet the requirements for beam width at the appropriate beam path distance. In most cases a number of alternative transducers could have been chosen to meet the design parameters, however, additional criteria were applied as follows:

(a) Lower frequencies were preferred to provide increased tolerance to imperfection misorientation.

(b) The transducer and housing size must allow placement of the transducer at the required position without interferring with the weld cap.

The combinations of frequency, diameter and focusing required to produce a particular beam width and maximum sound pressure at a given target path distance can be determined from fundamental acoustic principles. Atomic Energy of Canada Ltd., under a subcontract, developed a series of graphs to aid the transducer selection process (4). These graphs are shown in Figures 5 and 6. Their use is explained below, and illustrated with an example.

Figure 5 describes the relationship between beam diameter and path length for common transducer sizes with a frequency of 5.0 MHz. The equivalent steel path distance includes the effect of the transducer wedge and lens, which add approximately 15 mm to the actual target path distance. Also indicated on the figure is the shaded region where focusing is required in order to achieve the beam size required. In the region where focusing is indicated, focusing factors greater than 0.5 are avoided because the required beam size can usually be achieved without focussing by using a moderately higher frequency. Figures similar to Figure 5, for other frequencies, were also used to initially identify the alternative transducers.

In the region with focusing factors between 0.1 and 0.5, the actual beam widths are reported to be up to 30% larger (5) than indicated by the diagram, and must be considered in the transducer selection.

When focused transducers are selected it is not always possible to arrange that the inspection plane is located precisely at the focal point, however, the beam size does not increase significantly within the working range so that satisfactory operation can be achieved at other path distances within the working range. Figure 6 indicates the working range for different transducer sizes and focusing.

Example

The inspection design for plane C_1 in the 10 mm thick weld plate requires the following, from Table 1:

Actual beam width = 2.0 mm (focused beam width = 1.5 mm).
Actual steel path distance = 15.6 mm (effective path = 30.6 mm).

In order to avoid interference with the weld cap, the transducer size must be less than 15 mm.

Using Figure 5, and similar diagrams for other frequencies, alternative transducer sizes and focusing were identified corresponding to point A which indicates the required beam width and effective path length. The working range was determined from Figure 6 and other similar diagrams for each of the frequencies considered. The alternatives considered for plane C_1 are summarized below.

Frequency (MHz)	Diameter (mm)	Focusing Factor	Working Range (mm)
3.5	19.0	0.32	23.6 to 42.6
5.0	12.7	0.49	23.8 to 45.8
7.0	12.7	0.35	23.4 to 43.4

Although each of the transducers listed would be expected to produce a beam of the correct diameter at the inspection plane, only the 5 MHz and 7 MHz transducers meet the requirement for a transducer diameter less than 15 mm. The 5.0 MHz transducer was selected as the lowest frequency transducer that will meet the requirements.

6.3 Transducer Purchase

Transducers were purchased according to the specific design requirements identified in Table 1, and additional general requirements for accuracy of beam angles and frequency, absence of side lobes and signal to noise level, as indicated in Table 4. An order was placed with a custom transducer manufacturer for nine transducers, however, all were returned, primarily because of poor signal to noise levels, less than 12 dB. Another eight transducers were subsequently purchased from two separate suppliers and of these, five were retained and used for the project. Although several did not meet the specified requirements, and some compromises to the desired approach were required as described in Section 7.0, preliminary evaluation indicated their performance would allow evaluation of most of the inspection design principles, and allow the project to proceed without adding to the substantial delays which the purchasing had already caused.

7.0 TRANSDUCER PERFORMANCE

The five pulse-echo transducers selected are described in Tables 2 and 3. Three conventional transducers used during previous field trials are also described in Table 2 and were used for comparison purposes throughout this project.

The performance assessment of the conventional and selected transducers described in this section was carried out to determine:

(a) The beam size and working range which were the basis for the transducer selection, and

(b) Their compliance with the purchase specification (Table 4).

Transducer assessment was based on a series of tests. The test method, acceptance criteria and a discussion of the test results are presented in this section. The specified design requirements and the test results for the selected transducers and the conventional transducers are summarized in Tables 5 and 6 respectively.

7.1 Selected Transducers

7.1.1 Beam Width

The beam width at the appropriate beam path distance was determined from echo amplitude records produced on 2.0 mm diameter side-drilled holes perpendicular to the beam axis. In two cases, the focused transducers produced beam widths larger than the design size of the inspection plane. The cause of the deviation from the design is being investigated by Atomic Energy of Canada Ltd., the designer of the transducers.

Table 5 shows that the unfocused transducer No. 5, intended for inspection plane A, produced a beam width of 3.8 mm at the target position. This large beam width was a consequence of using the transducer at a surface position corresponding to 1.5 skips, because the transducer housing size was larger than stated by the supplier and interfered with the weld cap at the design position. The compromise avoided delays in purchasing another transducer, and the increased beam width did not cause any identified problems.

7.1.2 Working Range

The 6 dB working range was determined from a graph of echo amplitude versus beam path, illustrated in Figure 7 for transducer No. 1. The working range is considered to be the region where the echo amplitude is within 50% of the maximum. While the design required the target path to be within the working range, this was observed to occur with transducers No. 2 and No. 4 only. Results for transducers No. 1 and No. 3 indicate a focus position shorter than required resulting in a target path distance beyond the working range.

7.1.3 Signal to Noise

Signal to noise was of particular importance as it was the basis for determining the defect detection threshold. Signal to noise ratio was assessed from graphs (Figure 7) of signal and noise which were prepared for each transducer by measuring and recording the amplifier gain required for an 80% full screen height (FSH) signal from a 2 mm diameter side-drilled hole and an 80% FSH noise level at the same path distance. Noise measurements were carried out on the weld material.

As mentioned in Section 6.3, signal to noise levels in the purchased transducers were generally lower than the 30 dB specified and agreed to by the suppliers, particularily for the focused transducers. The inspection results obtained suggest signal to noise values less than 30 dB can be accepted, however, discussion of this aspect with suppliers will be required for future purchases.

It was determined that the low signal to noise level of transducers No. 1 to No. 4 was caused by internal reflections in the wedge. The addition of a damping material, Raychem S1052, to the front of the wedge reduced the internal reflections to an acceptable level, resulting in the signal to noise levels given in Table 5. The exception was transducer No. 3 which still had a signal to noise level below the minimum of 12 dB considered acceptable, and was not used in further testing.

7.1.4 Beam Angle

Beam angle was evaluated for each transducer using the IIW block. Initially the index position was determined by maximizing the echo signal from the 100 mm radius reflector on the IIW block and marking the location on the transducer corresponding with the zero point on the block. Beam angle was then determined by maximizing the echo from the 50 mm diameter hole and determining the angle on the graduated scale at the transducer index location.

Results show all selected transducers to provide a beam angle within the specified limit of ±2°.

7.1.5 Frequency

Peak frequency was assessed from the frequency spectrum supplied by the vendor with the transducer. All transducers were within the specified frequency range of ±10% of the peak frequency.

7.1.6 Squint Angle

The axis of the ultrasonic transducer housing is used to align the beam axis perpendicular to expected imperfections. Deviation of the two axes is called the squint angle. Squint angle was determined for each transducer by rotating the transducer housing to maximize the echo signal from a flat reflector as illustrated in Figure 8. The results show all transducers to be perfectly aligned within the housing.

7.1.7 Side Lobes

Large amplitude side lobes effectively increase the diameter of the beam, and therefore, can result in the problem of false defect indications. Side lobe measurements were taken from the echo amplitude record produced from a 2.0 mm diameter side-drilled hole perpendicular to the beam axis at the target path. Selected transducers showed no side lobes except for transducer No. 5 with a side lobe at -14 dB, greater than the -30 dB limit specified.

7.2 Conventional Transducers

The conventional transducers used were all enclosed in one housing, as illustrated in Figure 1.

Similar performance tests were used for conventional and selected transducers except for frequency where no spectrum was available for the conventional transducers and a nominal frequency was assumed.

7.2.1 Beam Width

Table 6 shows, as expected, beam widths at the target path longer than observed for the selected transducers except for transducer No. 8. This transducer produced a beam size equal to the size of inspection plane A which it was designed to examine and is the one case where the conventional transducer beam width is less than that of the selected transducers, however, the beam angle is misoriented by 20° from the inspection plane normal.

7.2.2 Working Range

Working range was not determined for unfocused transducers.

7.2.3 Signal to Noise

Signal to noise levels were acceptable in all cases.

7.2.4 Beam Angle

Beam angles were measured as indicated in Table 6.

7.2.5 Squint Angle

The squint angle for each transducer exceeded our limit of ±0.5° and would, therefore, require adjustment of the transducer axis to ensure beam and imperfection axis were perpendicular.

7.2.6 Side Lobes

Transducer No. 6 exhibited a side lobe at -8 dB relative to the main beam.

8.0 EQUIPMENT AND MATERIALS

8.1 Transducer Testing System

Figure 9 shows the ultrasonic instrument and x-y scanner which with an x-y plotter comprised the transducer testing system used to produce the analogue recordings of inspection results. The ultrasonic instrument was a Masterscan model UFD 310 manufactured by Balteau-Sonatest. The instrument provided a broad band (0.5-18 MHz) 100 dB dynamic range amplifier and was used to control the echo signal (amplitude) on the display screen. Screen-height and amplitude control linearity were established to be within 2% of a full screen according to articles T-532 and T-533 of ASME Section V. The time base was calibrated using the IIW A2 block to provide a resolution of 0.5 mm. The analogue output of the gated signal amplitude was recorded on the vertical axis of a Hewlett-Packard model 7046A x-y recorder, which was calibrated to indicate echo amplitude to an accuracy of 2%.

The x-y scanner manufactured by Atomic Energy of Canada Ltd. was used to control transducer movement and provide an analogue signal, corresponding to the distance travelled by the transducer, which was recorded on the horizontal axis of the recorder. Position was indicated to an accuracy of 0.5 mm. Figure 10 is an example of the analogue recordings produced which display the echo amplitude as a function of distance travelled by the transducer.

A 10W30 motor oil was used to couple the transducers to the test plate surface.

8.2 Test Plates

Two types of test plates were designed, one containing real weld imperfections and another containing machined notches and holes to simulate lack of fusion weld imperfections. The designs were based on an assessment of the imperfection types and their occurrence in GMA welds (Appendix 1.0). All plates were manufactured from CSA grade 448 MPa low carbon steel typical of that used for the making of line pipe.

8.2.1 Simulated Imperfection Plates

One simulated imperfection plate design, an example of which is shown in Figure 11, contained 1 mm deep notches and 2 mm diameter flat bottomed holes to simulate lack of fusion type weld imperfections along the planes of the weld preparation. The reflector designation corresponds approximately to the inspection plane, so that hole C1, for example, corresponds to a reflector on inspection plane C1. The hole and notch reflectors were made using a milling process to produce consistent shape and surface finish.

A second plate containing a series of 2 mm diameter flat bottomed holes was produced with the flat reflecting face oriented between horizontal and vertical in 5° increments as illustrated in Figure 12. The center of each flat face was located along the same line parallel to the plate surface so that the echo amplitude from reflectors at different orientations relative to the beam axis could be easily determined for a transducer.

8.2.2 Weld Imperfection Plates

Weld imperfection plates were designed to contain typical GMA planar lack of fusion type weld imperfections as described in Appendix 1.0. Special welding procedures described in Appendix 2.0 were developed to make each of the weld imperfections in flat plate. Each plate was designed such that the detection capability could be evaluated in each region of the weld. Welds joining plates with controlled amounts of high-low were prepared to evaluate the sensitivity to false indications and the detection performance in the presence of this condition.

9.0 EXPERIMENTAL PROCEDURE

9.1 Inspection Data Recording

The echo response data from simulated and real weld imperfections were obtained from the analogue recordings produced using the equipment described in Section 8.1.

The ultrasonic instrument gain was set and recorded to produce an 80% echo amplitude from a 2.0 mm side-drilled hole at the target distance for each transducer used. For the examination of the weld plates, the detection gate position and width were set using the calibrated time base so that the gated region began at a position 2 mm before the incident beam centerline intersected the inspection plane, and ended at the position where the beam centerline intersected the centerline of the weld as illustrated in Figure 13.

In order to avoid recording false indications from the weld root geometry with transducer No. 8, inspecting plane A, it was necessary to move the end of the gated position away from the centerline, reducing the coverage of the weld cross-section.

The x-y scanner was used to control the transducer movement after the initial transducer position was established. The positioning accuracy in each dimension was ±0.5 mm. Maximum scanning speed was 4.2 mm/sec.

The analogue recordings for the simulated imperfections represent the variation in echo as the transducer was moved perpendicular to the plane of the imperfection, and indicate the transducer position which produced the maximum echo response. For the weld plate examinations, the transducer was positioned at the location, relative to the weld centerline, where the maximum echo was expected from the target plane. The analogue recordings represent the echo response obtained as the transducer was moved parallel to the weld axis, at the fixed distance from the weld.

10.0 RESULTS AND ANALYSIS

10.1 Data Reduction

The most significant measure of detection performance is considered to be signal to noise ratio, which was determined from the analogue recordings. The signal amplitude was determined by averaging the maximum and minimum amplitude contained in a 5 mm distance along the weld, centered about the position of the analogue recording corresponding to each cross-section location. Cross-sectioning verified the presence and size of each weld imperfection.

Noise levels were determined for each transducer by recording the maximum amplitude recorded in a 5 mm distance along the weld, centered about the position on the analogue recording where metallographic examination confirmed that no imperfections were present. A minimum of eight locations were used, and the noise level shown in Table 7 for each transducer was considered to be the average of all the values.

In evaluation of the results obtained for simulted imperfections, the signal amplitude for each target was the maximum echo recorded, and the noise level for each transducer was used to calculate the corresponding signal to noise ratio.

10.2 Performance on Simulated Imperfections

Figures 14 and 15 present the signal to noise values calculated for each simulated imperfection in the 10 mm wall plate for the selected and conventional transducers respectively. The figures show the signal to noise for the target imperfection and neighbouring imperfections to be joined by a broken line for each transducer. Figure 14 shows the selected transducers to provide signal to noise levels in excess of 12 dB for all inspection planes in the 10 mm plate. Based on these results one would expect the selected transducers to provide satisfactory detection of weld imperfections in all regions of a weld.

Conventional transducers (Figure 15), show signal to noise levels as low as 2.5 dB in the midwall region. Detection of imperfections in the midwall region of real welds, therefore, would be expected to be very sensitive to the detection threshold.

Figure 16 presents the results for imperfections in planes A and C of the 20 mm wall plate for selected transducers only. The absence of results in planes D and E for the 20 mm plate was a result of the elimination of transducer No. 3 from further evaluation due to a very high noise level. No conventional transducers were evaluated for the 20 mm wall thickness material because of their poor performance on 10 mm wall plate.

Figure 16 shows the good performance observed with the selected transducer on planes A and C in the 10 mm plate was maintained with selected transducers on the 20 mm wall plate.

10.3 Corner Effects

The results of Figure 15 for the simulated imperfections detected by the conventional transducers indicate a substantially higher signal to noise level for the imperfection located closest to the surface in plane E compared to plane D, although both imperfections have a similar size and orientation. This observation suggested that the effect of target misorientation in plane E was minimized by the occurrence of a corner reflection, illustrated in Figure 17a, which produces a large echo response from defects close to the surface, compared to similar imperfections in the midwall where the return beam misses the transducer (Figure 17b).

The results of Figure 18 for conventional transducer No. 6 and selected transducer No. 1 illustrate the expected effect of echo amplitude decreasing with increasing angle between the beam axis and the target plane normal. These results, obtained on the plate illustrated in Figure 12, were used to estimate the "amplification" effect of the corner, which is summarized in Table 8. It appears that the corner effect is largely responsible for the good performance on the simulated imperfections in plane D for both the conventional and selected transducers.

Unfortunately this beneficial effect of a corner reflection cannot be relied upon in the presence of the weld cap which effectively removes the corner.

10.4 Performance on Real Weld Imperfections

10.4.1 Sensitivity and Missed Imperfections

The analysis which was carried out to assess transducer sensitivity on real weld imperfections related the signal to noise level to the projected throughwall depth of the weld imperfections. Projected throughwall depths were determined from metallographic cross-sections at selected locations.

Calculated signal to noise values are illustrated in Figure 19 which shows an example of the results for a single lack of fusion imperfection (Figure 20) detected by selected transducer No. 5 in plane A of the root in a weld in 10 mm plate.

The vertical and horizontal lines in the figure are related to the transducer performance goals mentioned earlier. The vertical line at 1.0 mm represents the minimum size to be detected and the horizontal lines at 12 dB and 6 dB represent two alternative detection thresholds. The data points indicate the signal to noise and corresponding imperfection depth at various positions along the length.

Graphs similar to Figure 19 were prepared for each transducer and inspection plane. Figures 21a and 21b show graphs for planar lack of fusion and non-planar porosity imperfections detected by selected transducer No. 2 examining plane C of the weld. Figures 22a and 22b are similar graphs for conventional transducer No. 7 also examining plane C of the weld. Transducer No. 7 shows inferior performance compared to transducer No. 2 for planar weld imperfections and confirms the results from the simulated imperfections which indicated unsatisfactory performance with the conventional transducer.

The probability of detecting imperfections greater than 1.0 mm in projected through wall dimension with a signal to noise of 6 dB or 12 dB is summarized in Tables 9 to 11 for each inspection plane and transducer. The probability of detection was defined as:

$$\text{Probability} = \frac{\text{No. of Imperfections Detected}}{\text{Imperfections Detected + Imperfections Missed}}$$

Table 9 shows the probability of detecting planar imperfections in the 10 mm thick weld plates and indicates that only the selected transducers examining planes A, C and E provide detection of all imperfections at the 12 dB threshold level. However, with the conventional transducers inspecting plane C, the probability of detection at a signal to noise of 12 dB was zero and at a signal to noise of 6 dB was only 0.17. These results clearly indicate the benefits of good inspection design and transducer selection and confirm the observations in the root region of the weld using simulated imperfections.

The detection probability for imperfections in plane D by selected transducer No. 3 is 0.86 at the 12 dB threshold level and 0.95 at the 6 dB level. While this is only slightly less than perfect probability of detection and may be satisfactory in some circumstances, it shows a decrease in detection performance compared to the results on planes A, C and E. A similar decrease in detection performance was expected in plane E based on consideration of the corner effect, but was not observed. This is believed to be due to the small population of only two imperfections available to determine detection probability. The reduced reliability of the pulse-echo technique to inspect plane D and strongly suspected unreliability for plane E resulted in an investigation of alternative techniques (see Section 11.0).

The conventional transducers clearly provide unsatisfactory performance in planes D and E of the real welds, unlike the good performance observed with the simulated imperfections, which was largely due to the beneficial corner effect.

Table 10 shows similar results to Table 9 for imperfections in planes A and C of the 20 mm thick weld plates. Although the probabilities are based on a limited number of imperfections, they do support the results of Table 9 for the 10 mm thick plates.

Table 11 shows the probability of detection of non-planar porosity to be less than 1.0 for all transducers examining the 10 mm weld plates. This is not unexpected given the relatively poor reflectivity of these imperfections, and is not of concern since such imperfections are generally innocuous. The results, however, do show considerably better detection in planes D and E with the selected transducers than in planes A and C. Comparison of the porosity in these planes indicates a relatively larger pore size in planes D and E (Figure 23) compared to that in planes A and C (Figure 24). Also, the elongated porosity in the body region is favourably oriented to the ultrasonic beam. Conventional transducers show poor detectability of porosity in all regions of the weld.

Selected transducer No. 5 showed excellent performance in detecting non-planar imperfections on plane A of the 20 mm welded plate based on the one imperfection examined.

10.4.2 False Indications

In addition to achieving satisfactory signal to noise values above a detection threshold, it is necessary to position the detection gate to avoid false indications from the cap and root surfaces. The analysis carried out to assess the potential for false indications was; therefore, limited to those transducers examining the regions nearest the cap and root surface geometry. As the potential for false indications is greatest where the weld high-low condition occurs, the analysis was carried out on plate 2 (10 mm thick) exhibiting a high-low of 2.2 mm or about 20% of the plate wall thickness.

The analysis examined the discrimination distance which is the length of sound beam path from the end of the gated region to the surface geometry echo (illustrated in Figure 13). Results of the analysis are shown in Table 12 for the root region and in Table 13 for the cap region. The schematic in Figure 13 indicates the dimensions reported in the tables and Figure 25 shows an A-scan photograph from which the discrimination distance c was measured.

The tables show measurements for nine consecutive locations 10 mm apart in an 80 mm length of weld No. 2. All measurements for transducers examining the root region were taken from the low side of the weld as illustrated in Figure 9 and measurements for the cap region from the high side of the weld. This was done to determine the minimum discrimination distance for the worst case condition. A positive distance indicates the gate end occurs prior to the geometry indication and no false imperfection indication would be recorded. A zero or negative distance indicates the geometry occurs at or inside the gated region which, therefore, could result in a false indication.

Table 12 shows the minimum discrimination distance for selected transducer No. 5 was 1.5 mm and indicates no false indications should occur unless transducer positioning error is greater than 1.2 mm. It was observed during the analysis for missed imperfections that no false indications were recorded with this transducer and confirms the results of this analysis.

Conventional transducer No. 8, however, did not show similar results. The minimum discrimination distance was 0.0 mm for this transducer indicating false indications could occur even without positioning errors. False indications using conventional transducer No. 8 were confirmed during the weld plate inspections by the "oily finger test" and resulted in the gate end being adjusted away from the weld root geometry to avoid recording these indications. From the analysis of the analogue recordings, it was determined that several indications recorded with conventional transducer No. 8 could not be related to real weld imperfections. These false indications and their corresponding signal to noise values are listed in Table 14

Table 13 shows the minimum discrimination distance for two transducers examining the cap region of the weld and indicates no false indications would occur at the gate positions established.

10.4.3 Detection Threshold

It was observed during the analysis that a 12 dB signal to noise detection threshold is a practical level for selected transducers which would ensure all significant real imperfections are detected and avoid false indications. While the 6 dB level showed similar imperfection detectability, it would result in some false indications with the selected transducers as shown in Table 15.

The results for conventional transducers indicate that any threshold level will be unsatisfactory. Results in Table 9 indicate a detection threshold for conventional transducers as low as 6 dB would not ensure detection of all significant real imperfections. Table 14 on the other hand, indicates thresholds as high as 12 dB would not eliminate all false indications with conventional transducers.

11.0 SUPPLEMENTARY WORK

Analysis of the results for inspection planes D and E, and consideration of the corner effect, indicated that the pulse echo detection technique in this area of the weld is likely to be unreliable. Two alternative techniques investigated were the creeping wave for imperfections close to the inspection surface (plane E) and the pitch-catch technique for imperfections deeper in the weld (plane D). To apply the pitch-catch technique required the throughwall dimension of plane E be increased from 1.5 mm to a minimum of 3.0 mm to ensure the beam path would not interfere with the weld cap as shown in Figure 26.

11.1 Pitch-Catch

The pitch-catch technique is a commonly used method for detection of near vertical defects (6) and therefore is well suited for the inspection of plane D. A performance evaluation of the technique was carried out on the simulated and real weld imperfections in 20 mm plate, using available transducers. Transducer No. 4 was used as the transmitter and a 40°, 5 MHz, 12.7 mm diameter unfocused transducer as the receiver with the distance between the two ranging from 22 mm to 41 mm for complete coverage of plane D. Instrument gain, detection gate width and signal to noise values were determined using similar procedures to those described earlier.

Signal to noise determined on the simulated imperfections showed levels in excess of 14 dB. Figure 27 presents the signal to noise values for four planar weld defects in plane D with projected throughwall depths ranging from 0.4 mm to 2.4 mm. Although the number of imperfections evaluated was limited, the performance was generally very good, when considering results obtained with the simulated defects also. It is recommended this method be further evaluated for inspection of plane D in the next phase of this project.

11.2 Creeping Wave

Use of the creeping wave is a relatively new method for defect detection and has good potential for detection of surface and near surface planar defects. Figure 28 illustrates the complex wave front produced by this transducer and indicates the creeping wave as a compression wave, parallel to the inspection surface.

The large beam size (Figure 29) of the creeping wave transducer used, unfortunately, limited its use to the 20 mm wall thickness material. Inspection of the 10 mm wall material resulted in false indications which could not be easily discriminated from real weld defects. The success of this transducer; therefore will depend largely on developing a design which will produce a beam depth of about 3 mm for inspection of plane E. Work to develop such a design is currently in progress.

The signal to noise of 17.8 dB for one planar defect in plane E with a projected throughwall depth of 0.7 mm indicates good performance. Signal and noise values were determined using the procedures outlined earlier.

12.0 DISCUSSION

Root Region

The results obtained in the root region of the weld (planes A and C) using the transducers selected to provide near perpendicular incidence with a controlled beam width indicated good performance, both in terms of detection, and freedom from false indications, in spite of the compromises which were made in accepting less than desired performance of the transducers.

The results obtained for the detection of real weld imperfections on plane A using the selected transducer No. 5 indicate the benefit of normal incidence in providing large signal to noise response, compared to the very poor response obtained using the conventional transducer No. 8. In this situation, the selected transducer was used with a target distance far beyond that intended because of the problem with the transducer housing size, however, the resulting beam size increase was not critical because the ideal beam direction minimized the problem in discriminating against geometry indications. Because of the larger beam size used for plane A, the two simulated imperfections in plane C also produced indications, as shown in Figure 14, although at a level below the proposed 12 dB threshold. This effect could give the erroneous impression that a single imperfection actually confined to plane C extended onto plane A and is deeper than it really is. A similar result was observed with the 20 mm wall thickness as shown in Figure 16. This effect is one of the reasons for desiring a beam width limited to the inspection plane.

The successful inspection of plane C, however, was considered to depend critically on avoiding unwanted transmission of the beam into the weld root reinforcement, so that control of the beam edge at the inside surface of the plate was the most important consideration. The use of a beam which was 5° from perpendicular and focused to minimize its width at the inside surface was successful, as indicated in Figure 17a, however, in future work, transducers to produce a beam with normal incidence, focused at the inside surface, should also be considered.

The performance of the transducers on real weld imperfections was accurately predicted by the performance on the simulated imperfections in the root region of the weld, indicating that inspection design can be evaluated by the performance on test plates with reflectors machined to simulate the typical planar imperfections in the root region.

Body and Cap Region

The geometry of the weld preparation for the fill pass regions of the weld prevented the use of shear waves perpendicular to the expected planar imperfections. The use of the selected 70° beams resulted in quite good performance in detecting real weld imperfections, significantly better than that obtained with the 55° beams produced with the conventional transducers, however, some imperfections were not detected with the 70° beams. In spite of the relatively good performance indicated for the selected transducers in planes D and E, a fundamental problem exists, which is not indicated by the performance on the simulated defects, as described in Section 10.3. The design of test plates to evaluate performance in the weld region close to the inspection surface requires further consideration to ensure that corner effects do not produce a misleading indication of good performance which cannot be reproduced on real welds.

Detection of imperfections in the body region (plane D) using the pitch-catch technique should be quite practical, however, verification of the performance on weld plates will be required, since there is insufficient data from the preliminary work done in this phase of the project. During the work to evaluate the pitch-catch technique, consideration should be given to also using each transducer of the pitch-catch assembly in the pulse-echo mode to provide redundant detection in the body region.

Detection of imperfections on plane E, closest to the outside surface, beneath the weld cap, appears to be the area where reliable detection is most difficult. The results obtained with the creeping wave transducer suggest it is capable of detecting imperfections in the region of plane E, however, modified designs to reduce the beam size in the through thickness direction are desirable to enable imperfection location to be determined more accurately. A new transducer design to produce the desired beam is being prepared for NOVA by Bundesanstalt Fur Materialprufung (BAM), and additional work to evaluate performance of the creeping wave transducer is planned.

Transducer Specification and Procurement

The approach to inspection design and transducer selection has been guided by the need to control the characteristics of the ultrasonic beam used to inspect each region of the weld and resulted in selection of focused transducers for most of the inspection zones. The important parameters for focused transducers are the working range, which is determined by the focal length, beam width and signal to noise ratio. Unsatisfactory transducer characteristics were found for each of these parameters.

The aspect of transducer characteristic causing the greatest problem was signal to noise level. A simple means of specifying and evaluating the noise level is needed which will allow the purchaser to indicate his requirements in a realistic manner than can be readily understood and evaluated by the manufacturers. The inability of all manufacturers to meet the specified signal to noise levels for the focused transducer would appear to be partly due to the manufacturers' lack of concern for client specifications on one hand, and some lack of clarity in the specification requirement on the other hand. Discussion with the manufacturers will be required to resolve this problem before any other focused transducers are purchased.

The other aspect of focused transducer performance that was less than satisfactory was the focal length and working range. Two of the four focused transducers produced a focal length less than specified, resulting in a target path beyond the working range. All of the transducers were designed with spherical focusing, which produces a relatively short working range (7,8). Conical and toroidal focusing designs are reported to provide a much longer working range with narrower beams (7,8), and will be investigated for the next phase of this project.

Inspection Design Approach

The inspection design approach using specialized beams to detect specific imperfections relies on accurate geometric knowledge of the weld region. The location of the transducers with respect to the weld centerline or edge of the weld preparation is an essential piece of required information, and means that a reference mark must be placed on the pipe during the bevelling operation which can be used after welding to locate the edge of the weld.

The importance of weld area geometry to inspection using focused beams has also been recognized in work sponsored by the American Gas Association. This work was aimed at using focused transducers to estimate the depth of weld imperfections, and attributed some significant location errors to longitudinal bending of the pipe wall adjacent to the weld. Such effects could introduce uncertainty in the beam path that would be detrimental to the proposed approach and will require careful attention during the next phase of this project to quantify pipe distortion and its effect on the inspection design.

The original design goal was to maintain a 6 dB beam width equal to the width of the inspection plane, however as noted, successful deviations from that goal were made for inspection of planes A and C and indicate that the design goal should really be control of the beam width to avoid false indications and to ensure uniform sensitivity through the thickness. Control of the beam width is also desirable to reduce uncertainty in the location of imperfections, and enable approximate estimates of throughwall depth to be made from the detection data for each zone of the weld, however, this is considered to be a secondary goal compared to the goal of avoiding false indications, and ensuring reliable detection of significant imperfections.

The production of test plates containing real imperfections is described in Appendix 2, however, the number of imperfections produced which could be used to reliably indicate transducer performance was less than expected. As mentioned in the Appendix, imperfections were frequently larger than desired, and as a result in some cases, imperfections were not sufficiently separated in the through wall direction to enable unambiguous correlation of an indication with a particular imperfection. This problem resulted in a rather small amount of usable data, particularily for plane E. The close proximity of individual imperfections also caused some difficulty in determining an appropriate noise level for the transducers, particularily those with wider beams, because indications interpreted to be noise may have been associated with real imperfections located in adjacent regions of the weld.

Future test welds should be designed so that only one intentional imperfection is located at any position along the length of the weld, and positions with intentional imperfections should be separated by a minimum of 50 mm of sound weld.

REFERENCES

1. Fingerhut, M. P. "Field Performance Evaluation of the Bandscan Automatic Ultrasonic Insepction System", Materials and Quality Management Report No. 15016.

2. Coote, R. I. and Fingerhut, M. P. "Ultrasonic Inspection of Girth Welds", Proceedings of the International Conference on Pipeline Inspection, Edmonton, June 1983, pp 203-279.

3. Fingerhut, M. P. "Assessment of the Bandscan Automatic Ultrasonic Inspection System", Materials and Quality Management Report No. 15013.

4. Kittmer, C. A. and Duncan, D. B. "Selection of Ultrasonic Transducers for Girth Weld Inspection", Atomic Energy of Canada Limited, Report No. CRNL-2775.

5. Kittmer, C. A. "Acoustic Lenses - Focusing in on Defects", Proceedings of the International Conference on Pipeline Inspection, Edmonton, June 1983, pp 161-178.

6. Krautkramer, J. and Krautkramer H. "Ultrasonic Testing of Materials", Third Edition, Springer-Verlag, 1983, pp 469, 522.

7. Murphy, R. V. "Toroidal, Conical and Spherical Lenses in Ultrasonic Inspection", Materials Evaluation, Vol. 39, March 1981.

8. Andrew, G. A. and Lamprey, C. W. "Focused Ultrasonic Transducers: Some Types and Characteristics, Qualtest-2 Conference and Exposition", October 25-27, 1983, Dallas, Texas.

9. Barnes, M. P. and Russell, A. N. "Foothills Pipelines 1981 Eastern Leg Construction Weld Quality Report", Materials and Quality Management Report No. 13054.

10. Middleton, C. A. "1982 Eastern Leg Construction Weld Quality Report", Materials and Quality Management Report No. 13060.

TABLE 1

INSPECTION DESIGN REQUIREMENTS
10 mm WALL THICKNESS

Plane*	Beam Angle (Degrees)	Surface Position Index to Weld Center Line (mm)	Equivalent Target Path (mm)	Required Beam Width at Target (mm)
A	52.5	12.52	29.9	2.4
C1	50	16.9	36.2	2.0
C2	50	19.6	38.4	2.0
D	70	50.0	65.0	2.8
E	70	56.0	71.3	1.5

*See Figure 1a.

20 mm WALL THICKNESS

Plane**	Beam Angle (Degrees)	Surface Position Index to Weld Center Line (mm)	Equivalent Target Path (mm)	Required Beam Width at Target (mm)
A	52.5	25.6	46.3	2.4
C1	50	28.8	51.7	2.0
C2	50	31.5	53.9	2.0
D1	70	78.0	94.9	3.2
D2	70	87.0	104.2	3.2
D3	70	96.0	113.6	3.2
D4	70	105.2	122.9	3.2
E	70	111.8	129.8	1.5

**See Figure 1b.

TABLE 2

TRANSDUCERS FOR INSPECTION OF 10 mm WALL THICKNESS PLATE

	Selected			Conventional		
Transducer Number	1	2	5	6	7	8
Inspection Planes	D + E	C1 + C2	A	D + E	C1 + C2	A
Refracted Angle in Steel Drawing	70	50	52.5	55	65	72
Frequency in MHz C = Center N = Nominal	5.0 C	5.0 C	7.5 C	4.0 N	4.0 N	4.0 N
Crystal Dimensions in mm	19.0	12.7	6.35 x6.35	8x10	8x10	8x10
Focusing Factor	0.47	0.49	None	None	None	None
Working Range	(49.5-99.5)	(23.8-45.8)	N/A	N/A	N/A	N/A

N/A - Not Applicable

TABLE 3

TRANSDUCERS FOR INSPECTION OF 20 mm WALL THICKNESS PLATE

Transducer Number	4	5
Inspection Planes	C1 + C2	A
Refracted Angle in Steel Drawing	50	52.5
Frequency in MHz C = Center N = Nominal	5.0 C	7.5 C
Crystal Dimensions in mm	19.0	6.35 x6.35
Focusing Factor	0.33	None
Working Range	(36.7-62.7)	N/A

N/A - Not Applicable

TABLE 4

TRANSDUCER SPECIFICATION

(a)	Center Frequency	±10% of the nominal frequency.
(b)	Beam Angle	±2° at 20°C.
(c)	Squint Angle	±0.5°.
(d)	Side Lobes	30 dB, relative to main beam.
(e)	Focus Position	±10% of design measured in steel from the beam entry point.
(f)	Signal to Noise	30 dB at the target path.

TABLE 5

SELECTED TRANSDUCER ASSESSMENT RESULTS

	Tests	Transducer No. 1 5.0 MHz, 19.0 mm ø		Transducer No. 2 5.0 MHz, 12.7 mm ø		Transducer No. 3 5.0 MHz, 25.4 mm ø		Transducer No. 4 5.0 MHz, 19.0 mm ø		Transducer No. 5 7.5 MHz (6.35x6.35)	
		Design	Actual	Design	Actual	Design	Actual	Design	Actual	Design	Actual
(a)	6 dB Beam Width at Target Path (mm)	3.0	3.1	2.0	2.6	3.2	2.9	2.0	2.9	2.5	3.8
(b)	6 dB Working Range (mm)	49.5-99.5	23.7-46.9	23.8-45.8	18.9-43.9	73.8-135.8	N/A	36.7-62.7	N/A	N/A	N/A
		Specified		Specified		Specified		Specified		Specified	
(c)	Signal to Noise at Target Path (dB)	30	16	30	22.5	30	6	30	20	30	28
(d)	Beam Angle (Dgr)	70	68.5	50	50.5	70	70	50	50	52.5	52
(e)	Center Frequency (MHz)	5.0	5.3	5.0	5.3	5.0	4.5	5.0	4.8	7.5	8.3
(f)	Squint Angle (Dgr)	0	0	0	0	0	0	0	0	0	0
(g)	Side Lobes (dB)	None	None	None	None	None	None	None	None	None	-14

N/A - Not Available

TABLE 6

CONVENTIONAL TRANSDUCER ASSESSMENT RESULTS

Tests	Transducer No. 6 4.0 MHz (8 x 10 mm) Actual	Transducer No. 7 4.0 MHz (8 x 10 mm) Actual	Transducer No. 8 4.0 MHz (8 x 10 mm) Actual
(a) 6 dB Beam Width at Target Path (mm)	5.8	4.6	2.4
(b) 6 dB Working Range (mm)	N/A	N/A	N/A
(c) Signal to Noise at Target Path (dB)	24	25	31
(d) Beam Angle (Dgr)	55	65	73
(e) Center Frequency (MHz)	4.0(a)	4.0(a)	4.0(a)
(f) Squint Angle (Dgr)	1	3	1
(g) Side Lobes (dB)	-8	None	None
(h) Focus Position (mm)	37.9(b)	35.4(b)	45.9(b)

(a) Nominal frequency.
(b) Wedge path estimated to be 15 mm, acrylic.
N/A - Not Available

TABLE 7

AVERAGED MAXIMUM NOISE LEVEL FOR EACH TRANSDUCER

Plate Thickness (mm)	Transducer Number	Noise Level[1] (dB)
10	1	-13.5
	2	-17.0
	5	-20.1
	6	-17.6
	7	-19.0
	8	-20.6
20	4	-16.5
	5	-21.2

[1] Relative to 2.0 mm diameter side-drilled hole at the target path.

TABLE 8

AMPLIFICATION OF ECHO SIGNAL DUE TO CORNER REFLECTION

Transducer Number	Disc Reflector	Distance From Surface (mm)	Misorientation Angle (DGR) for Simulated Defects	Amplitude[1] Expected (% FSH)	Amplitude Observed (% FSH)	Amplification Due to Corner Reflection (dB)
1	D2	2.0	16.5	17	54	10.0
1	D1	3.3	16.5	17	30	5.0
6	D2	2.0	30.0	2	32	24.0
6	D1	3.3	30.0	2	19	19.0

Note 1 - Amplitude for the misorientation angle was determined from Figure 18 and adjusted for differences in beam path distance between the misorientation plate and the simulated imperfection plate.

TABLE 9

DETECTION PROBABILITY FOR PLANAR WELD IMPERFECTIONS GREATER THAN 1.0 mm PROJECTED THROUGH WALL DEPTH IN 10 mm PLATE

Plane		Selected Transducer No.				Conventional Transducer No.		
		5	2	1	1	8	7	6
A	Total Defects	5				6		
	Probability With S/N > 12dB	1.0				0.67		
	Probability With S/N > 6dB	1.0				0.83		
C	Total Defects		6				6	
	Probability With S/N > 12dB		1.0				0.0	
	Probability With S/N > 6dB		1.0				0.17	
D	Total Defects			22				25
	Probability With S/N > 12dB			0.86				0.04
	Probability With S/N > 6dB			0.95				0.30
E	Total Defects				2			2
	Probability With S/N > 12dB				1.0			0.5
	Probability With S/N > 6dB				1.0			0.5

TABLE 10

DETECTION PROBABILITY FOR NON-PLANAR WELD DEFECTS GREATER THAN 1.0 mm PROJECTED THROUGH WALL DEPTH IN 20 mm PLATE

Plane		Selected Transducer No.	
		5	4
A	Total Defects	4	
	Probability With Avg. S/N > 12dB	1.0	
	Probability With Avg. S/N > 6dB	1.0	
C	Total Defects		1
	Probability With Avg. S/N > 12dB		1.0
	Probability With Avg. S/N > 6dB		1.0
D	Total Defects		
	Probability With Avg. S/N > 12dB		
	Probability With Avg. S/N > 6dB		
E	Total Defects		
	Probability With Avg. S/N > 12dB		
	Probability With Avg. S/N > 6dB		

TABLE 11

DETECTION PROBABILITY FOR NON-PLANAR WELD DEFECTS
GREATER THAN 1.0 mm PROJECTED THROUGH WALL DEPTH IN 10 mm PLATE

Plane		Selected Transducer No.				Conventional Transducer No.		
		5	2	1	1	8	7	6
A	Total Defects	4				4		
	Probability With Avg. S/N > 12dB	0.0				0.25		
	Probability With Avg. S/N > 6dB	0.25				1.0		
C	Total Defects		2				2	
	Probability With Avg. S/N > 12dB		0.0				0.0	
	Probability With Avg. S/N > 6dB		0.0				0.0	
D	Total Defects			7				8
	Probability With Avg. S/N > 12dB			0.43				0.0
	Probability With Avg. S/N > 6dB			0.71				0.0
E	Total Defects				6			
	Probability With Avg. S/N > 12dB				0.50			
	Probability With Avg. S/N > 6dB				0.83			

TABLE 12

MEASURED SOUND PATH DISTANCES IN THE ROOT REGION OF THE WELD
PLATE NUMBER 2, 2.2 mm HIGH-LOW

Transducer Position (mm)	Selected Transducer No. 5					Conventional Transducer No. 8				
	Sound Path Distance (±0.5 mm)			Min. C	Geometry Signal to Noise (dB)	Sound Path Distance (±0.5 mm)			Min. C	Geometry Signal to Noise (dB)
	a	b	c			a	b	c		
80	49.5	52.0	2.5	2.0	20.6	31.5	33.0	1.5	1.0	13.6
90	49.5	51.5	2.0	1.5		31.5	33.0	1.5	1.0	
100	49.5	51.5	2.0	1.5		31.5	33.0	1.5	1.0	
110	49.5	51.5	2.0	1.5		31.5	33.0	1.5	1.0	
120	49.5	51.5	2.0	1.5		31.5	33.0	1.5	1.0	
130	49.5	51.5	2.0	1.5		31.5	32.0	0.5	0.0	
140	49.5	52.0	2.5	1.5		31.5	32.5	1.0	0.5	
150	49.5	51.5	2.0	1.5		31.5	32.0	0.5	0.0	
160	49.5	52.0	2.5	2.0	18.4	31.5	32.0	0.5	0.0	18.3

a = Sound path to gate finish (mm).
b = Sound path to surface geometry (mm).
c = Discrimination distance (b - a) (mm).

TABLE 13

MEASURED SOUND PATH DISTANCES IN THE CAP REGION OF THE WELD
PLATE NUMBER 2, 2.2 mm HIGH-LOW

Transducer Position (mm)	Selected Transducer No. 1					Conventional Transducer No. 6				
	Sound Path Distance (±0.5 mm)			Min. C	Geometry Signal to Noise (dB)	Sound Path Distance (±0.5 mm)			Min. C	Geometry Signal to Noise (dB)
	a	b	c			a	b	c		
80	55.5	59.5	4.0	3.5	18.0	35.5	38.0	2.5	2.0	14.8
90	55.5	59.5	4.0	3.5		35.5	38.0	2.5	2.0	
100	55.5	60.0	4.5	4.0		35.5	39.0	3.5	3.0	
110	55.5	59.6	4.0	3.5		35.5	38.5	3.0	2.5	
120	55.5	59.5	4.0	3.5		35.5	39.5	3.5	3.0	
130	55.5	59.0	3.5	3.0		35.5	38.5	3.0	2.5	
140	55.5	58.5	3.0	2.5		35.5	37.5	2.0	1.5	
150	55.5	59.0	3.5	3.0		35.5	38.5	3.0	2.5	
160	55.5	59.5	4.0	3.5	16.6	35.5	38.0	2.5	2.0	15.4

a = Sound path to gate finish (mm).
b = Sound path to surface geometry (mm).
c = Discrimination distance, (b - a) (mm).

TABLE 14

SIGNAL TO NOISE OF FALSE DEFECT INDICATIONS IN THE ROOT REGION (dB)

Plate Number	Selected Transducer Number 5	Conventional Transducer Number 8
1	-	11.7
3	-	10.1
3	-	6.0
3	-	7.6
3	-	6.6
4	-	12.6
4	-	23.9

TABLE 15

SIGNAL TO NOISE OF FALSE DEFECT INDICATIONS WITH SELECTED TRANSDUCERS

Weld Plate Number	Selected Transducer Number	Signal to Noise
3	1	4.9
3	1	4.6
4	2	5.0
4	2	3.5
5	5	6.1

FIGURE 1

CONVENTIONAL TRANSDUCER ARRANGEMENT SHOWING TRANSDUCER ANGLES AND BEAM PATHS USED TO ACHIEVE COMPLETE COVERAGE OF THE WELD

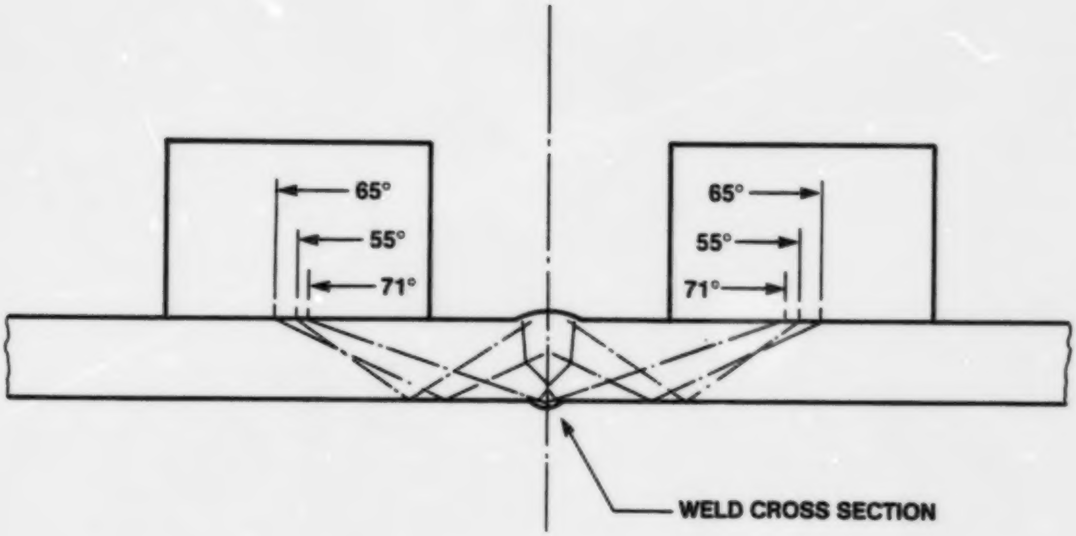

65°
55°
71°
65°
55°
71°
WELD CROSS SECTION

FIGURE 2
GAS METAL ARC WELD JOINT DESIGN SHOWING GEOMETRY OF INSPECTION PLANES

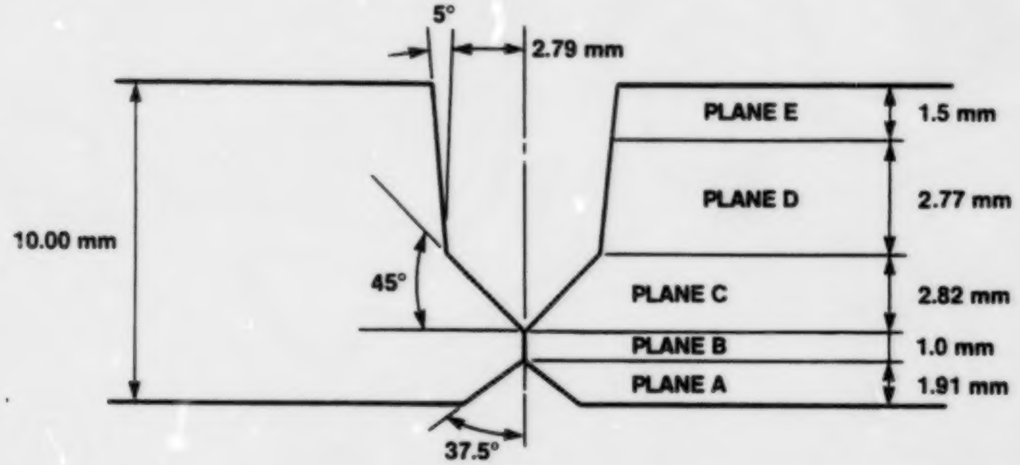
5°
2.79 mm
10.00 mm
PLANE E
1.5 mm
PLANE D
2.77 mm
45°
PLANE C
2.82 mm
PLANE B
1.0 mm
PLANE A
1.91 mm
37.5°

FIGURE 2A 10 mm WALL THICKNESS

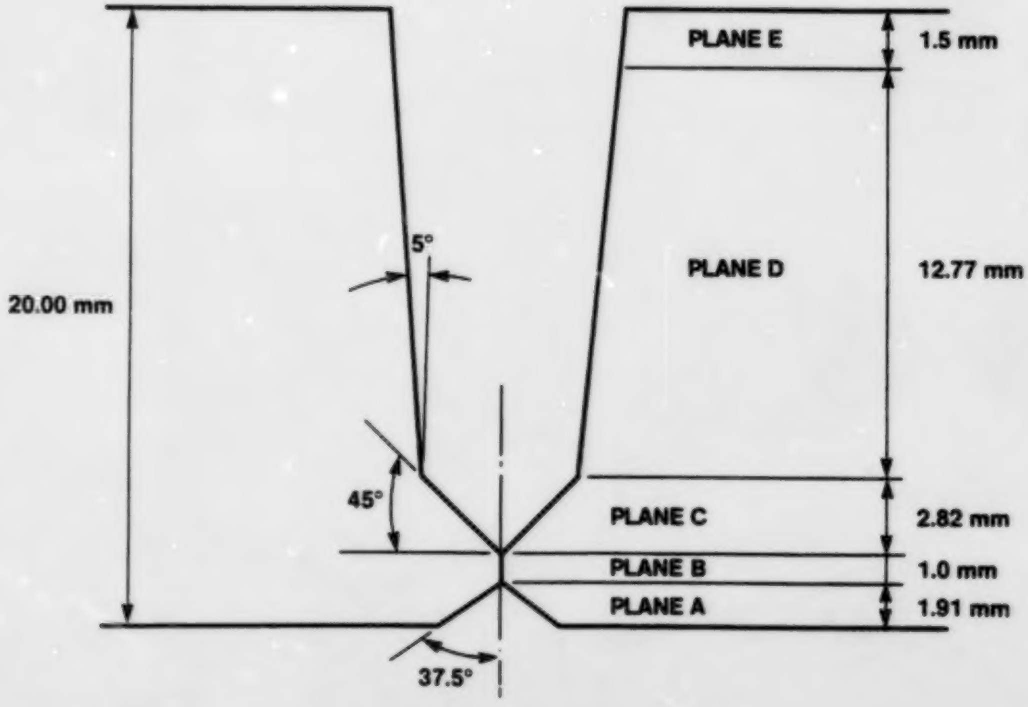
PLANE E
1.5 mm
5°
20.00 mm
PLANE D
12.77 mm
45°
PLANE C
2.82 mm
PLANE B
1.0 mm
PLANE A
1.91 mm
37.5°

FIGURE 2B 20 mm WALL THICKNESS

FIGURE 3
WELD JOINT CROSS-SECTION WITH INSPECTION DESIGN DIMENSIONS.

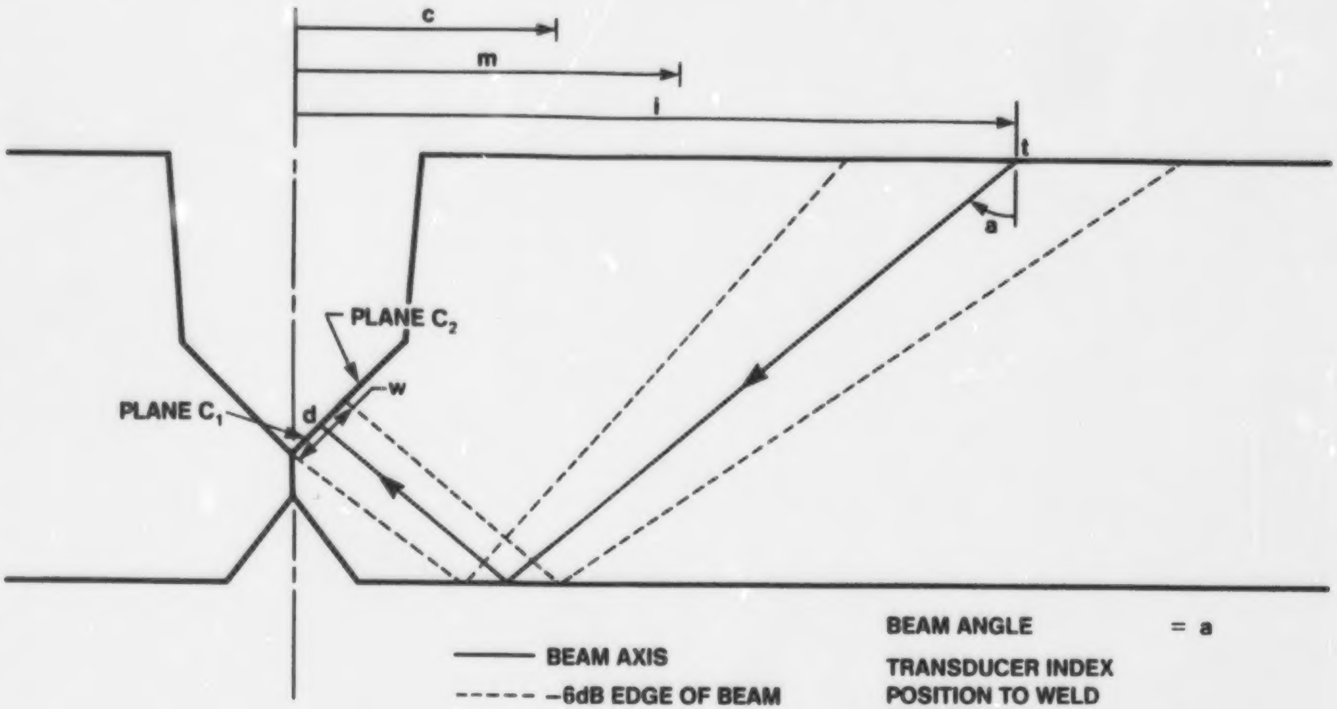
c
m
i
t
a
PLANE C_2
w
PLANE C_1
d
BEAM AXIS
–6dB EDGE OF BEAM

BEAM ANGLE = a

TRANSDUCER INDEX POSITION TO WELD CENTERLINE = i

TARGET DISTANCE = td

BEAM WIDTH AT THE TARGET = w

WELD CENTERLINE TO EDGE OF CAP = c

MINIMUM TRANSDUCER FRONT SURFACE TO WELD CENTERLINE = m

FIGURE 4A
INCREASED WELD CENTERLINE TO BEAM SKIP POSITION WITH A 5° INCREASE IN BEAM ANGLE

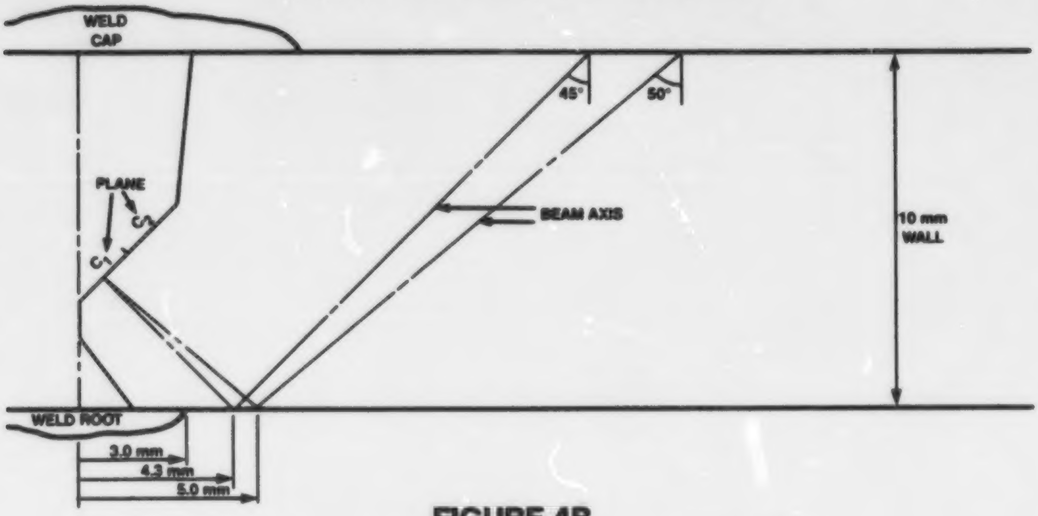
WELD CAP
45°
50°
PLANE
C1
C2
BEAM AXIS
10 mm WALL
WELD ROOT
3.0 mm
4.3 mm
5.0 mm

FIGURE 4B
INCIDENT ULTRASONIC BEAM OUTSIDE OF THE WELD ROOT GEOMETRY WHEN FOCUSED ON INSIDE SURFACE OF THE WALL

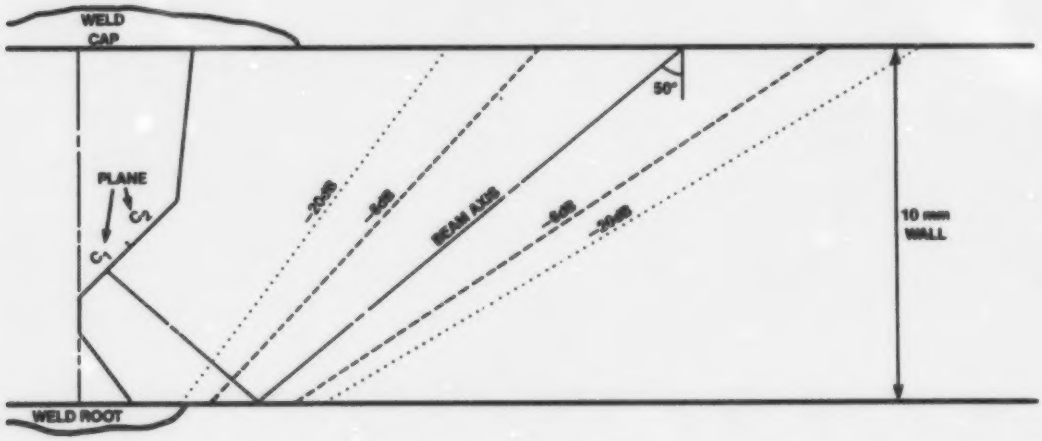
WELD CAP
50°
PLANE
C1
C2
-20dB
-6dB
BEAM AXIS
-6dB
-20dB
10 mm WALL
WELD ROOT

FIGURE 4C
INCIDENT ULTRASONIC BEAM WITHIN THE WELD ROOT GEOMETRY WHEN FOCUSED ON TARGET PLANE C1

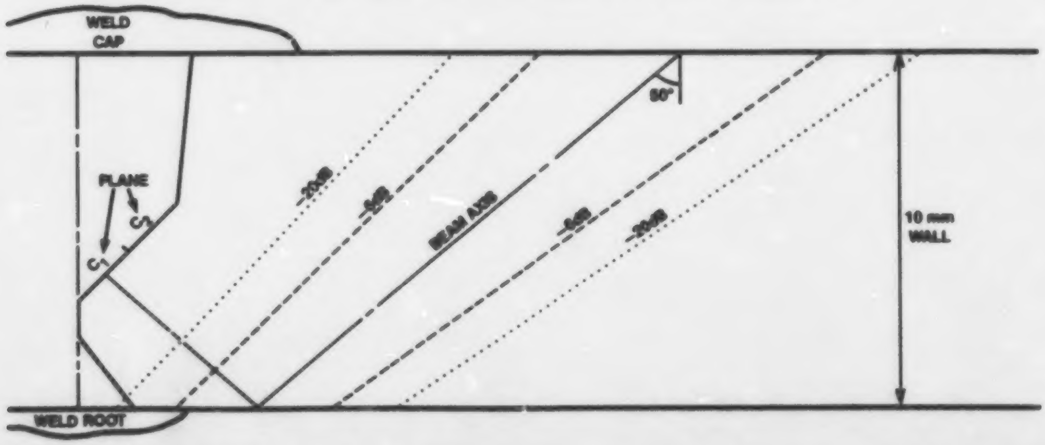
WELD CAP
50°
PLANE
C1
C2
-20dB
-6dB
BEAM AXIS
-6dB
-20dB
10 mm WALL
WELD ROOT

FIGURE 5
BEAM DIAMETER VERSUS TARGET PATH

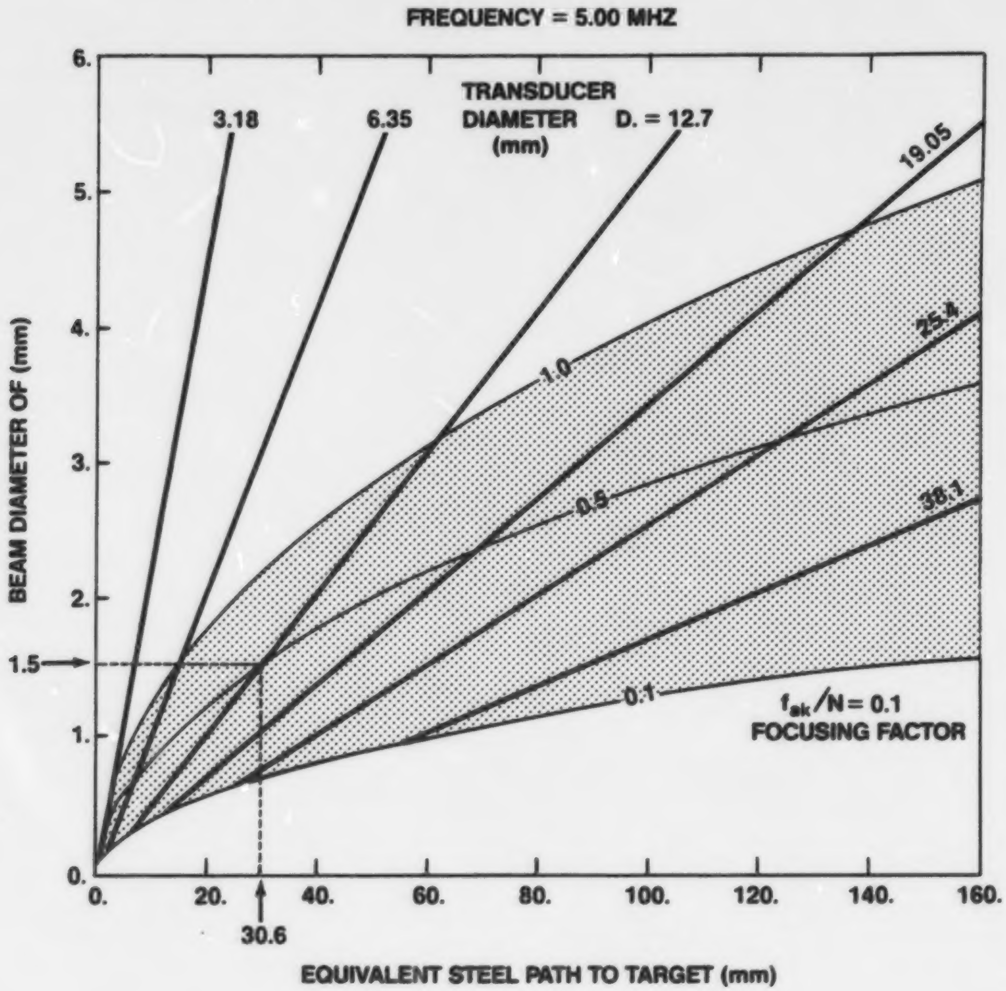

FIGURE 6
WORKING RANGE VERSUS TARGET PATH

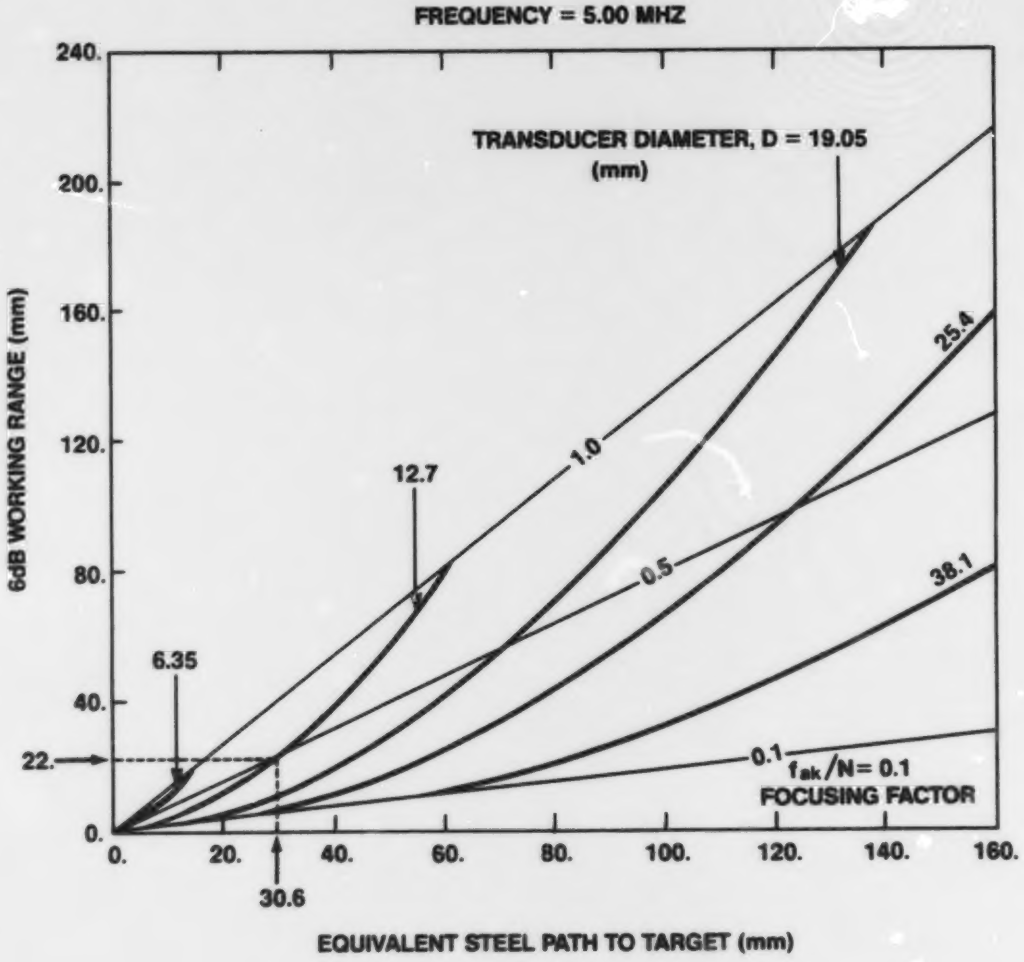

FIGURE 7
SIGNAL AND NOISE CURVES FOR TRANSDUCER NO. 1

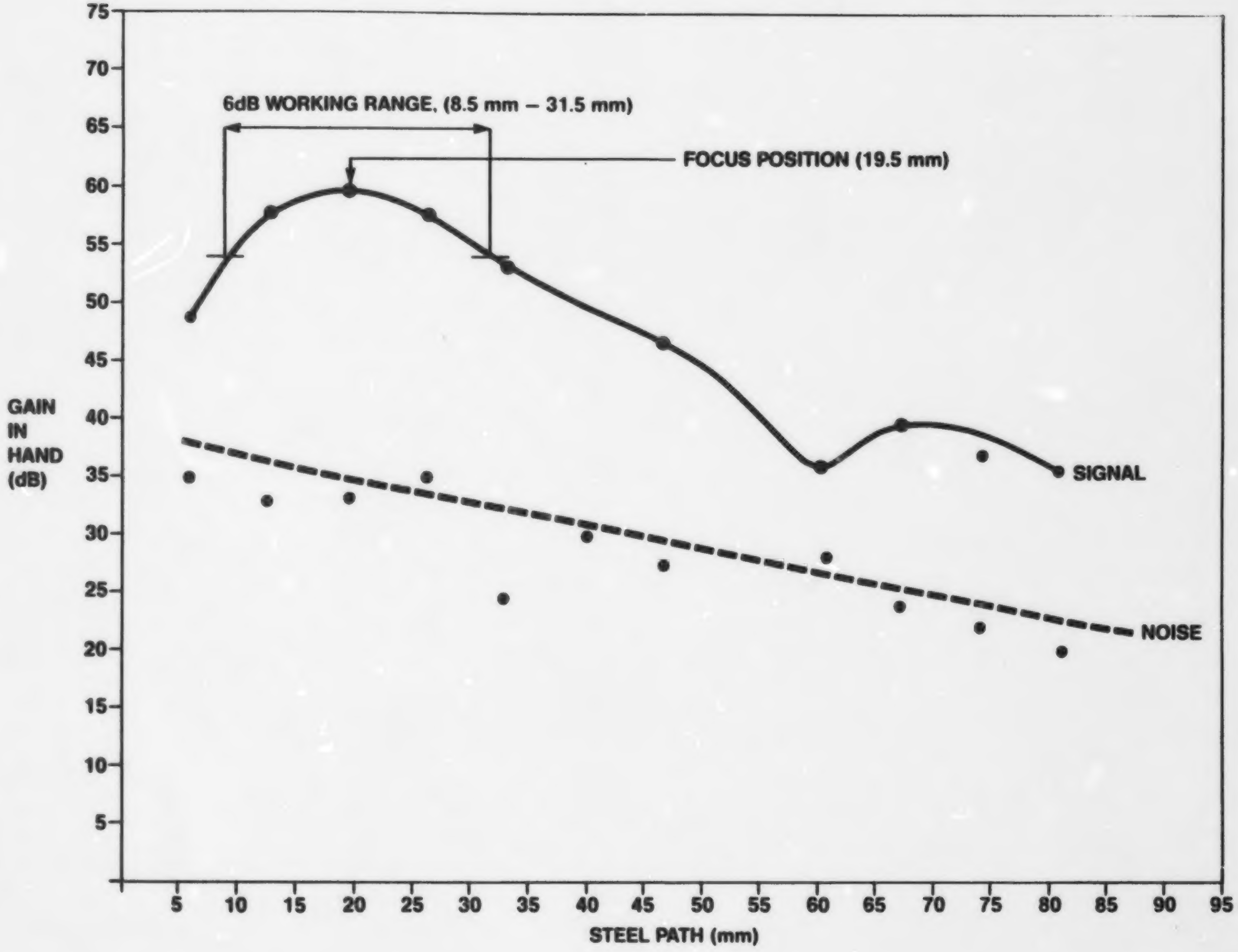

FIGURE 8
MEASURING SQUINT ON SIDE OF BLOCK

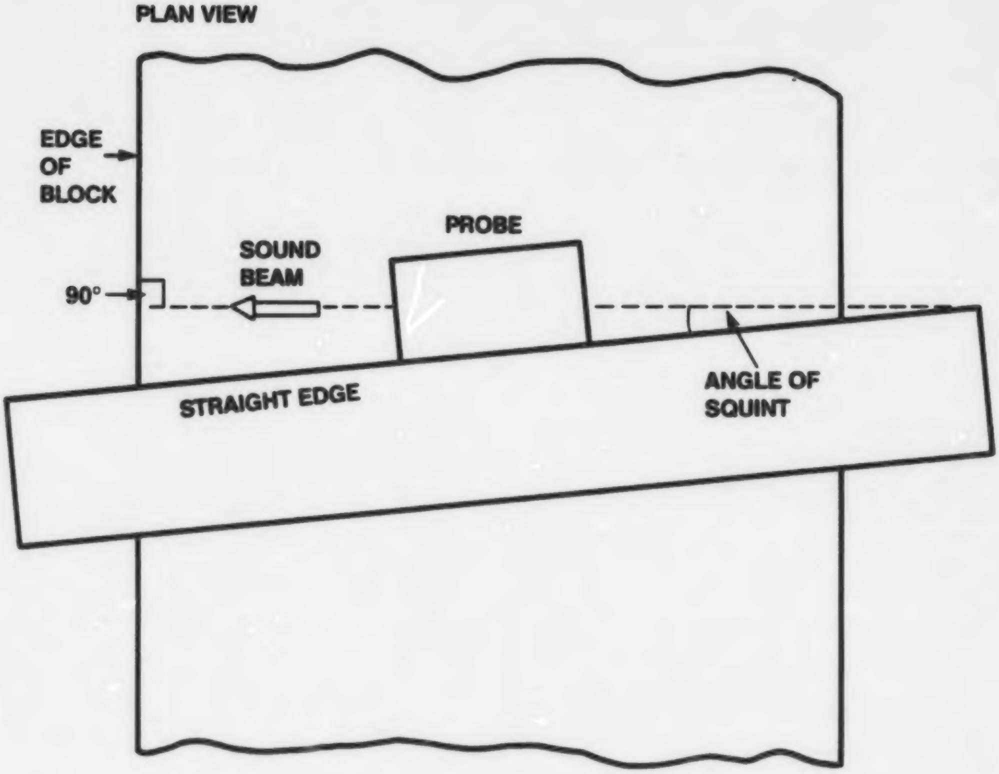
PLAN VIEW
EDGE OF BLOCK
PROBE
SOUND BEAM
90°
STRAIGHT EDGE
ANGLE OF SQUINT

PROBE IS TURNED TO GIVE A MAXIMUM SIGNAL

FIGURE 9
SYSTEM USED TO MANIPULATE TRANSDUCERS ON TEST PLATE SURFACE

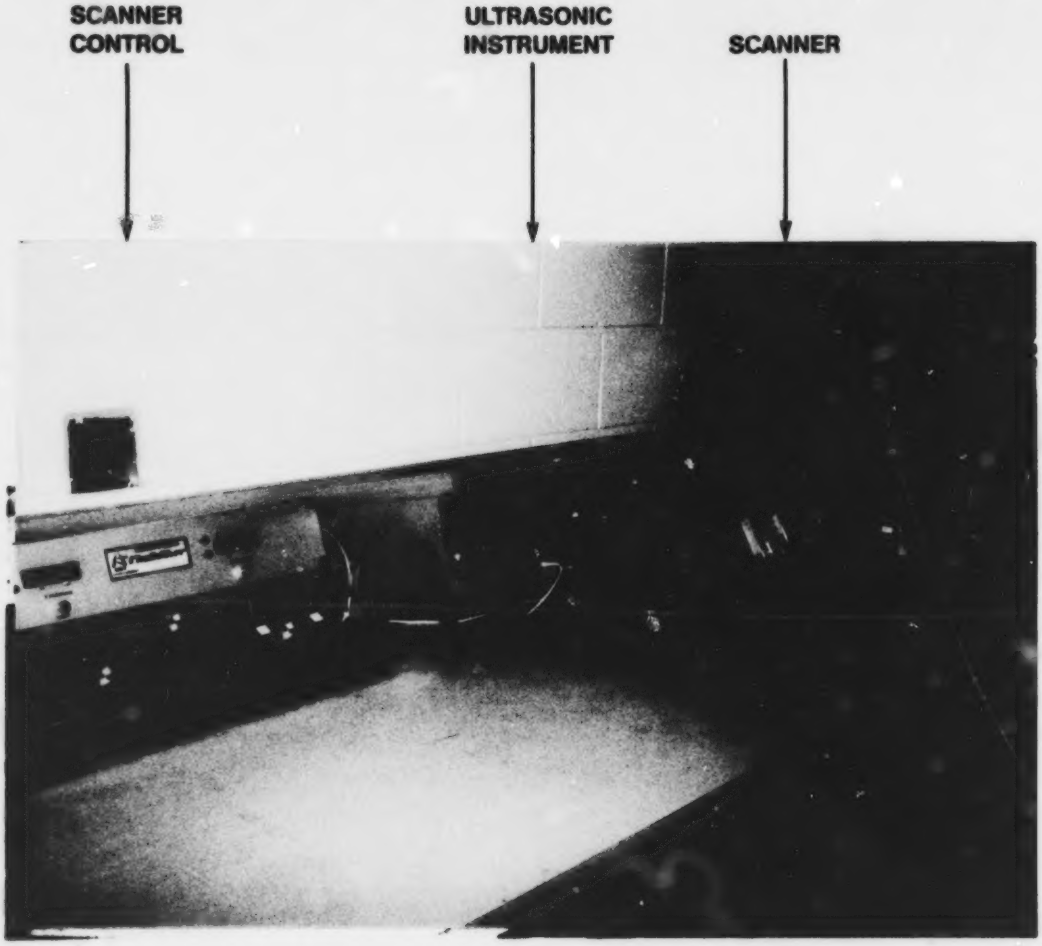
SCANNER CONTROL
ULTRASONIC INSTRUMENT
SCANNER

FIGURE 10
SAMPLE ANALOG RECORDING SHOWING ECHO AMPLITUDE VERSUS WELD LOCATION

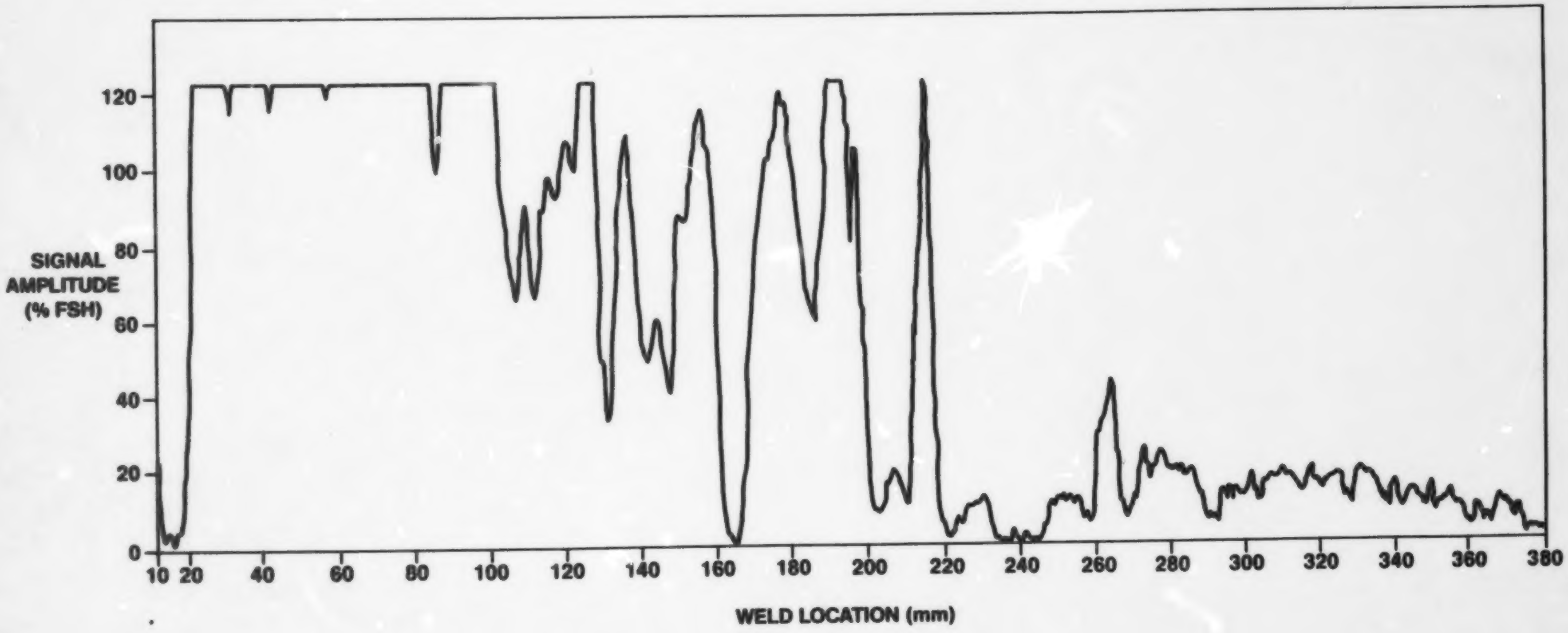

FIGURE 11
SIMULATED IMPERFECTION PLATE DESIGN

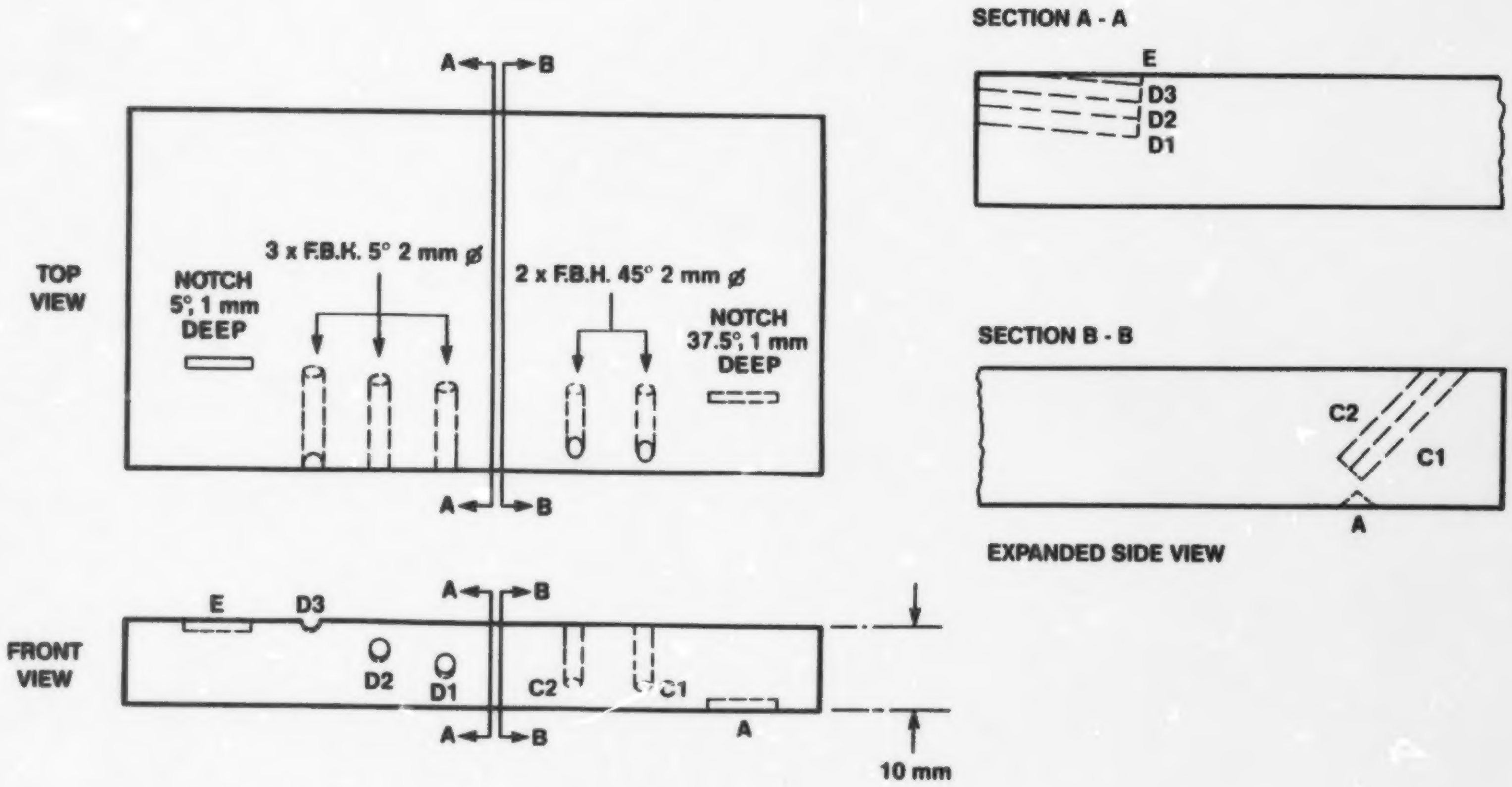
SECTION A - A
E
D3
D2
D1
A
B
TOP VIEW
NOTCH 5°, 1 mm DEEP
3 x F.B.K. 5° 2 mm ø
2 x F.B.H. 45° 2 mm ø
NOTCH 37.5°, 1 mm DEEP
SECTION B - B
C2
C1
A
EXPANDED SIDE VIEW
FRONT VIEW
E
D3
D2
D1
C2
C1
A
10 mm

FIGURE 12
MISORIENTATION PLATE DESIGN

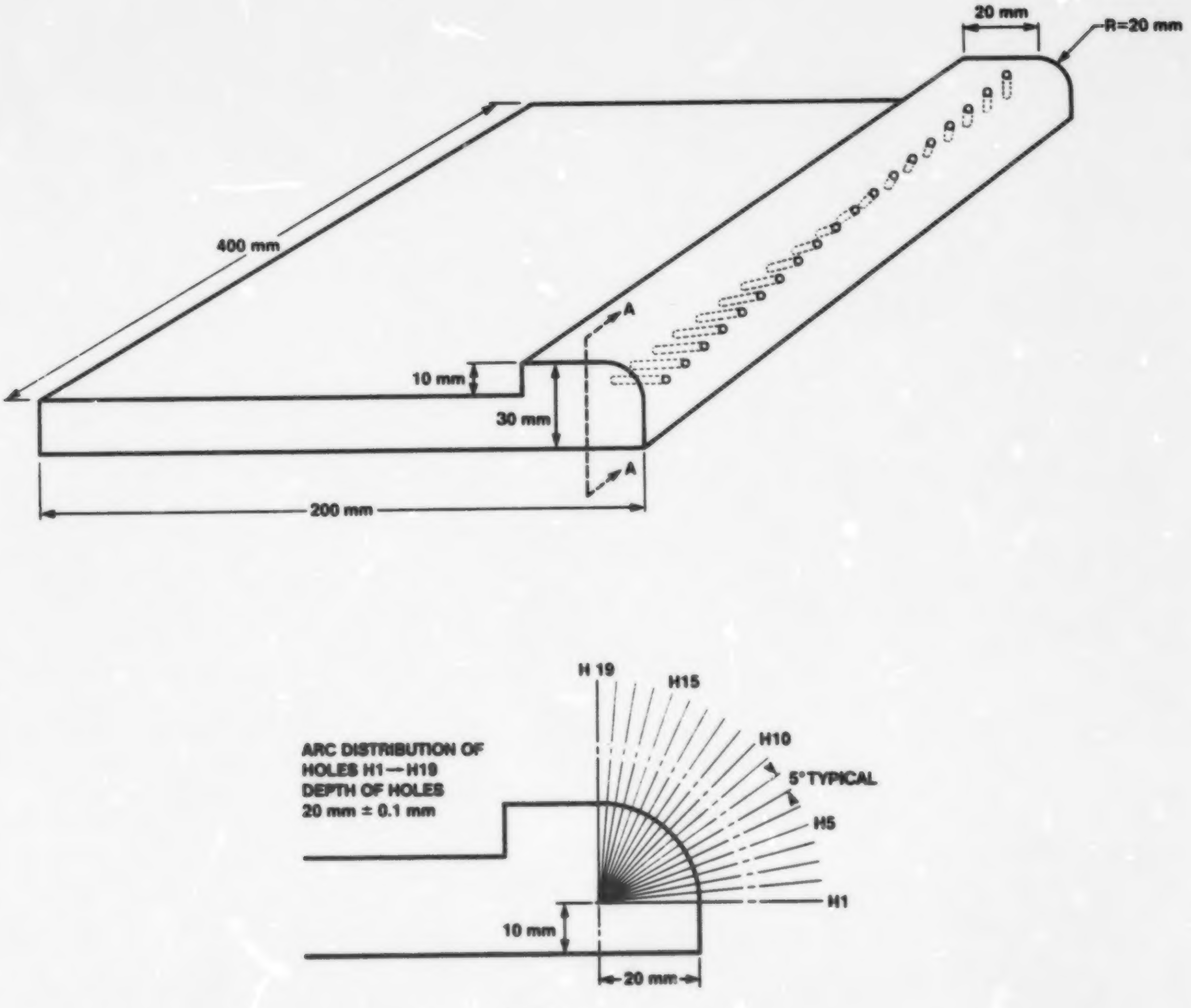
20 mm
R=20 mm
400 mm
A
10 mm
30 mm
A
200 mm
H 19
H15
H10
5° TYPICAL
H5
H1
ARC DISTRIBUTION OF
HOLES H1 — H19
DEPTH OF HOLES
20 mm ± 0.1 mm
10 mm
20 mm

VIEW A-A

FIGURE 13
SCHEMATIC OF GATE POSITION AND SIZE RELATIVE TO THE WELD ROOT GEOMETRY PLANE A

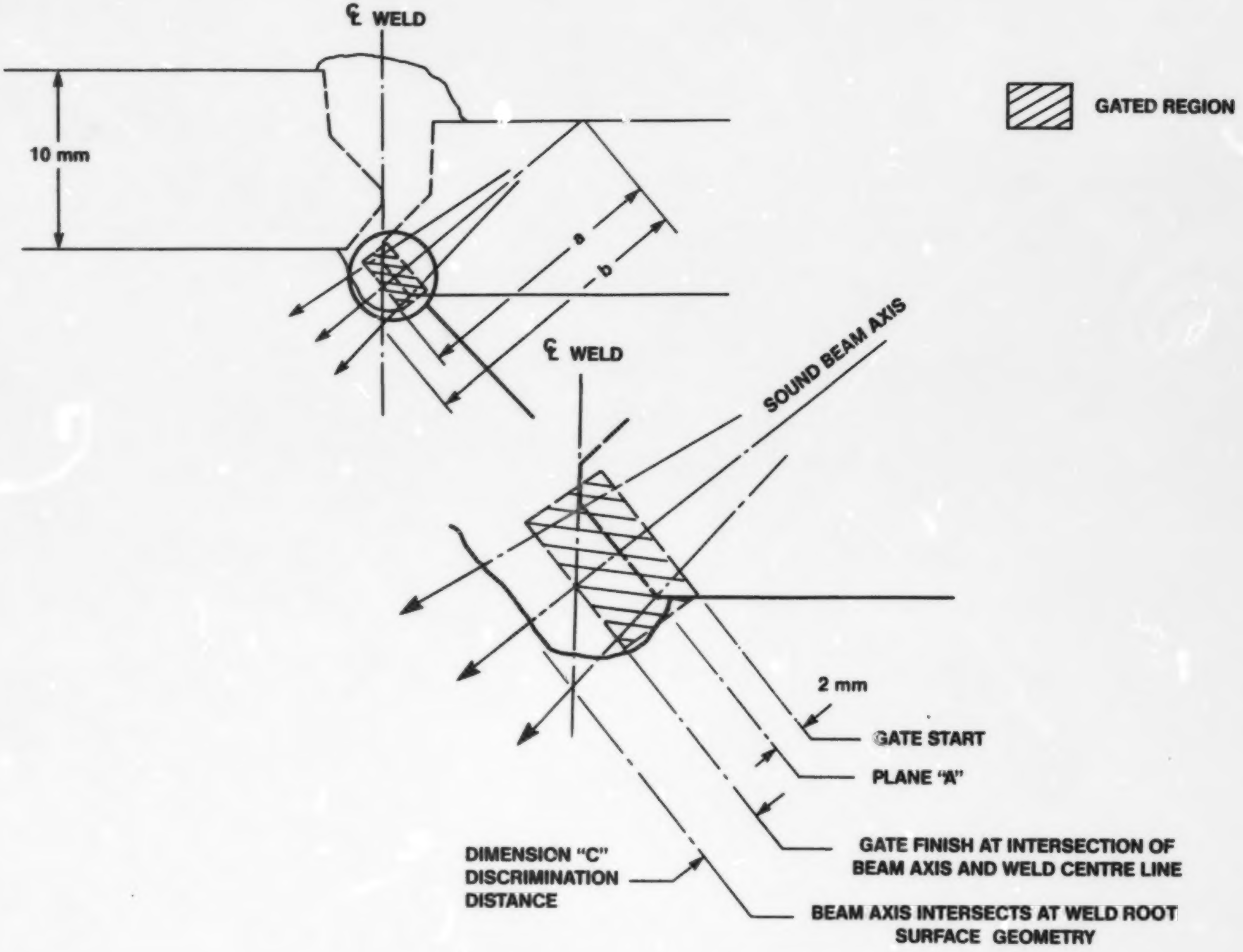
℄ WELD
10 mm
a
b
▨ GATED REGION
℄ WELD
SOUND BEAM AXIS
2 mm
GATE START
PLANE "A"
GATE FINISH AT INTERSECTION OF BEAM AXIS AND WELD CENTRE LINE
DIMENSION "C" DISCRIMINATION DISTANCE
BEAM AXIS INTERSECTS AT WELD ROOT SURFACE GEOMETRY

FIGURE 14

SIGNAL TO NOISE MEASURED ON SIMULATED IMPERFECTIONS WITH SELECTED TRANSDUCERS (10 mm WALL)

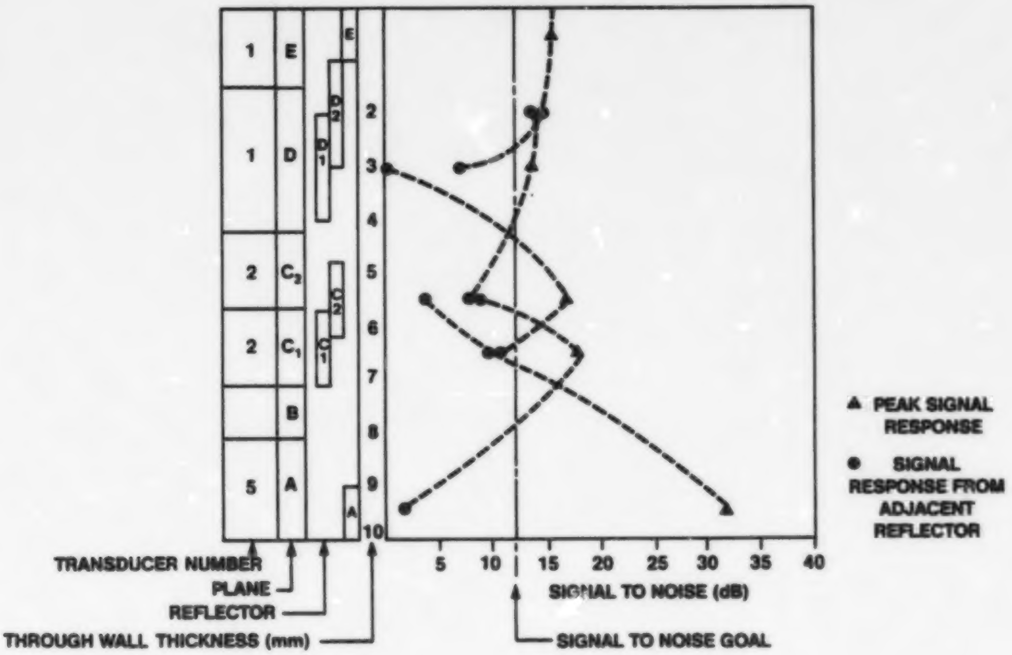

FIGURE 15

SIGNAL TO NOISE MEASURED ON SIMULATED IMPERFECTIONS WITH CONVENTIONAL TRANSDUCERS (10 mm WALL)

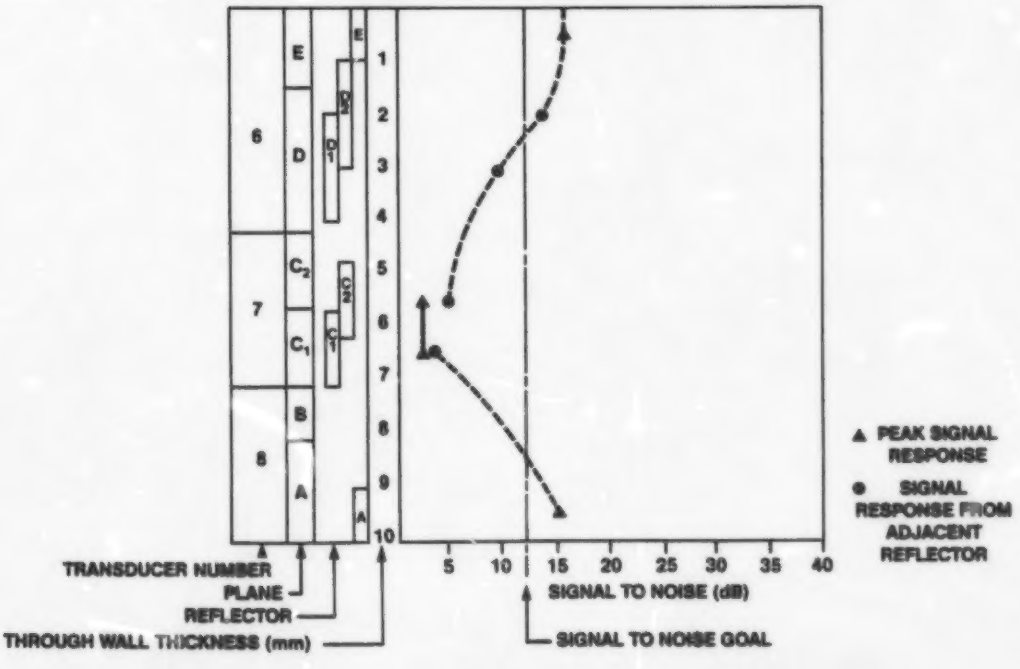

FIGURE 16
SIGNAL TO NOISE MEASURED ON SIMULATED IMPERFECTIONS WITH SELECTED TRANSDUCERS (20 mm WALL)

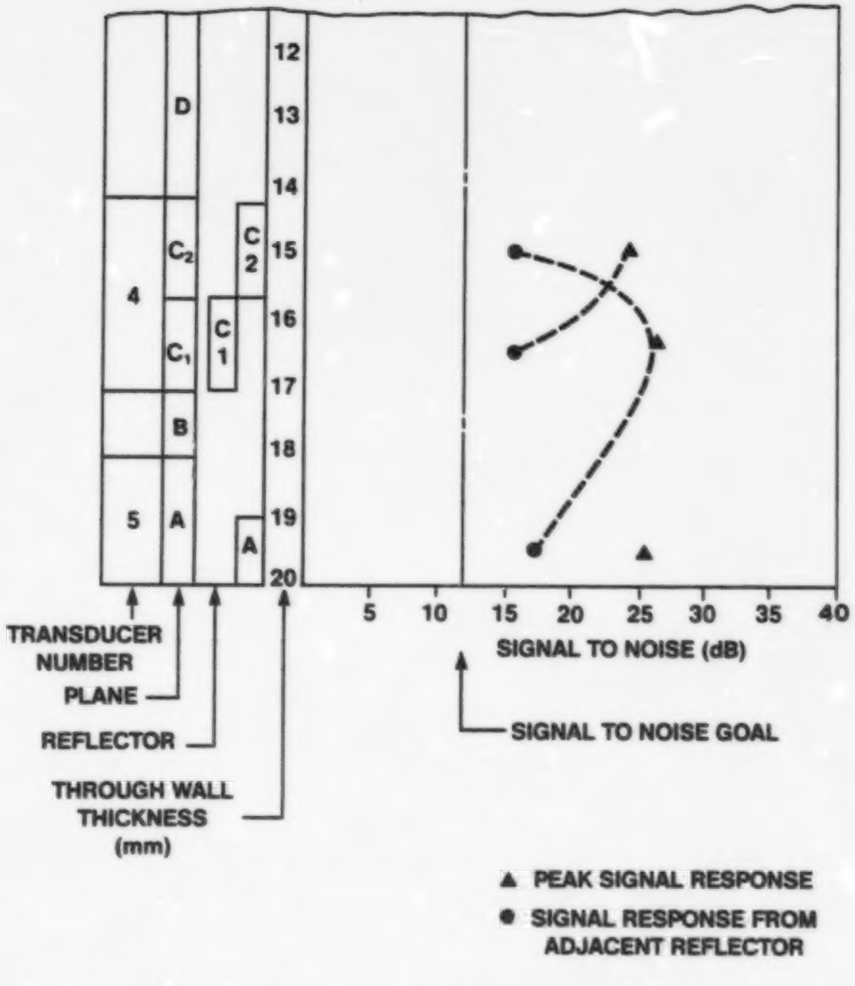

FIGURE 17A
BEAM PATH FOR "CORNER REFLECTION" FROM IMPERFECTION CLOSE TO PLATE SURFACE

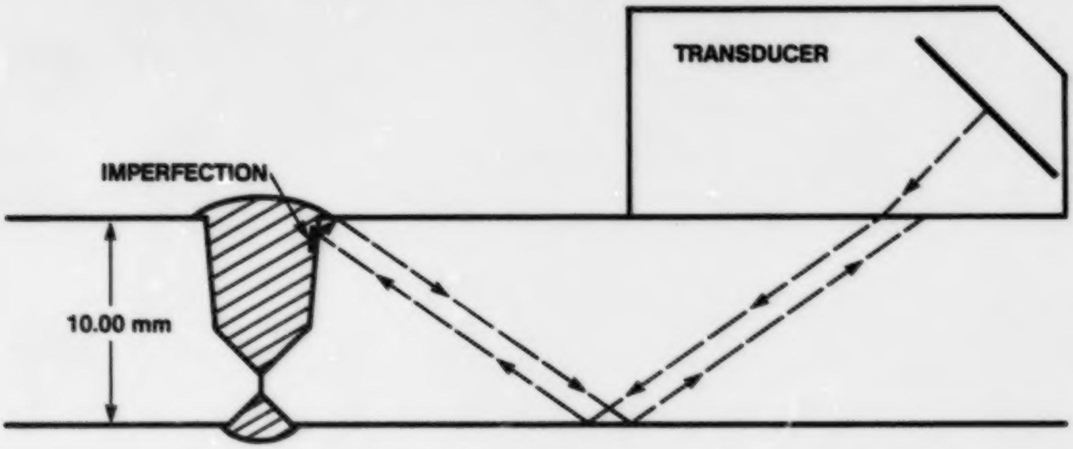
TRANSDUCER
IMPERFECTION
10.00 mm

FIGURE 17B
RETURN BEAM PATH MISSES TRANSDUCER FOR AN IMPERFECTION NOT CLOSE TO THE PLATE SURFACE

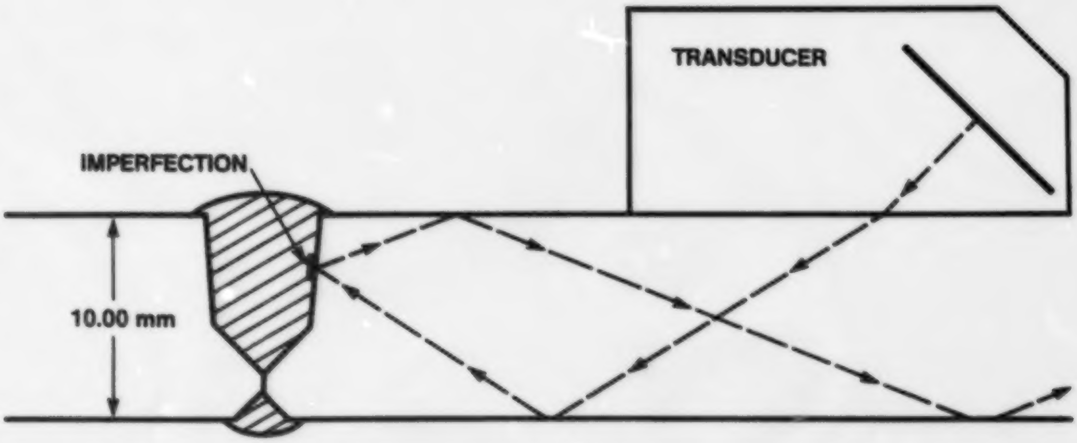
TRANSDUCER
IMPERFECTION
10.00 mm

FIGURE 18
SIGNAL AMPLITUDE VERSUS MISORIENTATION ANGLE

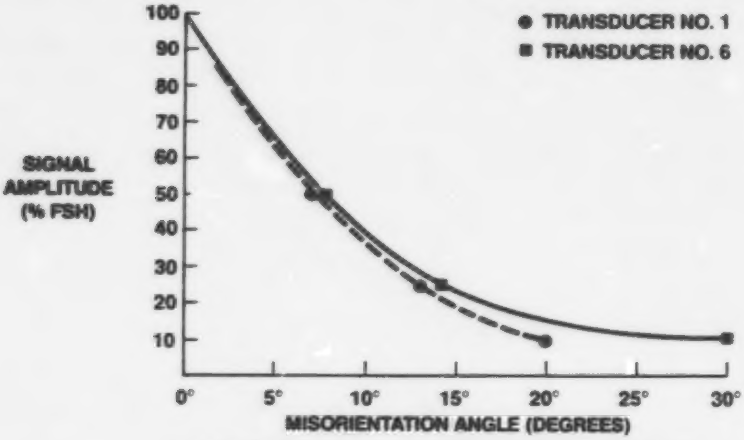

0° = PERPENDICULAR INCIDENCE, PATH DISTANCE FOR TRANSDUCER NO. 1 = 27.3 mm. PATH DISTANCE FOR TRANSDUCER NO. 6 = 17.4 mm

FIGURE 19
SIGNAL TO NOISE VERSUS IMPERFECTION PROJECTED THROUGH WALL DEPTH FOR SELECTED TRANSDUCER NO. 5 INSPECTING PLANE A

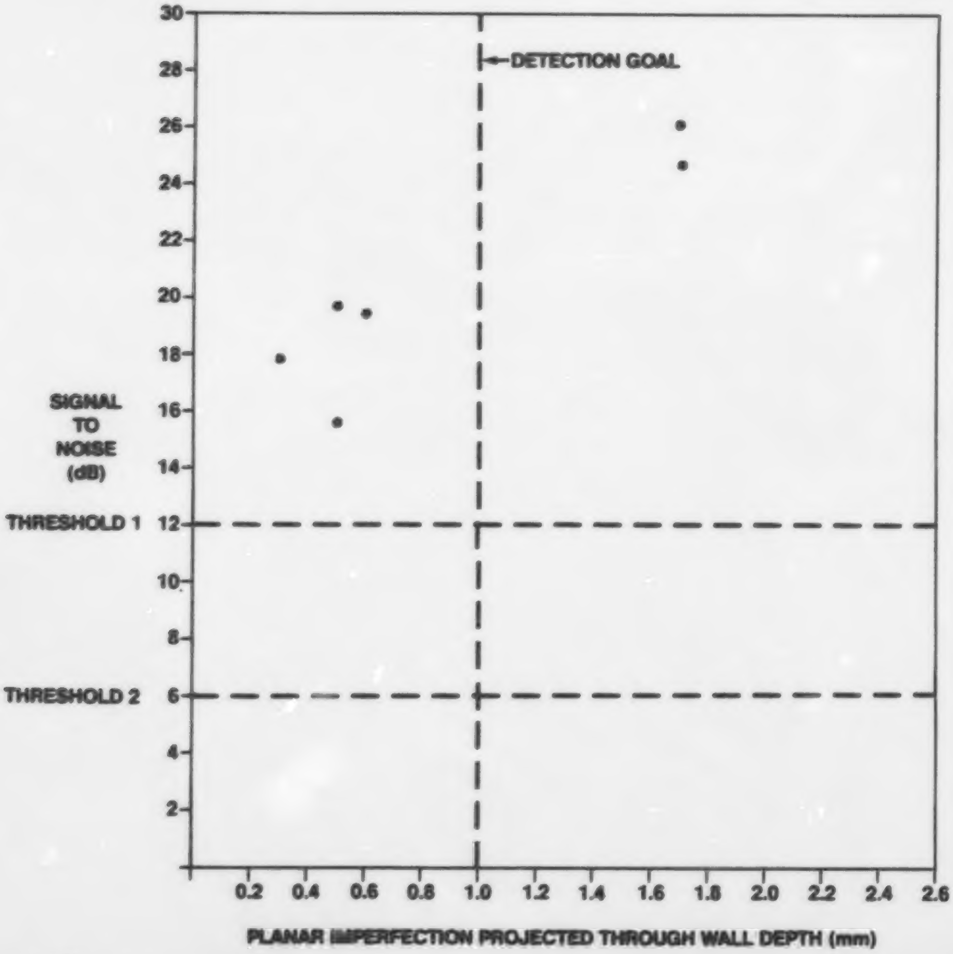

FIGURE 20
LACK OF ROOT FUSION DEFECT IN PLANE A

10.0 mm
LACK OF FUSION

FIGURE 21

SIGNAL TO NOISE VERSUS IMPERFECTION PROJECTED THROUGH WALL DEPTH FOR SELECTED TRANSDUCER NO. 2 INSPECTING PLANE C

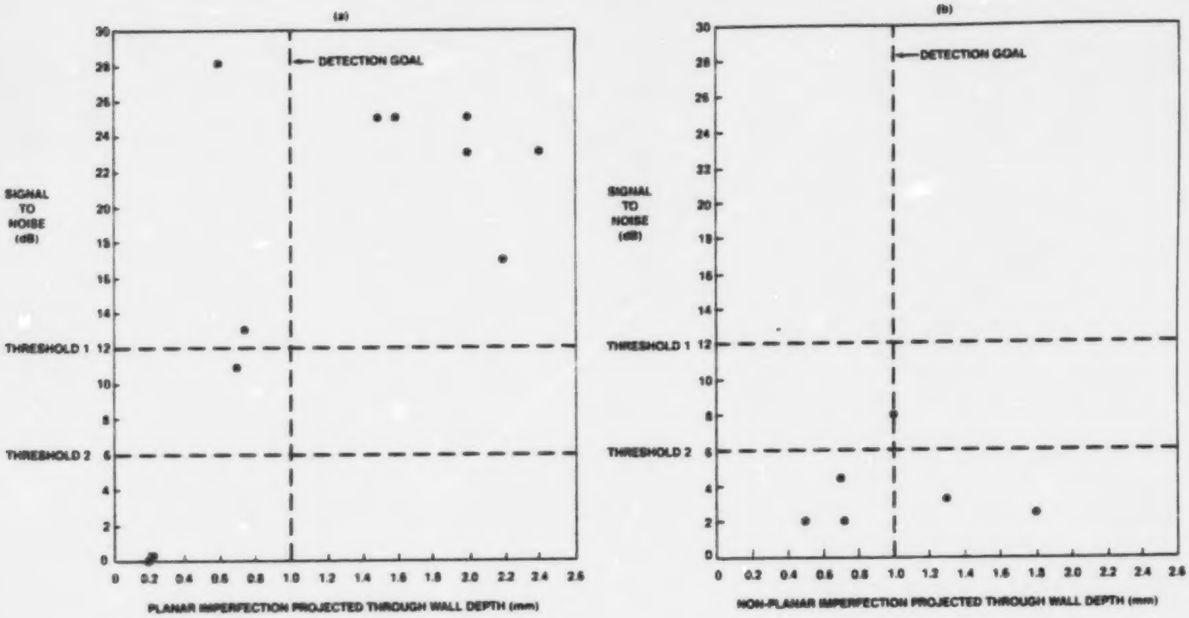

FIGURE 22

SIGNAL TO NOISE VERSUS IMPERFECTION PROJECTED THROUGH WALL DEPTH FOR CONVENTIONAL TRANSDUCER NO. 7 INSPECTING PLANE C

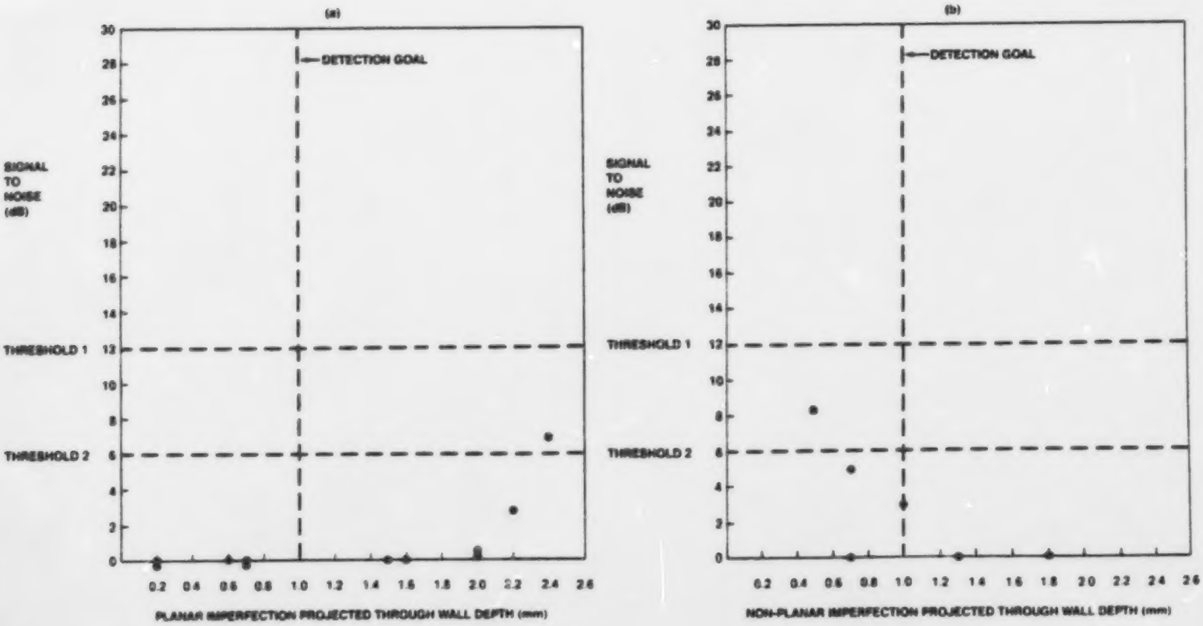

FIGURE 23
WELD CROSS SECTION SHOWING POROSITY IN THE CAP REGION

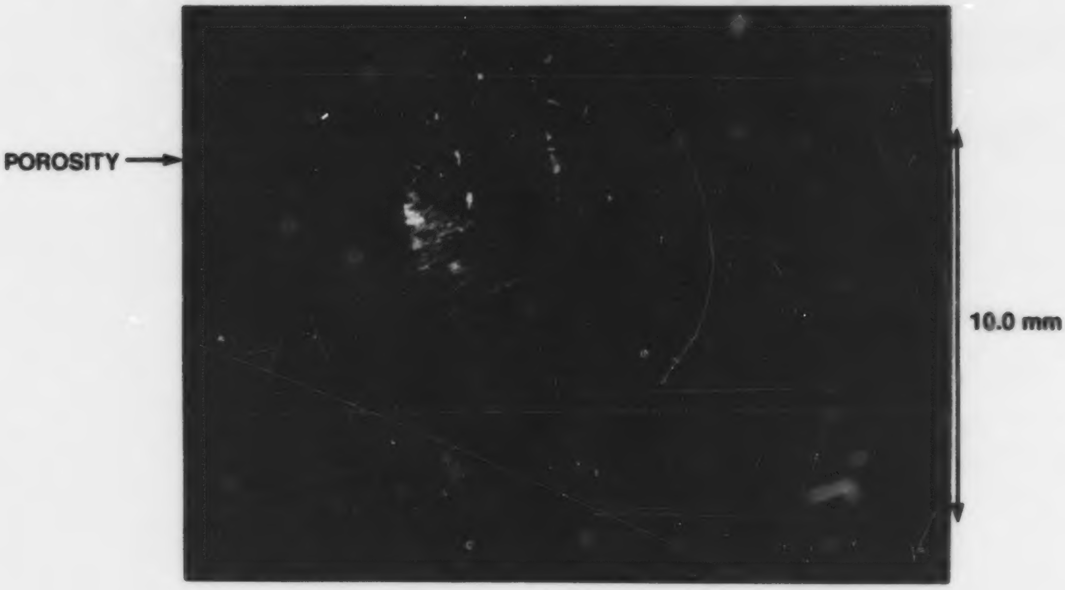
POROSITY
10.0 mm

FIGURE 24
WELD CROSS SECTION SHOWING POROSITY IN ROOT REGION

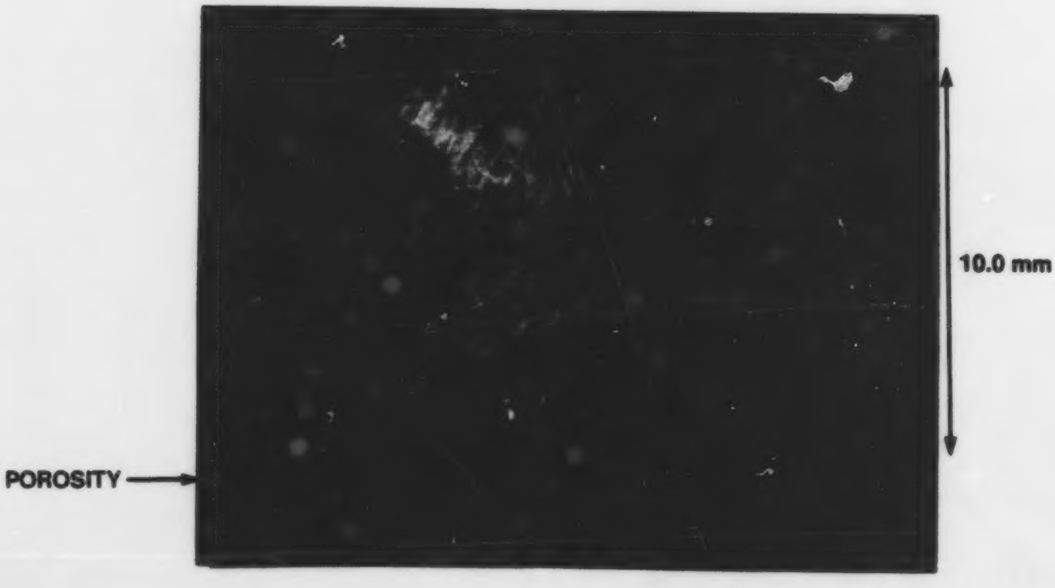
10.0 mm
POROSITY

FIGURE 25

"A" SCAN PHOTO SHOWING BAR GATE RELATIVE TO ROOT SURFACE INDICATION AND MEASURED DISCRIMINATION DISTANCE "C"

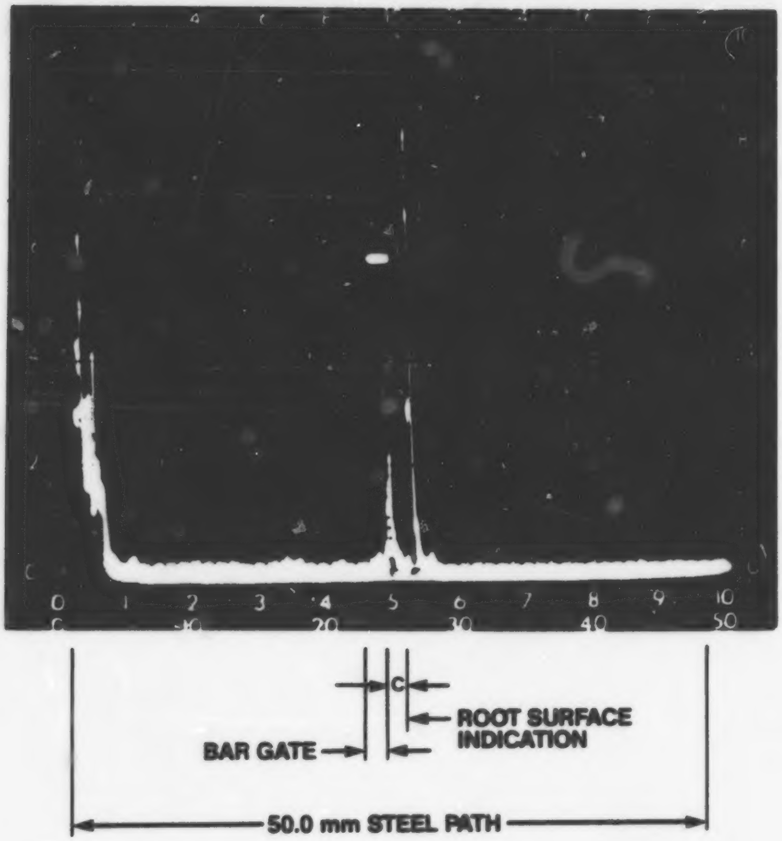

FIGURE 26
BEAM PATH OF PITCH-CATCH TECHNIQUE FOR
INSPECTION OF PLANE "D"

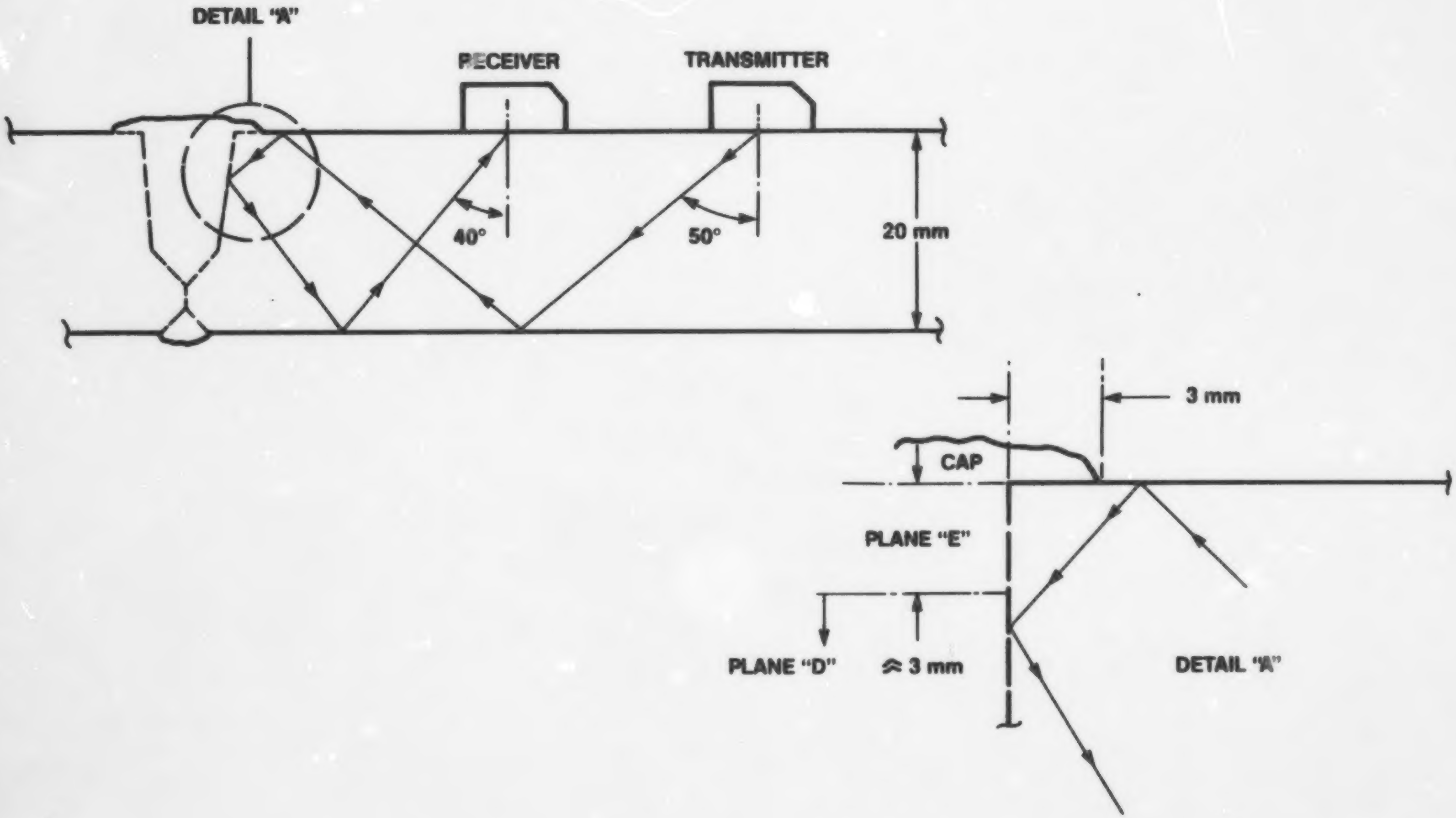
DETAIL "A"
RECEIVER
TRANSMITTER
40°
50°
20 mm
3 mm
CAP
PLANE "E"
PLANE "D"
≈ 3 mm
DETAIL "A"

FIGURE 27
SIGNAL TO NOISE VERSUS IMPERFECTION PROJECTED THROUGH WALL DEPTH FOR PITCH – CATCH INSPECTION OF PLANE D

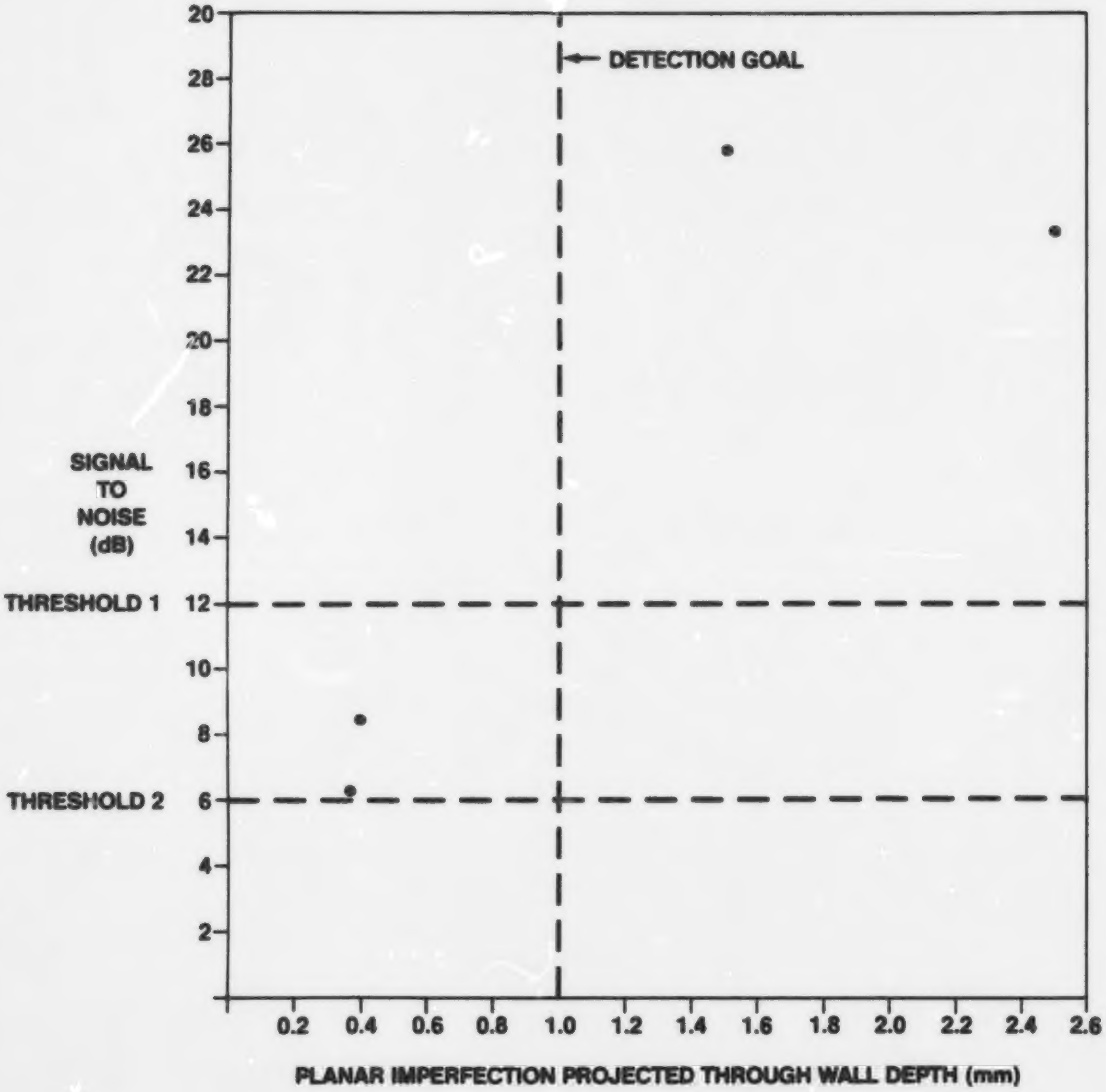

FIGURE 28
CREEPING WAVE AND OTHER WAVE TYPES PRODUCED BY THE CREEPING WAVE TRANSDUCER

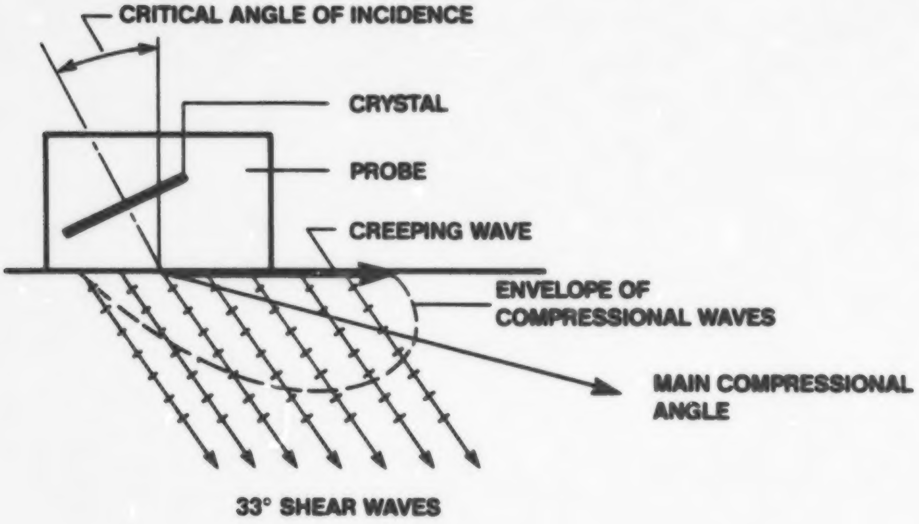
CRITICAL ANGLE OF INCIDENCE
CRYSTAL
PROBE
CREEPING WAVE
ENVELOPE OF COMPRESSIONAL WAVES
MAIN COMPRESSIONAL ANGLE
33° SHEAR WAVES

FIGURE 29
PULSE – ECHO RESPONSE OF CREEPING WAVE TRANSDUCER FROM SIMULATED IMPERFECTIONS IN 20 mm WALL PLATE

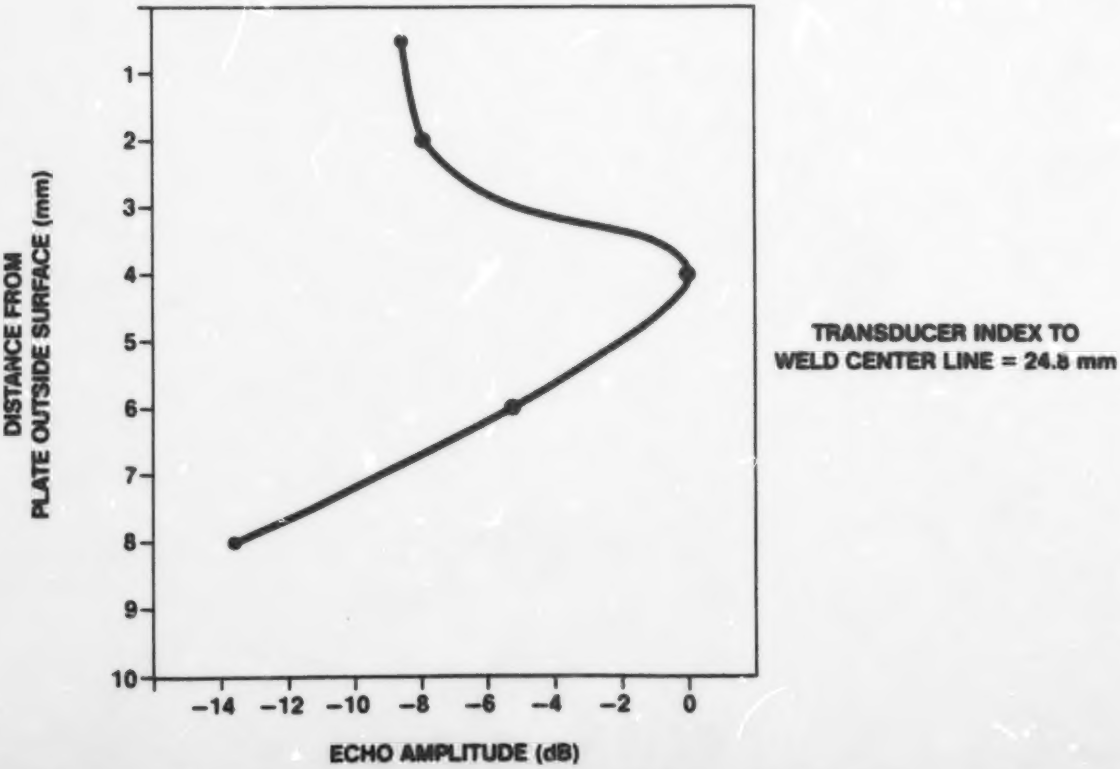

APPENDIX 1.0

DEFECTS IN GAS METAL ARC (GMA) WELDS

APPENDIX 1.0

Welding imperfections which occur with the GMA welding process are illustrated in the weld cross section schematics of Figures 1.1 to 1.12. Imperfections are organized into the planar and non-planar categories of CSA Z184 Appendix K and individual imperfections into seven different types. A description of each imperfection type is also provided.

Occurrence of GMA Imperfections

The occurrence of each of these imperfection types was determined from the GMA welding imperfection statistics tabulated for 23,312 GMA girth welds representing 623 km of 1067 mm pipeline construction (9,10). Wall thickness ranged from 12 to 19.2 mm. The welding imperfection statistics are shown in Table 1.1. The table shows planar imperfections make up the majority, and of these lack of fusion is the most common. Three types of imperfections which account for 92% of all the imperfections are: lack of fusion, 51% porosity, 24% and undercut, 17%.

Ten of the 14 welds identified to contain cracks contained root cracks initiating from the toe of the root bead. Three of the welds contained shrinkage cavities in the midwall region and one had a shrinkage cavity in the cap region.

The statistics are based on results reported by x-ray radiographic inspection and therefore reflect the method's ability to detect the imperfections made by the GMA process. Results from field trials with ultrasonic inspection show the incidence of imperfection indications to be approximately three times higher than for radiography. Metallographic analysis on a selected number of these welds, showing only ultrasonic indications identified real lack of fusion type welding imperfections. Ultrasonic results, therefore, indicate the incidence of lack of fusion is actually much higher than is currently reported by radiography. Radiographic inspection statistics and ultrasonic results both indicate planar lack of fusion as the predominant imperfection type.

Significance of Imperfections

The different types of imperfections have been ranked in categories related to fitness-for-purpose assessments as indicated in Table 1.2. Table 1.2 shows the most significant imperfections (I) are those that are planar and occur at the surface such as lack of fusion and cracks and the least important (IV) are volumetric, such as porosity that occurs in the body of the weld.

The welding statistics indicate that planar imperfections also occur in significantly greater numbers than volumetric imperfections, representing greater than 50% of all the GMA weld imperfection types reported by x-radiography during pipeline construction.

The types of welding imperfections, their occurrence and importance with respect to detection was used as a basis for the design of test plates containing real and simulated weld imperfections. Simulated imperfection test plates used to evaluate the performance of ultrasonic inspection techniques were, therefore, designed to contain flat bottomed hole and notch reflectors representing significant planar weld imperfections. Real imperfection test plates were designed to contain all imperfections except low cover and arc burn to determine the relative detectability to each, however, emphasized the planar lack of fusion imperfection type.

TABLE 1.1

GMA WELDING IMPERFECTION STATISTICS FOR 23,312 WELDS IN 1067 mm DIAMETER PIPE OF 12, 16 AND 19.2 mm WALL THICKNESSES

Planar Defects

Type	Region	No. of Welds	Percent of Total Welds
Lack of Fusion	All	2,603	11.17
Undercut	Cap & Root	857	3.67
Burn Through	Root	162	0.69
Crack	All	14	0.06
TOTAL		3,636	15.59

Non-Planar Defects

Type	Region	No. of Welds	Percent of Total Welds
Porosity	All	1,209	5.17
Low Cover	Cap	217	0.93
Arc Burn	Cap	13	0.06
TOTAL		1,439	6.16

TABLE 1.2

GAS METAL ARC WELDING IMPERFECTIONS RANKED ACCORDING TO IMPORTANCE OF DETECTION

Importance of Detection	Category	Location	Type
I	Planar	Surface	Lack of Fusion Undercut Burn Through Crack
II	Planar	Embedded	Lack of Fusion Crack
III	Volumetric	Surface	Porosity Low Cover Arc Burn
IV	Volumetric	Embedded	Porosity

PLANAR IMPERFECTIONS

LACK OF FUSION - An imperfection involving the lack of bond between weld passes or between the weld metal and the base metal and is illustrated in Figures 1.1 and 1.2. The lack of cross penetration imperfection shown in Figure 1.3 and defined as an imperfection occurring at the weld interior where the weld joint preparation incorporates abutting surfaces has also been included here due to its similarity in shape with the lack of fusion imperfection type.

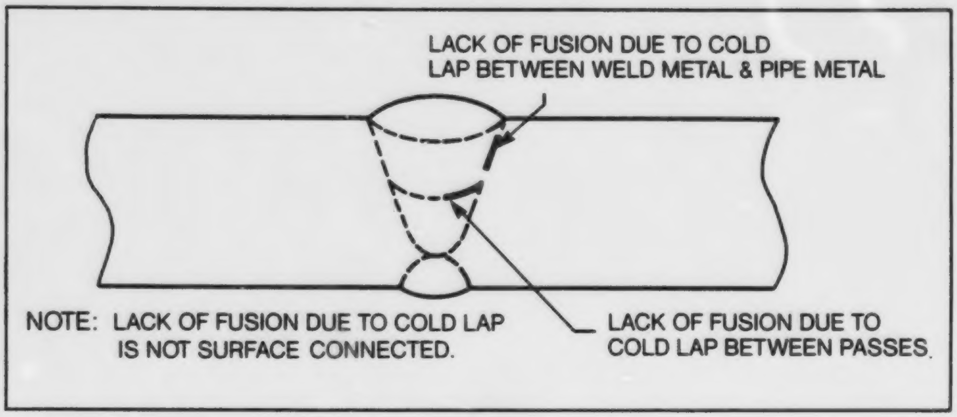
LACK OF FUSION DUE TO COLD
LAP BETWEEN WELD METAL & PIPE METAL
NOTE: LACK OF FUSION DUE TO COLD LAP
IS NOT SURFACE CONNECTED.
LACK OF FUSION DUE TO
COLD LAP BETWEEN PASSES.

FIGURE 1.1
Lack of fusion due to cold lap.

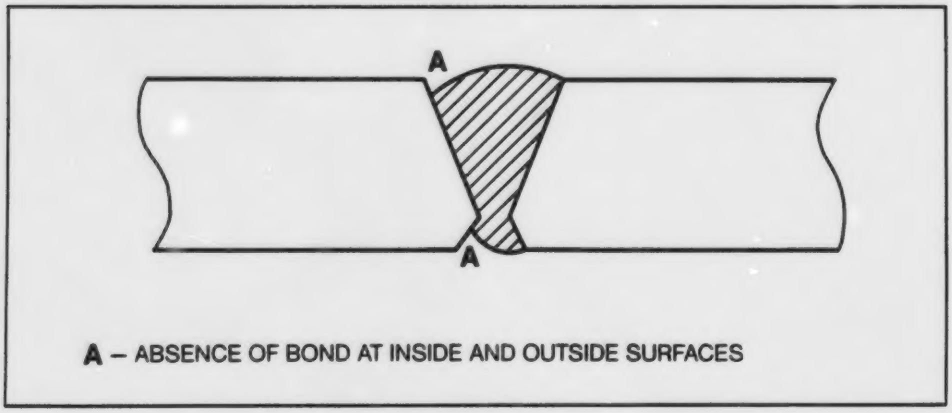
A
A
A – ABSENCE OF BOND AT INSIDE AND OUTSIDE SURFACES

FIGURE 1.2
Lack of fusion located between weld metal and base metal at inside and outside surfaces.

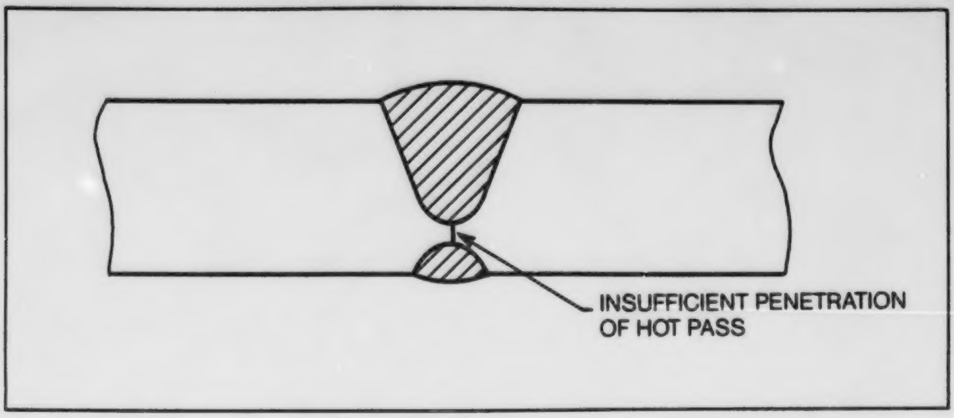
INSUFFICIENT PENETRATION
OF HOT PASS

FIGURE 1.3
Lack of cross penetration.

UNDERCUT - Undercutting is defined as a groove melted into the base metal adjacent to the toe or root of a weld and left unfilled by weld metal. A schematic representation of the condition is given in Figure 1.4.

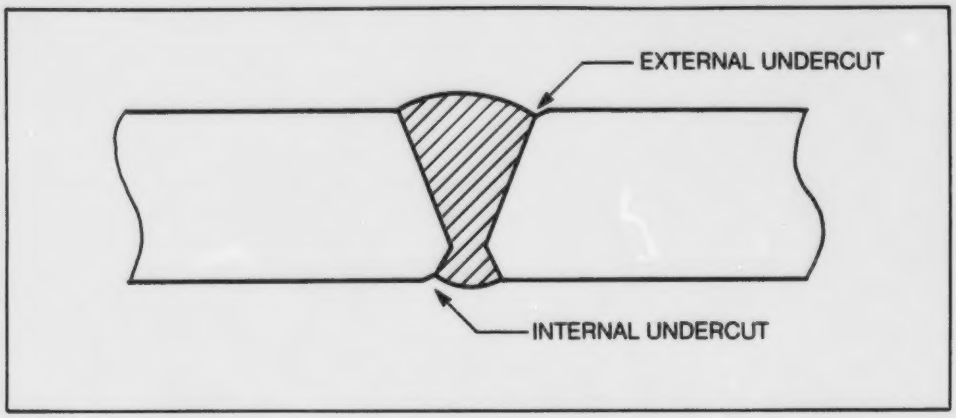
EXTERNAL UNDERCUT
INTERNAL UNDERCUT

FIGURE 1.4
Undercutting.

BURN THROUGH - Is defined as a region where excessive arc penetration has caused a cavity in the weld root.

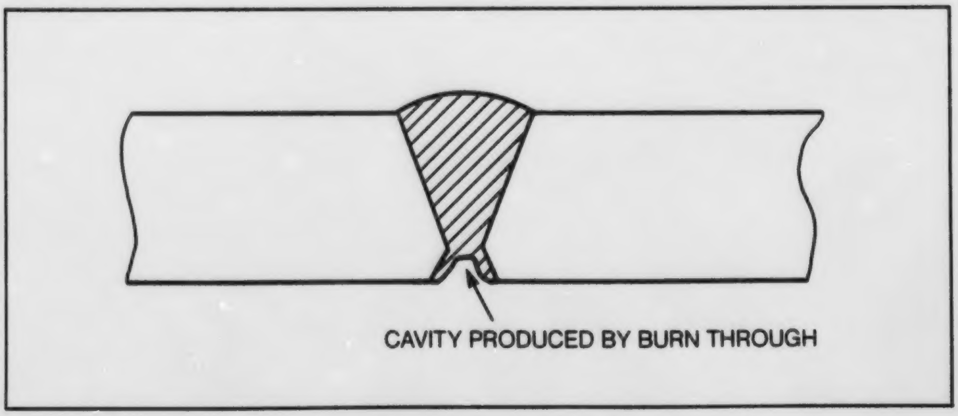
CAVITY PRODUCED BY BURN THROUGH

FIGURE 1.5
Burn through.

CRACK - A fracture type imperfection characterized by a sharp tip and high ratio length and height to opening displacement (Figure 1.6). An imperfection with similar characteristics is the shrinkage cavity which is defined as an interior imperfection occurring at the weld centerline where the application of an increased volume of weld metal and resultant cooling has left a void as illustrated in Figure 1.7.

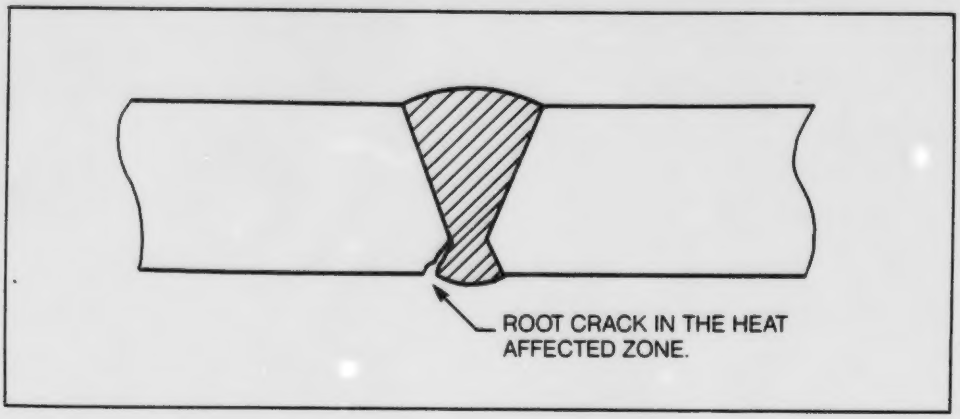
ROOT CRACK IN THE HEAT
AFFECTED ZONE.

FIGURE 1.6
Crack.

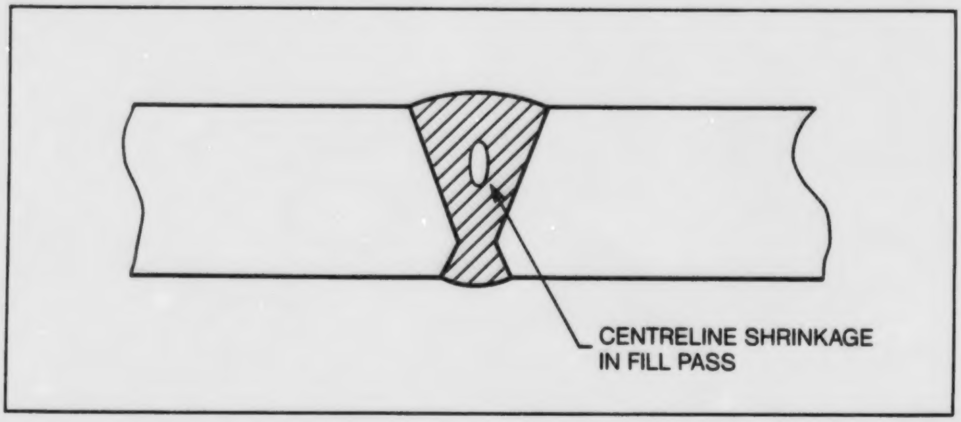
CENTRELINE SHRINKAGE
IN FILL PASS

FIGURE 1.7
Shrinkage cavity.

NON-PLANAR IMPERFECTIONS

POROSITY - Is defined as gas pockets having a circular section and occurring in the weld metal. Spherical porosity is illustrated in Figure 1.8. Piping or wormhole porosity (Figure 1.9) is characterized by an elongated gas pocket resulting from gas rising through solidifying weld metal and whose orientation tends to be partly in the through thickness direction and cluster porosity (Figure 1.10) which occurs as localized areas of spherical gas pockets along the lengh of the weld.

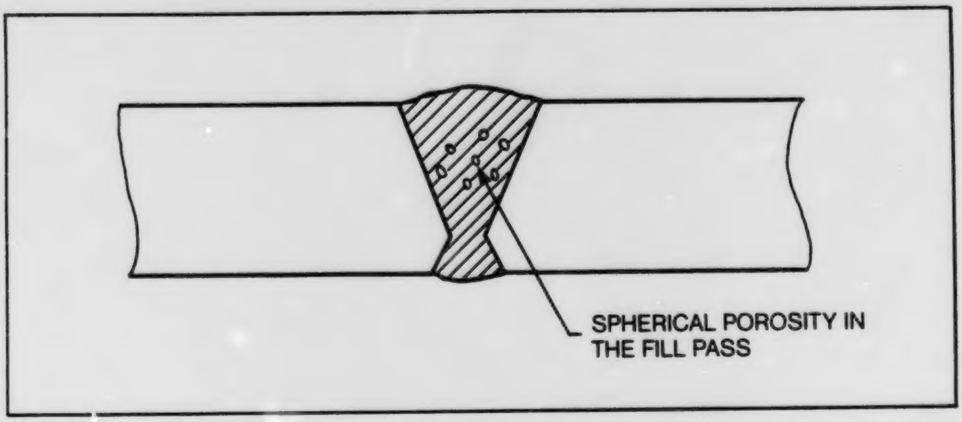
SPHERICAL POROSITY IN
THE FILL PASS

FIGURE 1.8
Spherical porosity.

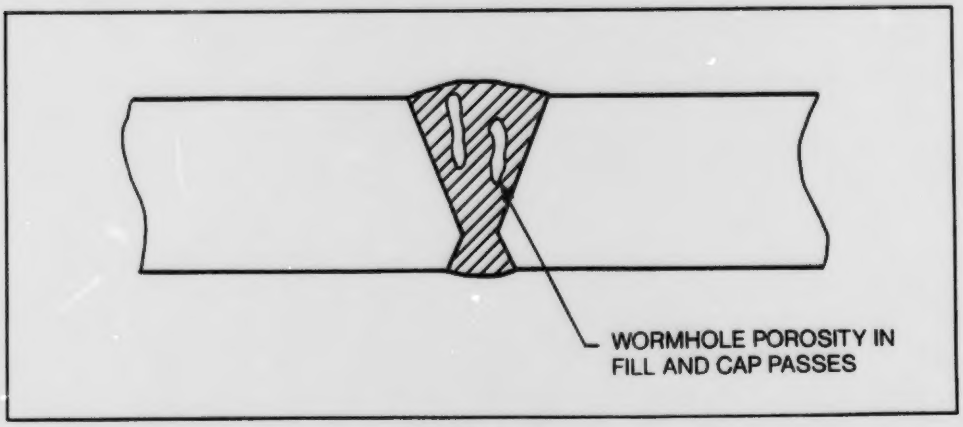
WORMHOLE POROSITY IN
FILL AND CAP PASSES

FIGURE 1.9
Piping of wormhole porosity.

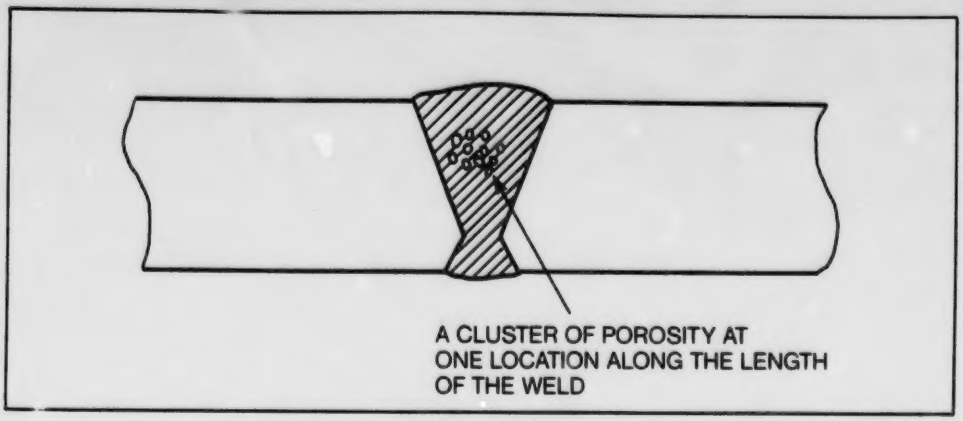
A CLUSTER OF POROSITY AT
ONE LOCATION ALONG THE LENGTH
OF THE WELD

FIGURE 1.10
Cluster porosity.

LOW COVER - A weld joint that has not been completely filled and the cap pass is below the pipe wall surface (Figure 1.11).

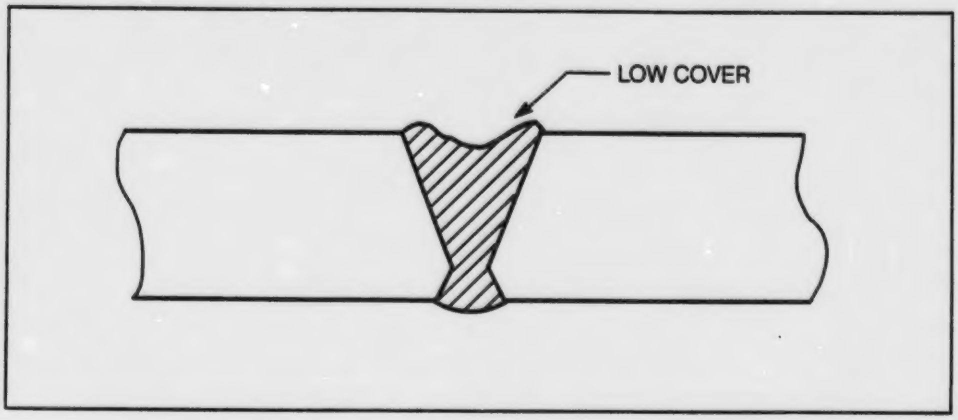

FIGURE 1.11
Low cover.

ARC BURN - A location where the welding electrode momentarily touched the pipe surface away from the weld joint (Figure 1.12).

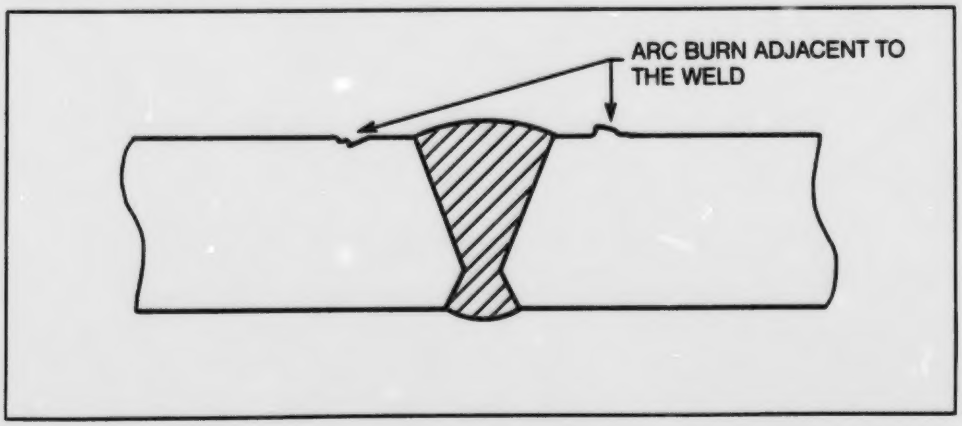
ARC BURN ADJACENT TO
THE WELD

FIGURE 1.12
Arc burn.

APPENDIX 2.0

PRODUCTION OF WELD DEFECTS

APPENDIX 2.0

1.0 INTRODUCTION

Welding techniques were developed whereby conventional mechanized gas metal arc welding procedures were modified to produce planar and non-planar weld imperfections for ultrasonic technique evaluations. Weld imperfections were designed to be a minimum of 3 mm apart in throughwall direction to ensure they were ultrasonically isolated (no two imperfections detectable by one ultrasonic beam) for identification purposes. Imperfection areas were categorized as; cap region, body region and root region as shown in Figure 2.1.

2.0 MATERIALS AND EQUIPMENT

Plate material representative of the high strength low alloy (HSLA) steels used in large diameter (>508 mm) gas pipeline construction was selected, see Table 2.1. Typical consumable chemistry is shown in Table 2.2.

Figure 2.2 shows the mechanized welding system which was used to simulate the CRC GMA pipeline welding procedure on flat plate. The system consisted of a variable speed travel carriage, track, oscillating head and a constant potential, variable current welding power source.

3.0 PROCEDURE DEVELOPMENT APPROACH

The gas metal arc welding process, in the short circuit mode of operation, is inherently very parameter sensitive. To achieve sound welds, arc parameters, voltage and circuit must be carefully balanced with mechanical parameters such as; travel speed, oscilliation speed and width, and torch angle. Isolated defects were produced in the appropriate region of each weld by upsetting this balance from existing qualified welding procedures. In general, when the welding system is operated on electrode positive with a constant potential power source and maintaining all other parameters constant, the following is observed:

- An increase in voltage will increase puddle fluidity.
- An increase in wire feed speed/amount will increase penetration.
- An increase in travel speed will reduce penetration.

Six, 10 mm thick plates and five, 20 mm thick plates were welded to produce both planar and non-planar defects. Table 2.3 shows a list of the defects which were attempted in each region of the weld with the procedures developed.

4.0 WELDING PROCEDURES

4.1 Root Region Defects

4.1.1 Lack of Sidewall Fusion

This defect was best manufactured using high travel speeds and low voltages. To maintain arc stability, wire-feed speed (current) was also reduced slightly. The combined effect of a moderate (15%) reduction in voltage and a more significant increase (56%) in travel speeds was used to ensure that the molten puddle would not wash and fuse into the joint sidewall thus producing lack of sidewall fusion. Welding parameters are shown in Table 2.4.

4.1.2 Lack of Cross Penetration

This defect occurs at the land portion of the joint bevel where the joint faces touch and was produced in a similar manner to that mentioned above. In addition, intentional arc misalignment from the center of the weld groove during the hot pass was used to assist in the production of this defect. Welding parameters are shown in Table 2.5.

4.1.3 Porosity

Porosity in the root pass was best achieved by limiting the shielding gas flow rate to less than 0.4 cubic feet per hour. This was the only parameter change for this defect. Welding parameters are shown in Table 2.6.

4.1.4 Crack

Internal root bead cracks were produced by using a damp 2.4 mm diameter SMA welding cellulosic electrode. The test plate was chilled to -18°C prior to welding and was allowed to cool to room temperature before the joint was completed using conventional mechanized GMA welding techniques. Welding parameters are shown in Table 2.7.

4.1.5 Undercut

This defect was also produced using a 2.4 mm diameter SMA cellulosic electrode. When producing undercut in the root it was necessary to weld the hot pass first to ensure the root pass does not burn through. A high voltage low current technique burns the bevel edges away producing the desireable weld defect. Welding parameters are shown in Table 2.8.

4.1.6 Burn Through

In the absence of the root bead, the hot pass will penetrate the inside of the pipe. In the area where burn through was desired, a grinder was used to open up the internal bevel, making the joint slightly wider with less land portion in the abutting area. Using a slower travel speed, with typical wire feed speeds and volts, the puddle was determined to easily burn through the thinned section. Welding parameters are shown in Table 2.9.

4.2 Body Region Defects

4.2.1 Lack of Sidewall Fusion

This was accomplished by focusing the contact tip towards one bevel and eliminating oscillation. This procedure concentrated the weld puddle on one side of the joint, so when the nect pass was deposited, lack of sidewall fusion was produced. Welding parameters are shown in Table 2.10.

4.2.2 Cold Lap

A lagging head angle of at least 15° cushioned the arc force penetration to the previous passes. Lowering the heat input (0.65 KJ/mm as compared to 0.85 KJ/mm for a normal fill pass) by reducing the wire feed speed and voltage also helped produce this defect. A grinder was used to reduce the hump in the weld pass produced, so the cap pass would not have an overly high mid point. Welding parameters are shown in Table 2.11.

4.2.3 Porosity

To ensure spherical porosity, shielding gas was limited to 0.7 cubic meters per hour. This was the only parameter change for this defect. Welding parameters are shown in Table 2.12.

4.3 Cap Region Defects

4.3.1 Lack of Sidewall Fusion

For this defect, the contact tip was positioned off the centerline of the joint and focused over either bevelled edge. This ensured that the molten puddle was deposited predominately to one side of the joint. Welding parameters are shown in Table 2.13.

4.3.2 Cold Lap

To produce this defect, primary consideration was given to the head angle. A lagging head angle of at least 15° must be used to help cushion the arc force, thus limiting penetration into the final fill pass. Low wire feed speed, voltage and slower travel, as recorded, are essential. Welding parameters are shown in Table 2.14.

4.3.3 Porosity

Porosity was achieved by limiting the shielding gas to less than 0.4 cubic meters per hour while maintaining proper welding parameters. Welding parameters are shown in Table 2.15.

4.3.4 Undercut

A reduction in wire feed speed and narrower oscillation width were used to produce this defect. A 4.0 mm diameter SMA welding cellulosic electrode was used to manufacture undercut. Welding parameters are shown in Table 2.16.

5.0 DISCUSSION

By careful control of the arc and mechanical parameters, weld defect were produced with a reasonable degree of consistency in the procedure development welds as determined by cross section of repeated welds. Lack of fusion and porosity defects were relatively easy to produce which is not surprising given they are the most predominant of the GMA weld imperfection types. Cracks in the root and shrinkage cavities in the body regions, however, could not be produced with the GMA welding process and were only achieved in the root region with SMA welding process with cellulosic electrodes. Similarily, the procedure for producing undercut in the root and cap regions required the use of the SMA welding process.

It was observed imperfections in welds produced using the procedures developed were typically larger than those produced during field welding. The production of imperfections of a more realistic size may have been possible, however, the effort to define that small window containing the parameters was not justified. The procedures developed did provide an effective method of obtaining all those GMA weld defects which do occur in the field, except a shrinkage cavity in the body region.

X-ray radiography inspection was used to confirm a minimum of one each of the defects listed in Table 2.3 had been produced in the six total 10 mm wall plates and five total 20 mm wall plates. Manual pulse echo shear wave ultrasonics was used particularily in the root region to confirm the presence of imperfections where radiography was known to experience difficulty in detection. No attempt was made to determine the throughwall location of the imperfections produced to assess if they were in neighbouring weld passes or ultrasonically isolated.

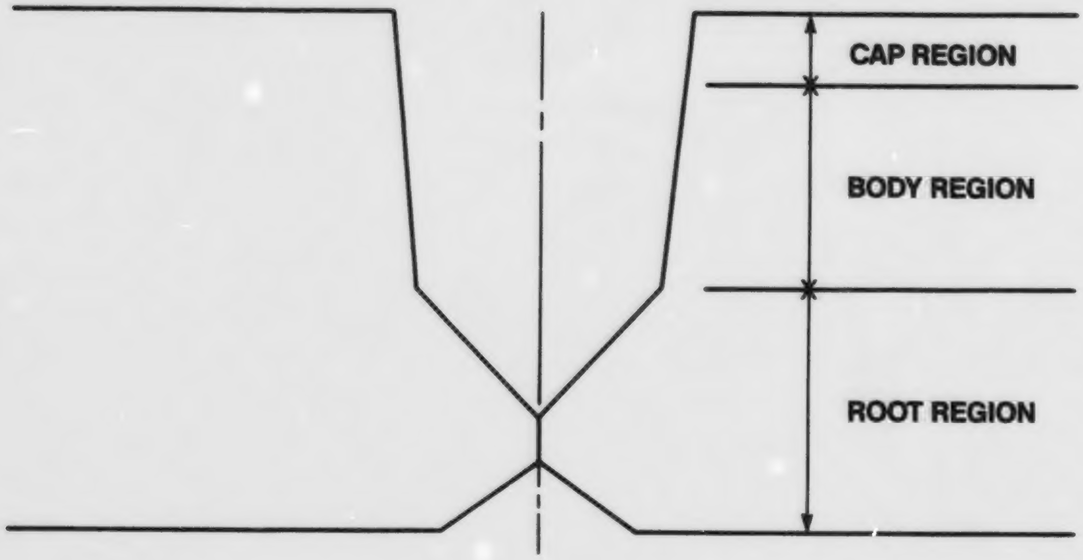
CAP REGION
BODY REGION
ROOT REGION

FIGURE 2.1

Weld Defect Regions

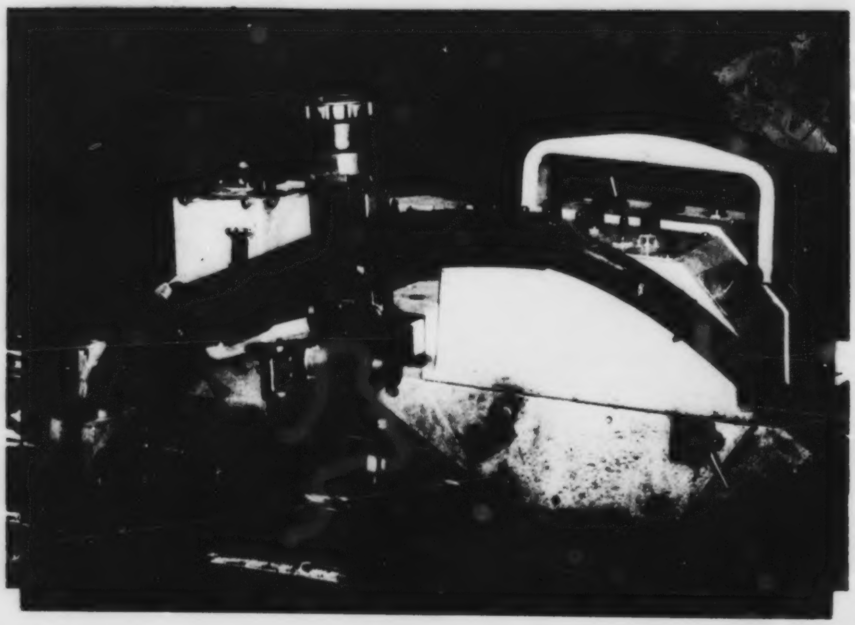

FIGURE 2.2

Mechanized welding system used to simulate the CRC gas metal arc welding process on flat plate.

TABLE 2.1

PLATE MATERIAL - CSA Z245.1 - 483 MPa

Thickness (mm)	C	Mn	P	S	Si	Cu	Ni	Cr	Mo	V	Cb
10	0.06	1.37	0.005	0.005	0.31	0.009	0.009	0.26	0.15	0.05	0.053
20	0.06	1.36	0.005	0.005	0.32	0.022	0.010	0.26	0.15	0.05	0.055

TABLE 2.2

TYPICAL CHEMICAL COMPOSITION - SFA-5.28

Consumable	C	Mn	Si	P	S	Ni	Mo	Cu	All Others
ER80S-D2	.07-.12	1.6-2.1	.5-.8	.025	.025	.15	.4-.6	.50	.50

TABLE 2.3

WELDING DEFECT SUMMARY

Root Region	Body Region	Cap Region
Lack of Sidewall Fusion	Lack of Sidewall Fusion	Lack of Sidewall Fusion
Lack of X-Penetration	Cold Lap	Cold Lap
Porosity	Porosity	Porosity
Crack		Undercut
Undercut		
Burn Through		

DETAILS OF TEST WELD

TABLE 2.4
MATERIAL: 10.00 mm W.T. x Gr. 414 MPa, Stelco Plate **DEFECT:** R_1(a) Lack of Side Wall Fusion

WELDING CONSUMABLE: Linde HI-84 ER 80S-D2 (0.9 mm Diameter)

RECORDED WELDING PARAMETERS

		ROOT (Internal)	HOT	FILL 1	CAP
Arc Speed mm/min		1000	1125	370	305
Wire Speed mm/min		8890	12700	10922	9652
Shielding Gas	Type	75% Ar 25% CO_2	100% CO_2	75% Ar 25% CO_2	75% Ar 25% CO_2
	Flow (cmh)	2.27	2.83	2.83	1.42
CTWD (mm)		6.35	8.89	12.7	7.92
Voltage		16.5	25.0	22.5	18.5
Amperage		190	250	225	205
Oscillation	Width (mm)	-	-	3	7
	Freq. (cpm)	-	-	150	150
Head Angle		0°	----	----	----

NOTE: CTWD - Contact Tip to Work Distance.
Electrical Characteristics - DC Reverse Polarity.
Preheat - 100° C.

DETAILS OF TEST WELD

TABLE 2.5

MATERIAL: 10.00 mm W.T. x Gr. 414 MPa, Stelco Plate **DEFECT:** R_1 (b) Lack of Cross Penetration

WELDING CONSUMABLE: Linde HI-84 ER 80S-D2 (0.9 mm Diameter)

RECORDED WELDING PARAMETERS

		ROOT (Internal)	HOT	FILL 1	CAP
Arc Speed mm/min		1000	1100	370	305
Wire Speed mm/min		8890	8890	10922	9652
Shielding Gas	Type	75% Ar 25% CO_2	100% CO_2	75% Ar 25% CO_2	75% Ar 25% CO_2
	Flow (cmh)	2.27	2.83	2.83	1.42
CTWD (mm)		6.35	8.89	12.7	7.92
Voltage		16.5	16.5	17.5	18.5
Amperage		190	190	205	205
Oscillation	Width (mm)	-	-	3	7
	Freq. (cpm)	-	-	150	150
Head Angle		0^o	----	----	----

NOTE: CTWD - Contact Tip to Work Distance.
Electrical Characteristics - DC Reverse Polarity.
Preheat - 100^o C.

DETAILS OF TEST WELD

TABLE 2.6

MATERIAL: 10.00 mm W.T. x Gr. 414 MPa, Stelco Plate **DEFECT:** R_2 Porosity

WELDING CONSUMABLE: Linde HI-84 ER 80S-D2 (0.9 mm Diameter)

RECORDED WELDING PARAMETERS

		ROOT (Internal)	HOT	FILL 1	CAP
Arc Speed mm/min		640	1125	370	305
Wire Speed mm/min		9652	12700	10922	9652
Shielding Gas	Type	75% Ar 25% CO_2	100% CO_2	75% Ar 25% CO_2	75% Ar 25% CO_2
	Flow (cmh)	$<$ 0.4	2.83	2.83	1.42
CTWD (mm)		6.35	8.89	12.7	7.92
Voltage		19.5	25.0	22.5	18.5
Amperage		205	250	225	205
Oscillation	Width (mm)	-	-	3	7
	Freq. (cpm)	-	-	150	150
Head Angle		0^o	----	----	----

NOTE: CTWD - Contact Tip to Work Distance.
Electrical Characteristics - DC Reverse Polarity.
Preheat - 100^o C.

DETAILS OF TEST WELD

TABLE 2.7

MATERIAL: 10.00 mm W.T. x Gr. 414 MPa, Stelco Plate **DEFECT:** R_3 Crack

WELDING CONSUMABLE: Linde HI-84 ER 80S-D2 (0.9 mm Diameter)

RECORDED WELDING PARAMETERS

		ROOT (Internal)	HOT	FILL 1	CAP
Arc Speed mm/min		205	1125	370	305
Wire Speed mm/min		-	12700	10922	9652
Shielding Gas	Type	-	100% CO_2	75% Ar 25% CO_2	75% Ar 25% CO_2
	Flow (cmh)	-	2.83	2.83	1.42
CTWD (mm)		-	8.89	12.7	7.92
Voltage		28.0	25.0	22.5	18.5
Amperage		85	250	225	205
Oscillation	Width (mm)	-	-	3	7
	Freq. (cpm)	-	-	150	150
Head Angle		0°	----	----	----

NOTE: CTWD - Contact Tip to Work Distance.
Electrical Characteristics DC Reverse Polarity.

DETAILS OF TEST WELD

TABLE 2.8
MATERIAL: 10.00 mm W.T. x Gr. 414 MPa, Stelco Plate DEFECT: R_4 Undercut

WELDING CONSUMABLE: Linde HI-84 ER 80S-D2 (0.9 mm Diameter)

RECORDED WELDING PARAMETERS

		ROOT (Internal)	HOT	FILL 1	CAP
Arc Speed mm/min		203	1125	370	305
Wire Speed mm/min		-	12700	10922	9652
Shielding Gas	Type	-	100% CO_2	75% Ar 25% CO_2	75% Ar 25% CO_2
	Flow (cmh)	-	2.83	2.83	1.42
CTWD (mm)		-	8.89	12.7	7.92
Voltage		28.0	25.0	22.5	18.5
Amperage		80	250	225	205
Oscillation	Width (mm)	-	-	3	7
	Freq. (cpm)	-	-	150	150
Head Angle		0°	----	----	----

NOTE: CTWD - Contact Tip to Work Distance.
Electrical Characteristics - DC Reverse Polarity.
Preheat - 100° C.

R_5

DETAILS OF TEST WELD

TABLE 2.9

MATERIAL: 10.00 mm W.T. x Gr. 414 MPa, Stelco Plate DEFECT: R_5 Burn Through

WELDING CONSUMABLE: Linde HI-84 ER 80S-D2 (0.9 mm Diameter)

RECORDED WELDING PARAMETERS

		ROOT (Internal)	HOT	FILL 1	CAP
Arc Speed mm/min		-	935	370	305
Wire Speed mm/min		-	12700	10922	9652
Shielding Gas	Type	-	100% CO_2	75% Ar 25% CO_2	75% Ar 25% CO_2
	Flow (cmh)	-	2.83	2.83	1.42
CTWD (mm)		-	8.89	12.7	7.92
Voltage		-	25.0	22.5	18.5
Amperage		-	250	225	205
Oscillation	Width (mm)	-	-	3	7
	Freq. (cpm)	-	-	150	150
Head Angle		0^{o}	----	----	----

NOTE: CTWD - Contact Tip to Work Distance.
Electrical Characteristics - DC Reverse Polarity.
Preheat - 100^{o} C.

DETAILS OF TEST WELD

B_1 (a)

TABLE 2.10

MATERIAL: 10.00 mm W.T. x Gr. 414 MPa, Stelco Plate **DEFECT:** B_1(a) Lack of Side Wall Fusion

WELDING CONSUMABLE: Linde HI-84 ER 80S-D2 (0.9 mm Diameter)

RECORDED WELDING PARAMETERS

		ROOT (Internal)	HOT	FILL 1	CAP
Arc Speed mm/min		640	1125	520	305
Wire Speed mm/min		9652	12700	10922	9652
Shielding Gas	Type	75% Ar 25% CO_2	100% CO_2	75% Ar 25% CO_2	75% Ar 25% CO_2
	Flow (cmh)	2.27	2.83	2.83	1.42
CTWD (mm)		6.35	8.89	12.7	7.92
Voltage		19.5	25.0	19.5	18.5
Amperage		205	250	250	205
Oscillation	Width (mm)	-	-	-	7
	Freq. (cpm)	-	-	-	150
Head Angle		0°	----	----	----

NOTE: CTWD - Contact Tip to Work Distance.
Electrical Characteristics - DC Reverse Polarity.
Preheat - 100° C.

DETAILS OF TEST WELD

TABLE 2.11

MATERIAL: 10.00 mm W.T. x Gr. 414 MPa, Stelco Plate **DEFECT:** B_1(b) Cold Lap

WELDING CONSUMABLE: Linde HI-84 ER 80S-D2 (0.9 mm Diameter)

RECORDED WELDING PARAMETERS

		ROOT (Internal)	HOT	FILL 1	CAP
Arc Speed mm/min		640	1125	100	305
Wire Speed mm/min		9652	12700	3810	9652
Shielding Gas	Type	75% Ar 25% CO_2	100% CO_2	75% Ar 25% CO_2	75% Ar 25% CO_2
	Flow (cmh)	2.27	2.83	2.83	1.42
CTWD (mm)		6.35	8.39	12.7	7.92
Voltage		19.5	25.0	14.5	18.5
Amperage		205	250	75	205
Oscillation	Width (mm)	-	-	3.5	7
	Freq. (cpm)	-	-	150	150
Head Angle		0°	----	15° Lag	----

NOTE: CTWD - Contact Tip to Work Distance.
Electrical Characteristics - DC Reverse Polarity.
Preheat - 100° C.

DETAILS OF TEST WELD

TABLE 2.12

MATERIAL: 10.00 mm W.T. x Gr. 414 MPa, Stelco Plate DEFECT: B_2 Porosity

WELDING CONSUMABLE: Linde HI-84 ER 80S-D2 (0.9 mm Diameter)

RECORDED WELDING PARAMETERS

		ROOT (Internal)	HOT	FILL 1	CAP
Arc Speed mm/min		640	1125	370	305
Wire Speed mm/min		9652	12700	10922	9652
Shielding Gas	Type	75% Ar 25% CO_2	100% CO_2	75% Ar 25% CO_2	75% Ar 25% CO_2
	Flow (cmh)	2.27	2.83	< 0.7	1.42
CTWD (mm)		6.35	8.89	12.7	7.92
Voltage		19.5	25.0	22.5	18.5
Amperage		205	250	225	205
Oscillation	Width (mm)	-	-	3	7
	Freq. (cpm)	-	-	150	150
Head Angle		0°	----	----	----

NOTE: CTWD - Contact Tip to Work Distance.
Electrical Characteristics - DC Reverse Polarity.
Preheat - 100° C.

DETAILS OF TEST WELD

$_1$ (a)

TABLE 2.13

MATERIAL: 10.00 mm W.T. x Gr. 414 MPa, Stelco Plate DEFECT: C_1 (a) Lack of Side Wall Fusion

WELDING CONSUMABLE: Linde HI-84 ER 80S-D2 (0.9 mm Diameter)

RECORDED WELDING PARAMETERS

		ROOT (Internal)	HOT	FILL 1	CAP
Arc Speed mm/min		640	1125	370	305
Wire Speed mm/min		9652	12700	10922	9652
Shielding Gas	Type	75% Ar 25% CO_2	100% CO_2	75% Ar 25% CO_2	75% Ar 25% CO_2
	Flow (cmh)	2.27	2.83	2.83	1.42
CTWD (mm)		6.35	8.89	12.7	7.92
Voltage		19.5	25.0	22.5	18.5
Amperage		205	250	225	205
Oscillation	Width (mm)	-	-	3	-
	Freq. (cpm)	-	-	150	-
Head Angle		0°	----	----	----

NOTE: CTWD - Contact Tip to Work Distance.
Electrical Characteristics - DC Reverse Polarity.
Preheat - 100° C.

DETAILS OF TEST WELD

TABLE 2.14

MATERIAL: 10.00 mm W.T. x Gr. 414 MPa, Stelco Plate DEFECT: C_1(b) Cold Lap

WELDING CONSUMABLE: Linde HI-84 ER 80S-D2 (0.9 mm Diameter)

RECORDED WELDING PARAMETERS

		ROOT (Internal)	HOT	FILL 1	CAP
Arc Speed mm/min		640	1125	370	125
Wire Speed mm/min		9652	12700	10922	4000
Shielding Gas	Type	75% Ar 25% CO_2	100% CO_2	75% Ar 25% CO_2	75% Ar 25% CO_2
	Flow (cmh)	2.27	2.83	2.83	1.42
CTWD (mm)		6.35	8.89	12.7	7.92
Voltage		19.5	25.0	22.5	15.5
Amperage		205	250	225	90
Oscillation	Width (mm)	-	-		
	Freq. (cpm)	-	-	150	150
Head Angle		0°	----	----	15° Lag

NOTE: CTWD - Contact Tip to Work Distance.
Electrical Characteristics - DC Reverse Polarity.
Preheat - 100° C.

C_2

DETAILS OF TEST WELD

TABLE 2.15

MATERIAL: 10.00 mm W.T. x Gr. 414 MPa, Stelco Plate DEFECT: C_2 Porosity

WELDING CONSUMABLE: Linde HI-84 ER 80S-D2 (0.9 mm Diameter)

RECORDED WELDING PARAMETERS

		ROOT (Internal)	HOT	FILL 1	CAP
Arc Speed mm/min		640	1125	370	305
Wire Speed mm/min		9652	12700	10922	9652
Shielding Gas	Type	75% Ar 25% CO_2	100% CO_2	75% Ar 25% CO_2	75% Ar 25% CO_2
	Flow (cmh)	2.27	2.83	2.83	$<$0.4
CTWD (mm)		6.35	8.89	12.7	7.92
Voltage		19.5	25.0	22.5	18.5
Amperage		205	250	225	205
Oscillation	Width (mm)	-	-	3	7
	Freq. (cpm)	-	-	150	150
Head Angle		0°	----	----	----

NOTE: CTWD - Contact Tip to Work Distance.
Electrical Characteristics - DC Reverse Polarity.
Preheat - 100° C.

DETAILS OF TEST WELD

TABLE 2.16

MATERIAL: 10.00 mm W.T. x Gr. 414 MPa, Stelco Plate **DEFECT:** C_3 Undercut

WELDING CONSUMABLE: Linde HI-84 ER 80S-D2 (0.9 mm Diameter)

RECORDED WELDING PARAMETERS

		ROOT (Internal)	HOT	FILL 1	CAP
Arc Speed mm/min		640	1125	370	305
Wire Speed mm/min		9652	12700	10922	8890
Shielding Gas	Type	75% Ar 25% CO_2	100% CO_2	75% Ar 25% CO_2	75% Ar 25% CO_2
	Flow (cmh)	2.27	2.83	2.83	1.42
CTWD (mm)		6.35	8.89	12.7	7.92
Voltage		19.5	25.0	22.5	18.5
Amperage		205	250	225	190
Oscillation	Width (mm)	-	-	3	3.5
	Freq. (cpm)	-	-	150	150
Head Angle		0°	----	----	----

NOTE: CTWD - Contact Tip to Work Distance.
Electrical Characteristics - DC Reverse Polarity.
Preheat - 100° C.

Volume

2

2

EVALUATION OF A UNIQUE CREEPING WAVE PROBE FOR EXAMINATION OF THE CAP REGION IN PIPELINE GIRTH WELDS

PART 2:

FINAL REPORT BY:

M.P. Fingerhut
A.G. Glover
D.V. Dorling

WORK ON THIS PROJECT WAS JOINTLY FUNDED BY NOVA CORPORATION OF ALBERTA AND THE PHYSICAL METALLURGY RESEARCH LABORATORIES, CANADA CENTRE FOR MINERAL AND ENERGY TECHNOLOGY, ENERGY MINES AND RESOURCES CANADA.

DSS FILE NUMBER: 23SQ-23340-2-9027-4
DSS CONTRACT SERIAL NUMBER: 0SQ82-00244
CANMET SCIENTIFIC AUTHORITY: DR. D.K. MAK

Report # 15047

October, 1988

65pp

MICROMEDIA

TABLE OF CONTENTS

PAGE

1.0 SUMMARY 1

2.0 CONCLUSIONS 2

3.0 RECOMMENDATIONS 3

4.0 INTRODUCTION 4

5.0 INSPECTION CRITERIA AND PROBE DEVELOPMENT 5

6.0 TRANSDUCER PERFORMANCE 8

- 6.1 Signal to Noise 8
- 6.2 Signal to Electronic Noise 9
- 6.3 Focus Position 9
- 6.4 Working Range 10
- 6.5 Beam Angle 10
- 6.6 Side Lobes 11
- 6.7 Index Point 11
- 6.8 Horizontal Beam Width 12

7.0 DEFECT DETECTION TEST EQUIPMENT AND MATERIALS 13

- 7.1 Equipment 13
- 7.2 Test Plates 14
  - 7.2.1 Machined Reflectors 14
  - 7.2.2 Weld Defect Plates 14

8.0 EXPERIMENTAL PROCEDURE 15

- 8.1 Instrument Settings 15
- 8.2 Testing Procedures 16
  - 8.2.1 Tests on Simulated Weld Defect Plates 16
  - 8.2.2 Tests on Real Weld Defect Plates 17

9.0 RESULTS AND ANALYSIS 18

- 9.1 Performance on Simulated Defects 18
- 9.2 Diffraction Effects 19
- 9.3 Performance on Real Weld Defects 20
  - 9.3.1 Sensitivity 20
  - 9.3.2 Detection Gate 23

10.0 DISCUSSION 25

REFERENCES
TABLES
FIGURES
APPENDIX

1.0 SUMMARY

This work is part of a program aimed at developing an ultrasonic inspection design for the nondestructive evaluation of pipeline girth welds made by the mechanized gas metal arc (GMA) welding process for onshore and offshore pipeline construction.

The earlier phases of the program demonstrated that focused probes in the pulse-echo mode are suitable for examination of the root region of the weld and that alternative approaches are required for examination of the remainder. The feasibility of using creeping waves for examination of the cap region was investigated and, as a result, a specification for an experimental creeping wave transducer developed(1). A probe was designed to this specification by Bundesanstalt fur Materialprufung (BAM) and built by Rontgen Technische Dienst (RTD). This report describes the work carried out to evaluate the performance of this experimental creeping wave transducer with respect to its ability to examine the cap region of mechanized GMAW welds in 9.5 mm material.

Evaluation of the experimental probe was carried out on simulated and real weld defects. The results showed that the probe achieved good detection performance not only in the cap region but also in the body regions of the 9.5 mm thick test plates. In addition some potential for detection of root region defects was demonstrated.

2.0 CONCLUSIONS

2.1 The unique creeping wave probe designed by BAM to NOVA's specification provides a beam oriented near perpendicular to expected defects in the cap region of the weld and was successful in detecting planar lack of sidewall fusion welding defects in this region with a signal-to-noise of greater than 12dB.

2.2 The creeping wave probe demonstrated good detection capability to the required depth of 3.4 mm from the plate surface with the ability to detect defects to a depth of 4.2 mm from the plate surface.

This indicates maximum pipe wall thicknesses of 10.9 mm may be satisfactorily examined before additional probes are required, assuming complete coverage in the root region is provided by other probes.

2.3 The creeping wave probe not only performed well in the detection of real weld defects in the cap region for which it was intended, but also showed potential for detecting and discriminating some planar defects in the root region.

3.0 RECOMMENDATIONS

3.1 Evaluate the performance of the creeping wave probe on the inspection of the cap region full scale welds for field application.

3.2 Determine the maximum pipe wall thickness which can be reliably examined with the creeping wave probe before additional probes are required.

3.3 Evaluate the application of creeping wave technology to investigate other surface breaking defects.

3.4 Evaluate the potential application of creeping wave technology to discriminate root region defects.

4.0 INTRODUCTION

It was shown in the earlier phases of this program that detection of planar (lack of fusion) type defects in the cap region of mechanized gas metal arc welds of the type produced by the CRC-Evans Automatic Welding system is unreliable(1) when using focused ultrasonic shear waves. Preliminary analysis also showed that ultrasonic probes using creeping waves with associated high-angle compression waves had a good potential for detecting these defects in the cap region. Creeping waves have the ability to travel parallel to the plate surface, as illustrated in Figure 1, uninterrupted by the weld cap reinforcement, weld spatter or other features that may exist on top of the pipe surface(2). The near-normal orientation of the creeping wave to the weld preparation in the cap region makes it particularly well suited for the detection of planar lack of fusion type defects.

In the previous work it was determined that, while these production creeping wave probes demonstrated good potential for cap pass defect detection, their large beam size produced indications from the root region which were not easily discriminated from those in the cap region of the weld. Success of this probe type would therefore depend largely on developing a design which will produce a beam depth of about 3 mm for inspection of the cap region of the weld, defined as plane E in Figure 2. A specification to meet this requirement was developed and this report describes the evaluation of the defect detection capabilities of a creeping wave probe designed and built to those specifications.

5.0 INSPECTION CRITERIA AND PROBE DEVELOPMENT

A reliable technique to detect defects anywhere in the weld should provide a signal-to-noise ratio of greater than 12dB for all defects larger than 1.0 mm in depth. The goal of a minimum value of 12dB signal-to-noise response was chosen so that a detection threshold level could be set which would not critically affect the inspection results. The value of 1.0 mm was chosen based on engineering critical assessments which showed that these depths of defects are tolerable regardless of length. The assessments assumed a weld crack tip opening displacement (CTOD) toughness of 0.1 mm, an applied strain of 0.5% and a pipe wall thickness of 10 mm, and indicated a surface defect 2.0 mm deep was tolerable for a complete pipe circumference. In order to take into account any variation in toughness the tolerable depth was reduced to 1.0 mm and is the limit below which defect detection performance is unnecessary.

As shown in Figure 1, creeping wave probes generate an envelope of compressional waves with a main compressional angle in the range of 75° to 79° depending on the size of the crystal(3). The benefit of the creeping wave is that it follows the surface and is not affected by weld spatter, surplus couplant or a change of geometry, such as a weld toe(2). Beneath the surface range of the creeping wave, the probes are no longer highly sensitive and responses may be observed from reflectors deep in the test piece as a result of the large compressional beam size. In 20 mm wall pipe this may not be a problem as detection gates could be used to differentiate between different regions. In 10 mm wall, however, the difference in path distance to a defect in the cap region and one in the root is only 3 mm (Figure 3) and it was found that detection gates could not be used effectively for discrimination of defects in the cap region from in the root region of the weld.

In addition to the compressional waves, continuous generation of shear waves at about 33° occur by mode conversion of the compression wave (Figure 1) and, as a result, the creeping waves have a steep energy decay and can only exist for short distance along the surface(4-5). It was anticipated, therefore, that interference from the weld cap may give limited surface positioning capabilities to these standard probes, and restrict the detection of lack of side wall defects immediately beneath the weld cap.

In order to overcome the likely problems resulting from excessive sensitivity of the large beam size, and weld cap interference, a specialized inspection probe was designed based on the specifications developed earlier and given in Table 1. These requirements are a result of measurements carried out during the preliminary investigation(1), and an evaluation by Battelle Pacific Northwest Laboratories (PNL) of five different creeping wave probes(6). The focus design results from a requirement to achieve a signal-to-noise ratio of 12dB and be able to inspect lack of fusion defects beneath the weld cap.

Table 1 also specifies a "working range", which is defined as the region along the beam path and about the focus of the beam where the echo amplitude has decreased by 50% (6dB). This working range is required to minimize the effect of minor variations in path distance to a defect. Working range limits starting at 2 mm and ending at 7 mm, measured horizontally in front of the probe, were determined based on those possible defect locations and probe positions relative to the edge of the weld preparation, as shown in Figure 4.

A creeping wave probe design to meet these specifications was carried out by BAM of West Germany starting in December 1986. Once designed, the probe was built by RTD of Holland and delivered to NOVA in July 1987.

6.0 TRANSDUCER PERFORMANCE

The creeping wave probe was identified as RTD-BAM 87-276 and can be simply described as a dual crystal (two 3.6 mm x 10.7 mm crystals), one to transmit - the other to receive, with a nominal frequency of 8 megahertz.

Assessment of the creeping wave probe was carried out to determine its characteristics and, in particular, its signal-to-noise ratios, focus position, working range and horizontal beam width, and to compare these with the design requirements. Probe assessment was based on tests described in NOVA Specification SUT-2 "Performance Specification for Medium Frequency, Shear Wave Angle Probes", given in Appendix 1. While this specification was clearly not intended for the detailed assessment of creeping wave probes, many of the test procedures are still relevant.

Figure 5 shows the design of the test plate used to assess the performance of this probe. The plate is ASME A516 Grade 70 normalized steel and hasa wall thickness of 9.5 mm. All the 1 mm diameter side drilled holes were produced by high speed drilling to provide a smooth and consistent hole surface finish, and spaced at intervals of 0.7 mm, 1.2, 1.7, 2.2, 2.7, 3.2, 3.7, 4.2, and 5.0 mm from the surface.

6.1 Signal to Noise

Signal-to-noise ratio is of particular importance as it is used as the basis for establishing the defect detection threshold. Signal and noise levels were assessed using the method in SUT-2 on the A516 Grade 70N test plate. The results are shown in Figure 6 and indicate a 36dB signal-to-noise difference at the design path distance of 12 mm. The design path total distance from the probe index to the weld preparation measured on the plate surface is 12 mm and was determined by summing dimensions a, b and c in Figure 7. This result is well in excess of the minimum 12dB specified for defect detection.

6.2 Signal To Electronic Noise

Electronic noise was also measured according to the method provided in SUT-2. Figure 6 shows a 45dB difference between the signal and electronic noise at the target path and exceeds the minimum of 40dB specified in SUT-2.

6.3 Focus Position

The Focus Position is that location along the beam path where the maximum echo-amplitude is measured. It was determined from measurements on 1.0 mm diameter side-drilled holes and found to be located at 5 mm horizontally in front of the probe contact surface and 3.2 mm below the test piece surface (with an accuracy of ±0.1 mm). While the focus position is within the specified horizontal range of 2 to 7 mm, it is slightly beyond the 0 to 3 mm vertical range specified. Nevertheless the slightly larger than specified maximum vertical distance to the focus was considered acceptable; the increase of 0.2 mm was not expected to result in a significantly higher sensitivity in the neighboring body region of the weld.

6.4 Working Range

The working range is of particular importance and was specified to accommodate anticipated variations in target path distance and to provide high sensitivity in the cap region of the weld only. The same techniques used to establish the focus position were used to establish the working range.

Figure 8 shows the specified and measured working ranges. The working range, measured horizontally as beginning at 0.5 mm and ending at 11 mm in front of the probe, clearly satisfies the minimum range requirements of 2 to 7 mm. The vertical range of 1 mm to 4.2 mm, however, exceeded the maximum specified and indicates a possible lack of sensitivity at the inspection surface (see Figure 8). While those echo responses measured near the inspection surface were less than 50% (6dB) of the echo measured at the focus, they were well above the targeted minimum signal-to-noise level of 12dB; hence, these lower responses are not expected to result in missed defects during an inspection. Based on the larger-than-specified vertical range, good detectability would be expected to a depth of at least 4.2 mm from the inspection surface.

6.5 Beam Angle

The creeping wave beam is known to travel along the plate surface, therefore its angle need not be measured. The main beam angle of the compression wave directly beneath the creeping wave, which performs much of the inspection in the cap region of the weld, was determined by maximizing the echo from a side-drilled hole which was 3.2 mm from the plate surface to the hole center. A refracted beam angle of 74° was calculated from the inspection geometry which is 0.5° less than that measured by RTD, the probe manufacturer.

The largest possible beam angle from the plate normal is clearly most desirable for examination of the cap region as this would have the envelope of compression waves positioned closest to the plate surface. While a larger beam angle may have been possible through the use of a larger piezoelectric crystal, this would have resulted in a probe to horizontal focus position much shorter than that specified to achieve targeted minimum signal-to-noise levels.

6.6 Side Lobes

Large amplitude side lobes to the main compression envelope effectively increase the through-wall size of the beam, which can result in the problem of false defect indications. Side lobe measurements were taken from the echo amplitude record produced from a series of 1.0 mm diameter side-drilled holes and the results shown in Figure 8, indicating that the echo signal rises and falls smoothly confirming that no side lobes are present.

6.7 Index Point

The index point was assumed to be accurate as marked on the probe housing at 6 mm from the front of the contact face. Measurements to confirm the index points could not be carried out by using a standard IIW calibration block as special devices are required.

6.8 Horizontal Beam Width

The horizontal beam width is that portion of the beam where the echo amplitude has decreased to 50% (6dB) of the maximum amplitude. This was determined from the record produced when scanning the beam across a 1.0 mm through-drilled hole. The probe index to hole distance was 12 mm representing typically the distance to a lack of sidewall fusion defect (Figure 7). A horizontal beam width of 3.0 mm was measured which is in accordance with that beam width specified in Table 1.

A beam width of no greater than 3 mm is required to ensure reasonable accuracy in measuring defect length.

7.0 DEFECT DETECTION TEST EQUIPMENT AND MATERIALS

7.1 Test Equipment

A probe testing system was set up consisting of the ultrasonic instrument with an x-y scanner, and an x-y plotter (Figure 9). The ultrasonic instrument was a Masterscan model UFD 310 manufactured by Balteau - Sonatest. The instrument provided a broad band (0.5-18MHz) 100dB dynamic range amplifier and was used to control the echo signal (amplitude) on the display screen. Screen horizontal and vertical linearity were established to be within 5% of full screen according to ASTM E317-79. The time base was calibrated using the IIW type 1 block to provide a resolution of 0.1 mm. Using a Hewlett-Packard model 7046 x-y recorder the analog output of the gated signal amplitude was recorded on channel 1 (vertical axis) which was calibrated to indicate echo amplitude to an accuracy of 2%. The analog output of the path distance (probe index to defect) was recorded on channel 2 (vertical axis) to an accuracy of 1.5%.

The x-y scanner leased from Atomic Energy of Canada Ltd. was used to control transducer movement and provide an analog signal corresponding to the distance traveled by the probe, which was recorded on the horizontal axis of the recorder. Position was indicated to an accuracy of 1 mm. Figure 10 is an example of the output of the analog readings and shows the echo amplitude and beam path distance displayed as a function of distance travelled by the probe on a plate containing machined reflectors.

7.2 Test Plates

Two types of test plates were used, one containing machined holes and notches and the other containing real weld defects.

7.2.1 Machined Reflectors

The design of the 10 mm thick test plate containing machined notches and holes to simulate lack of fusion defects is shown in Figure 11.

7.2.2 Weld Defect Plates

Welded test panels in 9.5 mm thick plates were designed to contain three typical GMA weld defects which occur in the weld cap and body region; incomplete fusion due to cold lap between the weld metal and parent metal (lack of sidewall fusion), incomplete fusion due to cold lap between adjacent weld passes (lack of interrun fusion), and external undercut. The location of the manufactured three weld defect types is shown schematically in Figure 12. The welds were designed such that the detection capability in the cap region of the weld could be evaluated. Weld geometry conditions such as high-low were not expected to present a problem for the creeping wave probe and hence were not included in the test program.

8.0 EXPERIMENTAL PROCEDURE

8.1 Instrument Settings

All tests were carried out at fixed ultrasonic instrument settings given in Table 2 for both simulated and real weld defect plates. The instrument gain level of 60dB was established to produce a 100% full screen echo on the 1.0 mm deep O.D. surface notch in the simulated weld defect plate shown in Figure 11 at a creeping wave path distance of 10 mm. This reflector and path produces the highest echo response and ensured that the instrument recording limits were not exceeded during testing.

For testing of the plate with simulated weld defects, the detection gate position and width were set, using the calibrated time base, so that the gated region began at a position 2 mm before the creeping wave intersected the plate O.D. surface notch, at the shortest test path distance, and ended 2 mm after the compression wave lobe intersected the I.D. surface notch at the longest test path distance. This 12 mm wide gate is illustrated in Figure 13 and was used to ensure that a measureable echo response from any of the simulated defects would not be missed during testing.

The narrower 4.8 mm gate shown in Figure 13 was used during testing of the welded test plates, which would ensure detection of defects in the cap and upper body regions only and eliminate any problems arising from the root region. The gate began 2 mm before the creeping wave intersected the inspection plane and ended where the creeping wave intersected the centerline of the weld as illustrated in Figure 13.

A recording threshold of 10% of full screen was used and represents a level of 12dB above the noise level measured according to the procedure provided in appendix 2. A threshold level of 12dB was determined during previous work to be a practical level for selected probes which would ensure the detection of real defects and avoid false indications(1).

In all tests, a wide band frequency instrument setting was used. No rejection was used to suppress noise levels. The required probe delay length was determined based on a known probe index-to-surface reflector distance. An instrument time base range of 20 mm was used to maximize path distance measuring accuracy.

8.2 Testing Procedure

Tests were carried out initially on the simulated weld defect plate to establish a basis for these instrument settings described above and to determine the probe positioning for the welded test panels.

8.2.1 Tests on Simulated Weld Defect Plate

A total of five tests were carried out on this plate beginning with the probe index-to-plate O.D. surface notch of 10 mm. In each subsequent test the probe index-to-surface notch distance was increased by one millimeter. The design index-to-notch distance was 12 mm and each shorter and longer distance represented a possible probe position error.

The x-y scanner was used to control the probe movement during each test after the initial probe position had been established. The positioning accuracy in each dimension was ± 0.5 mm. Maximum scanning speed was 4.2 mm /sec.

Echo response and path distance data were obtained from the analog recordings produced during each test using the equipment described in section 7.0.

8.2.2 Tests on Real Weld Defect Plates

A total of five 9.5 mm thick plates were examined. Each plate was examined once at the design index-to-weld inspection plane distance of 12 mm. A total of 19 locations were selected for metallographic cross-sectioning to verify the presence and size of the weld defects detected.

9.0 RESULTS AND ANALYSIS

The most significant measure of detection performance is considered to be the signal-to-noise ratio. A large signal-to-noise ratio is required to ensure reliable detection of defects.

The noise level used to determine the signal-to-noise ratio was that measured during the probe evaluation (Section 6.1) although it was realised that this may be somewhat different from a real weld. The signal level was determined from the analog recordings. The maximum signal amplitude measured was used to calculate signal-to-noise results for the simulated weld defects. The amplitude at selected locations on the analog recordings were used to determine results on the welded test panels. Weld cross-sectioning at the selected locations verified the presence and size of each defect.

9.1 Performance on Simulated Defects

The results shown in Figure 14 indicate high signal-to-noise levels through the plate thickness. In all but one case (defect C_1 simulating a lack of fusion defect in the hot pass, with a probe index to surface notch distance of 14 mm), signal-to-noise levels were well above the goal of 12dB. Based on these results, the creeping wave probe could be expected to provide satisfactory detection of planar defects in the fill and cap regions of a 10 mm thick GMA weld, and could even be used for the root region.

The results also indicate that if required there is an optimum probe position for examination of plane A of Figure 2 where the signal-to-noise is the highest. It would, therefore, appear feasible to monitor inspection planes A and E in the 9.5 mm W.T. with the creeping wave probes.

9.2 Diffraction Effects in Simulated Defects

During the examination of the simulated defects it was noted that the measured path distances to reflectors C_1, C_2, D_1 and E_1 indicated a longer path than would be expected if the echo returned along the same path as the incident beam. The path distances indicated by measured time-to-echo correlate well with the wave path shown in Figure 15 as discussed in reference 8. The path ABCDA assumes the incident compression wave to be diffracted at the bottom edge of the flat-bottomed hole reflector (B), at the top edge (C) and again at the plate surface (D) resulting in a wave returning to the probe along the plate surface. Table 3 shows measured path distances to be very close to those calculated according to the path ABCDA and within measurement error.Whilst this analysis may be true for simulated defects, buried real weld defects may not behave in the same way because point D (Figure 15) would no longer exist for a weld with the cap in place.

9.3 Performance On Real Weld Defects

9.3.1 Sensitivity

The analysis which was carried out to assess probe detection performance on real weld defects related the signal-to-noise level to the projected through-wall depth of the weld defects. Projected depths were determined from the metallographic cross-sections at selected locations.

Figure 16 shows the signal-to-noise level associated with the measured projected depth for each cross section location. The vertical and horizontal lines in the figure represent the probe performance goals specified. The vertical line at 1.0 mm represents the minimum size to be detected and the horizontal line at 12dB the detection threshold. The figure indicates that in all cases the presence of a lack of fusion defect greater than 1.0 mm in projected through wall depth resulted in a signal-to-noise level above 12dB, demonstrating satisfactory detection performance.

Also shown in the figure are the results of two cross sections which indicate that, at locations where no defect indication was recorded, no defects exist. In two cases, however, cross-sections were made at defect indication locations and no defect was found. In one case, the defect indication length based on a 6dB drop sizing technique was estimated to be 3 mm long. The same length of indication was recorded when measuring the horizontal beam width using a 1.0 mm diameter through drilled hole; a 1 mm long defect could have been removed during cross-sectioning of the sample.

In the second case, the cross-section is believed to have been made at a location where there was no defect and the defect indication was an integrated echo response from two adjacent defects. Sections made of one of the two adjacent indications confirmed the presence of a defect.

Undercutting defects were detected by the creeping wave probe, however, only in relatively few instances did they produce recordable indications (greater than the 12dB threshold level). One undercutting defect cross-sectioned at a location with a signal-to-noise level of 8dB was measured to be only 0.2 mm in depth. Recording of these shallow defects would require the use of lower threshold levels however defects less than 0.5 mm are acceptable regardless of length and hence changes in threshold levels are not required. Confirmation of this imperfection is commonly done by visual examination in the field.

All defects examined in the gated portion of the cap region of the weld produced recordable signal-to-noise levels of greater than 12dB and the results are shown in Figure 17. Each bar indicates the position of the defect from the plate surface and its projected through-wall depth. The boxed area indicates that portion of the weld where the maximum detection sensitivity was observed. Contained within the box is the top of the defect closest to the weld plate surface and the top of the one furthest from the weld plate surface and this represents a conservative estimate of the detection capability of the probe.

Figure 18 shows the defect represented by the bar labeled A in Figure 17. This defect was 1.2 mm in projected depth (greater than the 1.0 mm minimum) with its tip 3.4 mm from the plate surface, producing a signal-to-noise level of 27.2dB, and indicates detection of significant defects below plane E is possible with the creeping wave probe. These results are consistent with those determined on the simulated weld defects and with probe performance testing, which indicated detection capabilities at 4.2 mm from the plate surface.

Figure 19 shows the defect represented by the bar labelled B in Figure 17. This defect was less than 1 mm in projected depth and 0.6 mm from the plate surface and yet still provided a very large signal-to-noise level of 30.5dB. This indicates very good sensitivity near the inspection surface and is consistent with the high signal-to-noise level observed on the surface notch of the simulated weld defect plate (Figure 14, reflector E_2).

Figure 20 shows the defect represented by the bar labelled C in Figure 17. This crack, rare in this type of weld, was less than 1 mm in projected depth and 1.5 mm from the plate surface and provided a large signal-to-noise level of 22.5dB. This defect lies approximately 1 mm past the defined limits of inspection plane E toward the weld centerline, and indicates increased detection capability within the cap volume if required and not only at the inspection plane. This defect was detected experimentally because the complete inspection volume was displayed for these tests rather than just the gated region. This enhanced capability is also shown in Figure 21 which shows a defect detected on the inspection plane opposite to the one being examined. The defect has a projected depth of 0.6 mm and is 2.0 mm from the plate surface and produced a signal-to-noise level of 24.0dB at a path distance of 18.5 mm or 3.5 mm past the end of the specified detection gate.

9.3.2 Detection Gate

In addition to achieving satisfactory signal-to-noise values above a detection threshold level, it is necessary to position the detection gate to ensure defects will not be missed. The analysis used to determine the required detection-gate size relates the measured path distance at defect locations to the distance to the end-of-the-gate (see Figure 22). A defect to end-of-gate distance of at least 1 mm is required to ensure no errors arise from the tolerance of the probe positioning or from weld scanner tracking error during pipe weld inspection. A defect to end-of-gate distance of no greater than 2 mm is required to ensure that the possibility of false defect indications is eliminated.

The results of some of the inspection on the five test welds are shown in Table 4 which compares the defect distance to the end-of-gate path distance. Welds 2 and 3 indicate this path difference distance to be 2.8 and 3.3 mm respectively and for weld 5, 1.6 mm. These variables could therefore be further optimized to achieve the minimum 1.0 mm defect-to-end of gate tolerance. A similar analysis to assess the potential for false indications from the root region of the weld would also have to be carried out to ensure that the correct detection gate was specified as a function of wall thickness.

10.0 DISCUSSION

Inspection results indicate that the creeping wave probe design provided good detection performance of planar lack of fusion defects and freedom from false indications in the cap region of the weld. This performance was achieved even with a slightly larger beam size than was specified for the examination of plane E (cap region). The larger beam size, however, did result in a demonstrated defect detection capability on real defects to a depth of at least 3.4 mm. The results from simulated defects indicated detection at the required signal-to-noise level to a depth of 4.2 mm. The larger the region of satisfactory detection performance possible with this cap region probe, the larger the maximum pipe wall thickness which can be examined before additional body region probes are required. An increase in the creeping wave depth detection capabilities from 3.0 to 4.2 mm means that the maximum pipe wall-thickness which can be examined using only creeping wave and root region increases probes from 9.7 mm to 10.9 mm. A definitive maximum pipe wall-thickness will be determined during the final full scale pipe weld testing phase of the program.

The larger than specified beam size was the result of a compromise in the probe specification during its design. Smaller piezoelectric crystals were used to achieve the horizontal focus position requirements at the expense of the vertical focus position and working range requirements(9). These changes were made so that the difference in path distance from the probe index to the root and cap region of the weld in 10 mm (thin) wall material could be maximized. This meant that electronic gating could be used effectively to ensure the absence of possible root region indications; a feature that was not possible with the earlier probe designs. Tests on the simulated weld defect plate showed that at least 2.0 mm existed between the end of the detection gate and the position at which root defects could occur.

The results from the simulated tests weld defects tests also indicated that there may be an opportunity to discriminate between defects in both cap (plane E) and root region (plane a) with the creeping wave probe and still not give rise to false indication. This potential will remain to be evaluated during the future testing of mechanized girth welds made in 9.8 mm wall-thickness.

During the examination of buried reflectors in the simulated weld defect plate it was noted that path distances longer than expected were measured. The same was not observed when examining the welded test panels containing the real defects with the weld cap in place. It is speculated, however, that the reason for this increase in path length in the simulated weld defect analysis is because of wave diffraction from the corner of the flat bottom hole of the buried reflectors. Whilst this program has not fully investigated the phenonomen it is clear that these results indicate that buried flat-bottomed hole reflectors do not accurately represent real planar lack of fusion weld defects, hence should not be used for ultrasonic system calibration.

In a related study carried out by Jaffrey(8) wave diffracted indications were observed from surface reflectors oriented normal to the inspection plate surface and there was a concern that this factor might effect the results of the simulated defect inspections. Jaffrey's experimental set up, therefore, was duplicated during the present investigation using the 1 mm deep surface notch oriented at 5° to the plate normal. These tests confirmed his findings that the diffracted signal occurred at a path distance longer than the reflected signal by an amount equal to the plate wall-thickness, hence the diffracted signal would not interfere with the monitoring of the reflected creeping wave.

It was observed that echo amplitude levels measured during the examination of welded test panels were similar to the level measured on the 1 mm deep surface notch in the simulated weld defect plate, for the same ultrasonic instrument gain level. The surface notch was used throughout this program for determining probe position and establishing gate position and size. These results confirm that surface notches can and were used satisfactorily to calibrate the ultrasonic instrument for examination of the cap region in CRC type GMA welds.

The investigation has shown that a creeping wave probe can be designed and calibrated using a 1 mm deep surface notch to provide satisfactory defect detection performance in the cap region of the GMA weld in 9.5 mm wall-thickness plate. On this basis an experimental program has been designed to evaluate the probes performance on full scale girth welds in 9.8 mm and 20.6 mm thickness pipe, for potential field application.

REFERENCES

1. Fingerhut, M.P., Coote, R.I. and Hodgkinson, D., "The Selection of Ultrasonic Transducers for Inspection of Pipeline Girth Welds", Materials Engineering Services Report No. 15034.

2. Smith, P.H., "Practical Application of Creeping Waves", Welding Institute Research Bulletin, May, 1983.

3. Wüstenberg, H., Erhard, A. and Engl, G., "Improved Ultrasonic Flaw Detection and Analysis Techniques for in Service Inspections on Pressure Vessels", I. Mech. E., 1979.

4. Erhard, A., Wüstenberg, H. and Mondry, E., "Detection of Near Surface Cracks With Creeping-Longitudinal-Waves". Welding and Cutting, May 1983.

5. Erhard, A et al., "Creeping Wave Probes in Ultrasonic Testing - Physical Principles, Application in Welded Constructions", Welding and Cutting, May 1983.

6. Good, M., Private Communication, June 30, 1986.

7. Krautkramer, J. and Krautkramer, H., "Ultrasonic Testing of Materials", Third Edition, Springer-Verlag, 1983.

8. Jaffrey, D. et al, "Improved Detection of Near-Surface Defects With New Ultrasonic Probes and Signal Analysis Techniques", Fifth International Conference on Pressure Vessel Technology - Vol. II: Materials and Manufacturing, p. 693-702.

9. Wüstenberg H., Technical Report, March, 1988. Bundesanstalt für Materialforschung. Berlin.

TABLE 1

CREEPING WAVE PROBE DESIGN REQUIREMENTS

Focus Position

a) Horizontal distance to the focus between 2 mm and 7 mm measured from the front of the probe; and

b) Vertical distance to the focus between 0 mm and 3 mm from the plate surface.

Working Range

a) An amplitude at 2 mm and 7 mm measured horizontally from the front of the probe that is no less than one half the maximum at the focus; and

b) An amplitude at 3 mm depth from the plate surface that is not greater than one half the maximum amplitude at the focus.

Beam Width in the Working Range

A horizontal (6dB) beam width not greater than 3 mm in the direction parallel to plate surface.

TABLE 2

ULTRASONIC INSTRUMENT SETTINGS FOR TESTING ON SIMULATED AND REAL WELD DEFECTS

ULTRASONIC INSTRUMENT - BALTEAU-SONATEST, MASTERSCAN 310

	TESTING ON SIMULATED DEFECTS	TESTING ON REAL WELD DEFECTS
GAIN	60dB	60dB
GATE START	8 mm	10 mm
GATE FINISH	20 mm	15 mm
RECORDING THRESHOLD	@ 10% FSH	@ 10% FSH
RANGE	20 mm	20 mm
DELAY	23 mm	23 mm
REJECT	OFF	OFF
FREQUENCY	Wide-Band	Wide-Band

TABLE 3

MEASURED AND CALCULATED DATA DISTANCES TO EACH SIMULATED WELD DEFECT

SIMULATED WELD DEFECT NO	TYPE	ANGLE	MEASURED PATH DISTANCE (mm)	CALCULATED PATH DISTANCE (mm)
E	1 mm Notch	5	12.25	12.0
E	2.0 mm Ø FBH	5	14.00	13.9
E	2.0 mm Ø FBH	5	14.25	14.6
C	2.0 mm Ø FBH	45	17.25	16.8
C	2.0 mm Ø FBH	45	19.25	19.1
A	1 mm Notch	37.5	16.50	17.0

TABLE 4

CALCULATED PATH DISTANCE BETWEEN THE DEFECT AND THE END-OF-THE-DETECTION-GATE

WELD PLATE NO.	DEFECT TYPE	MAXIMUM PATH DISTANCE TO DEFECT (mm)	PATH DISTANCE TO THE-END-OF-THE GATE (mm)	CALCULATED PATH DISTANCE BETWEEN THE DEFECT AND THE END-OF-THE-GATE (mm)
1	Good Weld	--	14.8	--
2	LOF (Sidewall)	12	14.8	2.8
3	LOF (Sidewall)	11.5	14.8	3.3
5	LOF (Interrun)	13.2	14.8	1.6

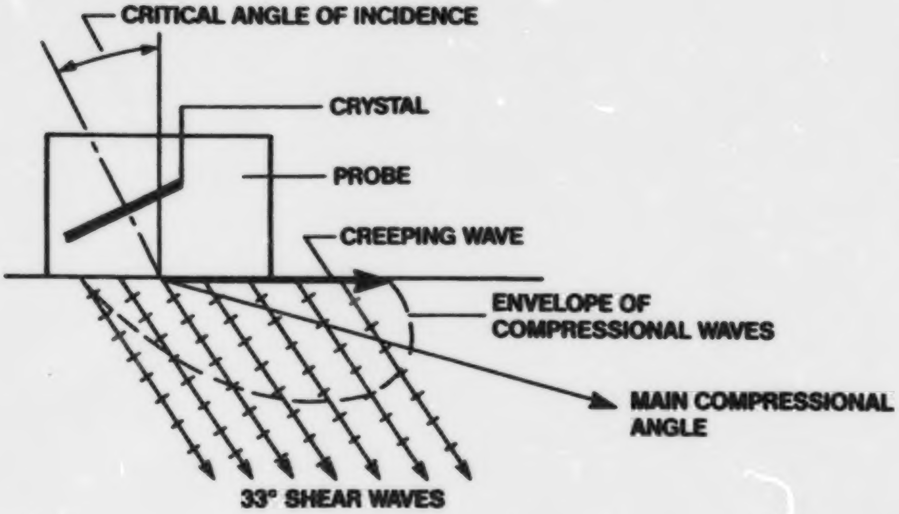
CRITICAL ANGLE OF INCIDENCE
CRYSTAL
PROBE
CREEPING WAVE
ENVELOPE OF COMPRESSIONAL WAVES
MAIN COMPRESSIONAL ANGLE
33° SHEAR WAVES

Figure 1: Creeping Wave and Other Wave Types Produced by the Creeping Wave Transducer.

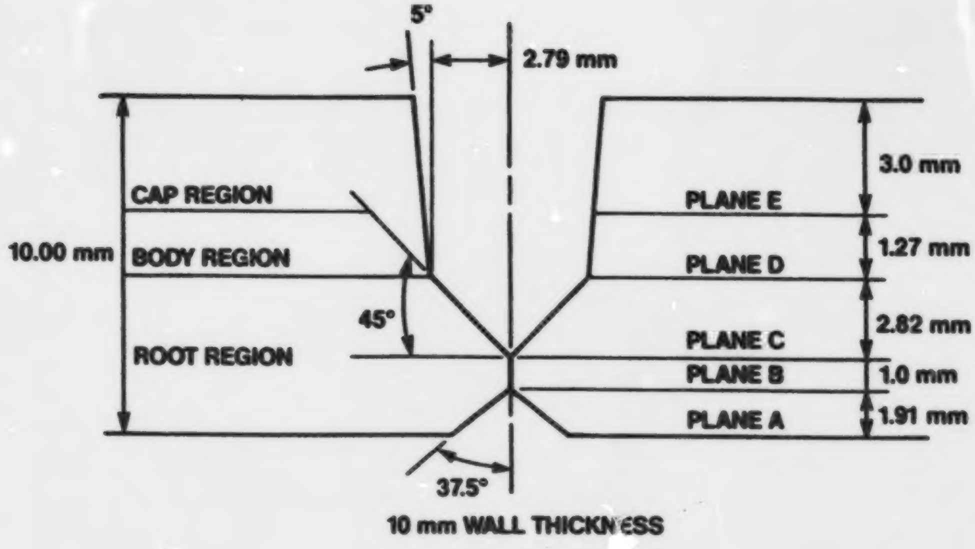
5°
2.79 mm
3.0 mm
CAP REGION
PLANE E
10.00 mm
BODY REGION
1.27 mm
PLANE D
45°
2.82 mm
PLANE C
ROOT REGION
PLANE B
1.0 mm
PLANE A
1.91 mm
37.5°
10 mm WALL THICKNESS

Figure 2: Gas Metal Arc Weld Joint Design Showing Geometry of Inspection Planes.

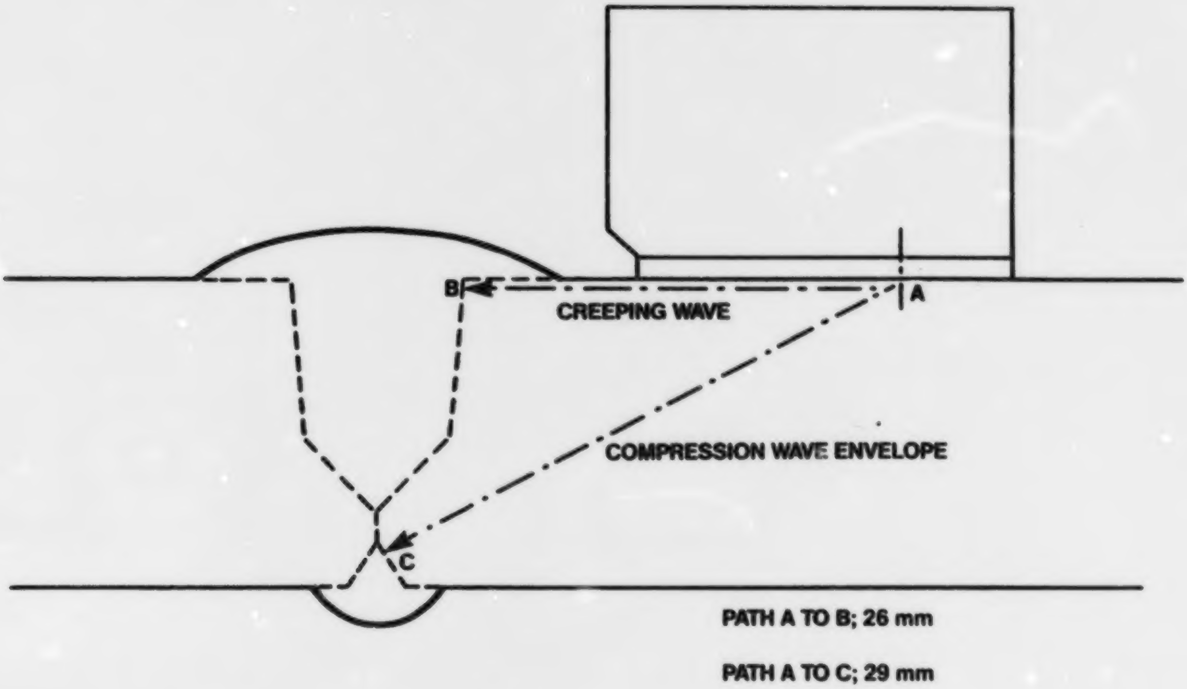
B
A
CREEPING WAVE
COMPRESSION WAVE ENVELOPE
C
PATH A TO B; 26 mm
PATH A TO C; 29 mm

Figure 3: Schematic Showing the Paths and Path Lengths From the Probe Index to Points B and C in the Weld Cross Section.

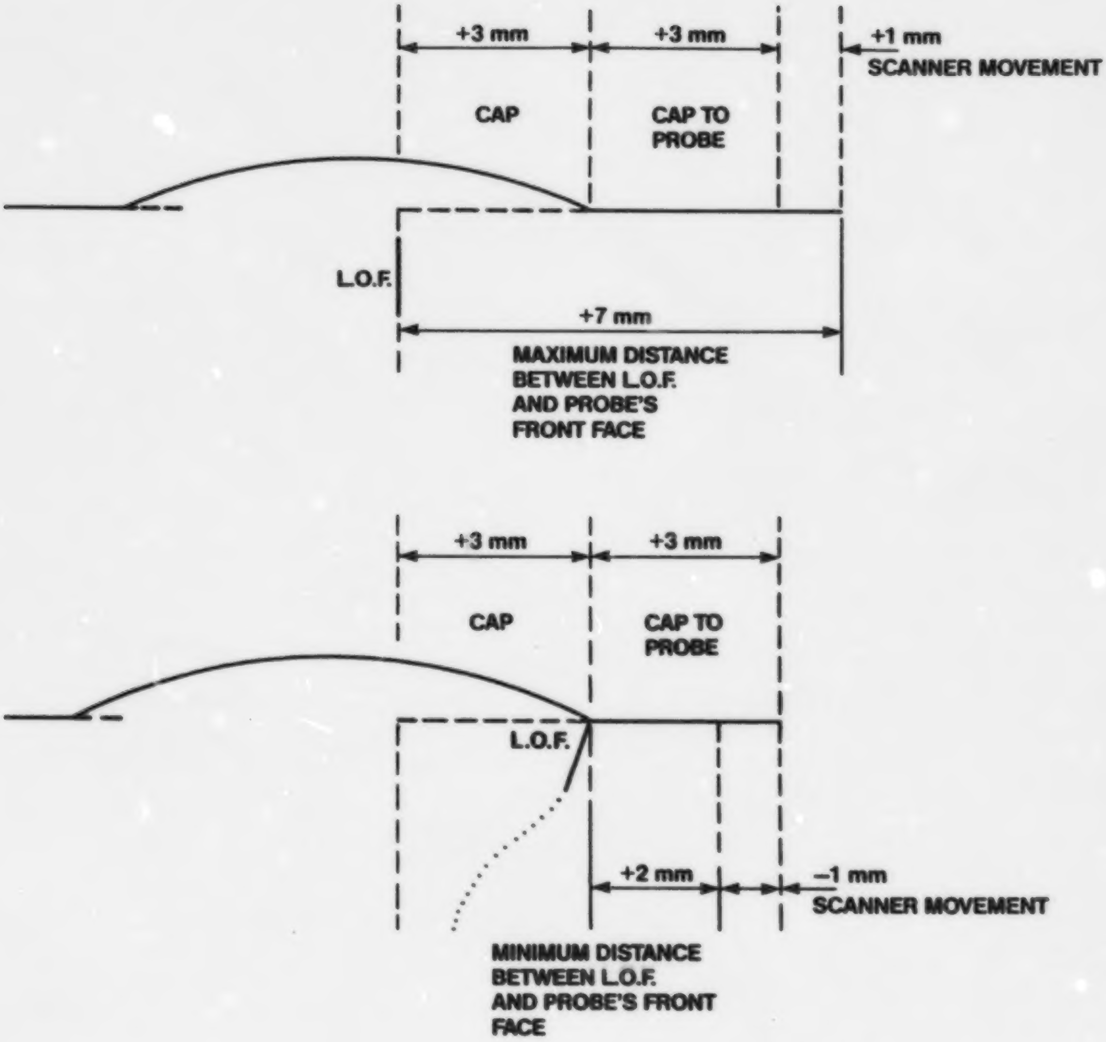
+3 mm
+3 mm
+1 mm
SCANNER MOVEMENT
CAP
CAP TO PROBE
L.O.F.
+7 mm
MAXIMUM DISTANCE BETWEEN L.O.F. AND PROBE'S FRONT FACE
+3 mm
+3 mm
CAP
CAP TO PROBE
L.O.F.
+2 mm
−1 mm
SCANNER MOVEMENT
MINIMUM DISTANCE BETWEEN L.O.F. AND PROBE'S FRONT FACE

Figure 4: Probe Position Relative to Lack of Fusion Defect.
(a) maximum distance (b) minimum distance

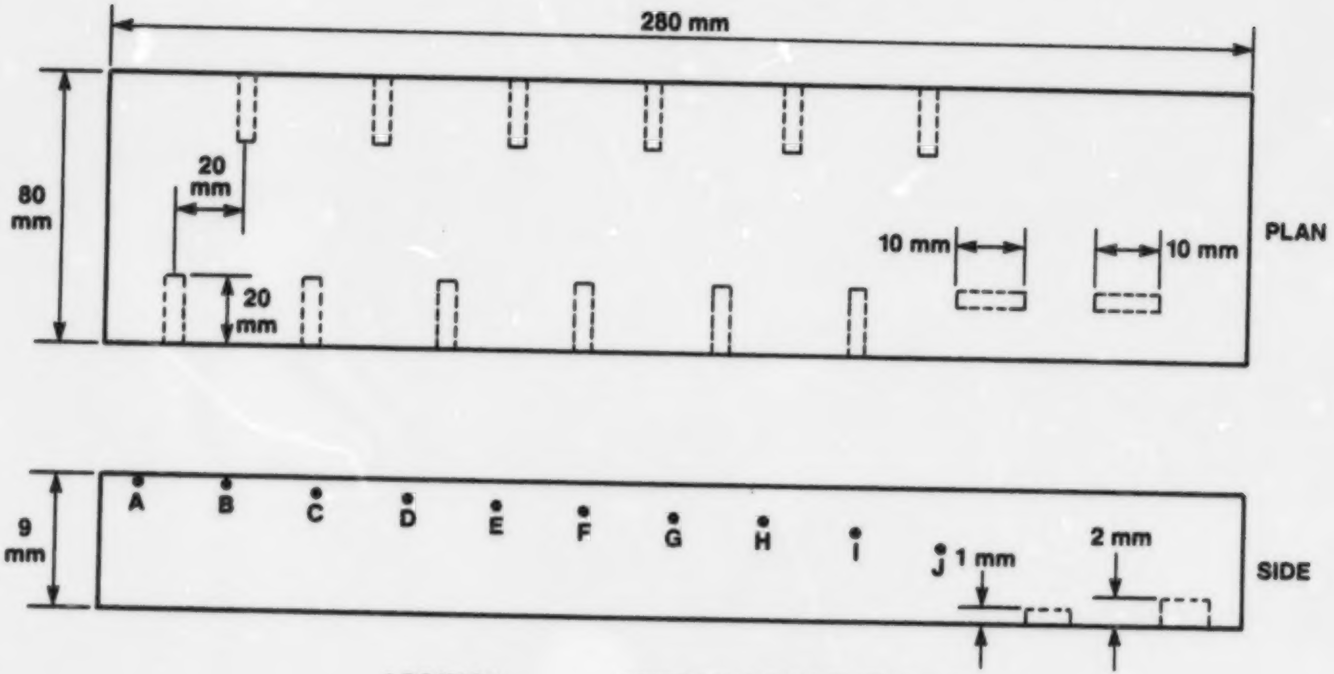
280 mm
80 mm
20 mm
20 mm
10 mm
10 mm
PLAN
9 mm
A
B
C
D
E
F
G
H
I
J
1 mm
2 mm
SIDE

LOCATION	DEPTH BELOW SURFACE (mm)
A	0.0
B	0.7
C	1.2
D	1.7
E	2.2
F	2.7
G	3.2
H	3.7
I	4.2
J	5.0

Figure 5: Design of Test Plate for Simulated Defects (Side Drilled Holes).

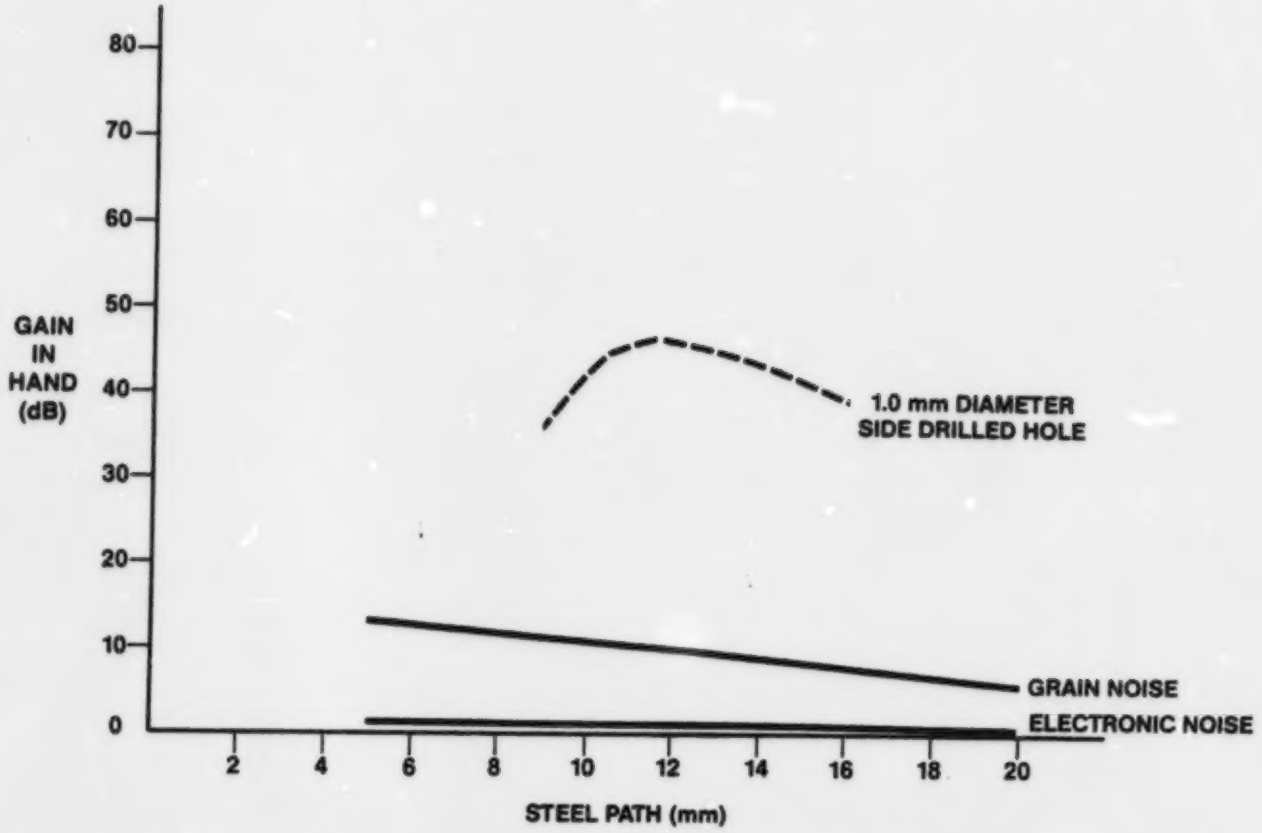

Figure 6: Results of Signal and Noise Analysis, Creeping Wave Transducer No. 87-276.

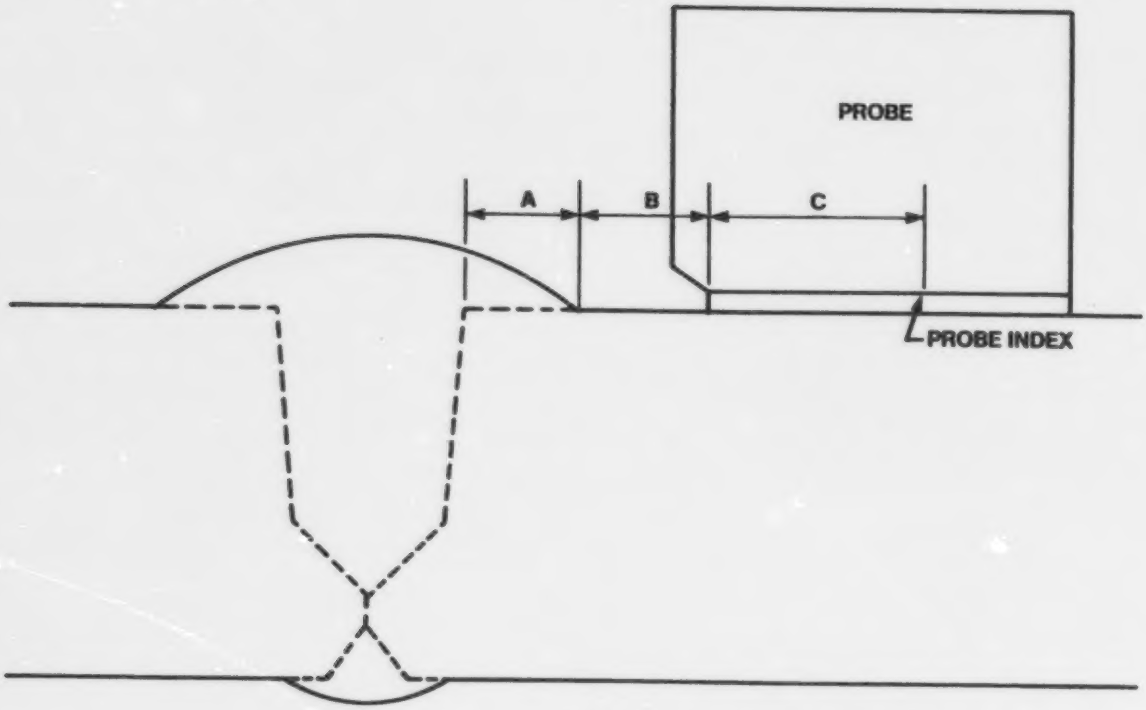

A = 3 mm, MAXIMUM CAP OVERLAP
B = 3 mm, MINIMUM TOE TO FRONT OF PROBE
C = 6 mm, FRONT OF PROBE CONTACT TO INDEX

Figure 7: Schematic of Weld Cross Section Showing Probe Design Position Relative to the Weld Cap and Weld Preparation.

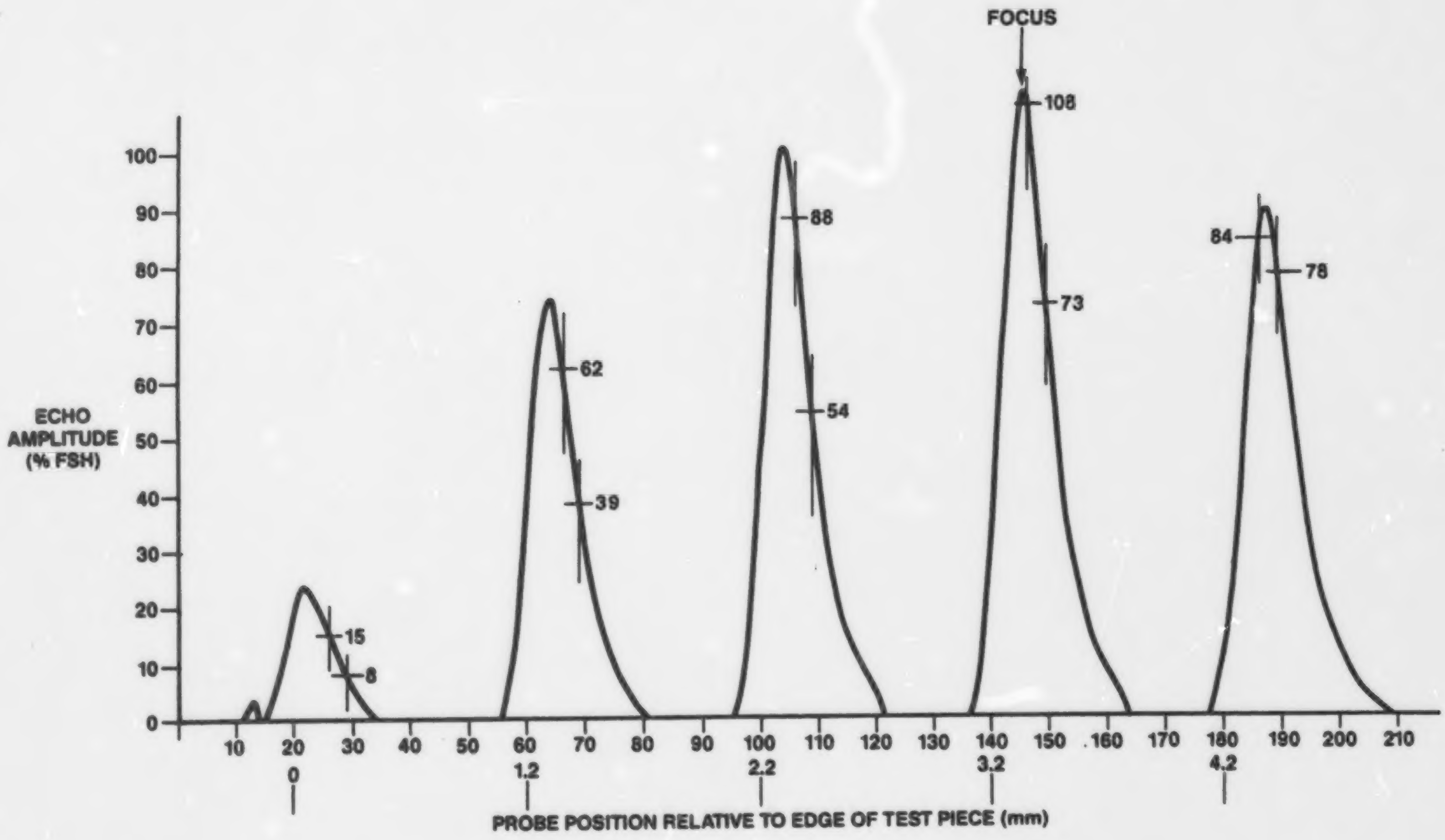

Figure 8: Amplitude Envelope from Five Side Drilled Holes at Different Path Distances, Showing No Side Lobes.

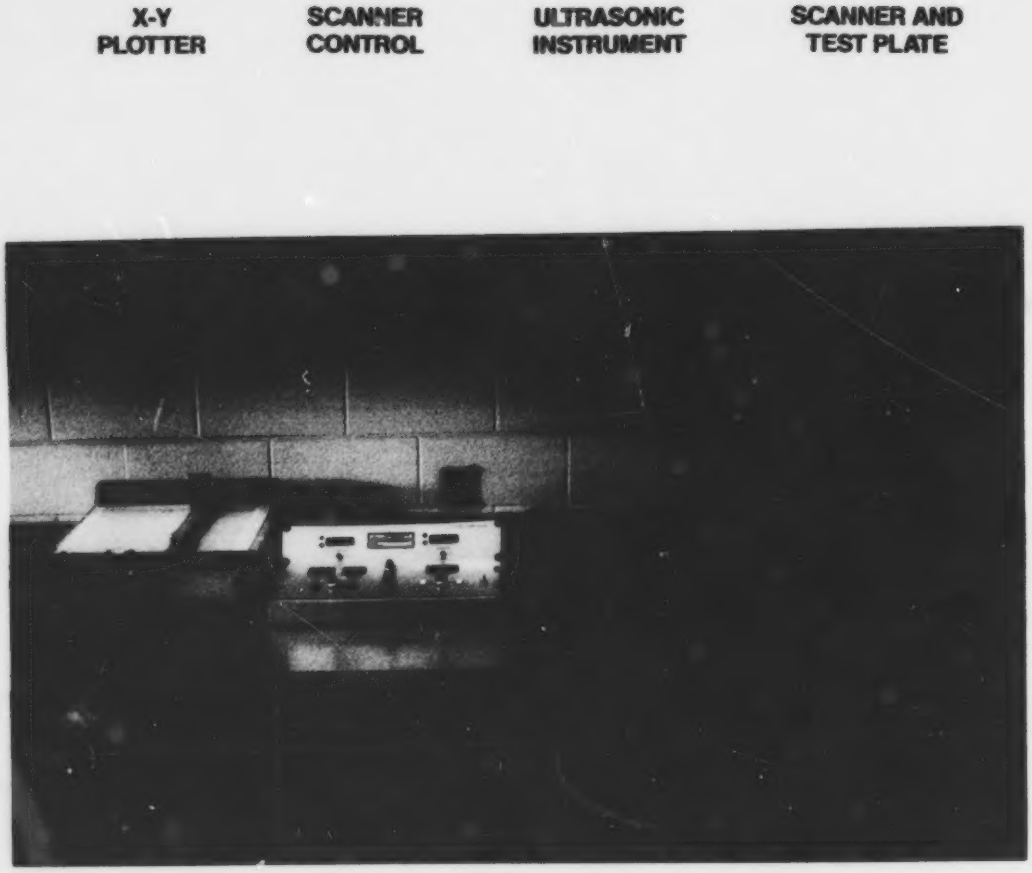
X-Y PLOTTER
SCANNER CONTROL
ULTRASONIC INSTRUMENT
SCANNER AND TEST PLATE

Figure 9: Ultrasonic Probe Testing System

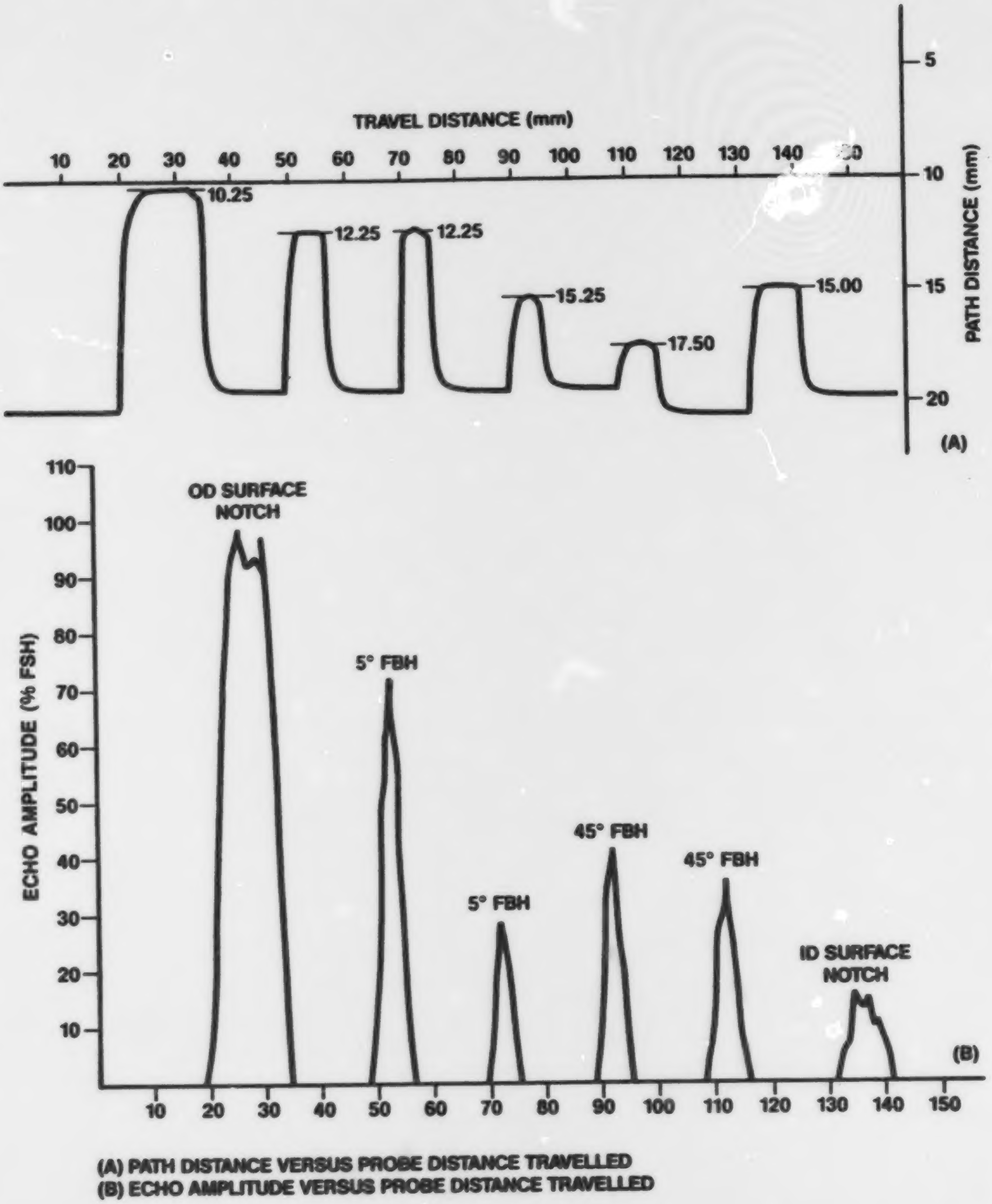

Figure 10: Analog Recording of Echo Amplitude, and Path Distance Versus Probe Distance Travelled.

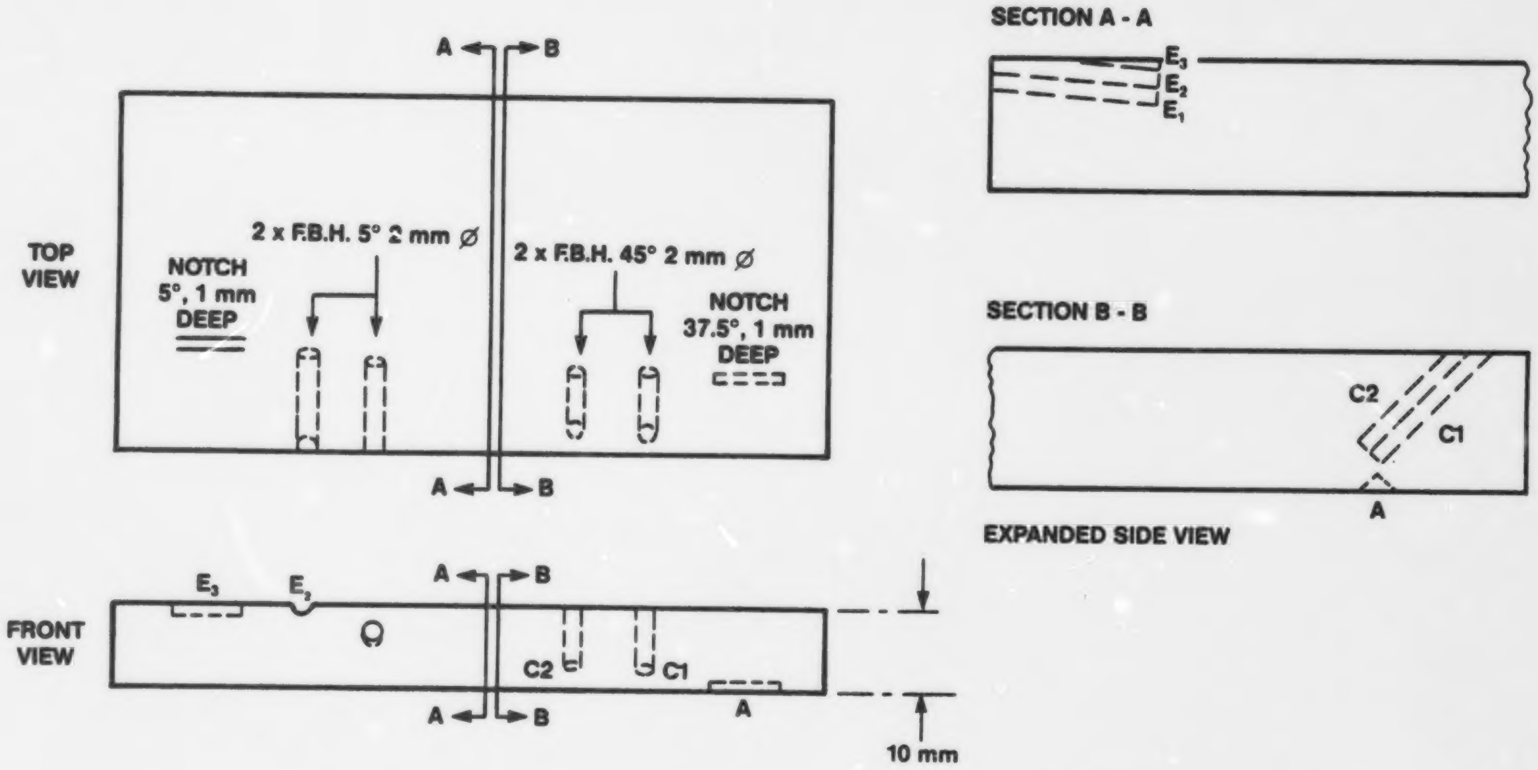
SECTION A - A
E_3
E_2
E_1
SECTION B - B
C2
C1
A
EXPANDED SIDE VIEW
A
B
TOP VIEW
NOTCH 5°, 1 mm DEEP
2 x F.B.H. 5° 2 mm Ø
2 x F.B.H. 45° 2 mm Ø
NOTCH 37.5°, 1 mm DEEP
A
B
FRONT VIEW
E_3
E_2
C2
C1
A
10 mm

Figure 11: Simulated Imperfection Plate Design.

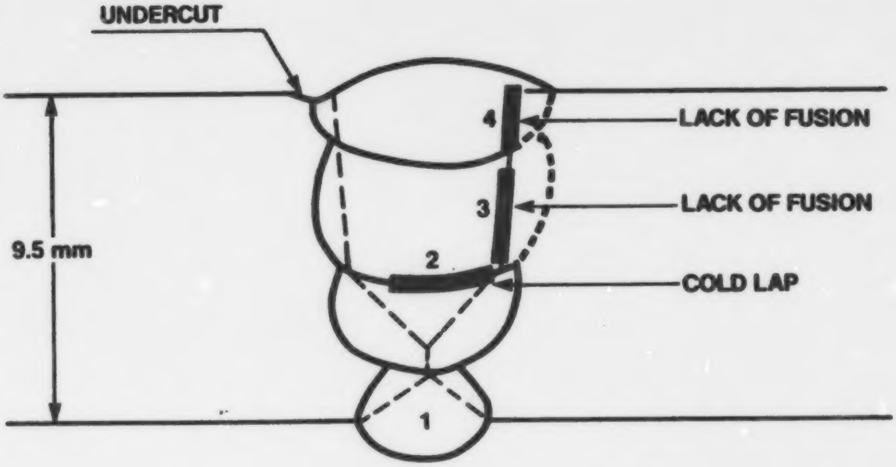
UNDERCUT
LACK OF FUSION
LACK OF FUSION
COLD LAP
9.5 mm
4
3
2
1

Figure 12: Details of Defects Introduced into Weld Test Plates.

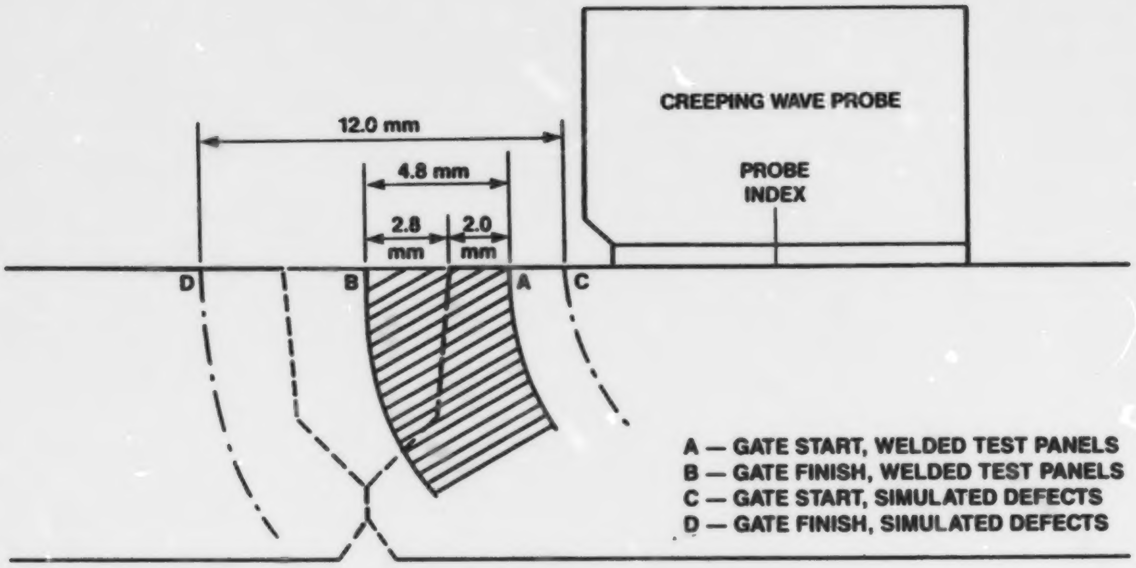
CREEPING WAVE PROBE
PROBE INDEX
12.0 mm
4.8 mm
2.8 mm
2.0 mm
D
B
A
C
A — GATE START, WELDED TEST PANELS
B — GATE FINISH, WELDED TEST PANELS
C — GATE START, SIMULATED DEFECTS
D — GATE FINISH, SIMULATED DEFECTS

Figure 13: Gated Regions Superimposed on Weld Joint Cross Section.

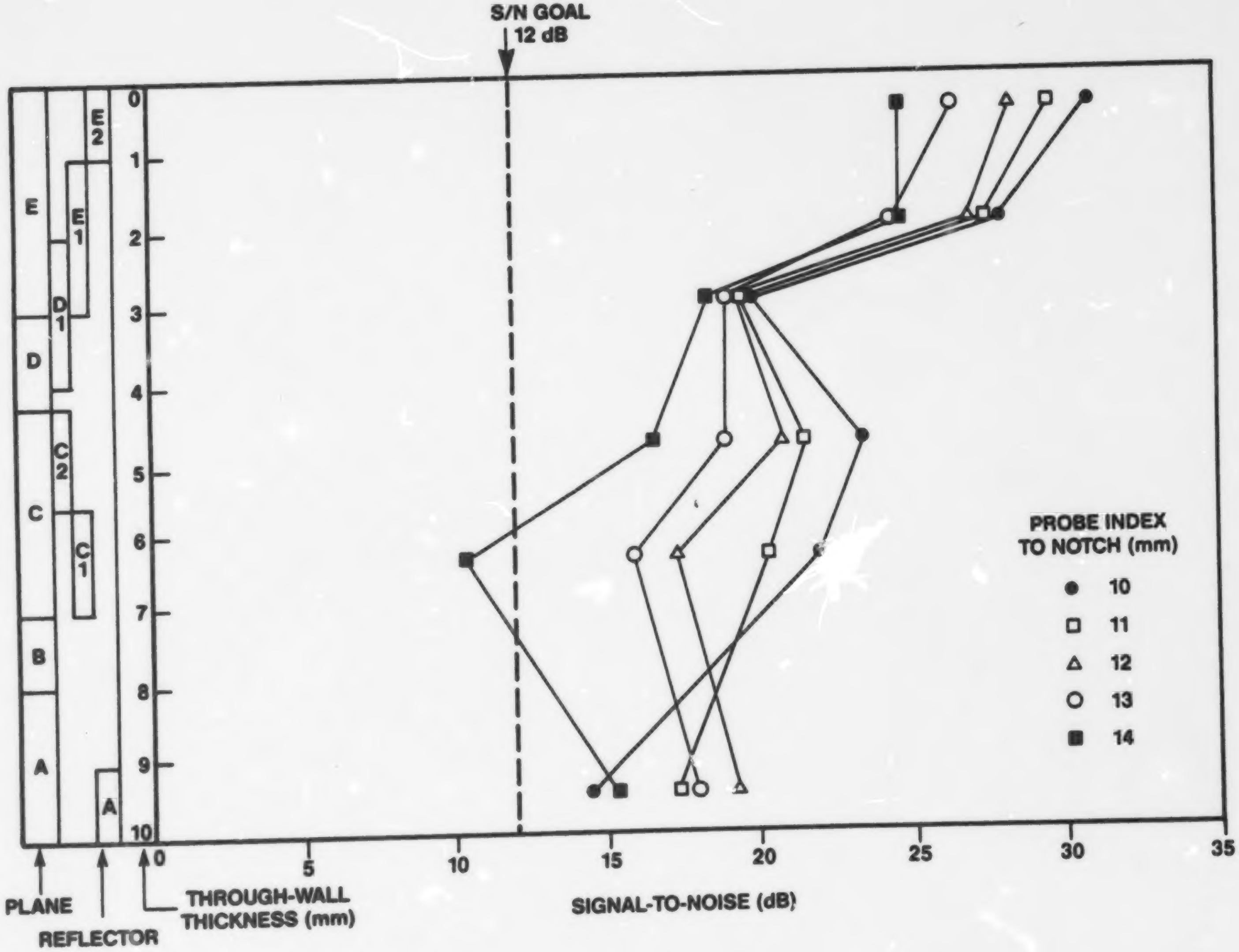

Figure 14: Signal-to-Noise- Measured on Simulated Defects with the Creeping Wave Probe.

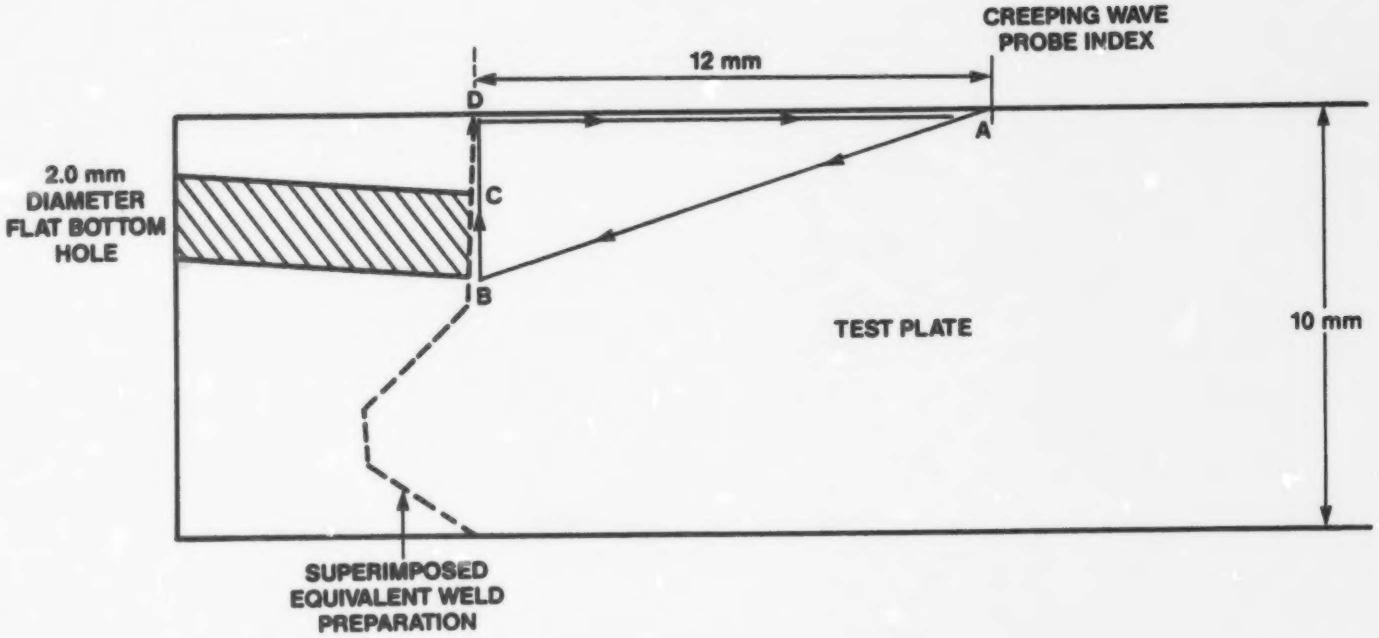
CREEPING WAVE
PROBE INDEX
12 mm
D
A
2.0 mm
DIAMETER
FLAT BOTTOM
HOLE
C
B
TEST PLATE
10 mm
SUPERIMPOSED
EQUIVALENT WELD
PREPARATION

Figure 15: Wave Path (ABCDA) Resulting from Postulated Diffraction on Simulated Weld Defect.

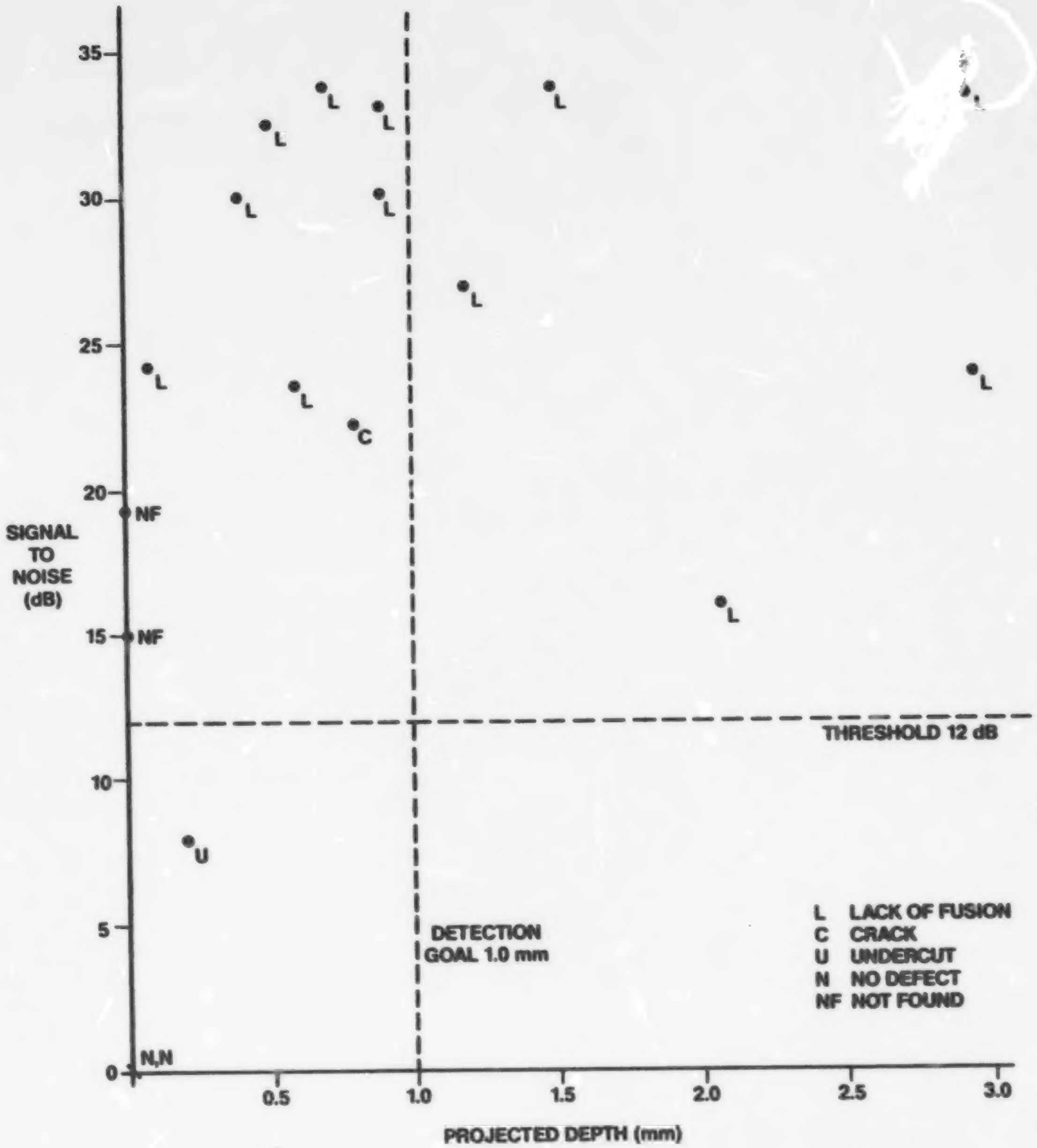

Figure 16: Signal-to-Noise versus Projected Through-Wall Depth on Weld Test Panels.

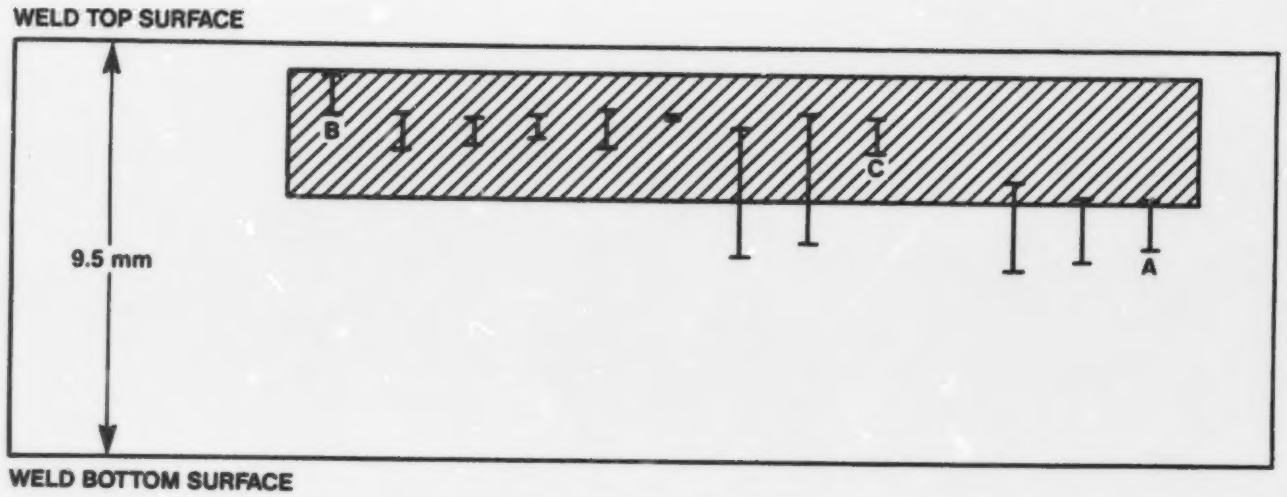
WELD TOP SURFACE
9.5 mm
B
C
A
WELD BOTTOM SURFACE

Figure 17: Plate Cross Section Showing the Through-Wall Position and Projected Through-Wall Depth of each Confirmed Defect.

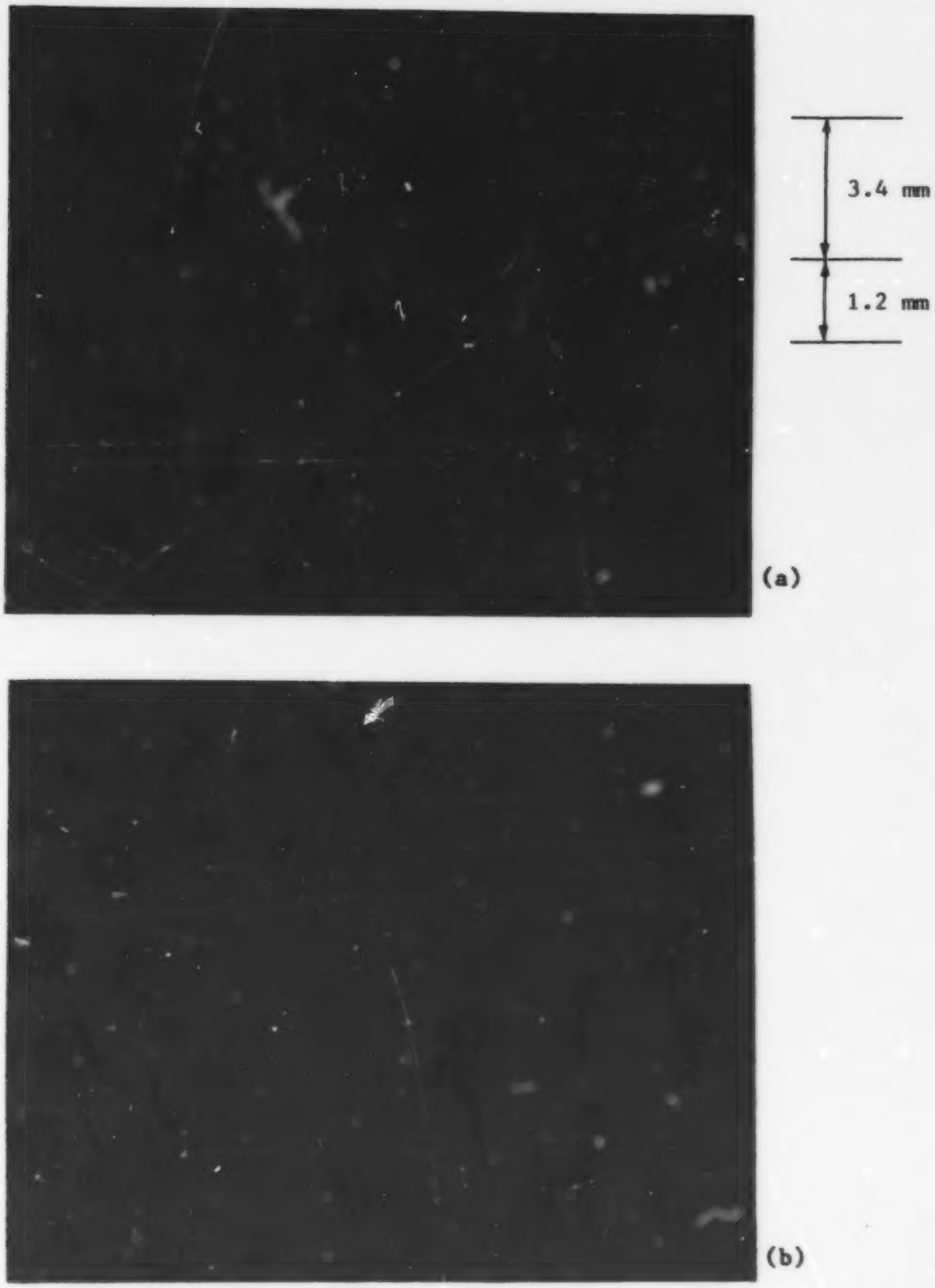

Figure 18: Weld Cross Section Showing Lack of Side Wall Fusion of Defect A (Figure 17).
(a) macrosection X 6.6 (b) details of defect X 50

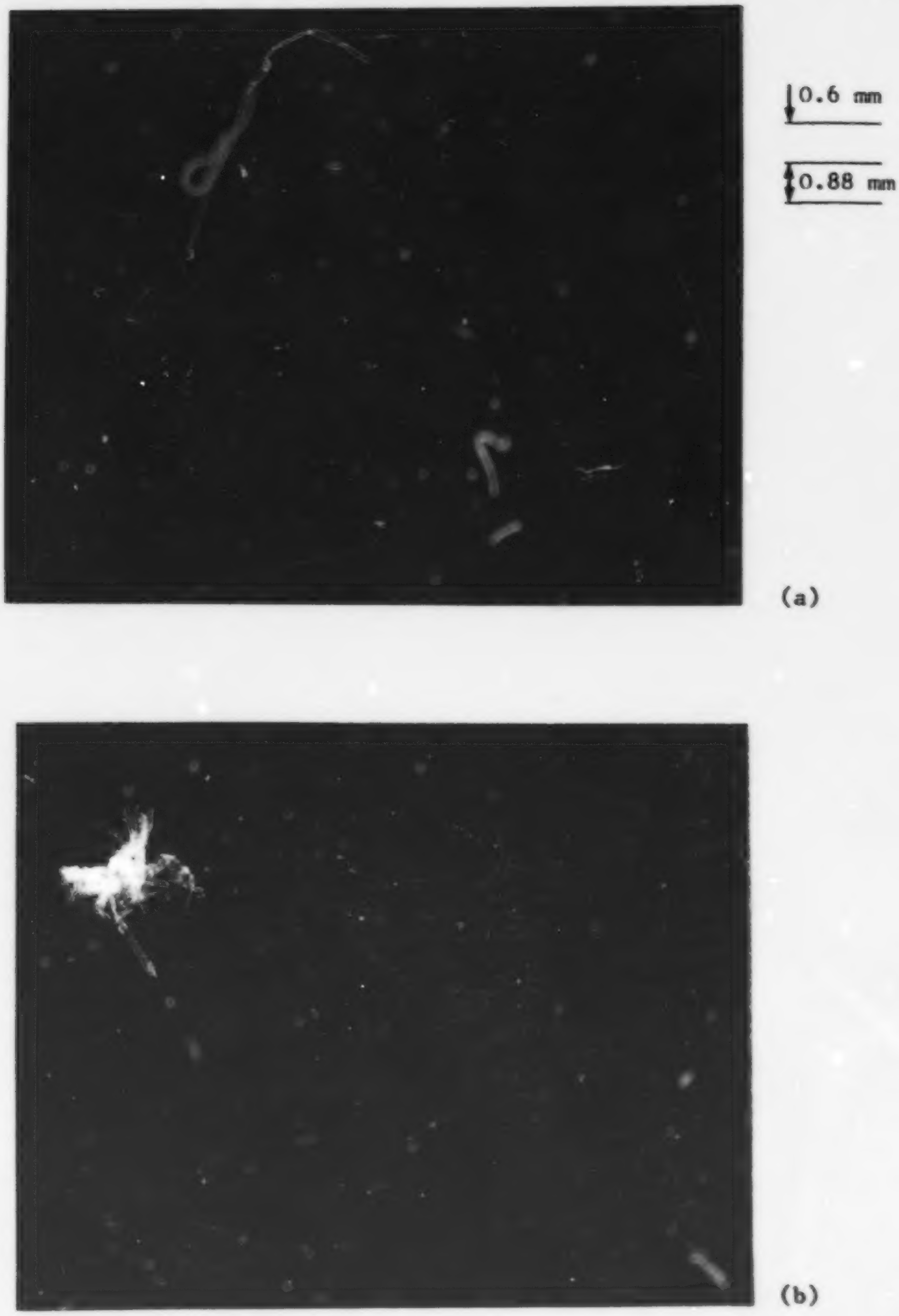

Figure 19: Weld Cross Section Showing Lack of Sidewall Fusion of Defect B (Figure 17).
(a) macrosection X 6.3 (b) details of defect X 50

1.5 mm
0.8 mm
(a)
(b)

Figure 20: Weld Cross Section of Crack in the Cap Region of the Weld, Defect C (Figure 17).
(a) macrosection X 6.3 (b) details of defect X 50

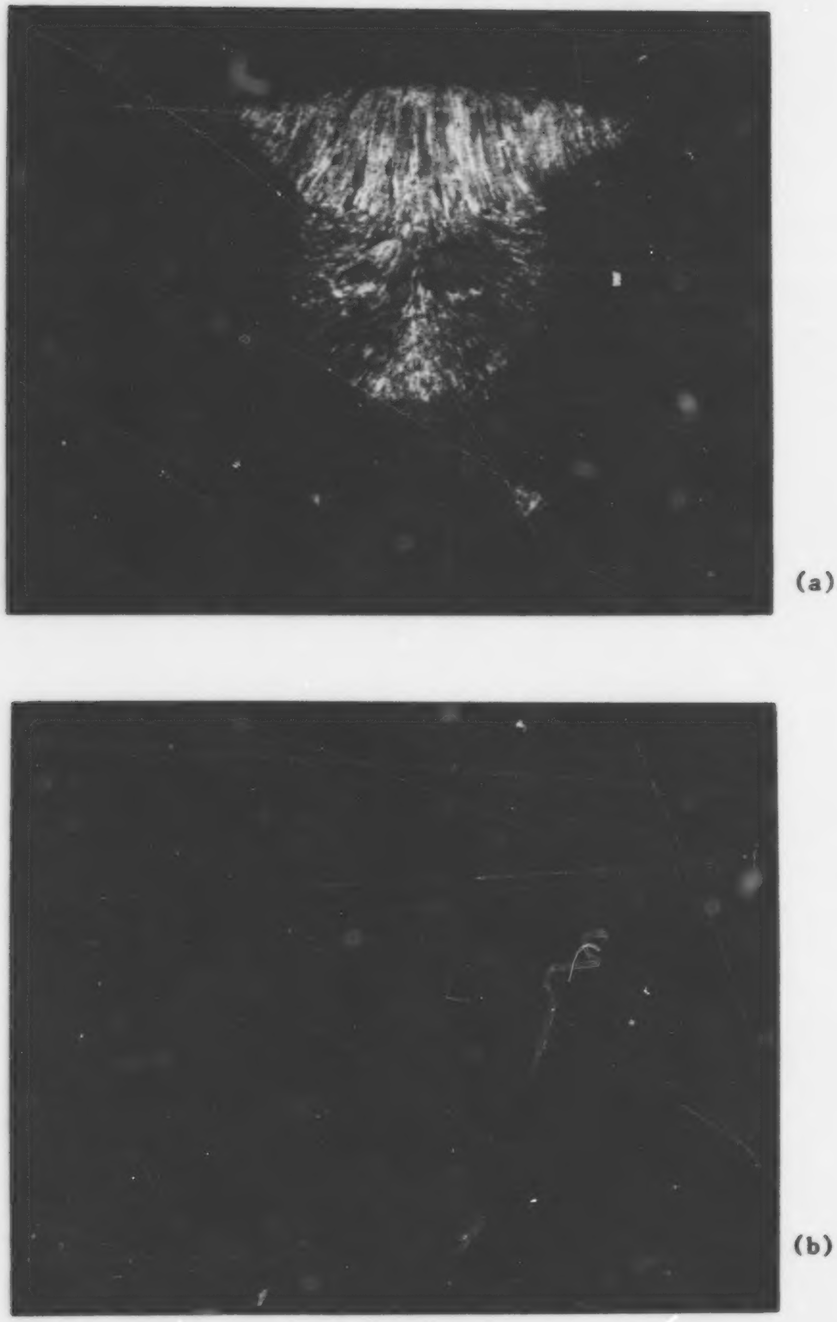
(a)

(b)

Figure 21: Defect Detected on Opposite Side of Inspection Plane.
(a) macrosection X 6.3 (b) details of defect X 50

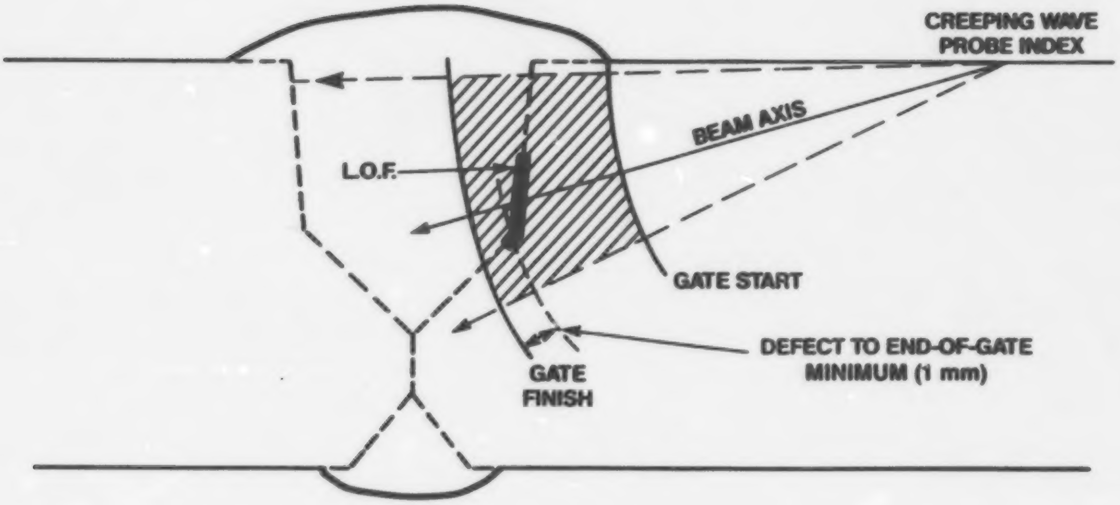
CREEPING WAVE PROBE INDEX
BEAM AXIS
L.O.F.
GATE START
DEFECT TO END-OF-GATE MINIMUM (1 mm)
GATE FINISH

Figure 22: Schematic of Gate Position and Size Required to Achieve Detection of Cap and Body Region Defects and Eliminate False Indications.

APPENDIX 1

SUT - 2

PERFORMANCE SPECIFICATION FOR
MEDIUM FREQUENCY, SHEAR
WAVE ANGLE PROBES

TABLE OF CONTENTS

1.0 SCOPE

2.0 REFERENCES

3.0 DEFINITIONS

4.0 TEST EQUIPMENT

5.0 FLAW DETECTORS AND ELECTRICAL MATCHING

8.0 METHODS OF TEST AND ACCEPTANCE LEVELS

- 8.4.1 SIGNAL AND NOISE CURVES
- 8.15 BEAM WIDTH

FIGURES

- 5. SAMPLE, SIGNAL AND NOISE CURVES

APPENDIX A

REPORT SHEET FOR ULTRASONIC PROBE RESULTS

.../2

1.0 SCOPE

This specification details the additions and replacements to the requirements of the Electricity Supply Industry (ESI) Standard 98-2 for the testing and acceptance of ultrasonic shear wave angle probes and follows the numbering and format of ESI 98-2. Where a conflict exists the requirements of this specification shall apply.

2.0 REFERENCES

ESI standard 98-9, "ULTRASONIC FLAW DETECTORS"

3.0 DEFINITIONS

CROSS-DRILLED HOLES: Cylindrical holes drilled parallel to the test surface and at right angles to the vertical plane of the probe.

PROBE FACE: The face of the probe in contact with the surface of an inspected component through which the ultrasound is transmitted and received.

SIDE LOBES: Side Lobes are peaks or pronounced shoulders in the amplitude profile in the vertical of the sound beam which lie at higher or lower refracted angles than the main beam.

PURCHASER: NOVA Corporation of Alberta

4.0 TEST EQUIPMENT

4.1 One ultrasonic flaw detector, with A-scan display for use with single or twin crystal probes of nominal frequency in the range of 1-10 MHz and which satisfies the requirements of ESI Standard 98-9.

5.0 FLAW DETECTORS AND ELECTRICAL MATCHING

The manufacturer shall certify that probes supplied will meet the requirements of this specification when used with the flaw detector(s) identified on the Purchase Order.

.../3

8.0 METHODS OF TEST AND ACCEPTANCE LEVELS

If the flaw detector has more than one frequency range setting covering the nominal frequency of the probe, the tests shall be conducted using the control setting which gives the best separation of signal from noise (see clause 8.4.1). This frequency setting is not necessarily the one which gives the highest echo amplitude. This setting together with the probe test results shall be recorded on the report sheet in appendix A.

8.4.1 SIGNAL AND NOISE CURVES

This section is in addition to the requirements of section 8 of standard 98-2.

NOISE CURVE

METHOD: Using the A2 (or thicker) block adjust the range controls of the flaw detector until the screen width corresponds to 0 to 100 mm for shear waves. Remove the probe from the block and clean off all couplant. Adjust the calibrated attenuator to bring each internal echo in turn to half screen height. Measure the range of each echo and the corresponding gain left in hand on the attenuator in decibels, and plot these as points on a graph of gain in hand versus range as shown in figure 5.

Continue plotting the internal echoes at increasing range until the gain of the flaw detector is at maximum and electronic noise is clearly visible. If the internal echoes have not fallen below the electronic noise level by the 100 mm range, recalibrate the range 100 to 200 mm or as appropriate and continue plotting. If, when all the gain controls are set to maximum, the noise level has still not reached half screen height, estimate the (negative) gain remaining in hand from the following scale:

Noise at 30% full screen height: - 4 dB in hand
Noise at 25% full screen height: - 6 dB in hand
Noise at 20% full screen height: - 8 dB in hand
Noise at 10% full screen height: -14 dB in hand
Noise at 5% full screen height: -20 dB in hand

.../4

SIGNAL CURVE

Maximize in turn the echoes from 1.5 mm diameter cross-drilled holes of at least eight ranges in the A5 block (or block in Clause 4(iv) if appropriate). Four holes shall lie in the range of 0 to 100 mm and four in the range 100 to 200 mm. To satisfy this requirement some measurements will have to be made at full skip.

For each hole adjust the calibrated attenuator to bring the maximized echo to half screen height and plot a point showing the gain remaining in hand at that range, on the graph as shown in Figure 5. The curve of gain shall be drawn to be a best fit to the plotted points.

ACCEPTANCE LEVEL:

The noise curve shall be at least 20 dB weaker than the signal curve at the target path distance specified by the purchaser and no less than 16dB at path distances of 20 mm greater and 10 mm less than the target path.

8.15 BEAM WIDTH AT THE TARGET:

This shall replace section 8.15 in Standard 98-2.

METHOD: The width of the refracted beam shall be determined according to ASTM volume 03.03 (metallography; nondestructive testing) proposed practice for evaluating the characteristics of ultrasonic search units section A6.4.4

ACCEPTANCE LEVEL:

The measured beam width at the target distance shall not differ from that specified by purchaser by more than 10%.

.../5

APPENDIX A

REPORT SHEET FOR ULTRASONIC PROBE RESULTS (SINGLE CRYSTAL)

Specification Applied: ESI Standard 98-2 for Ultrasonic Probes: Medium Frequency, Miniature Shear Wave, Angle Probes

Probe Manufacturers and Identification: ____________________

Probe Specification and Dimensions: ____________________

Flaw Detector, Cable and Critical Control Settings: ____________

Electrical Matching: ____________________

Mechanical Construction (including subjective comments): __________

Operator and Date: ____________________

Operator's Signature: ____________________

Summary of Test

Result	Clause	Parameter	Requirement for Single Crystal Angle Probe
______	7	Identification	Marked on probe: manufacturer, probe type, beam angle, frequency, crystal size and shape.
______	8.1	Depth of Shoe Probes	The available depth shall be indicated and shall be at least 1 mm.
______	8.2	Probe Wear (Used Probes)	Probe face shall be proud of the manufacturer's wear allowance marks.
______	8.3	Shoe Flatness	Flat within 0.05 mm.
______	8.4	Overall Gain	At least 50 dB gain in hand.
______	8.4.1	Signal to Noise Ratio	Noise shall be at least 20 dB weaker than the signal at the target path.
______	8.5	Signal to Electronic Noise	Noise shall be at least 40 dB weaker than the signal at the target path.

Result	Clause	Parameter	Requirement for Single Crystal Angle Probe
	8.6	Index Point	Marked index point shall be within 1 mm of measured one.
	8.7	Beam Angle	For nominal beam angles less than 45° +/- 1.5°, for greater than 45° +/- 2°.
	8.8	Squint	Not exceeding 1.5° for single crystal probes nor 2° for twin crystal probes.
	8.10	Longitudinal - Angle Beam	At least 35 dB weaker than shear beam. Measured at 100 mm range.
	8.11	Surface Waves	At least 34 dB weaker than shear wave for beam angles below 65°. At least 24 dB weaker for higher angles. Measured at 100 mm range.
	8.13	Side Lobes	At least 20 dB weaker than the main beam, except angle greater than 64° shall be at least 15 dB weaker than the main beam.
	8.14	Subsidiary Maxima	Fluctuations in echo amplitude shall not exceed that caused by interference with grass.
	8.15	Beam Width	Measured beam width shall be within 10% of design width.
	8.16	Pulse Shape	Single Peaked: Any secondary peaks in tail of pulse at least 20 dB less tnan main peak.
	8.17	Cycle Spacing	Less than +/- 15% variation between each cycle.
	8.18	Frequency	Within +/- 10% of the nominal frequency.
	8.19	Pulse Length	Not exceeding 2.5 microseconds between points on the unrectified pulse at 10% of peak amplitude.

A tick in the "Results" column should be used to indicate compliance with the Standard.

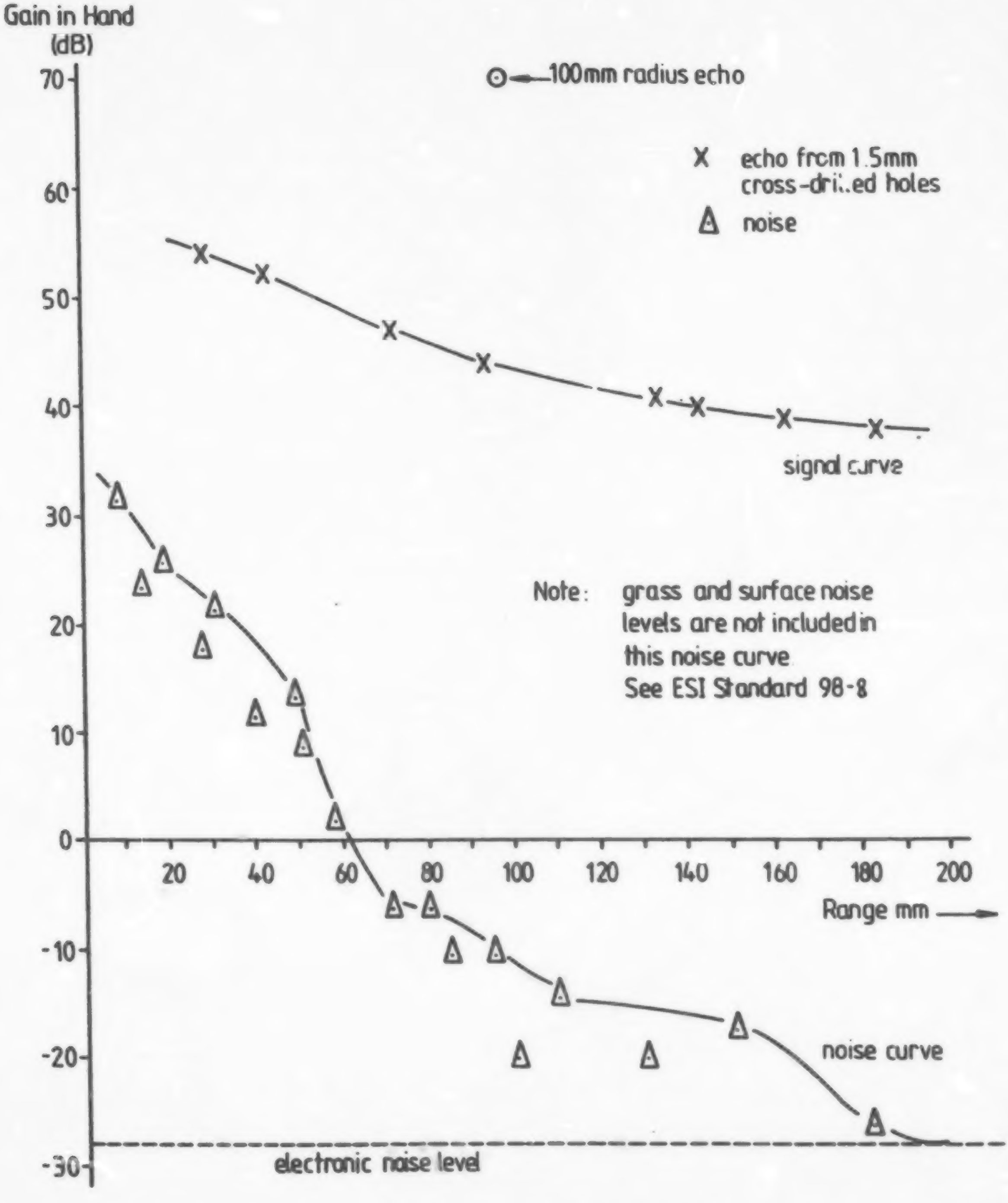

Fig signal and noise curves

80/451

APPENDIX 2

SUT - 1

PROCEDURE FOR THE DETERMINATION OF THE DETECTION THRESHOLD LEVEL FOR MECHANIZED ULTRASONIC EXAMINATION

1.0 SCOPE

This document provides that procedure which shall be used for determining the detection threshold level for mechanized ultrasonic examination.

2.0 APPLICATION

This procedure shall only be used for determining detection threshold for ultrasonic probes which satisfy the requirements of SUT-2.

3.0 REFERENCES

SUT-2, Performance specification for medium frequency shear wave angle probes.

4.0 GROUPS AFFECTED

(a) Project Engineering
(b) Design Engineering
(c) Engineering Services

5.0 THRESHOLD LEVEL

(a) Determine from the noise curve produced according to SUT-2 the instrument gain level required to produce the 50% screen height signal at the target path distance.

(b) Calibrate the instrument gain level for examination using the appropriate reference reflector.

(c) Determine the screen height noise signal at the gain level selected in (b) according to the following formula:

$$n = 10^{x} \left(\frac{a-b}{20} - \log 50 \right)$$

where a = the instrument gain level for a 50% screen height noise signal;

b = calibrated instrument gain level;

n = noise level in percent of screen height

Note: $\left(\frac{a-b}{20} - \log 50\right)$ will always be a negative number.

(d) The threshold level will be 12dB above the screen height noise level (n).

$$T = 10^{x} \left(\frac{12}{20} + \mathrm{Log}\ n \right)$$

Where T = the threshold level in percent of screen height.

Volume

3

MECHANIZED ULTRASONIC INSPECTION OF PIPELINE GIRTH WELDS

3

Part 3: Evaluation of the Pitch-Catch Technique For Examination of the Body Region

FINAL REPORT BY:

A.G. Glover
M.P. Fingerhut
D.V. Dorling

WORK ON THIS PROJECT WAS JOINTLY FUNDED BY NOVA CORPORATION OF ALBERTA AND THE METALS TECHNOLOGY LABORATORIES, CANADA CENTRE FOR MINERAL AND ENERGY TECHNOLOGY, ENERGY MINES AND RESOURES CANADA

DSS FILE NUMBER: 23SQ-23340-2-9027-4
DSS CONTRACT SERIAL NUMBER: OSQ82-00244
CANMET SCIENTIFIC AUTHORITY: DR. D.K. MAK

Report #15048

October, 1988

49 pp

TABLE OF CONTENTS

PAGE

1.0 SUMMARY 1

2.0 CONCLUSIONS 3

3.0 RECOMMENDATIONS 4

4.0 INTRODUCTION 5

5.0 EXPERIMENTAL 7

- 5.1 General 7
- 5.2 Inspection Design 7
- 5.3 Transducer Selection 12

6.0 EVALUATION OF PITCH-CATCH TECHNIQUE 14

- 6.1 Test Equipment 14
- 6.2 Test Plates 15
  - 6.2.1 Machined Reflectors 15
  - 6.2.2 Weld Defect Plates 15

7.0 EXPERIMENTAL PROCEDURE 16

- 7.1 Instrument Settings 16
- 7.2 Testing Procedure 17
  - 7.2.1 Tests on Simulated Weld Defect Plate 17
  - 7.2.2 Tests on Real Weld Defect Plates 18

8.0 RESULTS AND ANALYSIS 19

- 8.1 Performance on Simulated Defects 19
- 8.2 Performance on Real Weld Defects 20

9.0 DISCUSSION 22

REFERENCES
TABLES
FIGURES
APPENDICES

1.0 SUMMARY

This Report is the third in a series of four research reports aimed at developing an ultrasonic inspection design for the nondestructive evaluation of pipeline girth welds made by the mechanized gas metal arc (GMA) welding process for onshore and offshore pipeline construction.

Part 1 of the program described an inspection design method and criteria for the selection of ultrasonic transducers for the inspection of pipeline girth welds. This study showed that focussed probes in the pulse-echo mode are suitable for the examination of the root region of the weld and that alternative approaches are required for examination of the remainder of the weld. Part 2 of the program studied the use of creeping wave transducers for the examination of the cap region and showed that they could successfully be used with the specified inspection criteria and transducers. Part 3 of the program, described in this report, studies the use of the pitch-catch technique to examine the body of the weld.

In previous parts of this program the approach has been to use specialized beams to detect specific imperfections and to, wherever possible, have the ultrasonic beam normal to the plane of the imperfection. It was shown during the Part 1 investigations, however, that the pitch-catch technique may be the only appropriate way to investigate defects in the body region. This present report describes the work carried out to evaluate the performance of the pitch-catch

technique with respect to its ability to examine the body region of mechanized GMAW welds in 19.5 mm thick material. Note that previous analysis in Part 2 has shown wall thicknesses of 9.73 mm and less can be inspected without the use of body region probes and hence no inspection design was carried out for the 9.5 mm wall thickness.

Evaluation of the pitch-catch technique was carried out on simulated and real weld defects. The results showed that the technique achieved good detection performance in the body region of thick section weldments and the technique should be evaluated on full scale welds.

2.0 CONCLUSIONS

2.1 An inspection design method and criteria can be specified for the detection of lack of sidewall fusion defects in the body region of mechanized gas metal arc welds. The criteria specified a pitch-catch technique using a 2.25 MHz 45° transmitter and a 2.25 MHz 55° receiver probe. A single pair of these transducers can inspect wall thicknesses from 9.7 mm to 23.0 mm.

2.2 The pitch-catch technique evaluated on 19.5 mm wall thickness materials demonstrated that the detection goal of 1 mm projected depth with a signal-to-noise ratio of greater than 12dB could be met, and that no problems occurred with false indications or missed defects.

2.3 High sensitivities to small defects in the body region were obtained using a single pair of pitch-catch probes that inspected the body region as a single plane.

2.4 Indexing of the weld preparation prior to welding, as well as actual calibration test pieces, will be required for field welding evaluations.

3.0 RECOMMENDATIONS

3.1 Evaluate the use of the pitch-catch technique in combination with focussed probes and creeping wave transducers on full scale laboratory test welds.

3.2 The potential of dividing the inspection plane into two regions should be investigated, so that more uniform inspection plane sensitivities can be achieved.

4.0 INTRODUCTION

The objective of this work has been to develop an inspection design criteria and transducer selection methodology for the mechanized ultrasonic inspection of mechanized gas metal arc welds in 10 and 20 mm wall thickness. Previous work had shown that problems associated with missed imperfections and false indications were fundamentally related to the characteristics of the ultrasonic beam used, and to the design of the inspection geometry. The approach used in this program therefore was to use specialized beams to detect specific imperfections and thus overcome problems of variable response from the range of imperfection types and location. The goal is to obtain a large echo signal, relative to the background noise from specific imperfections in the region being examined by a particular beam. The goal was a signal-to-noise ratio greater than 12dB for all imperfections with a projected depth exceeding 1.0 mm.

Initial work in Part 1 (1) showed that the pulse-echo technique used to examine body region defects (identified as Plane D, Figure 1) was satisfactory for simulated defects but unreliable for real defects. The satisfactory performance on simulated defects was only obtained because of the beneficial corner effect. The use of a two-probe method (commonly called pitch-catch) has been shown to reliably detect defects that are located normal to the plate surface, and hence a preliminary trial was carried out using this technique during Part 1.

The trial was carried out using available transducers and showed that performance was good enough to warrant a full scale evaluation.

The body region of the CRC type mechanized gas metal arc weld is defined as that portion located between the cap and root region of the weld as shown in Figure 1. Inspection of the root region (Planes A and C) by focussed probes covers a fixed depth of 5.73 mm; inspection of the cap region (Plane E) by the creeping wave technique(2) covers a minimum depth of 3.00 mm, giving a total minimum fixed depth of 8.73 mm for the root and cap region. On this basis, therefore, the minimum wall thickness that will require a body region inspection for 20 mm wall pipe will be 9.73 mm (allowing for the 1.00 mm minimum detection criteria). This present study, therefore, is limited to designing an inspection criteria for the body region of the 20 mm wall thickness case, and no inspection design was carried out for the 9.5 mm case.

5.0 EXPERIMENTAL

5.1 General

The experimental program consisted of developing an inspection design, specifying and evaluating transducers, and evaluating the performance on simulated and real defects in 19.5 mm wall thickness material. All the work was based on the primary need to detect lack of side wall fusion type defects, even though interrun fusion defects may also be present in the body of the weld. The sidewall type is oriented predominantly normal to the pipe surface and subject to longitudinal stress, whereas the interrun is oriented primarily parallel to the pipe surface with a comparatively small normal component and not subject to significant stress. The lack of sidewall fusion is therefore a more critical defect to detect as analyzed by fitness-for-purpose assessments.

5.2 Inspection Design

At the start of the project some primary goals were set for the inspection design of each plane of the weld and these included an ultrasonic shear wave beam which is perpendicular to the inspection plane, and a 6dB beam width confined to the inspection plane. In practice it was necessary to select designs for the body and cap regions of the weld which did not exactly meet these goals. In the case of the body region, the inspection plane would require the use of

85° refracted beams and extremely large target distances; both of which are not practicable. Initial work (1) used a beam with a refracted angle of 70° and accepted the loss of sensitivity due to the 15° misorientation between the beam and the inspection plane. Evaluation of the performance in detecting weld defects in the body region proved unsatisfactory and led to a trial of the pitch-catch technique. The preliminary trials proved satisfactory and led to the present inspection design approach.

The basic principle of the pitch-catch technique is illustrated in Figure 2, which shows that the acoustic pulse from the transmitter is reflected from the defect and detected by the receiver. The schematic in Figure 2 also illustrates that the inspection Plane D must commence 3 mm below the surface in order to eliminate any problems with interference from the cap region.

The design approach developed for inspection by the pitch-catch technique was as follows:

(a) To use shear wave beams (within the 6dB envelope) with incident angles along the beam path of greater than 35° to avoid mode conversion of the shear waves to compression waves and resultant energy loss. Incident angles of no larger than 45° on the inspection plane (defect) are also required to ensure that when inspecting the zone closest to the cap that any loss of energy occurring from the beam intersecting the weld cap is minimized.

(b) To specify the shortest possible beam path which would allow placement of the transducers without interfering with the weld cap.

In order to specify transducers to satisfy these criteria a series of design tables were established based on the geometry of the weld joint and standard trigonometry. The beam path and weld geometry configuration are given in Figure 3, and these were used to determine beam angles at each reflecting surface along the path from transmitter to receiver. Using this information, design tables (Appendix 1) were established for the maximum and minimum beam angles for the 6dB envelope at each reflecting plane. Three transducer diameters of 6.3, 9.5 and 12.7 mm were analyzed at frequencies of 2.25, 3.5, and 5.0 MHz to determine which combinations met criteria (a) above. Combinations which produced incident angles less than 35° and would give mode conversions, and those that would lead to interference from the weld cap were rejected. From these results only those transducer pairs having a 45° transmitter and 55° receiver satisfy the beam angle design requirements. Using this requirement and the geometry configuration from Figure 3, the inspection design parameters for the examination of the body region in 19.5 mm test panels can be established and are given in Table 1.

Previous analysis (1) of the selection of transducers has indicated that a compromise in the beam width at the target is usually required when using common transducer crystal diameters and frequencies, however, inspection criteria goals can still be met. In the case of the pitch-catch technique, transducers having a larger than required beam width will not give rise to false indications and would therefore be acceptable, however beam widths smaller than required could lead to reduced sensitivities and missed imperfections.

Analysis showed that a 6dB beam width large enough to inspect the complete inspection plane could be achieved using a single pair of transducers. The minimum detection requirement of a 1.00 mm deep defect on the inspection plane also translates to an equivalent length of 0.77 mm beam width at the inspection plane. A minimum, therefore, was placed on the required beam width at the target, which includes an allowance for the 0.77 mm, and this is included in Table 1.

Three other factors were considered in the inspection design and these were the effect of local diameter changes, the number of probe pairs/wall thickness relationship, and ability to detect interrun lack of fusion. In terms of diameter changes these occur during the girth welding and result in some localized bending of the pipe adjacent to the girth weld. As long as both the transducers of the pitch-catch arrangement are located within the same deflected angle region of the pipe surface, the inspection geometry and beam angles at the reflecting surfaces are the same as in the ideal case of no pipe deflection, and no adjustment to the design approach would be required. If the two transducers are on different angles of curvature then allowance would have to be made for this. In the present case, however, of 20 mm wall pipe measurements showed that no significant deflections occur at the girth weld and no allowances are needed to be made.

From geometry considerations it was determined (based on a 45° transmitter angle and 55° receiver angle) that inspection of the body region could be achieved using a single pair of common transducers for wall thicknesses ranging from 9.7 to 23.0 mm. The upper limit of 23.0 mm arises only from use of a commonly available receiver transducer of 25.4 mm. The 25.4 mm size arises from calculations that this would be the minimum size required for the detection of the 6dB portion of the transmitted beam.

The pitch-catch technique is primarily designed to achieve detection of lack of sidewall fusion, and its ability to detect lack of interrun fusion is limited due to the inconsistency in the shape and orientation of the defect. The optimum case for detecting lack of interrun fusion would be to use a transmitter transducer in the pulse-echo technique with the lowest possible transducer frequency. Lower frequencies are preferred to provide increased tolerance to defect misorientation particularly to improve the chance of detecting lack of interrun fusion. The upper bound of 5.0 MHz was therefore used in the design to ensure detection of poorly oriented reflection while not severely restricting the range of transducers available for selection.

5.3 Transducer Selection

The diameter, frequency and focussing required for the transmitter transducers with the appropriate frequency and diameter to meet the requirements for beam width at the target path in 19.3 mm thick material (Table 1) were selected according to the process described in the previous sections. Two transducer choices which satisfied the transmitter inspection design requirements are shown in Table 2.

The approach to selecting receiver transducers at the time was simply to:

(a) match the frequency with that of the transmitter transducer and;

(b) have as large a crystal diameter as possible to maximize the detection surface, and no less than required to detect the 6dB portion of the transmitted beam.

As shown, in the discussion, subsequent analysis on the sensitivity at the inspection plane could lead to improvements in the specification of the receiver transducer. The transmitter and receiver transducer selections made for the examination of the body region in the 19.3 mm wall thickness test panels are shown in Table 3. The transmitter transducer was a 2.25 MHz, 45° Shear, 10x10 mm crystal manufactured by Sonatest. The receiver transducer was a 2.25 MHz, 55° Shear, 20x20 mm crystal manufactured by Harisonic.

The transmitter probe was evaluated according to NOVA Specification SUT-2 (3), and the results given in Appendix 2. The results of the signal-to-noise evaluation are given in Figure 4, which shows a signal-to-noise ratio of 35dB at the target path distance of 42.9 mm. The beam width of the probe at the target path distance of 42.9 mm was 7.0 mm. This is slightly below the minimum of 7.1 mm required but is not anticipated to create any problems with minimum defect depth detection capability. No detailed analysis of the receiver probe was carried out except to assess the signal-to-noise level of the tandem probe arrangement on a 19.5 mm thick test plate. The result of 30dB was well in excess of the minimum 12dB required.

6.0 EVALUATION OF PITCH-CATCH TECHNIQUE

6.1 Test Equipment

A tandem probe testing system was set up consisting of the ultrasonic instrument with an X-Y Scanner, and an X-Y Plotter, Figure 5. The ultrasonic instrument was a Masterscan model UFD310, manufactured by Balteau-Sonotest. The instrument provided a broadband (0.5 - 18 MHz) 100dB dynamic range amplifier and was used to control the echo signal (amplitude) on the display screen. Screen horizontal and vertical linearity were established to be within 5% of full screen according to ASTM E317-79. The time base was calibrated using the IIW type 1 block to provide a resolution of 0.1 mm. Using a Hewlett-Packard Model 7046 X-Y Recorder the analog output of the gated signal amplitude was recorded on Channel 1 (vertical axis) which was calibrated to indicate echo amplitude to an accuracy of 2%. The analog output of the path distance (probe index-to-defect) was recorded on Channel 2 (vertical axis) to an axis of 1.5%.

The X-Y Scanner, leased from Atomic Energy of Canada Ltd., was used to control transducer movement and provide an analog signal corresponding to the distance travelled by the probe, which was recorded on the horizontal axis of the X-Y Recorder; position was indicated to an accuracy of 1 mm.

6.2 Test Plates

Two types of test plates were used, one containing machined holes and notches, and the other containing real weld defects.

6.2.1 Machined Reflectors

A test plate was machined from 19.8 mm thick A516 Gr. 70 normalized plate containing a series of 2.0 mm diameter flat bottomed side drilled holes and slots. These reflectors simulated defects in root, body, and cap regions. The body defects were designed to simulate lack of sidewall fusion at depths of 2, 4, 6, 8 and 10 mm; a schematic of the test plate is shown in Figure 6.

6.2.2 Weld Defect Plates

Welded test panels in 19.0 mm thick plates were designed to contain either no defects or defects typical of lack of side wall fusion. Five test panels were welded using typical mechanized GMA procedures, Panel 1 contained no defects and Panels 2 to 5 contained lack of sidewall fusion defects; each test panel had the defect located in a different fill pass. The welds were designed such that the detection capability in the body region could be evaluated. Weld geometry conditions such as high-low were not expected to present a problem for the pitch-catch technique and hence were not included in the test program.

7.0 EXPERIMENTAL PROCEDURE

7.1 Instrument Settings

All the tests were carried out at fixed ultrasonic instrument settings given in Table 4 for both simulated and real weld defects.

The instrument gain level of 50dB on the simulated defects was established to produce a 100% full screen height echo from a 2.0 mm diameter flat bottomed hole in the body region. The D2 hole (Figure 6) was used, as this reflector produced the highest echo response (Figure 7) and ensured that the instrument recording limits were not exceeded during testing of the simulated weld defect plate. During the testing of weld defects it was determined that lower gain levels (as shown in Table 4) were required in order to ensure that recording instruments limits were not exceeded.

For testing of the plate with simulated defects, the detection gate position and width were set using the calibrated time base, so that the gated region began at a position 5 mm before the beam axis intersected the inspection plane (D) and finished 5 mm after the intersection. The gate size was selected to ensure the gate started 2 mm prior to the shortest path expected and ended 2 mm after the longest path expected for a fixed probe surface position.

Testing of the real weld defects used the same gate start position, but the gate width was increased by 5 mm. This increase in gate size was to enable possible detection of defects up to the weld centerline.

In all tests a frequency of 1.5 to 3.5 MHz was used with no rejection to suppress noise levels. The required probe delay length was determined based on a known probe index-to-surface reflector distance. An instrument time base range of 50 mm was used to maximize path distance accuracy.

7.2 Testing Procedure

Tests were initially carried out on the simulated weld defect plate to establish a basis for those instrument settings described in Section 7.1 and to determine the probe position for the welded test panels.

7.2.1 Tests on Simulated Weld Defect Plate

A total of five tests were carried out on the test plate shown in Figure 6 beginning with the probe index-to-edge of weld preparation of 48 mm. In each subsequent test this distance was increased by 1 mm, up to 52 mm. The probe index-to-edge of weld preparation of 50 mm was based on trial tests which showed it to be optimum based on echo height; each shorter and longer distance represents possible probe positioning errors. The X-Y Scanner was used to control the probe movement during each test after the initial probe position had been established. The positioning accuracy in each dimension was 0.5 mm.

Maximum scanning speed was 4.2 mm/sec. Echo response and path distance data were obtained from the analog recording produced during each test using the equipment described in Section 6.0. A recording level of 10% of full screen was used and represents a level of 12dB above the noise level measured according to procedure SUT-1 (4).

7.2.2 Tests on Real Weld Defect Plates

A total of five 19.0 mm thick plates were examined. Each plate was examined once at the optimum transmitter probe index-to-weld preparation distance of 50 mm. During these tests the gain level was reduced in comparison to the simulated defects because the defect sizes were producing large echo amplitudes, exceeding 100% full screen height at 50dB. The gain level was therefore adjusted for each inspection to ensure that calculations of signal-to-noise ratios could be accurately made. A total of 16 locations were selected for metallographic cross-sectioning to verify the presence and size of the weld defects detected.

8.0 RESULTS AND ANALYSIS

The most significant measure of detecting performance is considered to be the signal-to-noise ratio. A large signal-to-noise ratio is required to ensure reliable detection of defects. The noise level used in the determination of the signal-to-noise ratio of the simulated and real defects was that measured during the probe evaluation, namely 80% full screen height at 70dB gain. The signal level was determined from the analog recordings; the maximum signal amplitude measured was used to calculate signal-to-noise results for the simulated defects; the amplitude at selected locations on the analog recordings were used to determine results on the welded test panels. Weld cross-sectioning at the selected locations verified the presence and size of each defect.

8.1 Performance on Simulated Defects

The results of the analysis of defects in the through-thickness location at different probe index positions are given in Figure 7. In all cases for the body region, Plane D, signal-to-noise levels exceeded the goal of 12dB. Defects located in the C region were not in a favourable orientation and were not expected to be detected. Similarly the pitch-catch inspection criteria was not designed for defects in the A or E planes, and although these defects were found they were well below the threshold value of 12dB. Based on these results the pitch-catch technique could be expected to provide satisfactory detection of planar defects in the body region of a 20 mm thick GMA weld. The results also show a higher echo response from reflectors deep in Plane D than those nearer the surface.

8.2 Performance on Real Weld Defects

The analysis carried out to assess the performance on real welds defects related the signal-to-noise level to the projected through-wall depth of the weld defects. Projected depths were determined from metallographic cross-sections at selected locations. A total of 16 locations were sectioned corresponding to random positions from the analog reading. The defects were designed to be in the 1st, 2nd, 3rd and 4th fill, however during sectioning it was found that many locations had defects in several fill locations. The overall results are summarized in Table 5 and plotted in terms of signal-to-noise versus total depth in Figure 8. The vertical and horizontal dotted lines in figure represent specified performance goals; 1.0 mm minimum projected depth at a 12dB minimum detection threshold. The results show that in all cases lack of sidewall fusion defects greater than 1 mm in projected through-wall depth resulted in a signal-to-noise level above 12dB, demonstrating satisfactory performance.

Analysis of the results in Table 5 and Figure 8 also show that defects less than 1.00 mm deep can also be satisfactorily detected at threshold levels greater than 12dB. Some of the individual defects in sections 4.1 and 4.2 of only 0.4 to 0.8 mm deep (Figure 9) give signal-to-noise ratios of 19-29dB. Whilst the results from the simulated defects showed improved resolution from those defects at greater depths (Figure 7), no such clear indication was obtained from the real weld defects. This was primarily because multiple defects were present on the sidewall in many cases, Figure 10. Small defects within the body of the weld were clearly well resolved as shown in Figure 11. Individual defects near the surface of the weld were also well resolved (Figure 12).

In addition to achieving satisfactory signal-to-noise values above a detection threshold level, it is necessary to position the detection gate to ensure defects will not be missed. The analysis used to determine the required detection-gate size relates back to the measured path distance at the defect locations. The inspection of the near vertical Plane D makes the definition of the gate size relatively easy. The preliminary analysis shows that a tolerance of at least 1 mm is required to ensure that no errors arise from the tolerance of the probe positioning or from weld scanner tracking error during pipe weld inspection. Maximum gate size can also be specified to the centerline of the weld will ensure that the possibility of false defect indications is eliminated. During weld inspection defects were also detected on the far side of the weld (Figure 13), which were clearly outside of the gate and normally would be gated out during the mechanized inspection.

9.0 DISCUSSION

The study has concentrated on the ability of the pitch-catch technique to detect defects in the body region of 19.5 mm mechanized gas metal arc welds. Only the 19.5 mm wall thickness was investigated as it had been previously shown that the body region of a 9.5 mm wall thickness could be adequately inspected using the creeping wave technique. Detailed analysis of the inspection criteria resulted in specifying a 2.25 MHz 45° transmitter probe with a 9.5 mm diameter and a 2.25 MHz 55° receiver probe with a 25.4 mm diameter. This combination of probes could be used to inspect the body region of wall thicknesses from 9.7 to 23.0 mm. The low frequency was specified to maximize the sensitivity on lack of sidewall fusion defects as well as lack of interrun fusion defects, although the technique was primarily designed for lack of sidewall fusion defects.

Analysis of the characteristics of the transmitter probe showed that it met all the specified design requirements with the exception of beam width. This was specified at 7.5 mm, however it was actually 7.0 mm. Initial analysis showed that a minimum beam size of 7.1 mm was required to ensure that defects 1.0 mm and greater were detected. Subsequent results, however, showed that defects less than 1.0 mm could still be detected with the minimum beam size of 7.0 mm.

Inspection results of the pitch-catch technique on simulated and real defects indicated that the inspection design methodology provided good detection performance on planar lack of fusion defects and potential freedom from false indications in the body region of the weld. Signal response from the real weld defects was much better than from the simulated defects because of the defect size, again reinforcing the requirement of setting up the sensitivity levels on actual calibration blocks containing milled and real defects for use in full scale tests. The performance goals of 1 mm projected detectable depth at signal-to-noise ratios of greater than 12dB were easily met on real weld defects. Defects with a through wall dimension of 0.4 mm were also found with signal-to-noise levels greater than 12dB. Destructive examination did not find any defects larger than 1 mm that gave a signal-to-noise ratio of less than 12dB. Defects were also detected that were less than 3 mm from the surface, which again exceeds the minimum requirements. The specification of a minimum dimension of 3 mm from the surface is designed to ensure that no missed defects occur because of loss of signal in the cap region. This region will normally be inspected by the creeping wave probe.

The results of the tests on the simulated defects in the body region show that while the signal-to-noise ratio always exceeded 12dB a gradual decrease in the ratio occurred as the probe index-to-weld preparation is increased or reduced from the optimum. This confirms that the original weld preparation edge or centerline will have to be indexed prior to welding when utilizing the inspection procedure in the field. The results also confirm that poor results would be obtained from defects located on Plane C and oriented at a 45° angle to the vertical. This plane however will be investigated by the root pass focussed probes.

The inspection design criteria used in the present approach has been to inspect the body region using a single pair of transducers. This means that a single 6dB beam width at the inspection plane has to be capable of covering the complete body region. The results of the inspection on simulated defects in Figure 7 point to a potential problem with using this philosophy. An increase of approximately 12dB occurs between those defects near the surface (D5) and those in the middle of the inspection plane (D3). Therefore in order to detect small defects near the D5 location, equivalent small defects at D3 will give high signal-to-noise ratios. Indicating, therefore, that very small defects detected with large amplitude signals are close to "false indications". Similar results can also be seen from the real weld defects where very small defects in the middle of the weld were detected with large signal-to-noise ratios. Whilst this may not be a problem with very short defects (i.e. defects less than 1.00 mm in depth and with no significant length), it could present a problem if the defect had reasonable length if this really does prove to be a problem in the field then one solution would be to divide the inspection plane into two. In this manner the beam width required at the inspection plane is halved and the sensitivity spread response to small and large defects within each region is reduced, thus further reducing the likelihood of false indications. By dividing the inspection plane in two would mean that two pairs of transmit-receive transducers would be required rather than one pair.

Another improvement that could be made would be in the specification of the receiver transducer. In the present case the requirement was to be able to receive the 6dB edge of the beam. An improved approach would be to assess the receiver as a transmitter and to specify its requirements on the basis of a 6dB beam width at the inspection plane. This should improve the sensitivity spread at the plane. In conjunction with this the inspection could then be carried out in a switching mode by alternating the receiver to a transmit mode and vice-versa.

No detailed analysis was performed in lack of interrun defects, however, their detection could be improved by using the transmitter transducer in the pulse-echo mode. During an actual field evaluation, therefore, the system could be set up electrically to switch the transmit to a pulse-echo mode and to combine this with a subsequent switch to the receive mode with the other transducer transmitting. In this way a three stage inspection would be carried out using transmit-receive, switch to receive-transmit, switch to transmit pulse-echo.

The program has shown that an inspection criteria can now be specified for the complete inspection of gas metal arc welds from the root to the cap without the possibility of false indications or missed defects. The next stage of the program is therefore to produce full scale girth welds for laboratory investigation.

REFERENCES

1. Fingerhut, M.P., Coote, R.I. and Hodgkinson D., "The Selection of Ultrasonic Transducers for the Inspection of Pipeline Girth Welds". Part 1. December 1986 NOVA Tech. Lit. #15034

2. Fingerhut, M.P., Glover, A.G. and Dorling, D.V., "Evaluation of a Unique Creeping Wave Probe for Examination of the Cap Region in Pipeline Girth Welds". Part 2. September 1987 NOVA Tech. Lit. #15047

3. NOVA Specification SUT-2, "Performance Specification for Medium Frequency, Shear Wave Angle Probes".

4. NOVA Specification SUT-1, "Procedure for the Determination of the Detection Threshold Level for Mechanized Ultrasonic Examination".

TABLE 1

INSPECTION DESIGN REQUIREMENTS FOR PLANE D IN 19.3 mm WALL TEST PANELS

TRANSDUCER	BEAM ANGLE (°)	SURFACE POSITION INDEX TO CENTER LINE OF WELD (mm)	REQUIRED MINIMUM BEAM WIDTH AT THE TARGET (mm)	EQUIVALENT TARGET PATH (mm)
TRANSMITTER	45	33.8	7.1	58.1
RECEIVER	55	70.0	Not Specified	84.3

TABLE 2

ALTERNATIVE TRANSMITTER TRANSDUCER SELECTIONS CONSIDERED

NO.	FREQUENCY (MHz)	DIAMETER (mm)	BEAM WIDTH AT THE TARGET (mm)
1	2.25	9.5	9.0
2	3.50	6.3	8.7

TABLE 3

TRANSMITTER AND RECEIVER TRANSDUCER SELECTIONS FOR INSPECTION OF THE BODY REGION IN 19.3 mm WALL THICKNESS PLATES

TRANSDUCER	FREQUENCY (MHz)	DIAMETER (mm)
TRANSMITTER	2.25	9.5
RECEIVER	2.25	25.4

TABLE 4

ULTRASONIC INSTRUMENT SETTINGS FOR TESTING ON SIMULATED AND REAL WELD DEFECTS

ULTRASONIC INSTRUMENT - BALTEAU-SONATEST, MASTERSCAN 310

	TESTING ON SIMULATED DEFECTS	TESTING ON REAL WELD DEFECTS
GAIN	50dB	30-40dB
GATE START	57 mm	57 mm
GATE FINISH	67 mm	72 mm
RECORDING THRESHOLD	@ 10% FSH	@ 5% FSH
RANGE	50 mm	50 mm
DELAY	1.4 mm	1.4 mm
REJECT	Off	Off
FREQUENCY	1.5 to 3.5 MHz	1.5 to 3.5 MHz

TABLE 5

RESULTS OF PITCH-CATCH PERFORMANCE ON REAL WELD DEFECTS

WELD NUMBER	CROSS-SECTION NUMBER	DEFECT DEPTHS (mm)	DEPTH OF TOP DEFECT FROM SURFACE (mm)	TOTAL PROJECTED DEPTH (mm)	SIGNAL TO-NOISE dB
1	1.1	No Defects	-	-	0
2	2.1	0.3	1.2		
		2.4	6.9		
		1.9	12.0	4.6	35
	2.2	0.4	1.5		
		1.3	7.1		
		2.6	11.9	4.3	38
	2.3	0.3	1.8		
		8.1	5.9	8.4	41
	2.4	0.6	2.5		
		6.9	7.3		
		1.0	6.2	8.5	41
3	3.1	0.7	7.8	0.7	29
	3.2	2.1	7.7	2.1	34
4	4.1	0.8	5.2	0.8	19
	4.2	0.4	5.0	0.4	29
	4.3	7.9	2.4		
		1.4	0.9		
		0.8	11.1	10.1	36
	4.4	5.3	2.0	5.3	31
	4.5	4.8	2.2	4.8	33
	4.6	0.8	2.5		
		0.2	3.9		
		0.6	5.1		
		0.3	11.5	1.9	20
5	5.1	2.4	1.4	2.4	27
	5.2	3.4	0.6		
		3.0	11.2	6.4	32
	*	(0.8)	(13.0)		
	5.3	2.2	2.0	2.2	18

* Deep on opposite side (ignored in total depth calculation)

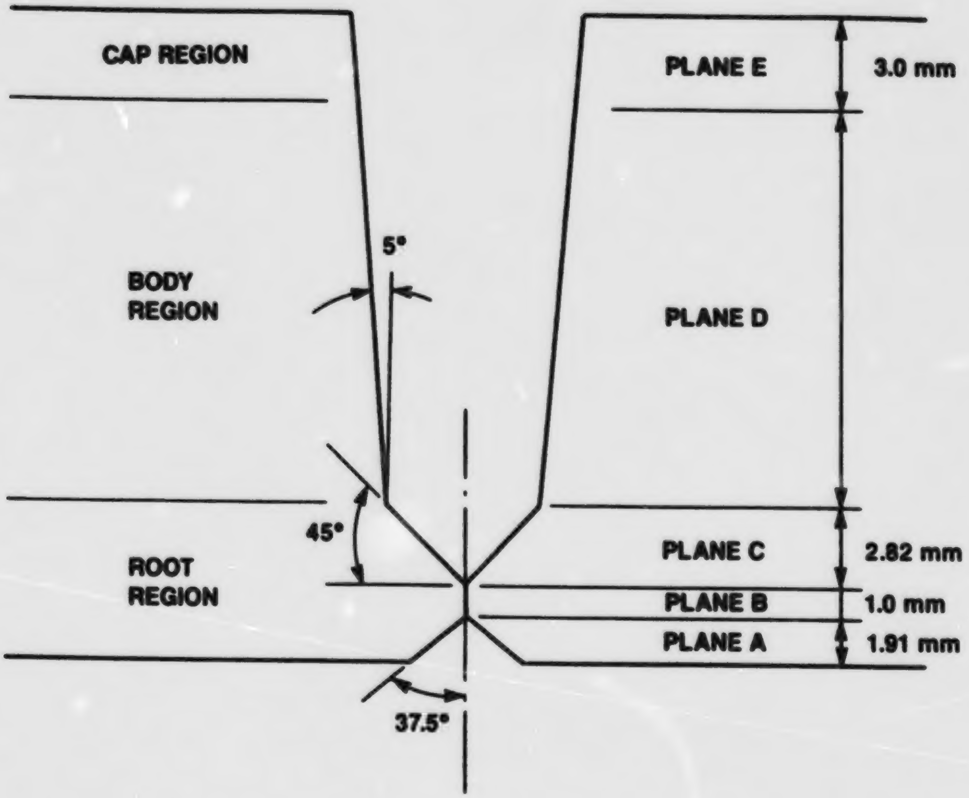
CAP REGION
PLANE E
3.0 mm
5°
BODY REGION
PLANE D
45°
ROOT REGION
PLANE C
2.82 mm
PLANE B
1.0 mm
PLANE A
1.91 mm
37.5°

Figure 1: Geometry of Gas Metal Arc Weld, Showing Definition of Body Region, Plane D.

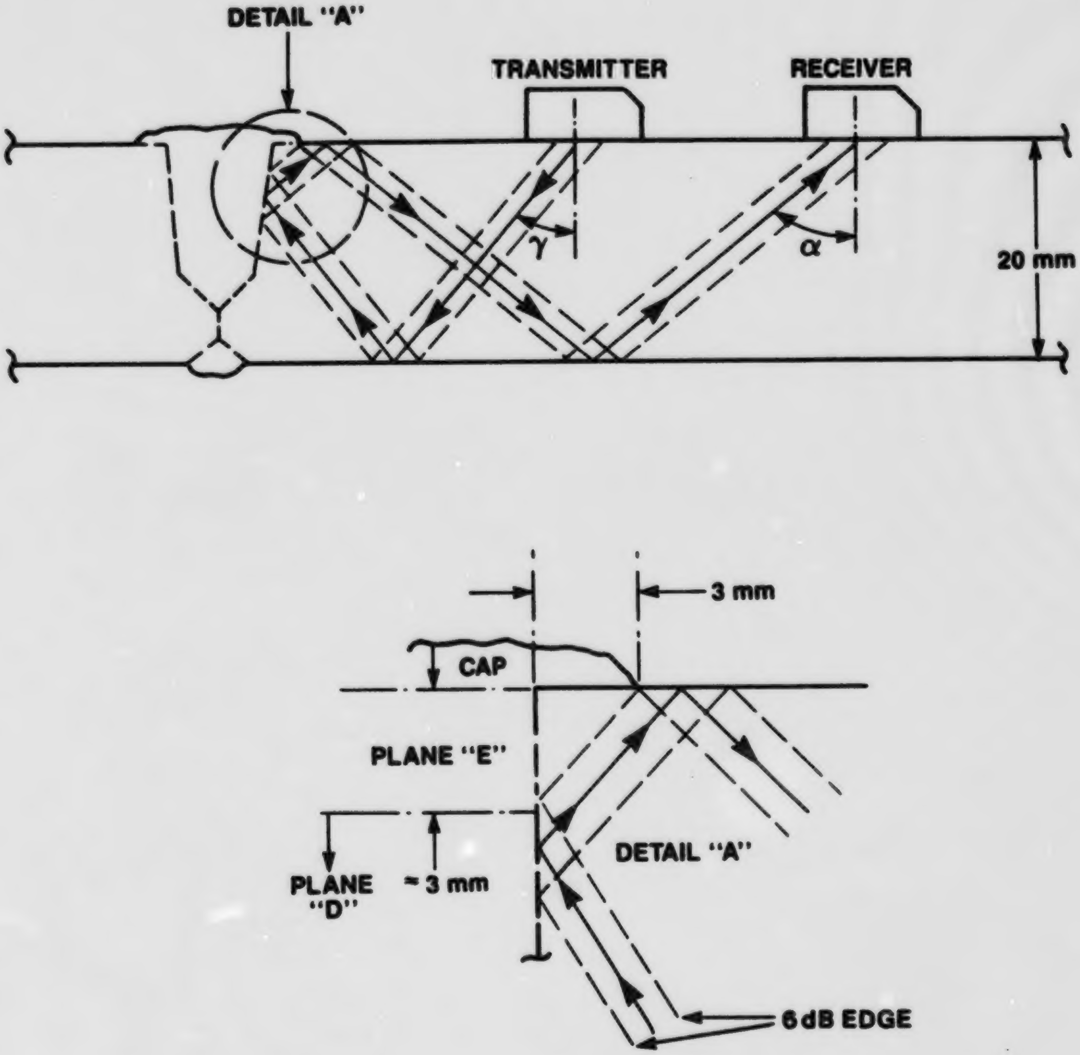
DETAIL "A"
TRANSMITTER
RECEIVER
γ
α
20 mm
3 mm
CAP
PLANE "E"
PLANE "D"
≈ 3 mm
DETAIL "A"
6dB EDGE

Figure 2: Elements of the "Pitch-Catch" Technique.

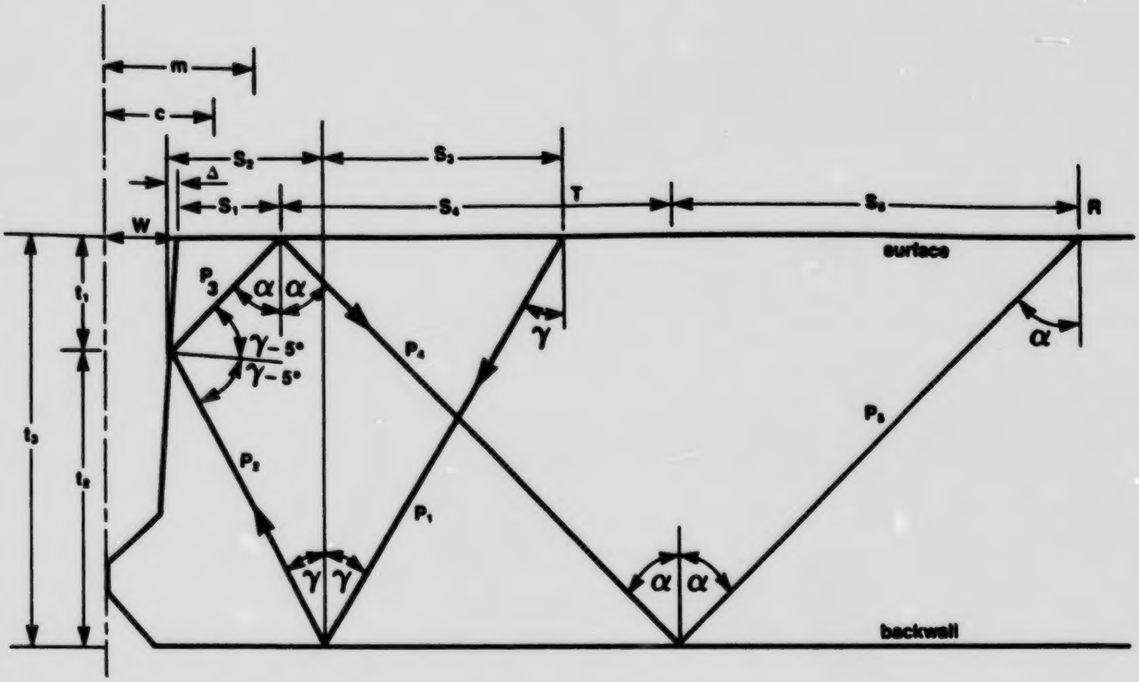
m
c
S_2
S_3
Δ
S_1
S_4
T
S_5
R
W
surface
P_3
α α
$\gamma - 5°$
$\gamma - 5°$
P_4
γ
α
t_1
t_3
t_2
P_2
P_1
P_5
γ γ
α α
backwall

γ = TRANSMITTER TRANSDUCER BEAM ANGLE
α = RECEIVER TRANSDUCER BEAM ANGLE
P_1, P_2 = TRANSMITTER TO TARGET PATH
P_3, P_4, P_5 = RECEIVER PATH
W = WELD CENTRELINE TO EDGE OF WELD PREP
Δ = EQUIVALENT SURFACE DISTANCE FROM EDGE OF WELD PREP TO BEAM AXIS REFLECTION POINT ON INSPECTION PLANE
S_1 = SURFACE DISTANCE FROM EDGE OF WELD PREP TO RECEIVER BEAM SKIP LOCATION
S_2 = SURFACE DISTANCE FROM REFLECTION POINT TO BACKWALL SURFACE
S_3 = SURFACE DISTANCE FOR ONE-HALF SKIP TRANSMITTER BEAM PATH
S_4, S_5 = SURFACE DISTANCE FOR ONE-HALF SKIP RECEIVER BEAM PATH
t_1 = INSPECTION SURFACE TO BEAM AXIS REFLECTION POINT ON INSPECTION PLANE
t_2 = BACKWALL SURFACE TO BEAM AXIS REFLECTION POINT ON INSPECTION PLANE
t_3 = WALL THICKNESS
C = WELD CENTRELINE TO EDGE OF WELD CAP
m = MINIMUM TRANSDUCER FRONT SURFACE TO WELD CENTRELINE DISTANCE.

Figure 3: Weld Joint Cross Section and Inspection Design Reference Dimensions.

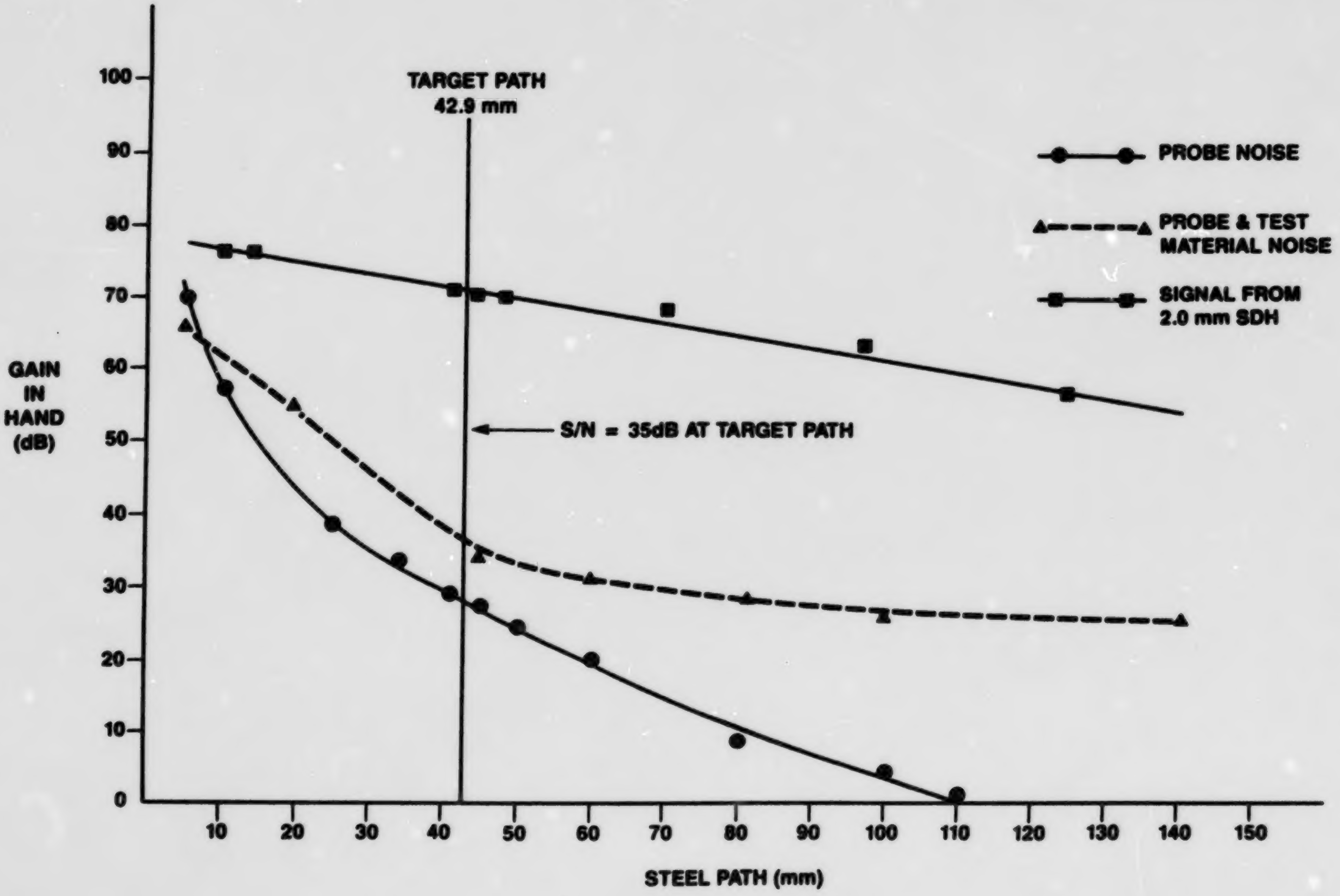

Figure 4: Signal-to-Noise Analysis for Transmitter Probe.

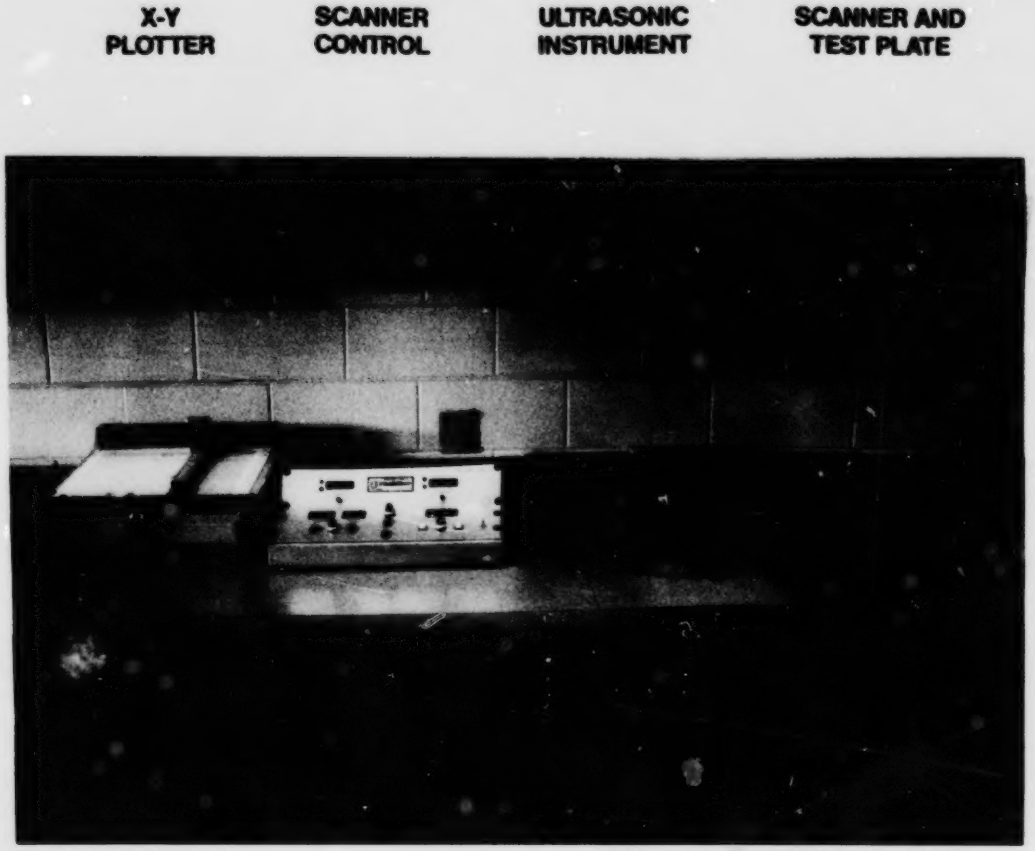
X-Y PLOTTER
SCANNER CONTROL
ULTRASONIC INSTRUMENT
SCANNER AND TEST PLATE

Figure 5: Ultrasonic Probe Testing System.

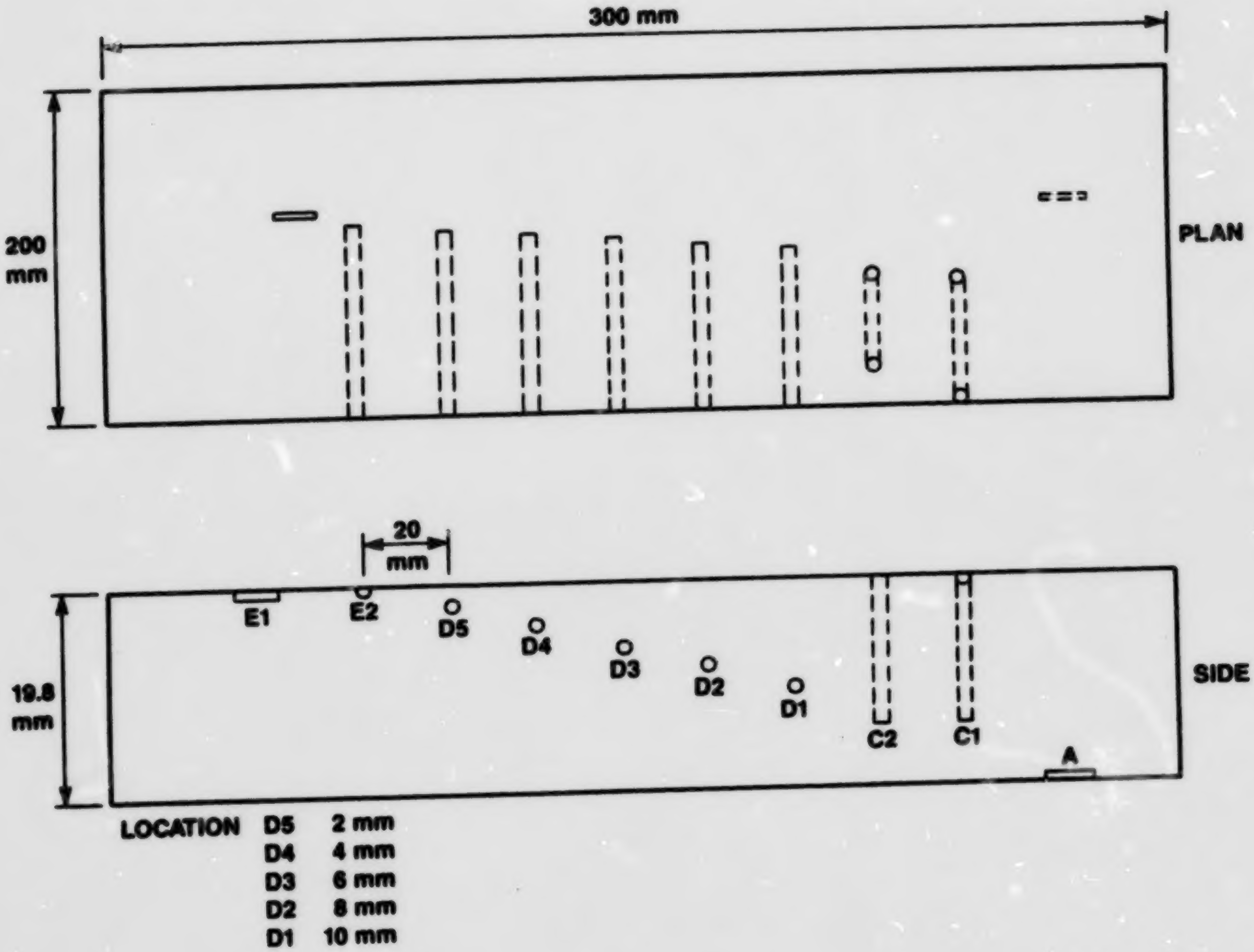
300 mm
200 mm
PLAN
20 mm
E1
E2
D5
D4
D3
D2
D1
C2
C1
A
19.8 mm
SIDE
LOCATION
D5 2 mm
D4 4 mm
D3 6 mm
D2 8 mm
D1 10 mm

Figure 6: Schematic of Test Plate for Simulated Defects.

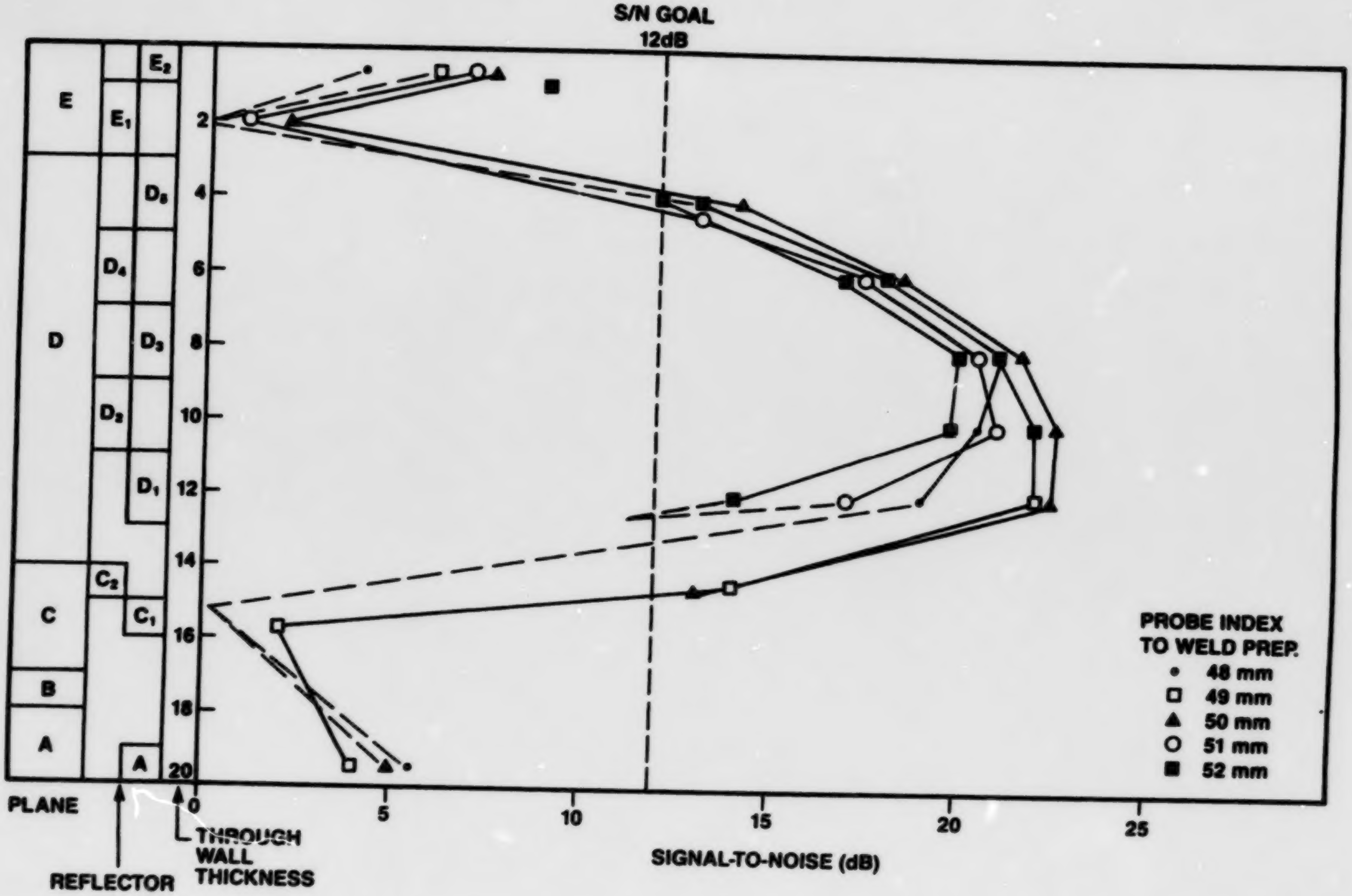

Figure 7: Signal-to-Noise Measured on Simulated Defects with the Pitch-Catch Technique.

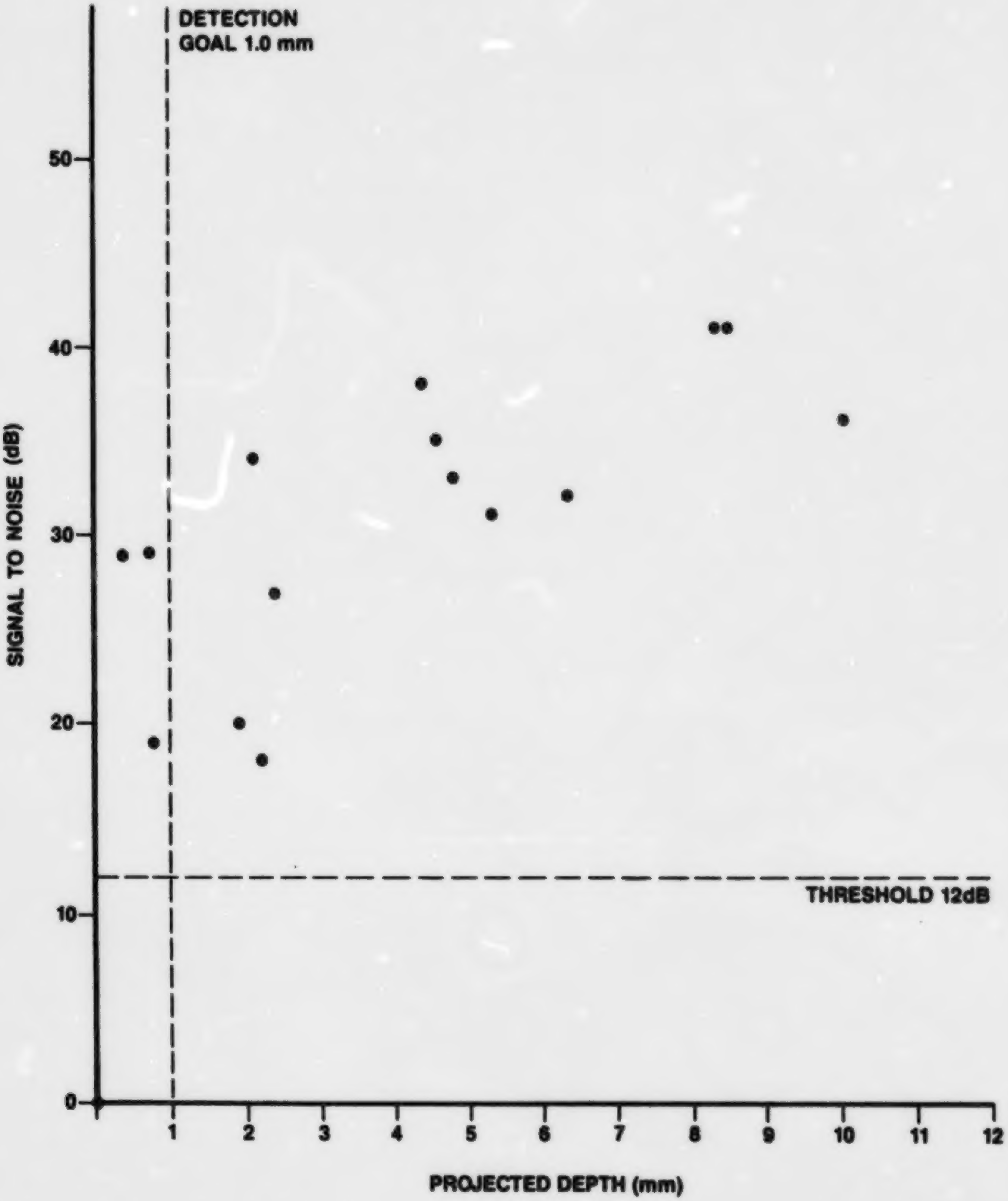

Figure 8: Signal-to-Noise versus Projected Through-Wall Depth (Total) on Weld Test Panels.

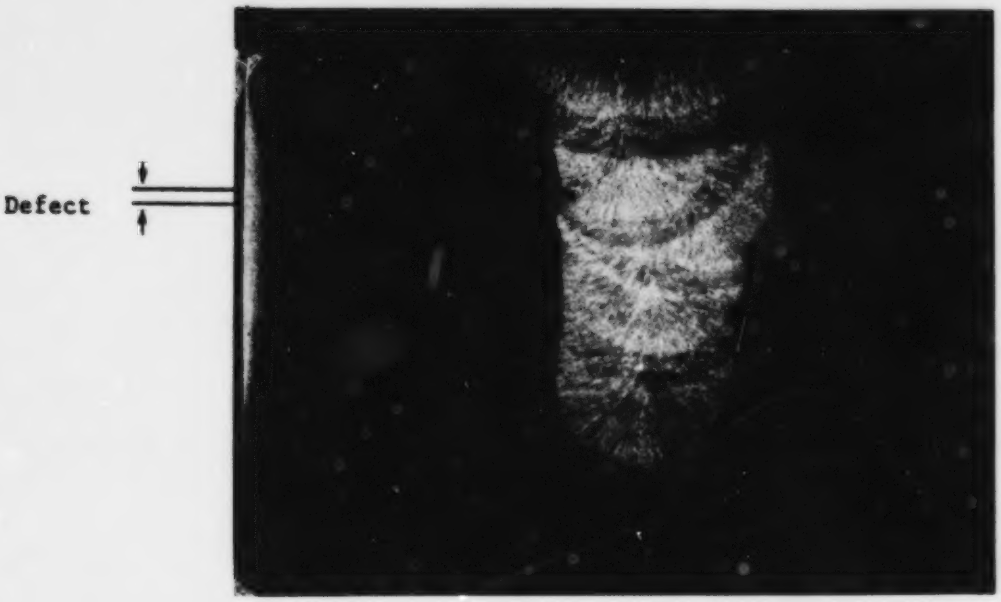

Figure 9: Section Through Weld 4, Location 4.1 Showing Defect 1.0 mm, Magnification X 3.5

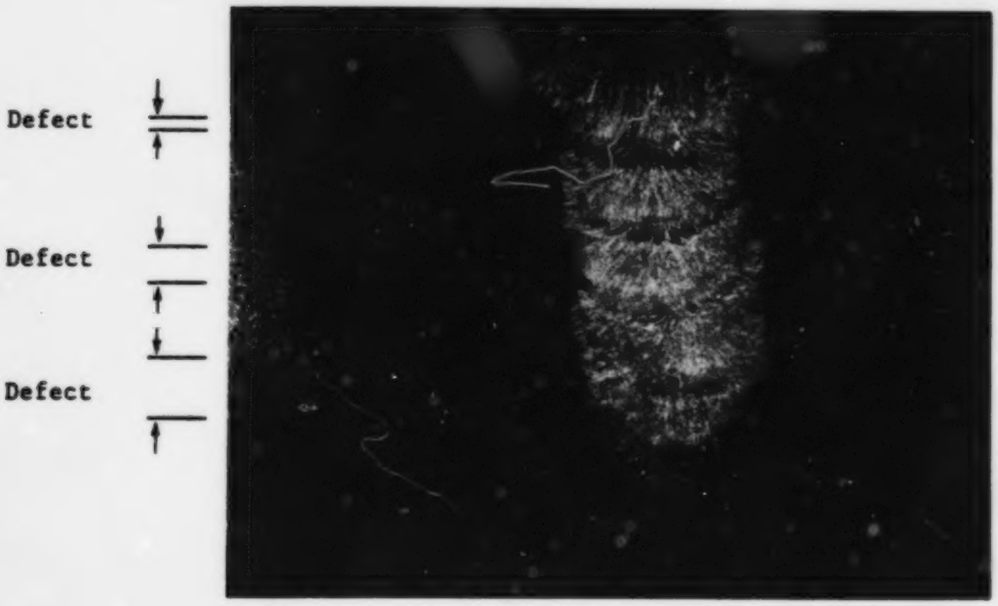
Defect
Defect
Defect

Figure 10: Section Through Weld 2, Location 2.2, Showing Three Defect Locations, Magnification X 3.5

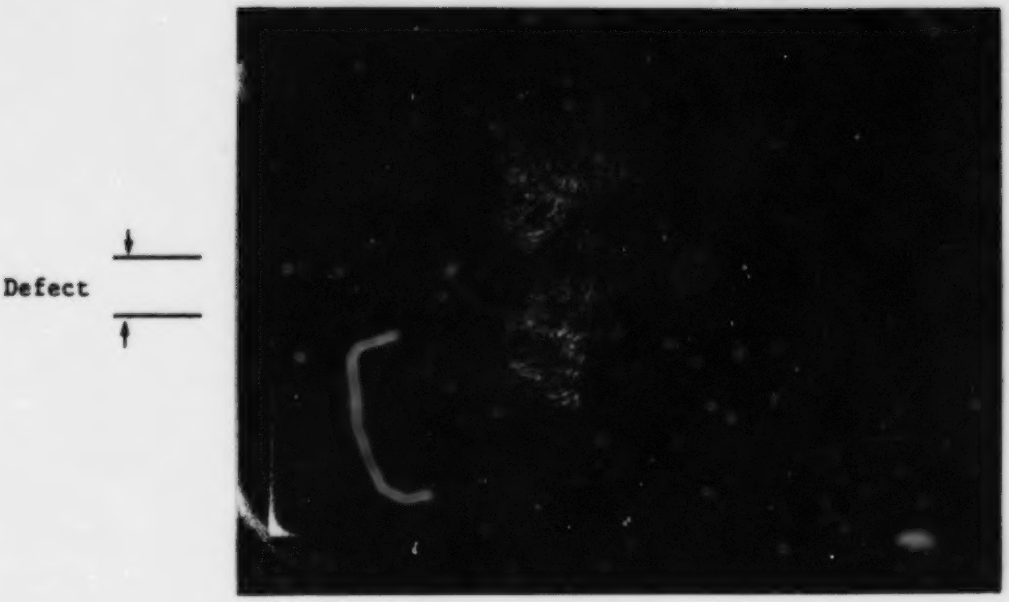

Figure 11: Section Through Weld 3, Location 3.2, Showing Individual Defect, Midwall, Magnification X 3.5

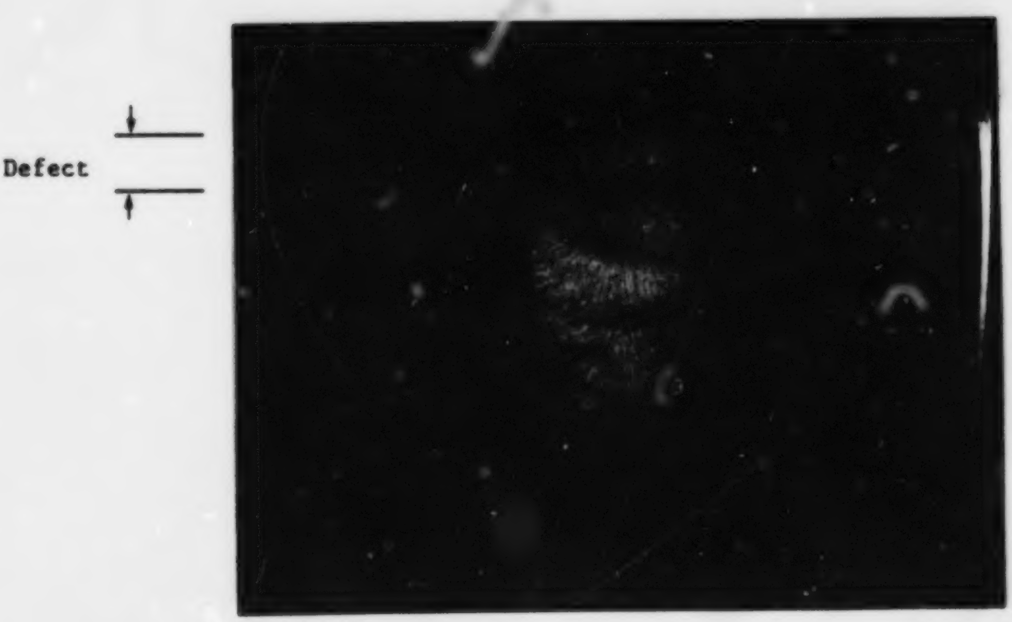

Figure 12: Section Through Weld 5, Location 5.1, Showing Defect Located Near Cap, Magnification X 3.5

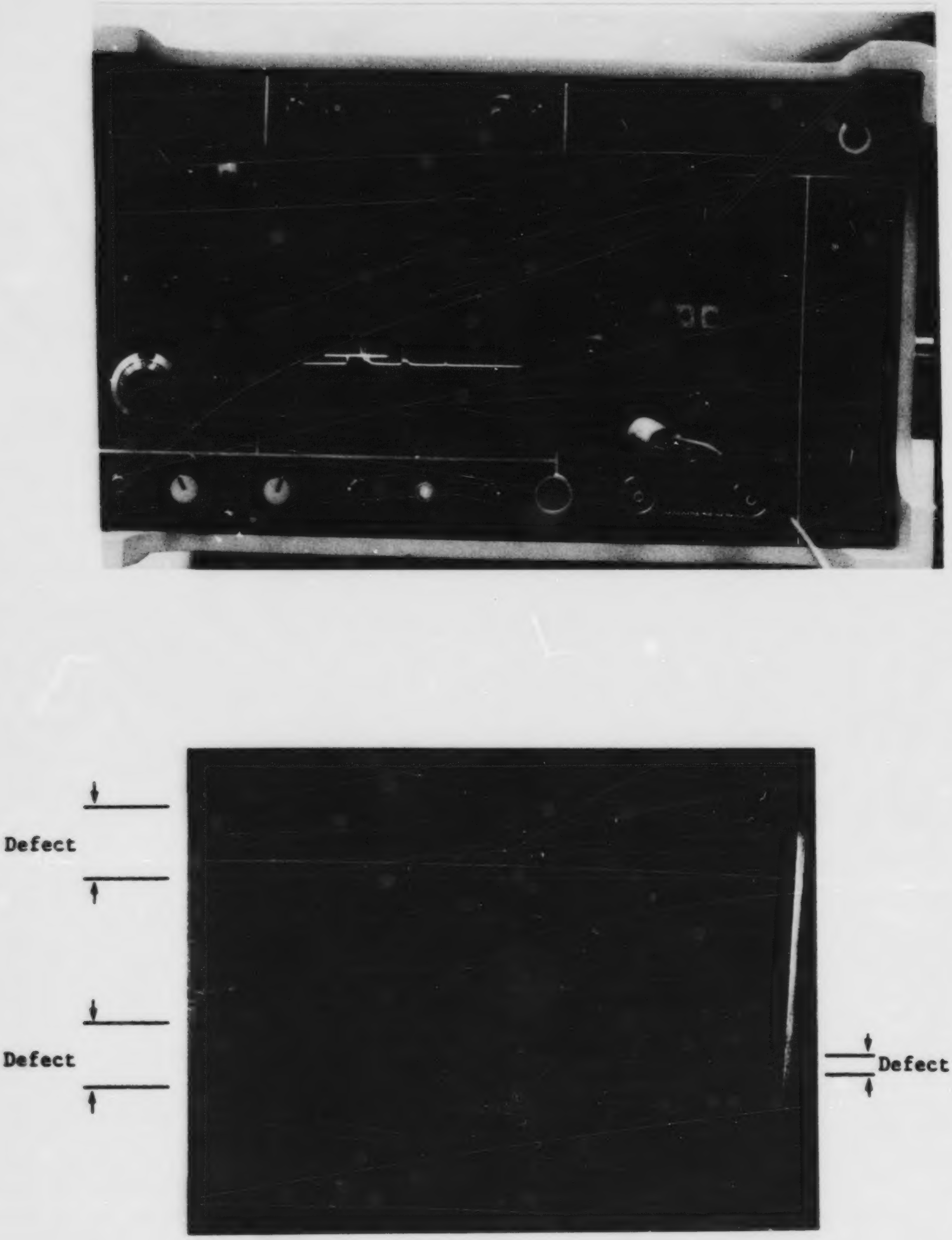
Defect
Defect
Defect

Figure 13: Ultrasonic Display and Cross Section Showing Defect on Far Side of Weld Outside The Gate, Macrosection X 3.5

APPENDIX 1

PITCH-CATCH TECHNIQUE INSPECTION DESIGN TABLES

PITCH-CATCH TECHNIQUE INSPECTION DESIGN TABLES

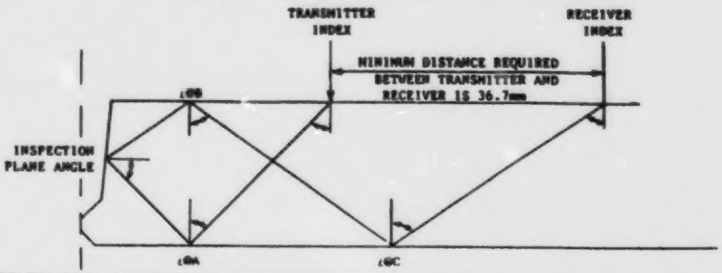
TRANSMITTER INDEX
RECEIVER INDEX
MINIMUM DISTANCE REQUIRED BETWEEN TRANSMITTER AND RECEIVER IS 36.7mm
INSPECTION PLANE ANGLE
∠ΘB
∠ΘA
∠ΘC

	FREQ. (MHz)	TRANSMITTER			POINT A			INSPECTION PLANE			POINT B			POINT C			RECEIVER			MINIMUM RECEIVER TRANSDUCER DIAMETER REQUIRED (mm)
		BEAM ANGLE	MAX ANGLE	MIN ANGLE	BEAM ANGLE	MAX ANGLE	MIN ANGLE	BEAM ANGLE	MAX ANGLE	MIN ANGLE	BEAM ANGLE	MAX ANGLE	MIN ANGLE	BEAM ANGLE	MAX ANGLE	MIN ANGLE	BEAM ANGLE	MAX ANGLE	MIN ANGLE	
TRANSMITTER TRANSDUCER DIAMETER 6.3mm	2.25	35	41.6	28.4	35	41.6	28.4	50	56.6	43.4	45	51.6	38.4	45	51.6	38.4	45	51.6	38.4	
	3.5	35	39.2	30.8	35	39.2	30.8	50	54.2	45.8	45	49.2	40.8	45	49.2	40.8	45	49.2	40.8	R_1
	5.0	35	38.0	32.0	35	38.0	32.0	50	53.0	47.0	45	48.0	42.0	45	48.0	42.0	45	48.0	42.0	
	2.25	40	46.6	33.4	40	46.6	33.4	45	51.6	38.4	50	56.6	43.4	50	56.6	43.4	50	56.6	43.4	
	3.5	40	44.2	35.8	40	44.2	35.8	45	49.2	40.8	50	54.2	45.8	50	54.2	45.8	50	54.2	45.8	
	5.0	40	43.0	37.0	40	43.0	37.0	45	48.0	42.0	50	53.0	47.0	50	53.0	47.0	50	53.0	47.0	R_2
	2.25	45	51.6	38.4	45	51.6	38.4	40	46.6	33.4	55	61.6	48.4	55	61.6	48.4	55	61.6	48.4	
	3.5	45	49.2	40.8	45	49.2	40.8	40	44.2	35.8	55	59.2	50.8	55	59.2	50.8	55	59.2	50.8	32.8
	5.0	45	48.0	42.0	45	48.0	42.0	40	43.0	37.0	55	58.0	52.0	55	58.0	52.0	55	58.0	52.0	20.8
	2.25	50	56.6	43.4	50	56.6	43.4	35	41.6	28.4	60	66.6	53.4	60	66.6	53.4	60	66.6	53.4	14.31 A
	3.5	50	54.2	45.8	50	54.2	45.8	35	39.2	30.8	60	64.2	55.8	60	64.2	55.8	60	64.2	55.8	
	5.0	50	53.0	47.0	50	53.0	47.0	35	38.0	32.0	60	63.0	57.0	60	63.0	57.0	60	63.0	57.0	R_1
TRANSMITTER TRANSDUCER DIAMETER 9.5mm	2.25	35	39.4	30.6	35	39.4	30.6	50	54.4	45.6	45	49.4	40.6	45	49.4	40.6	45	49.4	40.6	
	3.5	35	37.8	32.2	35	37.8	32.2	50	52.8	47.2	45	47.8	42.2	45	47.8	42.2	45	47.8	42.2	R_1
	5.0	35	37.0	33.0	35	37.0	33.0	50	52.0	48.0	45	47.0	43.0	45	47.0	43.0	45	47.0	43.0	
	2.25	40	44.4	35.6	40	44.4	35.6	45	49.4	40.6	50	54.4	45.6	50	54.4	45.6	50	54.4	45.6	
	3.5	40	42.8	37.2	40	42.8	37.2	45	47.8	42.2	50	52.8	47.6	50	52.8	47.6	50	52.8	47.6	
	5.0	40	42.0	38.0	40	42.0	38.0	45	47.0	43.0	50	52.0	48.0	50	52.0	48.0	50	52.0	48.0	R_2
	2.25	45	49.4	40.6	45	49.4	40.6	40	44.4	35.6	55	59.4	50.6	55	59.4	50.6	55	59.4	50.6	
	3.5	45	47.8	42.2	45	47.4	42.2	40	42.8	37.2	55	57.8	52.2	55	57.8	52.2	55	57.8	52.2	21.6
	5.0	45	47.0	43.0	45	47.0	43.0	40	42.0	38.0	55	57.0	53.0	55	57.0	53.0	55	57.0	53.0	13.9
	2.25	50	54.4	45.6	50	54.4	45.6	35	39.4	30.6	60	64.4	55.6	60	64.4	55.6	60	64.4	55.6	9.7 A
	3.5	50	52.8	47.2	50	52.8	47.2	35	37.8	32.2	60	62.8	57.6	60	62.8	57.6	60	62.8	57.6	
	5.0	50	52.0	48.0	50	52.0	48.0	35	37.0	33.0	60	62.0	58.0	60	62.0	58.0	60	62.0	58.0	R_1
TRANSMITTER TRANSDUCER DIAMETER 12.7mm	2.25	35	38.3	31.7	35	38.3	31.7	50	53.3	46.7	45	48.3	41.6	45	48.3	41.6	45	48.3	41.6	
	3.5	35	37.1	32.9	35	37.1	32.9	50	52.1	47.9	45	47.1	42.9	45	47.1	42.9	45	47.1	42.9	R_1
	5.0	35	36.5	33.5	35	36.5	33.5	50	51.5	48.5	45	46.5	43.5	45	46.5	43.5	45	46.5	43.5	
	2.25	40	43.3	36.7	40	43.3	36.7	45	48.3	41.7	50	53.3	46.7	50	53.3	46.7	50	53.3	46.7	
	3.5	40	42.1	37.9	40	42.1	37.9	45	47.1	42.9	50	52.1	47.9	50	52.1	47.9	50	52.1	47.9	R_2
	5.0	40	41.5	38.5	40	41.5	38.5	45	46.5	43.5	50	51.5	48.5	50	51.5	48.5	50	51.5	48.5	
	2.25	45	48.3	41.7	45	48.3	41.7	40	43.3	36.7	55	58.3	51.7	55	58.3	51.7	55	58.3	51.7	
	3.5	45	47.1	42.9	45	47.1	42.9	40	42.1	37.9	55	57.1	52.9	55	57.1	52.9	55	57.1	52.9	16.1
	5.0	45	46.5	43.5	45	46.5	43.5	40	41.5	38.5	55	56.5	53.5	55	56.5	53.5	55	56.5	53.5	10.3 A
	2.25	50	53.3	46.7	50	53.3	46.7	35	38.3	31.7	60	63.3	56.7	60	63.3	56.7	60	63.3	56.7	7.2
	3.5	50	52.1	46.7	50	52.1	47.9	35	37.1	32.9	60	62.1	57.9	60	62.1	57.9	60	62.1	57.9	
	5.0	50	51.5	48.5	50	51.5	48.5	35	36.5	33.5	60	61.5	58.5	60	61.5	58.5	60	61.5	58.5	R_1

R_1 = Rejectable, incident angle < critical angle for mode conversion.
R_2 = Rejectable, incident angle on inspection plane would lead to weld cap interference.
A = Acceptable

APPENDIX 2

EVALUATION OF TRANSMITTER PROBE ACCORDING TO SUT-2

APPENDIX

REPORT SHEET FOR ULTRASONIC PROBE RESULTS (SINGLE CRYSTAL)

Specification Applied: ESI Standard 98-2 for Ultrasonic Probes: Medium Frequency, Miniature Shear Wave, Angle Probes

Probe Manufacturers and Identification: SA_2 - 45° SONATEST

Probe Specification and Dimensions: 10 X 10 mm, lead zirconate titanate, 2.25 MHz

Flaw Detector, Cable and Critical Control Settings: SONATEST 310

Electrical Matching: ____________________

Mechanical Construction (including subjective comments): Appears to be well constructed.

Operator and Date: 88 01 21

Operator's Signature: Martin P. Fingerhut

Summary of Test

Result	Clause	Parameter	Requirement for Single Crystal Angle Probe
SA_2 - 45°	7	Identification	Marked on probe: manufacturer, probe type, beam angle, frequency, crystal size and shape.
2 mm	8.1	Depth of Shoe Probes	The available depth shall be indicated and shall be at least 1 mm.
NONE	8.2	Probe Wear (Used Probes)	Probe face shall be proud of the manufacturer's wear allowance marks.
FLAT	8.3	Shoe Flatness	Flat within 0.05 mm.
82 dB	8.4	Overall Gain	At least 50 dB gain in hand.
35	8.4.1	Signal to Noise Ratio	Noise shall be at least 20 dB weaker than the signal at the target path.
	8.5	Signal to Electronic Noise	Noise shall be at least 40 dB weaker than the signal at the target path.

Result	Clause	Parameter	Requirement for Single Crystal Angle Probe
AS MARKED	8.6	Index Point	Marked index point shall be within 1 mm of measured one.
44.5	8.7	Beam Angle	For nominal beam angles less than 45° +/- 1.5°, for greater than 45° +/- 2°.
1.5°	8.8	Squint	Not exceeding 1.5° for single crystal probes nor 2° for twin crystal probes.
34 dB	8.10	Longitudinal - Angle Beam	At least 35 dB weaker than shear beam. Measured at 100 mm range.
50 dB	8.11	Surface Waves	At least 34 dB weaker than shear wave for beam angles below 65°. At least 24 dB weaker for higher angles. Measured at 100 mm range.
NONE	8.13	Side Lobes	At least 20 dB weaker than the main beam, except angle greater than 64° shall be at least 15 dB weaker than the main beam.
NONE	8.14	Subsidiary Maxima	Fluctuations in echo amplitude shall not exceed that caused by interference with grass.
7.0 mm specified 7.5	8.15	Beam Width	Measured beam width shall be within 10% of design width.
	8.16	Pulse Shape	Single Peaked: Any secondary peaks in tail of pulse at least 20 dB less than main peak.
	8.17	Cycle Spacing	Less than +/- 15% variation between each cycle.
	8.18	Frequency	Within +/- 10% of the nominal frequency.
	8.19	Pulse Length	Not exceeding 2.5 microseconds between points on the unrectified pulse at 10% of peak amplitude.

A tick in the "Results" column should be used to indicate compliance with the Standard.

PROBE: SA2-45°

SONATEST

This probe is manufactured in accordance with:-

B.S. 5750

It conforms to:-

ESI 98.8

and is

C.E.G.B. APPROVED

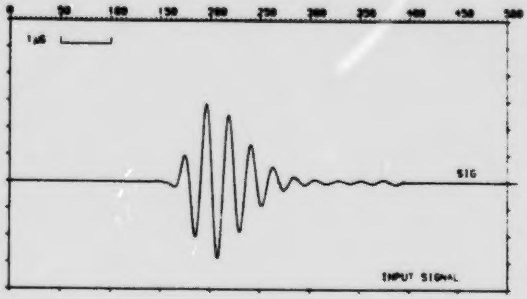

TYPICAL REAL TIME WAVEFORM

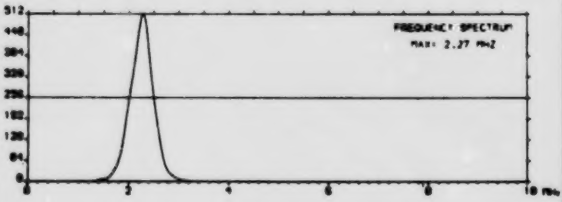

TYPICAL FREQUENCY SPECTRUM

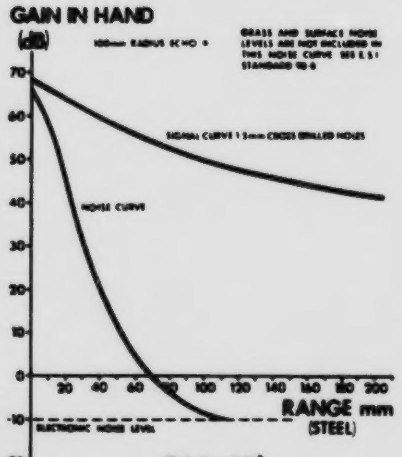

SA2-45°

TYPICAL SIGNAL AND NOISE CURVES

TYPE: Miniature single crystal, shear wave angle probe.

CONSTRUCTION: Fixed angle perspex shoe, stainless steel case, epoxy top.

CONNECTOR: Top or rear entry Male subvis or female micro - dot.

TUNING: Internal inductor.

CRYSTAL: 10mm x 10mm, lead zirconate titanate 2.25 MHz

NOMINAL FREQUENCY: 2.3 MHz ± 10%.

ANGLE: 45° ± 1.5° in steel at 20° C.

PULSE LENGTH: Typically 2.4 micro sec. ± 0.2 micro sec. not greater than 2.7 micro sec. Measured at 10% to 10% of peak amplitude.

EMISSION POINT: Within 1mm of marked index. (Typically within 0.5mm)

NOMINATED FLAW DETECTORS:

UNIT TYPE	BANDWIDTH
UFD7	1 – 3 MHz
Sitescan 100	1.5 – 3.5 MHz

NOMINATED CABLE: 50 ohms. Type Sonatest PC.

ELECTRICAL IMPEDANCE: 100 ± 10 ohms. (measured at peak frequency, with type PC lead.

TYPICAL SIGNAL TO PROBE NOISE RATIO: 83 dB for 100mm radius echo.

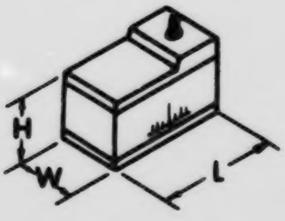

H:- 19 mm
L:- 27 mm
W:- 16 mm

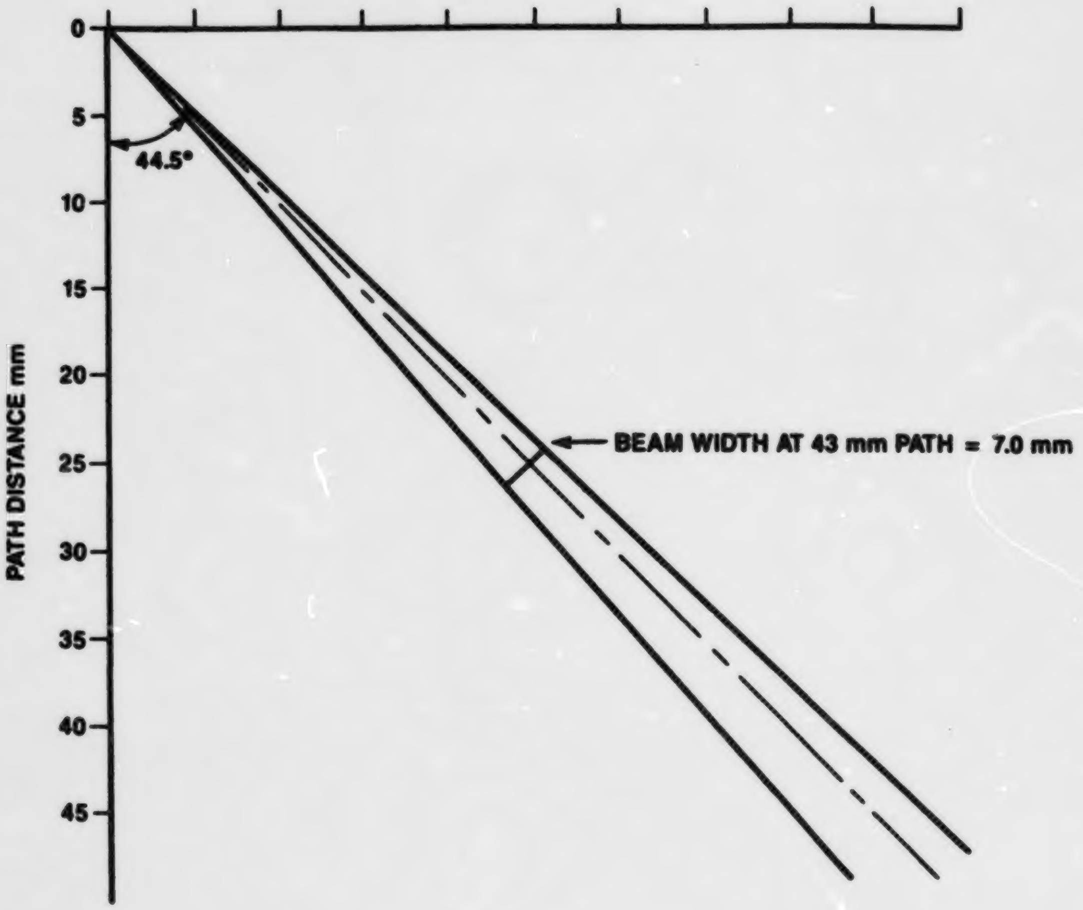

Figure 2.1: Beam Width in Transmitter Probe Sonatest No. SA2-45°

Volume

4

MECHANIZED ULTRASONIC INSPECTION OF PIPELINE GIRTH WELDS 4

Part 4: Evaluation of Inspection Criteria On Full Scale Girth Welds

FINAL REPORT BY:

A.G. Glover
M.P. Fingerhut
D.V. Dorling

WORK ON THIS PROJECT WAS JOINTLY FUNDED BY NOVA CORPORATION OF ALBERTA AND THE METALS TECHNOLOGY LABORATORIES, CANADA CENTRE FOR MINERAL AND ENERGY TECHNOLOGY, ENERGY MINES AND RESOURCES CANADA

DSS FILE NUMBER: 23SQ-23340-2-9027-4
DSS CONTRACT SERIAL NUMBER: OSQ82-00244
CANMET SCIENTIFIC AUTHORITY: DR. D.K. MAK

Report #15049

November, 1988

110 pp

MICROMEDIA

TABLE OF CONTENTS

PAGE

1.0 SUMMARY 1

2.0 CONCLUSIONS 3

3.0 RECOMMENDATIONS 5

4.0 INTRODUCTION 6

5.0 EXPERIMENTAL 9

5.1 Materials 9
5.2 Welding 9
5.3 Inspection Criteria and Transducer Specification . 10
5.3.1 Root Region 10
5.3.2 Body Region 11
5.3.3 Cap Region 14

6.0 FULL SCALE EVALUATION 16

6.1 Test Equipment 16
6.2 Evaluation on 9.8 mm Wall Pipe 17
6.3 Evaluation on the 20.6 mm Wall Pipe 20

7.0 RESULTS AND ANALYSIS 23

8.0 DISCUSSION 27

REFERENCES
TABLES
FIGURES
APPENDICES

1.0 SUMMARY

This report is the fourth in a series of four research reports aimed at developing an ultrasonic inspection design for the non-destructive evaluation of pipeline girth welds made by the mechanized gas metal arc (GMA) welding process for onshore and offshore pipeline construction.

Part 1 of the program described an inspection design method and criteria for the selection of ultrasonic transducers for the inspection of pipeline girth welds. This study showed that focussed probes in the pulse-echo mode are suitable for the examination of the root region of the weld and that alternative approaches are required for examination of the remainder of the weld. Part 2 of the program studied the use of creeping wave transducers for the examination of the cap region in thick wall pipe and the cap and body region for thin wall pipe. The work showed that they could be used with a specified inspection criteria and specially designed transducers. Part 3 of the program studied the successful use of the pitch-catch technique to examine the body region of the weld in thick walled pipe. Part 4 of the program, described in this report, combines the technology developed in the three previous reports into the overall inspection of field girth welds.

Throughout the program emphasis has been placed on developing an approach which uses specialized beams to detect specific imperfections

and to inspect the weld in a series of regions. This present report describes the work carried out to evaluate the performance of the complete inspection criteria on two full scale welds in 9.8 mm and 20.6 mm thick pipe. The root region was inspected using focussed probes, the cap region was inspected using creeping wave transducers, the body region was inspected using either creeping wave transducers for the 9.8 mm or the pitch-catch technique for the 20.6 mm.

Evaluation of the technique was carried out on field welds made using the CRC-Evans process and containing deliberately introduced defects. The probes were connected to an RTD-Rotoscan inspection system designed for high speed mechanized ultrasonic inspection of circumferential welds. The results showed that the inspection criteria developed achieved good detection performance in the three regions of the weld and that missed defects and false indications can be eliminated. The system will need some refinement prior to field evaluation and this relates primarily to improved cabling on the creeping wave transducer to eliminate electronic noise, improved probe housing and holder arrangements, selective threshold set up, and improved switching of the pitch-catch transducers with also reduced sensitivity.

2.0 CONCLUSIONS

2.1 An inspection design method and criteria can be specified for detection of defects in a mechanized gas metal arc weld using mechanized ultrasonic inspection. The criteria specified focussed probes for the root region, pitch-catch technique for the body region and creeping wave transducers for the cap region.

2.2 The inspection criteria evaluated on 9.8 mm and 20.6 mm wall thickness girth welds demonstrated that the detection goal of 1 mm projected depth with a signal-to-noise ratio of greater than 12dB could be met, and that no problems occurred with false indications or missed defects.

2.3 The inspection confirmed that planar lack of fusion defects could be detected ultrasonically and that these types of defects could be missed radiographically.

2.4 The results confirmed that detailed calibration and indexing of the probes was required prior to inspection. The placement of the probes relative to the weld preparation was also critical and hence reference points are required prior to welding.

2.5 The calibration of the probes requires that specific calibration test pieces are available and are of the correct wall thickness prior to carrying out field inspection.

2.6 Threshold levels for each probe system must be able to be individually set for each sequence during field investigations.

2.7 High electronic noise levels were experienced on the creeping wave signals primarily as a result of the cabling system used with these higher frequency probes.

3.0 RECOMMENDATIONS

3.1 Final preparations should be made to evaluate the inspection criteria on a pipeline project constructed using mechanized gas metal arc welds.

3.2 Improvements should be made in the cabling system to reduce the electronic noise from the creeping wave transducer.

3.3 Improvements should be made in the probe casings to eliminate any problem with wear and weld interference during field evaluation. Designs should be made for the probe holder to allow inspection from both sides of the weld simultaneously and to permit exact positioning of the probe in relation to the design position.

3.4 The question of sensitivity levels of the pitch-catch arrangement should be addressed prior to field evaluation.

3.5 The field system should have a recording system that permits individual threshold levels to be set, and permits switching of transmit-receive mode of the pitch-catch transducers.

4.0 INTRODUCTION

Non-destructive testing is an important part of the pipeline construction process, providing the information used to control girth weld quality according to the appropriate construction specification. Cost effective pipeline construction demands reliable and rapid inspection and currently depends on the x-ray radiography method. Although the incidence of girth weld failures from defects undetected by radiography is low, such incidents have occurred, and radiography is recognized to have some inherent limitation for the detection of inclined planar defects (1,2).

The desire to improve productivity during pipeline construction has led to the increased use of mechanized gas metal arc (GMA) welding projects which use mechanized welding systems are likely to produce more planar types of defects than shielding metal arc welding, and therefore may require changes to the inspection system especially in situations where the girth weld will be subjected to higher levels of longitudinal stress.

NOVA initially evaluated the use of ultrasonic inspection of mechanized girth welds using a standard mechanized system, which highlighted problems relating to the inspection system and weld geometry. The fixed transducer system uses an array of transducers, located at a fixed distance from the weld centerline, which is moved around the circumference. The transducer elements and detection gates are chosen with the intention of covering the cross-sectional area where imperfections occur while excluding the surface areas in the root and cap which would produce echoes unrelated to the presence of imperfections. The mechanical simplicity of fixed transducer systems, which facilitates rapid inspection, results in other complications related primarily to the transducers used. Figure 1 shows a schematic of a weld cross-section and a conventional transducer arrangement to achieve complete coverage of the weld volume. The inspection design is based on each transducer providing through-wall coverage of a fixed amount. The index positions for all transducers in the array are nearly coincident on the pipe surface so that the transducer array can be conveniently constructed into one housing. The resulting transducer selections provide inspection beams which are necessarily broad and oriented to provide complete coverage of the weld with little regard to the orientation of the expected imperfections, leading to missed imperfections and false indications.

The problems of missed imperfections and false indications are considered to be fundamentally related to the characteristics of the ultrasonic beam used, and to the design of the inspection geometry. In order to overcome these problems, the approach in this present study has been to develop an inspection criteria using specialized beams to detect specific imperfections. The goal has been to achieve a large echo signal, relative to the background noise, from specific imperfections in the region being examined by a particular beam.

In order to inspect the mechanized gas metal arc weld it was divided schematically into three regions (Figure 2); the root, the body and the cap. The inspection criteria was developed based on assessing specific defects in each of the regions. Part 1 of the report (3) reviewed the inspection criteria philosophy and specifically addressed the inspection of the root region. Part 2 of the report (4) evaluated and validated the use of creeping wave transducers to inspect the cap region. Part 3 of the report (5) analyzed the use of the pitch-catch technique to detect defects in the body region. This final report takes the inspection criteria developed in the previous three reports and applies it to the inspection of two full scale gas metal arc welds in 9.8 mm and 20.6 mm wall thickness, 914 mm diameter line pipe.

5.0 EXPERIMENTAL

5.1 Materials

Two pipe materials were used for the evaluation; one a 914 mm diameter by 9.8 mm wall thickness, the other a 914 mm diameter by 20.6 mm wall thickness, both materials were grade 483 line pipe.

5.2 Welding

Welding was performed by CRC-Evans, Houston, and utilized standard mechanized gas metal arc welding equipment and procedures. The two welds produced were designed to contain defects in cap, body and root regions of the weld. In addition to lack of sidewall fusion and interrun fusion defects each weld was designed to contain high-low and cap misalignment conditions typical of the worst cases which have been experienced in the field. Segments of the weld were also designed to contain no defects. The 9.8 mm wall thickness weld was divided into 6 segments, and the 20.6 mm wall thickness weld divided into 8 segments. It was proposed that only one defect per segment be introduced, although this was difficult to control during actual welding and some of the defect locations also varied during the actual production. The schematics of the proposed distribution of defects in the two welds are shown in Figures 3 and 4.

5.3 Inspection Criteria and Transducer Specification

The approach in this overall study has been to develop an inspection criteria using specialized beams to detect specific imperfections and to achieve a large echo signal relative to the background noise. The inspection has to be able to detect a 1 mm deep defect in the through-wall orientation and achieve a signal-to-noise ratio of greater than 12dB. This has been achieved on test plates by dividing the weld into three regions; root, body and cap as shown in Figure 2.

5.3.1 Root Region

The primary goals of the design of the inspection system for this weld region were to achieve an ultrasonic shear wave beam which is perpendicular to the inspection plane and a 6dB width confined to the inspection plane. In order to meet these requirements for Planes A and C, the pulse-echo technique was used with focussed transducers. The geometry of the weld preparation determines the required beam angle, transducer location and target path distance for each inspection plane (shown in Figure 5 for Plane C). The inspection of Plane C was divided into two zones to avoid any problems with the beam intersecting the root reinforcement (Figure 6). In addition, the focus of the beam was adjusted so that it focussed on the inside pipe wall rather than at the inspection plane, again designed to prevent false indications from the weld reinforcement. Plane B, which is less than 1.00 mm in depth is not inspected in the root region philosophy. In order to inspect Planes A and C, a three transducer system was specified, two for Plane C and one for Plane A. The transducers specified for Plane C were focussed probes, 5 MHz frequency, 45°, with a 6dB beam width at the inspection plane of 2 mm. The transducer specified for Plane A was a focussed probe 5 MHz frequency, 52.5°, with a 6dB beam width at the inspection plane of 2.5 mm. It was also required that the same transducers be used for inspecting both the 9.8 and 20.6 mm wall thickness. This meant that the design of the transducers had to be such that the converging part of the beam was used in the 9.8 mm case and the diverging part of the beam used in the 20.6 mm case. Axicon focussed probes with their region of relatively constant beam width were therefore selected rather than spherically focussed probes. The three focussed probes were designed and built by The Welding Institute, UK, and their detailed report is given in Appendix 1. The actual design requirements and probe characteristics are given in Tables 1 and 2.

The probes were assessed at TWI according to SUT-2 and the results given in Appendix 1. These results were confirmed by NOVA and additional signal-to-noise assessments performed. These results are given in Figures 7, 8, and 9 and confirm that the probes meet all of NOVA's specifications.

5.3.2 Body Region

The dimensions of the cap bead overlap give rise to the definition of where the body region must commence in terms of its inspection distance below the pipe surface. This is defined in Figure 10 as 3 mm beneath the surface, which ensures that no problems occur with missed indications because of signal loss in the cap pass. In fact the creeping wave transducer as determined in the next section, is designed to inspect to a depth of 4.2 mm. The transducers described in section 5.3.1 can inspect the root region to a defined depth of 5.73 mm (Figure 2). Hence the root and cap regions can be inspected to a total depth of 9.93 mm. In which case only the body region of the 20.6 mm wall will need additional transducers and the root and cap ones which will be sufficient for the 9.8 mm wall.

The geometry of the weld preparation for the body region (fill passes) prevents the use of shear waves perpendicular to the expected planar defects and, although high angle beams can produce good results on simulated defects in test plates, these results cannot be reproduced on real weld defects. The pulse-echo technique was therefore replaced with a pitch-catch technique which has been commonly used for detection of near vertical defects, as described in reference 5. The results from that study showed that the body region in welds 9.3 mm to 23.0 mm could be inspected using a single pair of transmitter-receiver probes of the following specification; 2.25 MHz, 45° transmit and 2.25 MHz, 55° receive.

In order to facilitate the probe handling for the full scale evaluation it was determined that the two probes could be contained within a single housing and still meet the stringent indexing requirements. The probes were placed in a 80 x 40 x 35 mm housing and supplied by RTD, reference 88-III. The ultrasonic beam plots and frequency data sheets for the probes are given in Appendix 2.

The depth of the body region for inspection is 11.87 mm which is equivalent to a projected depth on the 5° inclined weld preparation of 11.91 mm. In order to ensure this is uniquely inspected by the fixed position of the transmitter probe requires a 6dB beam width of 9.12 mm at the inspection plane. Allowing for an accepted error of a minimum defect size of 1 mm on the inspection plane means that the 6dB beam width at the target should be no less than 8.35 mm. The results of the beam width analysis at 6dB at the target path distance of 46 mm of the transmitter probe are shown in Figure 10, illustrating that the actual beam width is 8.5 mm, and will meet the inspection criteria.

The previous results (5) showed that there was a possibility that the sensitivity of a single pair of pitch-catch probes at the mid body region could lead to detection of small defects at high signal-to-noise ratios. The transmitter-receiver pair chosen for the full scale evaluation, however, were designed to minimize this potential problem and hence were the only ones chosen for the full-scale evaluation.

The pitch-catch probe was evaluated according to SUT-2 and met all of its requirements. The signal-to-noise results are given in Figure 11, evaluated on a 20 mm thick plate with reference side drilled holes at specific locations, and giving a S/N of 42dB at the target path distance.

5.3.3 Cap Region

Detection of imperfections on Plane E, closest to the outside surface, beneath the weld cap is potentially the most difficult. The pitch-catch technique for the body region is unable to examine the weld region within 3 mm of the inspection surface (Figure 12) without encountering false indications from the cap geometry, hence the cap region to be inspected was considered to be 3 mm deep. Initial studies of the cap region showed that the use of creeping waves (Figure 13) had a good potential for detecting cap region defects. The near normal orientation of the creeping wave to the weld preparation in the cap region makes it particularly well suited for the detection of planar lack of fusion defects. The design of conventional creeping wave transducers, however, means that a large beam size is normally produced which will have the effect of also detecting defects in the root and could lead to false or ambiguous indications. In order to overcome this problem of a large beam size, problems with weld cap interference, and to ensure that a suitable probe focus and working range were achieved, a specialized creeping wave probe was designed and built. A specialized probe was evaluated in report 2 (4) and found to meet all the specified requirements. As this particular probe was evaluated only on flat specimens a second probe was designed and built specifically to be used on the full scale evaluation. The probe was designed by BAM, Berlin and built by RTD and designated RTD-BAM 88-110. The details of the dual crystal 8 MHz creeping wave probe are given in Appendix 3. The probe in the transmit and receive mode was further analyzed according to SUT-2 and found to meet all of its requirements. The dual crystal was found to have a 90° creeping wave with a 76.2° main compression wave with a focus position 2.7 mm below the pipe surface with an effective working range down to 4.4 mm. The increased working range slightly reduced the sensitivity at the surface but it was still well above the minimum 12dB required (Figure 14).

6.0 FULL SCALE EVALUATION

The approach taken in the full scale evaluation was as follows;

- evaluate the welds using radiography
- install the RTD-Rotoscan equipment
- establish weld preparation reference
- establish probe index to weld preparation distance
- establish gate positions
- calibrate system on simulated weld defects
- establish threshold settings
- carry out test runs from reference side
- carry out test runs from opposite reference side
- qualify specific defect locations
- co-ordinate results
- section welds at specific locations and compare to ultrasonic and radiographic results.

6.1 Test Equipment

The transducers were accommodated in a modified probe holder (Figure 15) and driven around the weld on a standard band using a customized CRC welding bug to manipulate the probes. The system was interfaced to the RTD-Rotoscan system (Figure 16), consisting of a Sonolog 82 Ultrasonic Unit and Multichannel Scanner, control unit and eight channel strip chart recorder. The couplant used throughout the test program was water and this was flooded continuously ahead of the probes, Figure 17.

The RTD-Rotoscan inspection system is designed for the high speed mechanized ultrasonic inspection of circumferential welds. The system has a go-no go recording system which permits rapid assessment of defects exceeding a predetermined threshold level. The system was also interfaced to a Sonolog 82 ultrasonic system which can independently record echo amplitude and transit distances for the complete scan. The system can be operated manually or automatically. In the manual mode the system performs like a conventional flaw detector, transmitting and receiving on specified probes and provides an A-scan display. Under the automatic operation, the control unit transmits the required probe numbers to a switch box which in turn ensures that the correct transmit probe is excited and that the received signal is fed into the amplifier. In this mode the operation is described in terms of sequences. A sequence is defined as a transmit/receive probe combination and associated with it is a series of operating parameters such as gate position and amplifier gain. The present set-up recorded the signals on an eight channel recorder which only permitted a combination of four probes at a time to be assessed.

6.2 Evaluation on 9.8 mm Wall Pipe

A reference line 30 cm from the edge of the weld preparation had been set up prior to welding and this was used to index the probe positions in relation to the weld geometry. Four transducers were used for the evaluation, 001, 002 and 003 in the pulse echo mode for the root regions and 88-110 in the transmit-receive mode for the cap and body regions. The index positions of the transducers were rechecked using IIW VI block and a kidney block and their actual indices marked on the housing. Finally the index positions and beam angles of the three root region probes were verified on a 10 mm thick test plate containing simulated defects. Once these positions had been verified the gate start and stop positions could be indexed and these were all set to start at 2 mm prior to start of the inspection plane and stop at the weld centerline (Table 3).

Each of the probes were calibrated to give a 80% full screen height signal from a 2.0 mm diameter flat bottom hole for the root region and a 1.0 mm surface notch for the creeping wave transducer. These results are given in Table 3 and compared to the equivalent noise level measured on the pipe. These results were used to determine the threshold level setting and this is given in Table 3. The probe positions were fixed in the probe holder so that their reference position to the weld preparation were at the design locations, and these are given in Table 3.

Completion of all of the calibrations and set-up permitted the program sequence to be inputted into the RTD controller and this is given in Table 4. The weld was first inspected from the reference side of the weld in a series of eight runs, relative to different design locations and triggering sequences; these are summarized in Table 5. The complete inspection of each run takes 72.5 seconds.

Upon completion of these runs the probes were repositioned on the opposite side of the weld to the reference line (referred to as opposite reference, OR). The calibration levels were rechecked and same values as given in Table 3 were used as the design basis. A sequence of nine reported runs were performed using the sequence in Table 4 with the exception of sequence 5 which was not carried out. The details of the nine runs are given in Table 6. The scanning time for this second set of runs was 74.2 seconds per circumference.

In both sets of runs transit distance measurements were performed. The Sonolog ultrasonic system on the RTD equipment was set to provide measurement from the start of the gate. The instrument was set so that the measurement of the gate width could be achieved with a resolution of 0.1 mm at a voltage output range of 0 - 10 V. During the initial evaluation it was found necessary to remove the 20dB filter on the transit distance recording channel because the filter delayed the response and skewed the transit measurement results.

An initial problem also occurred with the acquisition of data from the creeping wave transducer. This arose because the combination of the high frequency of the probe and the cabling system resulted in a high amplified noise level at the recorder. This was overcome in this particular evaluation by making the cabling to the amplifier as short as possible, which could be done in the laboratory. In addition the threshold level was set at 20% screen to prevent recording noise in the creeping wave probe channel. This level was used for each channel as the present configuration of the Sonolog system does not provide for setting the threshold individually for each sequence. Setting the threshold level at 20% screen, however, does not effect the recording of echo amplitude, although the transit distance is not recorded unless the signal is above the threshold.

During the second series of runs from the opposite side of the reference line it was noted that transit distances in the plane A, root region, were being recorded prior to the end of the gate. Runs were therefore performed with the triggering not only from the highest point of the highest indication in the gate but also to the leading edge of the first indication exceeding the threshold level set at 20% (Table 6). Also at one point where deliberate excessive cap overlap had been introduced probe 003 became uncoupled at design + 1 mm spacing because the probe rode up the cap (Figure 18).

6.3 Evaluation on the 20.6 mm Wall Pipe

A similar 30 cm reference line had been set up from the edge of the weld preparation prior to welding the 20.6 mm wall pipe and this was used to index the probe positions in relation to the weld geometry. Five transducers were used for the evaluation, 001, 002 and 003 in the pulse-echo mode for the root regions, 88-111 in the pitch-catch mode for the body region and 88-110 in the transit receive mode for the cap region.

The index positions and beam angles of the probes were rechecked using calibration probes prior to the commencement of the inspection on the pipe. It was found that there was some discrepancy between the angles now found on root region probes and those used in the 9.8 mm wall investigation. The slight decrease in angle was thought to be due to the absence of a stainless steel casing across the front of the probes. This allowed some wear to occur during the initial investigation resulting in a tilt forward of the probe and a slightly shallower angle. Evaluation of probe 003 on the 20 mm thick calibration also revealed two maximas to be occurring at path distances separated by 2.8 mm. As no side-lobes were identified during the probe assessment one possible explanation was that this was due to a tip diffraction effect. All these factors were taking into account during the setting of the calibration levels and gate positions. Another factor that had to be taken into account was the difference in the calibration plate test piece and the pipe wall thickness. In the present case the calibration plate was 19.8 mm thick and the nominal 20.6 mm thick pipe was actually 21.1 to 21.4 mm in thickness. The approach therefore was to establish the gate position based on the path distance determined from the calibration block reflectors and add on to this the effective increase in path distance from the pipe wall difference whilst making allowance for the actual probe angle.

Each of the probes were calibrated to give a 80% full screen height signal from a 2.0 mm diameter flat bottom hole for the root and body region and a 1.0 mm surface notch for the creeping wave transducer. The complete settings for the inspection of the 20.6 mm wall pipe are given in Table 7.

Completion of all of the calibrations and set-up permitted the program sequence to be inputted into the RTD controller and this is given in Table 8. As only eight channels were available for recording the root and cap regions (Planes A, C and E) were evaluated first, and then the root (Plane A), body (plane D) and cap region (Plane E) subsequently. The weld was first inspected from the reference side of the weld and the the details of these are summarized in Table 9.

On completion of the inspection of the weld from the reference side, the probes were repositioned and re-indexed on the opposite side (OR) to the reference line. The calibrations were rechecked and trial runs were performed to monitor echo amplitudes, and the gate positions were confirmed. These trials showed that in some instances confirmed root defects occurred at the end of the gated region for probe 003 and hence the probe was repositioned 1 mm closer to the weld based on calculated surface position. On completion of all checks the run sequences shown in Table 10 were carried out.

Threshold levels and filter levels were set as per the 9.8 mm wall investigation for all of the 20.6 mm sequences.

7.0 RESULTS AND ANALYSIS

The results of the inspection were compared in terms of the initial radiography, the ultrasonic examination and detailed metallographic sections. The main emphasis was placed on the performance of the ultrasonic examination, which was monitored in terms of the chart output. Each record consists of eight lines of data, referenced at the top of the chart by distance markers. On the chart the data is presented in terms of pairs, e.g. channels 1 and 2 are recorded data from a single probe; channel 1 represents the echo amplitude and Channel 2 records the equivalent path distances. Echo amplitudes are recorded for each signal that exceeds the reference threshold level of 12dB and the transit distances are also checked to ascertain that the indication is within the gate. The only exception to this was the creeping wave probe where assessments were made at threshold levels of 6dB level.

No problems were experienced during the operation of the RTD system and couplant was maintained throughout the weld inspection. Some trial runs which are not fully reported were rejected because they did not give meaningful results. This was the case for example when a sequence was used that triggered the amplitude on the highest echo in the gate and transit distance was triggered on the first echo exceeding the threshold level; another sequence rejected was system triggering on highest echo but threshold adjusted to 30% FSH. Throughout the program the creeping wave was triggered on the highest echo in the gate. When triggering on the first echo in the gate, creeping wave indications were not recorded. This situation will be overcome once noise levels on the cabling are reduced.

The program was also sequenced to look at two sets of gates in the root region. Use of dual gates to monitor the root region has been shown to have several advantages. When the defect indication is at a near the end of a detection gate, the presence of an indication and a corresponding transmit distance in the other gate monitoring the root region indicates that the indication in the gate is unique. The presence of only an indication in the detection gate and no transmit distance would suggest the probe is improperly positioned. The dual gates can therefore provide the evidence that the system is accurately tracing the weld. The dual gate system can also be used to identify root geometry effects.

Throughout the program runs were performed at probe distances corresponding to the design, closer to the weld, and further from the weld. Generally it was found that defects were correctly identified at the design distance and within ±0.5 mm. Once the probes were positioned at the designed ±1 mm distance, it was noted that occasionally, the signal from a root defect would be located at the very edge of the gate or even missed. This factor highlights the importance of accurate probe positioning and weld preparation indexing.

Each run and channel was reviewed and indications noted that exceeded the threshold levels and exceeded 10 mm in length (a nominal screening), and the corresponding maximum and minimum path distances were recorded for each indication. A similar exercise was carried out for the radiographic examination and the results plotted out in terms of its location and type of defect noted. The records from both were combined and presented in a single format. The simplified versions are given in Figures 19, 20, 21 and 22, with the original detailed versions given in Appendix 4.

These charts were used to assess position to be sectioned for metallographic comparison. The locations were chosen where both radiographic and ultrasonic indications occurred, and where no indications occurred. In the case of the 9.8 mm wall, specific ultrasonic indications occurred on one side of the weld or the other and hence sections were taken based on reference side and opposite reference side indications. For the 20.6 mm wall defects were present on both sides of the weld at the same location hence one section could represent both reference side and opposite reference side of the weld. The results are compared in Table 11 for the 9.8 mm and Table 12 for the 20.6 mm, both tables also highlight the metallographic results.

In the case where neither radiography nor ultrasonics indicated a defect, no defect was found on sectioning (Figure 23, sections 5 and 9, 9.8 mm). Defects detected by ultrasonics and not by radiography were confirmed by metallography. Figure 24 shows defects found only by ultrasonics in the fill and root, Figure 25 shows lack of sidewall fusion at the cap only found by ultrasonics. Figures 26a and 26b confirm a root defect found by ultrasonics and identified as bead misalignment by radiography. Figure 27 indicates a lack of side wall fusion defect between the hot an fill pass detected both by the creeping wave transducer and because part of the defect extends down along the hot pass plane also by probe 001. Figures 23 to 27 inclusive were all sections from the 9.8 mm wall pipe.

The sections from the 20.6 mm wall also confirmed the findings of the ultrasonic examination. Figures 28 and 29 reveal a hot pass root defect and a lack of sidewall fusion that were missed by radiography. Figure 30 shows a lack of side wall fusion defect and external undercut detected by ultrasonics but only reported as external undercut by radiography.. Figure 31 illustrates lack of side wall fusion in the 1st fill detected by both radiography and ultrasonics, plus root bead misalignment confirmed by the root geometry inspection. Figure 32 shows a region in the root that was identified as a root geometry effect and bead misalignment. The root geometry effect shows up on the dual gate. Probe 003 is also picking up the original weld preparation that has not been melted in because of the bead misalignment. True lack of fusion in the root was found in the 9.8 mm wall (Figure 26b) and a comparison of the echo amplitude plots from both types of defects is shown in Figure 33. A low amplitude signal is obtained from the unmelted root region (Figure 32) as compared to the root lack of fusion (Figure 26b), plus the gain level for the 003 probe was set as 25dB for the 20.6 mm wall, and 14dB for the 9.8 mm wall.

8.0 DISCUSSION

Mechanized gas metal arc welding has been increasingly used as a production welding system for large-diameter gas pipeline construction projects. Because of the types of potential defects produced by the technique consideration has been given to using ultrasonics as an alternative inspection method. In order to keep pace with production, however, the ultrasonic system must be mechanized. It has been shown by previous analyses (3) that using a fixed array transducer system gives rise to problems with missed and false indication. This present study has shown that in order to successfully utilize a mechanized ultrasonic inspection system that the key factor is the specification of the inspection transducer arrangement. This can be achieved by consideration of the weld geometry and defect orientation, and analyzing each specific region of the weldment. The geometry of the weld preparation determines the required beam angle, transducer location and target path distance for each inspection plane.

The investigation has shown that the weld can be inspected using three weld regions; the root, body and cap region. Each of these regions has specific requirements in terms of their inspection. The root bead and hot pass constituted the root region and can be inspected using focussed probes in the pulse-echo mode. One probe assesses the root pass sidewall fusion and two probes assess the hot pass sidewall fusion. The interrun region between the root and hot pass is not assessed during the inspection. The body of the weld can be inspected by either the pitch-catch technique or the creeping wave technique.

In essence a weld 10 mm thick and less can be inspected using a creeping wave transducer and three root region transducers, at larger thicknesses additional pitch-catch transducers would be required to inspect the body region. The cap of the weld can be inspected using creeping wave transducers. Both the pitch-catch and creeping wave transducers were operated in the transmit-receive mode for the present study. Details of the specific transducers were given in the main text, however they were all specified to achieve a signal-to-noise ratio of greater than 12dB at a threshold of a 1 mm projected depth defect. In order to meet this requirement and overcome geometry interaction effects the probes had to be specifically built with tight requirements on beam width at 6dB, focus positions and working ranges. All of the probes for the present investigation met the criteria required and performed according to the NOVA Specification SUT-2.

Detailed examination of the two laboratory welds using radiography and ultrasonics confirmed that ultrasonics is capable of detecting significant planar indications whereas radiography can miss some of these defects (Tables 11 and 12). The results of the ultrasonic inspection also confirm that by using the specifically designed inspection criteria the problems with false and missed imperfections can be eliminated. In all the cases examined, indications on the ultrasonic records could be confirmed by metallographic sectioning. There were, however, some areas relating to the inspection that will have to be clarified prior to a final full scale evaluation in the field.

One of the main problems arose with noise levels from the creeping wave transducer. The higher frequency of this particular probe resulted in higher noise pick up and a higher amplified noise level at the data acquisition system. The majority of this noise resulted from electronic noise from the cabling system used and was overcome in the present investigation by placing the amplifier as close to the probe as possible. This will not be an option in the field and hence a revised cabling system will be required. The noise level from the creeping wave transducer also highlighted another problem with setting the threshold levels. In the present system the threshold level could not be individually set for each sequence. Consequently the 20% threshold level set for the creeping wave also controlled the threshold level on all other probes. Whilst this did not affect the echo amplitude signals it did mean that the transit distances were not recorded until the threshold level was exceeded; some transit data might well be lost in this mode. This can be overcome in field trials by using Sonolog 83 or 86 units which do have the capability of setting individual levels for each probe.

Another factor that was highlighted during the investigation was the ability to correctly index the weld preparation so that the design gates can be achieved. It was shown that examinations outside of the ± 0.5 mm could result in defects being at the end of gates or even outside the gate once ± 1.0 mm was achieved. Analysis of the cap in relation to it's apparent mid point and actual mid point shows that it can vary by at least as much as 1.0 mm and hence could not be used as an index point in the field. For the present investigation the edge of the weld preparation was indexed to a reference point on the pipe and subsequently used as the design reference point. In the field therefore the initial placing of the band is noted at a fixed distance from the weld edge and this will have to be clearly marked prior to welding. Once welding commences, even though the band will remain in place for the subsequent ultrasonic examination, there is a tendency for it to move slightly and hence the need for a deliberately marked reference line.

The work has also shown that some improvements will be required in the probe casings and probe holders prior to field use. Although these probes were designed for laboratory experiments it was anticipated that they would be rugged enough for field application. It was noted, however, that the beam angle of the focussed probes changed slightly after completion of the test runs on the 9.8 mm wall. This was due to a small amount of wear occurring on the front of the probe and this could have been eliminated with the use of a wear strip. In addition, some modification to all of the probes was required to allow them to be placed as close as possible to the weld cap, especially in the case where excessive cap bead overlap occurred. This can be overcome in the field by chamfering the front edge of the probe housing. A specially designed probe holder will also be required for the field that will contain all of the probes and allow individual movement of the probe so that it can be set at its design distance from the weld preparation. The probe holder will also be required to allow the inspection of the weld from both sides at the same time. These modifications will all permit the successful investigation of mechanized gas metal arc welds using mechanized ultrasonic inspection.

While these changes will improve the field inspection it is not anticipated that there will have to be any significant changes to the inspection criteria used. All of these probes behaved as specified and no problems with missed imperfections were encountered. The three root region probes showed that defects could be uniquely identified in the area and indications from root geometry problems could be eliminated. The use of dual gates in the root pass region also ensured that problems with root geometry could be entirely eliminated. In the root region it is also important that the signal should be triggered off the first echo. During the present investigation triggering was either on the first echo or the highest echo in the gate. The latter was used in the present investigation only because of electronic noise problems from the creeping wave transducer. Once this is eliminated by improved cabling the system will be triggered only on the first echo in the gate. True root defects were consistently identified by the ultrasonics inspection which had been missed by radiography. The root region probe arrangement will not, and has not been designed to, detect lack of cross weld penetration, which also falls below the 1 mm projected through wall depth criteria.

The pitch-catch technique performed well on the 20.6 mm wall investigation and was able to identify lack of sidewall fusion defects that were missed by radiography. The pitch-catch technique was only used in the transmit-receive mode and without switching the transducers to the opposite mode. Regions of lack of interrun fusion would therefore not be detected unless they occurred with lack of sidewall fusion (Figure 31). These types of defects are ideally suited for the detection in the pulse-echo mode and this should be considered for the field investigation. Whilst the pitch-catch technique using a single pair of transducers detected all lack of fusion defects there is still some concern that it may be too sensitive. The problem arises with some small defects that were detected on the sidewall. A good example of this is Figure 30 which shows a series of small defects along the sidewall. Whilst careful screening of the signal may be able to resolve that it is coming from defects at different depths at the present stage the report only shows it to be coming from one. These small defects may well be close to being rated as "false" indications. This arises because the use of a single pair of transducers to inspect the complete body region requires a high sensitivity in the central region (5). This can be easily overcome by dividing the plane into two and using two pairs of transducers, which will mean that small defects will fall below the 12dB criteria.

The creeping wave transducer performed well (except for the electronic noise discussed earlier) and was able to inspect the cap and body region of the 9.8 mm wall, and the cap region of the 20.6 mm wall with no problems. Assessment of the results at two threshold levels of 6dB and 12dB revealed no specific problems except that some small surface defects were detected when sections were taken at thresholds that exceeded 6dB but were less than 12dB.

All of the work with these specific transducers has also shown that careful calibration is required prior to the commencement of the inspection. Specific calibration test pieces will be required for the field evaluations, and these will have to be on the same wall thickness as the test welds.

The work has shown that with the proposed modifications ultrasonic inspection of gas metal arc welds can be achieved without giving rise to false indications and missed defects providing that the inspection criteria and methodology are critically defined and implemented. The techniques developed over the past few years are now ready to be implemented into full scale field evaluations.

REFERENCES

1. Halmshaw, R., and Hunt, C.A., "Can Cracks Be Found By Radiography?" Br. J. NDT May 1975.

2. Lumb, R.F., "Non-Destructive Testing of Pipeline Girth Welds in the 1980s" Br. J. NDT July 1982.

3. Fingerhut, M.P., Coote, R.I., and Hodgkinson, D., "The Selection of Ultrasonic Transducers for Inspection of Pipeline Girth Welds" NOVA Tech. Lit. 15034 December 1986.

4. Fingerhut, M.P., Glover, A.G., and Dorling, D.V., "Evaluation of a Unique Creeping Wave Probe for Examination of the Cap Region in Pipeline Girth Welds" NOVA Tech. Lit. 15047 Oct. 1988.

5. Glover, A.G., "Mechanized Ultrasonic Inspection of Pipeline Girth Welds, Part 3 Pitch-Catch Technique NOVA Tech. Lit. 15048 Oct. 1988.

TABLE 1

DESIGN REQUIREMENTS

PROBE NO.	NOMINAL BEAM ANGLE (°)	REFLECTOR RANGES mm 9.8 mm W.T. RANGE R_1)	 20.6 mm W.T. (RANGE R_2)	REQUIRED BEAM WIDTHS (mm)
001	45	20	35.25	2.0
002	45	20	35.25	2.0
003	52.5	14.5	21.3	2.5

TABLE 2

PROBE CHARACTERISTICS ROOT REGION

(12.7 mm dia PZT-7a crystals of nominal frequency 5 MHz)

PROBE NO.	CRYSTAL FREQUENCY MHz	FOCUSING FACTOR N/F	DELAY PATH IN PERSPEX (mm)	ESTIMATED FOCAL RANGE IN STEEL (mm)	ACTUAL FOCAL RANGE IN STEEL (mm)*
001	4.996	1.68	15	21.9	23
002	4.900	1.68	15	21.9	22
003	5.147	1.97	15	16.9	17

*Appendix 1

TABLE 3

CALIBRATION SETTINGS FOR 9.8 MM WALL INSPECTION

PROBE NO.	REGION INSPECTED	CALIBRATION LEVEL (80% FSH) dB	NOISE LEVEL (80% FSH) dB	THRESHOLD LEVEL %	GATE START (mm)	GATE LENGTH (mm)
003	Root Plane A	14	48	6.4	15.0 (18.5)*	3.5 (4.0)*
002	Root Plane C	8	44	5.2	17.6	4.0
001	Root Plane C	13	46	7.2	19.2	5.0
88-110	Cap & Body Planes D & E	59	73	63.7	5.6	2.7

*Gate used for Test Runs 6, 7 and 8

PROBE	PROBE INDEX POSITION TO WELD PREPARATION (DESIGN) mm
003	9.0
002	11.0
001	13.5
88-110	12.0

TABLE 4

PROGRAM SEQUENCE 9.8 MM WALL

PROBE NUMBER	PROBE TYPE	MODE	SEQUENCE	TRANSMIT CHANNEL	RECEIVE CHANNEL	GAIN dB	WEDGE (mm)	RECORDING
003	FOC	P/E	4 (5)*	5 (5)	5 (5)	14	17.0	7,8 (8,4)
002	FOC	P/E	3	4	4	8	19.0	5,6
001	FOC	P/E	2	3	3	13	18.0	3,4
88-110	CW	T/R	1	1	2	59	9.4	1,2

* Runs 6, 7, 8, different gate see Table 3

TABLE 5

RUN SEQUENCE ON 9.8 mm WALL, REFERENCE SIDE

RUN NUMBER	PROBE LOCATION	
01	Design	Normal Sequence
02	Design + 0.5 mm	Normal Sequence
03	Design + 1.0 mm	Normal Sequence
04	Design - 0.5 mm	Normal Sequence
05	Design - 1.0 mm	Normal Sequence
06	Design - 1.0 mm	Sequence 5, Plane A, Gate Change
07	Design	Sequence 5, Plane A, Gate Change
08	Design + 1.0 mm	Sequence 5, Plane A, Gate Change

TABLE 6

RUN SEQUENCE ON 9.8 mm WALL, OPPOSITE REFERENCE SIDE

RUN NUMBER	PROBE LOCATION	GATE TRIGGER
09	Design	Trigger on highest indication
10	Design	Trigger on first echo
11	Design + 0.5 mm	Trigger on first echo
12	Design + 0.5 mm	Trigger on highest indication
13	Design + 1.0 mm	Trigger on highest indication
14	Design + 1.0 mm	Trigger on first echo
15	Design - 0.5 mm	Trigger on first echo
16	Design - 1.0 mm	Trigger on first echo
17	Design - 1.0 mm	Trigger on highest indication

TABLE 7

CALIBRATION SETTINGS FOR 20 mm WALL INSPECTION

PROBE NUMBER	REGION INSPECTED	CALIBRATION LEVEL (80% FSH) dB	NOISE LEVEL (80% FSH) dB	THRESHOLD LEVEL %	GATE START (mm)	GATE LENGTH (mm)
003	Root Plane A	25	59	6.4	32.1 (35.6)*	3.5 (4.0)*
002	Root Plane C	10	49	3.5	33.4	4.0
001	Root Plane C	17	49	7.9	36.1	5.0
88-111	Body Plane D	30	68	4.0	62.6	10.0
88-110	Cap	59	73	64	5.6	3.7

* Gate used for Subsequent Runs

PROBE	PROBE INDEX POSITION TO WELD PREPARATION (DESIGN) mm
003	23.4
002	20.4
001	25.4
88-111	32.4
88-110	12.0

TABLE 8

PROGRAM SEQUENCE 20.6 mm WALL

NUMBER	TYPE	MODE	SEQUENCE	TRANSMIT	RECEIVE	GAIN GAIN dB	WEDGE DELAY (mm)	RECORDING	
				CHANNEL				INITIAL	SUBSEQUENT
003	FOC	P/E	4 (5)*	5	5	25	17.2	7,8	7,8 (5,6)
002	FOC	P/E	3	4	4	10	19.0	5,6	--
001	FOC	P/E	2	3	3	17	18.0	3,4	--
88-111	P-C	T/R	6	6	7	30	17.0	--	3,4
88-110	CW	T/R	1	1	2	59	9.4	1,2	1,2

* Used for Gate Change

TABLE 9

RUN SEQUENCE ON 20.6 mm WALL, REFERENCE SIDE

RUN NUMBER	PROBE LOCATION	
18	Design	Trigger on first echo Normal Sequence
19	Design	Trigger on first echo Second Sequence
20	Design	Trigger on highest echo (as 19)
21	Design - 1 mm	Trigger on first echo
22	Design - 1 mm	Trigger on first echo
23	Design + 1 mm	Trigger on first echo
24	Design + 1 mm	Trigger on highest echo

TABLE 10

RUN SEQUENCE ON 20.6 mm WALL, OPPOSITE REFERENCE SIDE

RUN NUMBER	PROBE LOCATION	
25	Design	Trigger on highest echo Revised Sequence
26	Design	Trigger on first echo
27	Design - 1 mm	Trigger on first echo
28	Design - 1 mm	Trigger on highest echo
29	Design + 1 mm	Trigger on highest echo
30	Design + 1 mm	Trigger on first echo
31	Design - 2 mm	Trigger on first echo
32	Design	Trigger on first echo Normal sequence root
33	Design	Trigger on highest echo Normal Sequence
34, 35	Rerun of 28, 29	

TABLE 11

INSPECTION RESULTS 9.8 mm WALL

		ULTRASONIC INDICATION					
CROSS SECTION	LOCATION (mm)	PROBE NO.	ECHO AMPLITUDE	RADIOGRAPHIC INDICATION	REF	OPP REF	METALLOGRAPHY
1	192	88-110	50	SWF(CAP)	x		SWF Cap
2	426	88-110	70	-	x		SWF Fill
		001	15	-	x		Root Defect Fig. 24
		002	30	-	x		
3	505	88-110	45	LCP(H+F)	x		SWF Fill Root
		001	40		x		
		002	50		x		
		003	50		x		
4	623	002	80	LCP	x		LSWF Hot Pass
5	722	-	-				No Defect Fig. 23
6	2670	003	100	SWF(H)	x		No Root
7	2468	88-110	60	SWF(H+F)	x		LSWF Fill
		001	30		x		Top Edge of Hot Pass Fig. 27
8	2750	88-110	90	SWF(H+F)	x		LSWF Fill
		001	30		x		Top edge of Hot Pass
9	2840	-	-				No Defect
10	1297	88-110	>100	-		x	Fusion defect between Fill & Cap
11	1462	003	80	Bead Misalign		x	Root Defect Fig. 26a, 26b
12	1708	002	15	-		x	Partially missed root
13	1958	88-110	80	-		x	LSWF Cap Fig. 25

TABLE 12

INSPECTION RESULTS 20.6 mm WALL

		ULTRASONIC INDICATION					
CROSS SECTION	LOCATION (mm)	PROBE NO.	ECHO AMPLITUDE	RADIOGRAPHIC INDICATION	REF	OPP REF	METALLOGRAPHY
1	263	88-111	15	-	x		Very small LSWF
		88-111	100	SWF(HP+F)		x	LSWF
2	737	88-111	100	SWF(HP+F)	x	x	LSWF
		003	Root Geom	BMA	x		L Interrun Fusion Fig. 31 Bead Offset
3	1005	88-111	25		x	x	Very Small LSWF OR
4	1445	88-111	55	EUC	x	x	LSWF +EUC Fig. 30
		88-110	40-50		x	x	
5	1720	88-111	35	SWF(H+F)	x	x	Small LSWF
		88-110	65	EUC	x	x	
6	2520	88-111	50	-	x		LSWF Fig. 28
		002	20	-		x	Hot Pass Fig. 29
7	640	003	30	HP+SWF	x		LSWF
		003	20 Root Geom		x	x	Root LSWF Fig. 32
		88-111	50		x	x	

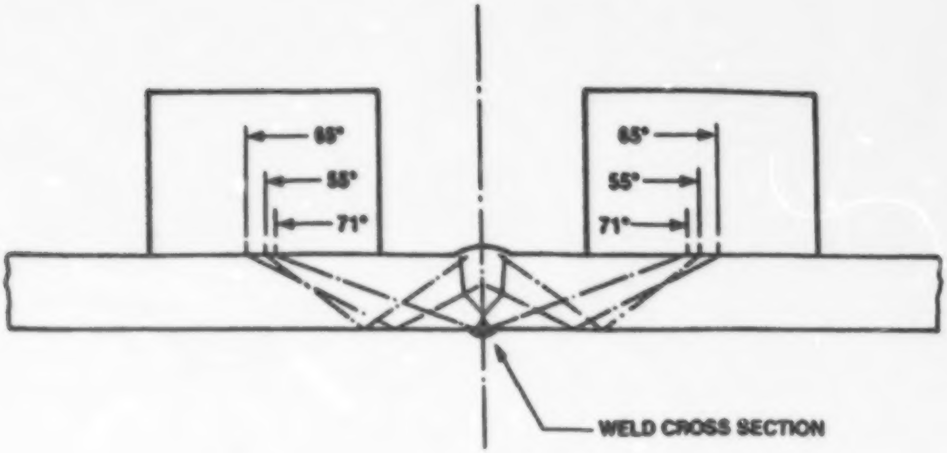
65°
55°
71°
65°
55°
71°
WELD CROSS SECTION

Figure 1: Conventional Transducer Arrangement Showing Angles and Beam Paths Used to Achieve Complete Coverage of the Weld.

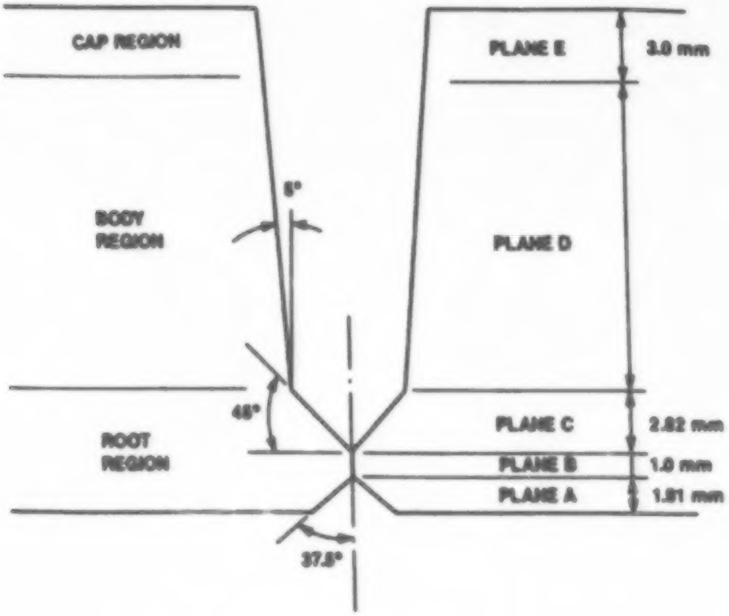
CAP REGION
BODY REGION
ROOT REGION
5°
45°
37.5°
PLANE E
PLANE D
PLANE C
PLANE B
PLANE A
3.0 mm
2.82 mm
1.0 mm
1.81 mm

Figure 2: Location of Inspection Planes within the Weld.

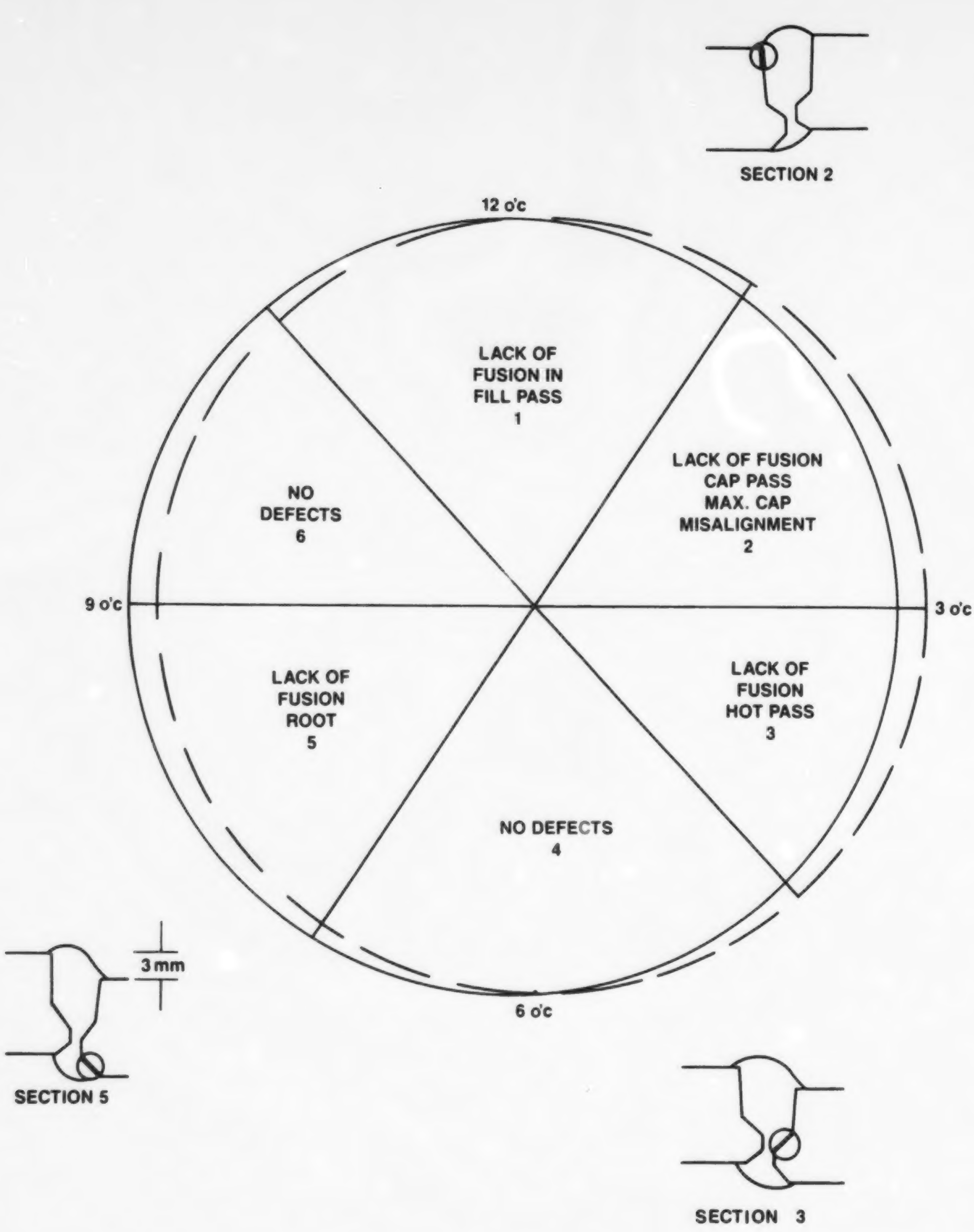
SECTION 2
12 o'c
LACK OF FUSION IN FILL PASS 1
LACK OF FUSION CAP PASS MAX. CAP MISALIGNMENT 2
NO DEFECTS 6
9 o'c
3 o'c
LACK OF FUSION ROOT 5
LACK OF FUSION HOT PASS 3
NO DEFECTS 4
3 mm
6 o'c
SECTION 5
SECTION 3

Figure 3: Schematic of Defects and Misalignment in 9.8 mm Wall Thickness Weld.

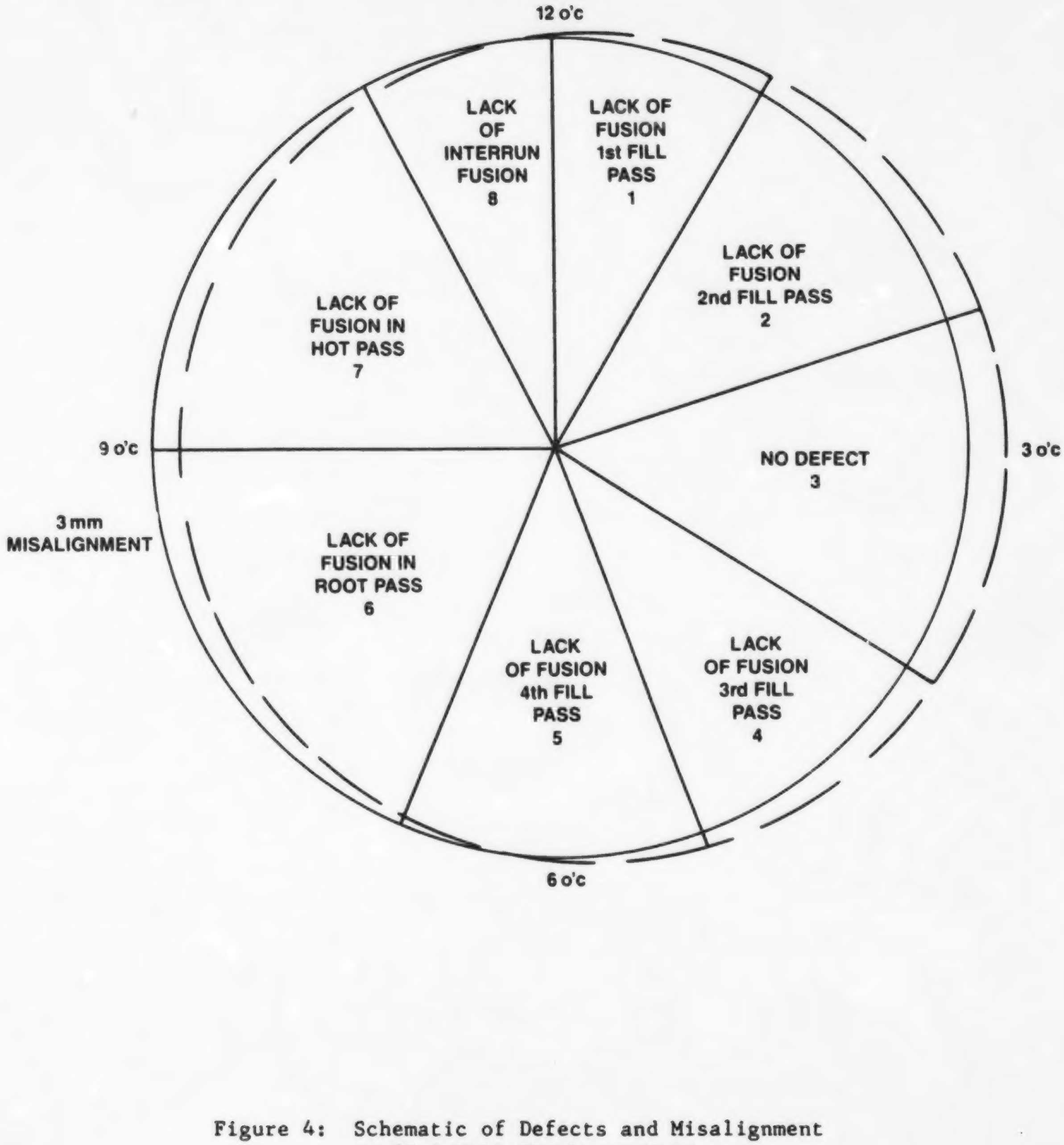
12 o'c
LACK OF INTERRUN FUSION 8
LACK OF FUSION 1st FILL PASS 1
LACK OF FUSION 2nd FILL PASS 2
LACK OF FUSION IN HOT PASS 7
9 o'c
NO DEFECT 3
3 o'c
3 mm MISALIGNMENT
LACK OF FUSION IN ROOT PASS 6
LACK OF FUSION 4th FILL PASS 5
LACK OF FUSION 3rd FILL PASS 4
6 o'c

Figure 4: Schematic of Defects and Misalignment in 20.6 Wall Thickness Weld.

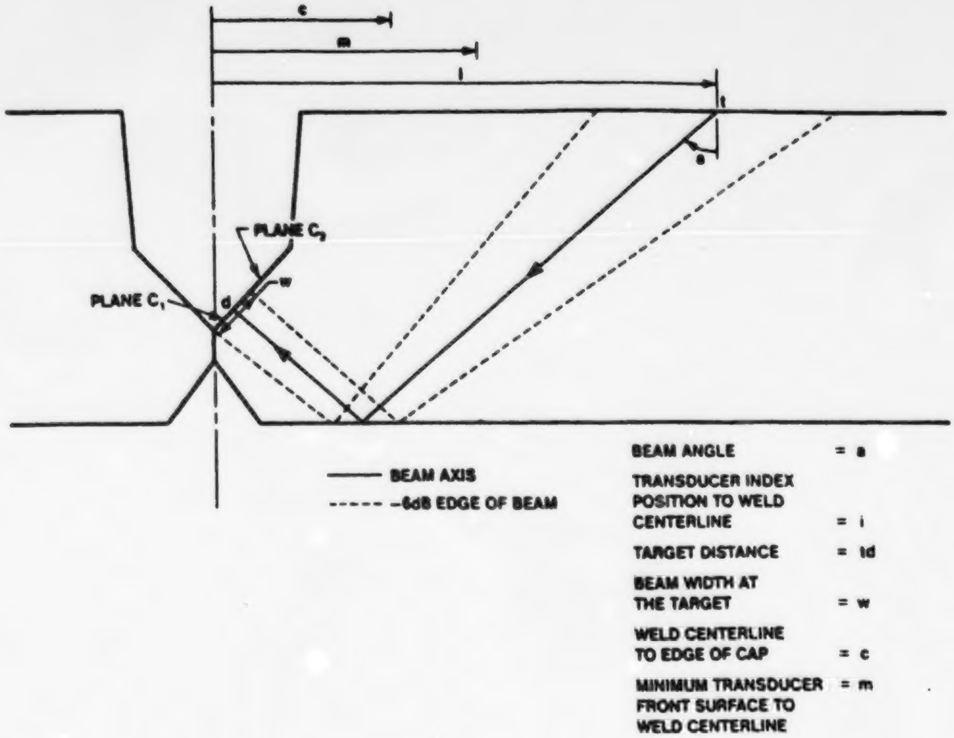
c
m
i
t
a
PLANE C₂
w
PLANE C₁
d
BEAM AXIS
-6dB EDGE OF BEAM
BEAM ANGLE = a
TRANSDUCER INDEX POSITION TO WELD CENTERLINE = i
TARGET DISTANCE = td
BEAM WIDTH AT THE TARGET = w
WELD CENTERLINE TO EDGE OF CAP = c
MINIMUM TRANSDUCER FRONT SURFACE TO WELD CENTERLINE = m

Figure 5: Inspection Design Dimensions, Plane C.

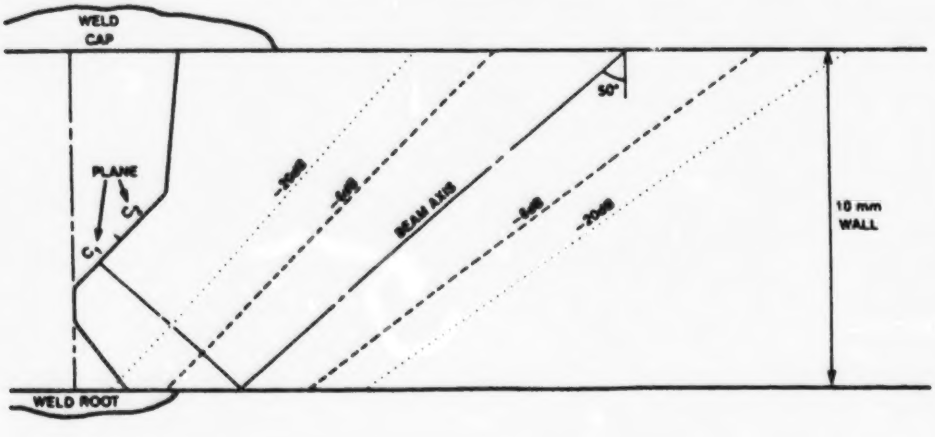
WELD CAP
50°
PLANE
C₁
C₂
-20dB
-6dB
BEAM AXIS
-6dB
-20dB
10 mm WALL
WELD ROOT

Figure 6: Inspection of Plane C and Focus Criteria.

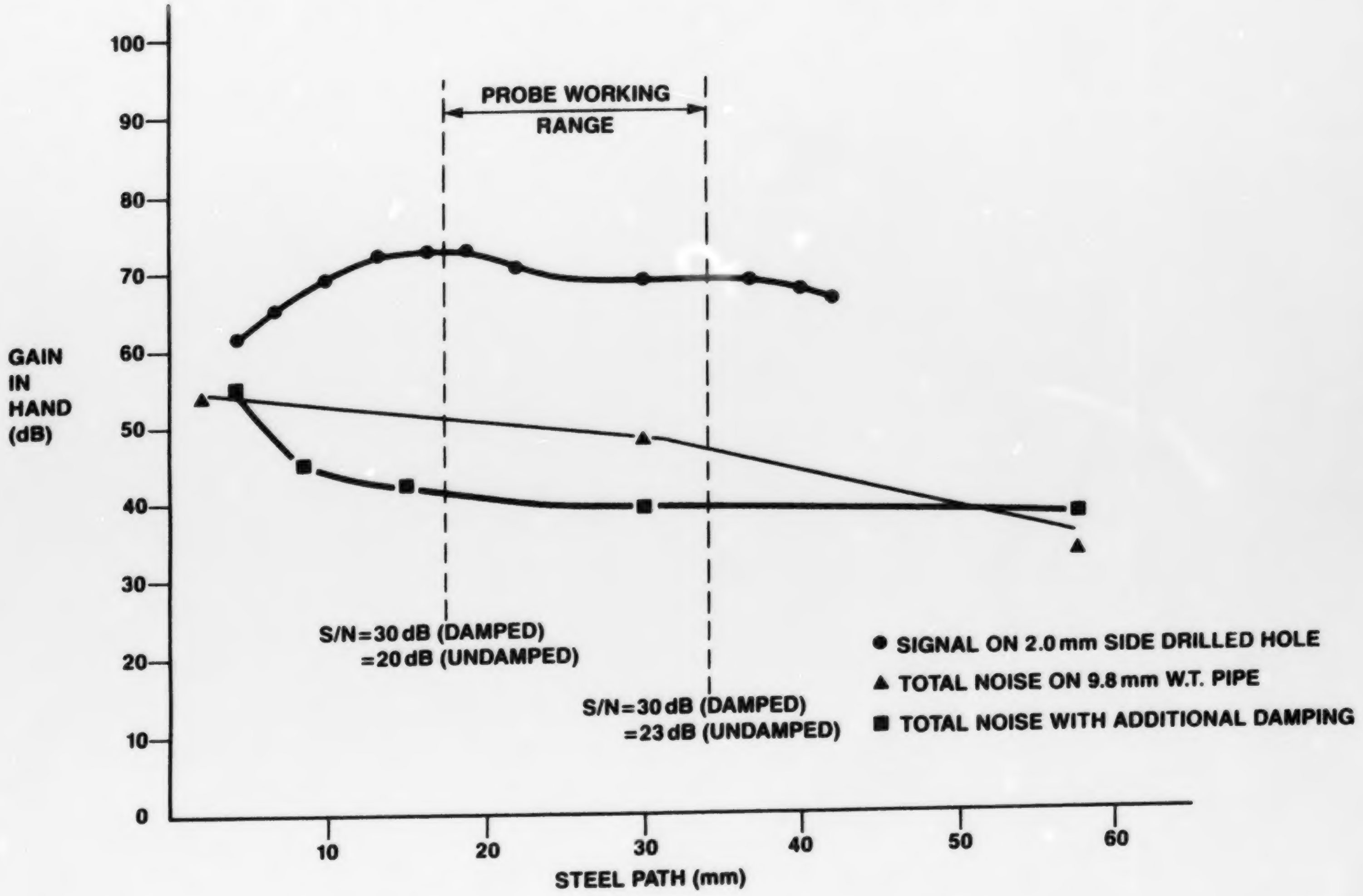

Figure 7: Signal-to-Noise Ratio, 45° Transducer Ref. 001.

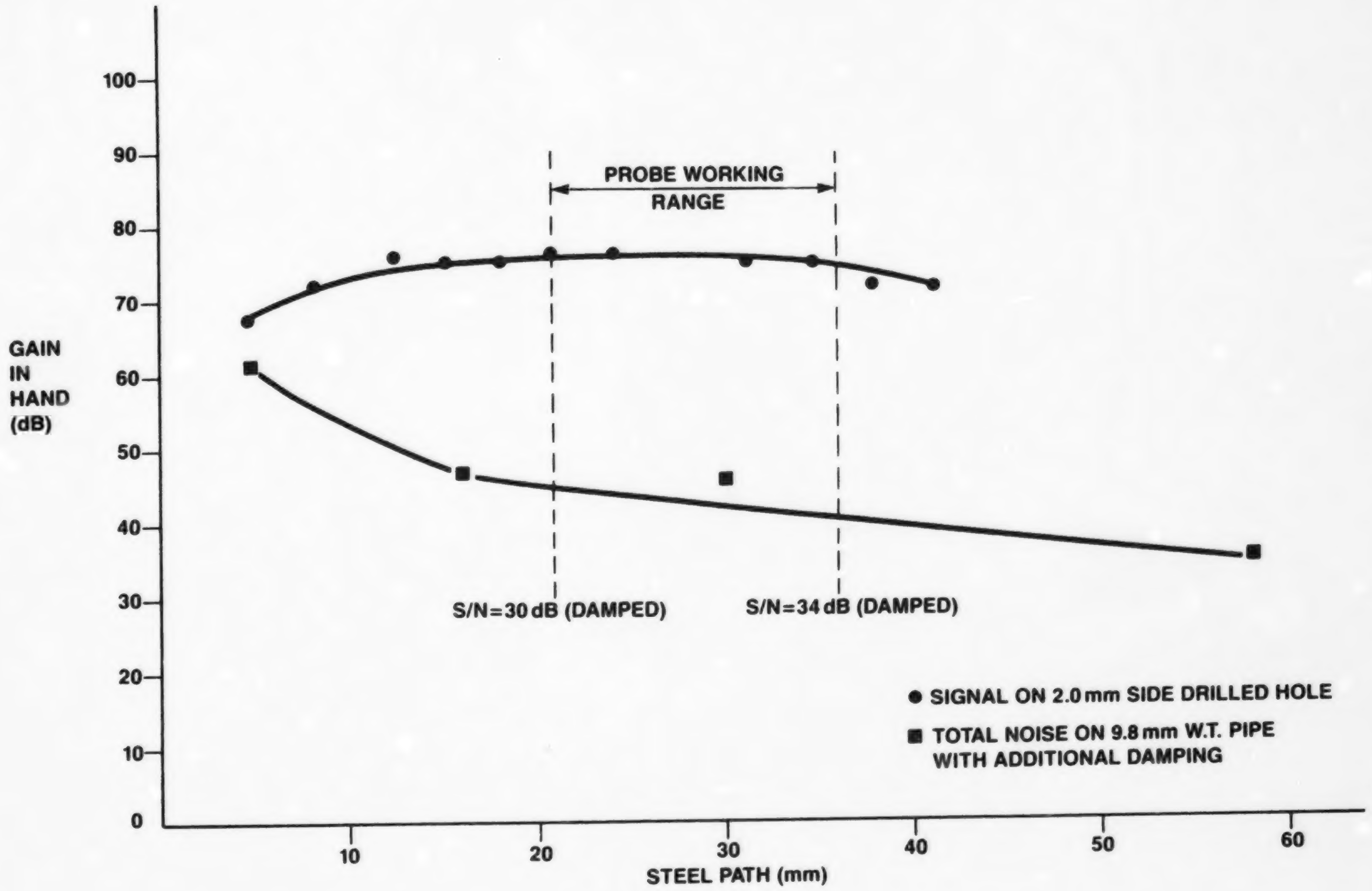

Figure 8: Signal-to-Noise Ratio, 45° Transducer Ref. 002.

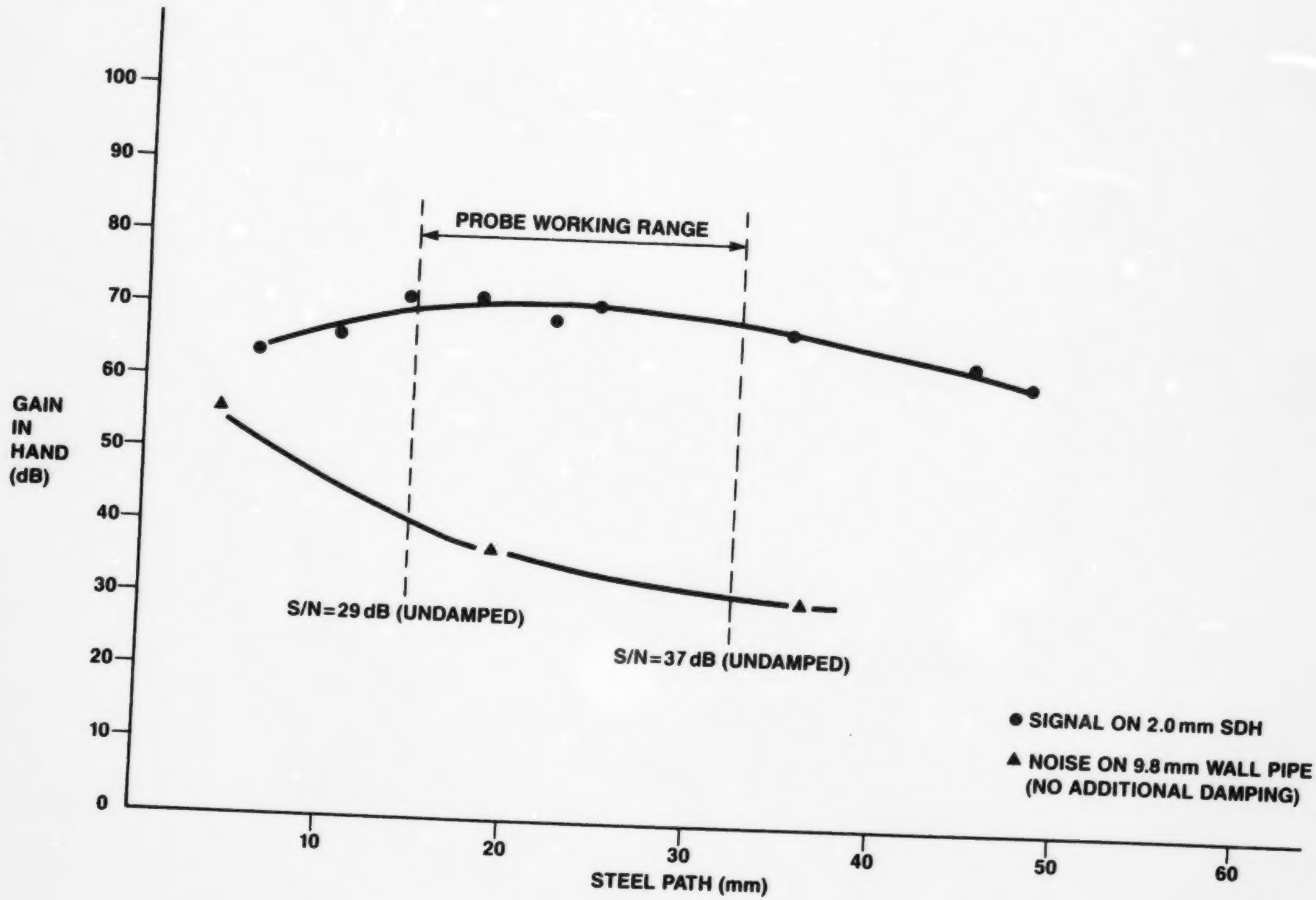

Figure 9: Signal-to-Noise Ratio, 52.5° Transducer Ref. 003.

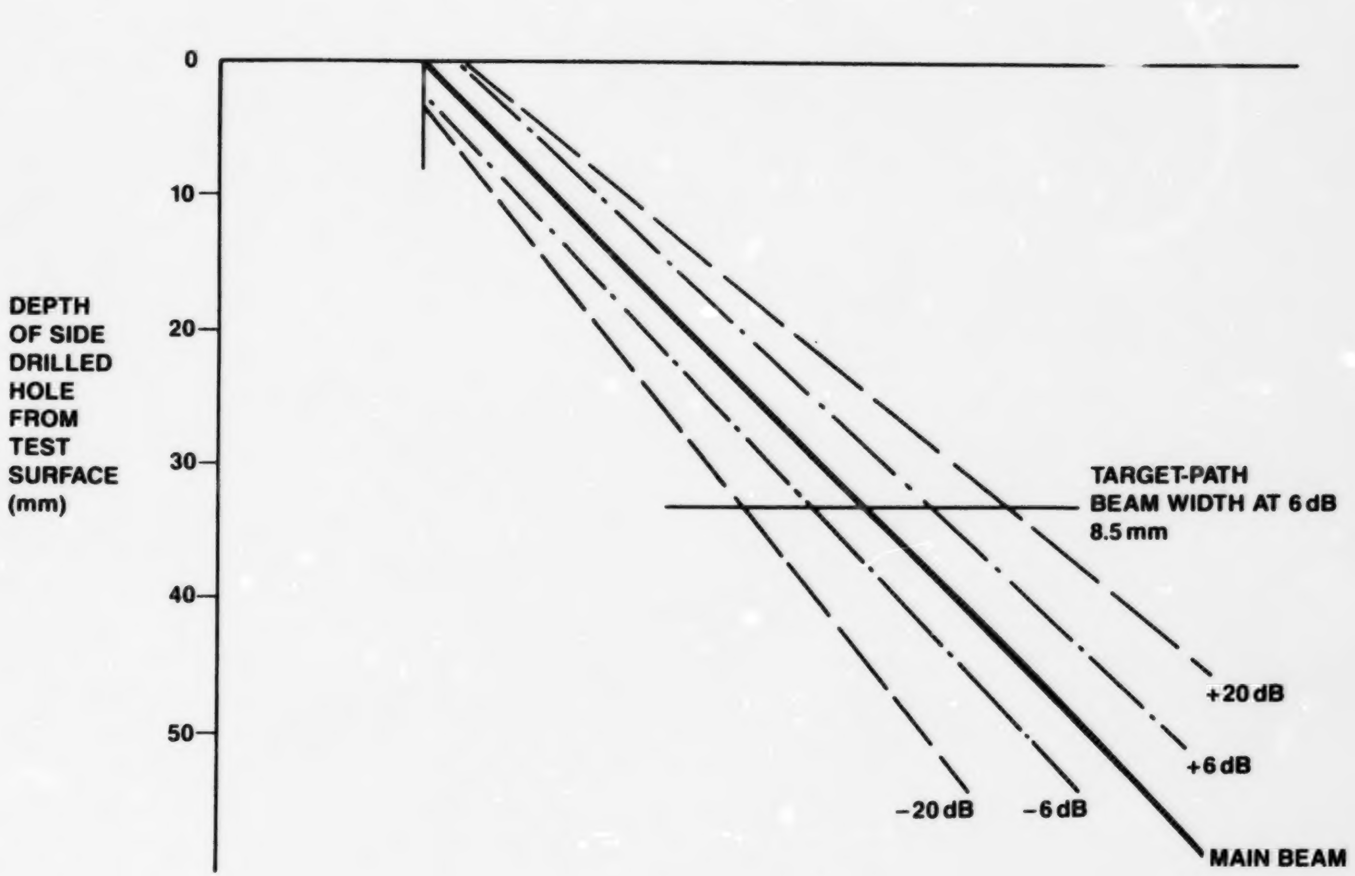

Figure 10: Beam Width Measurements of Transmitter Probe #88-111.

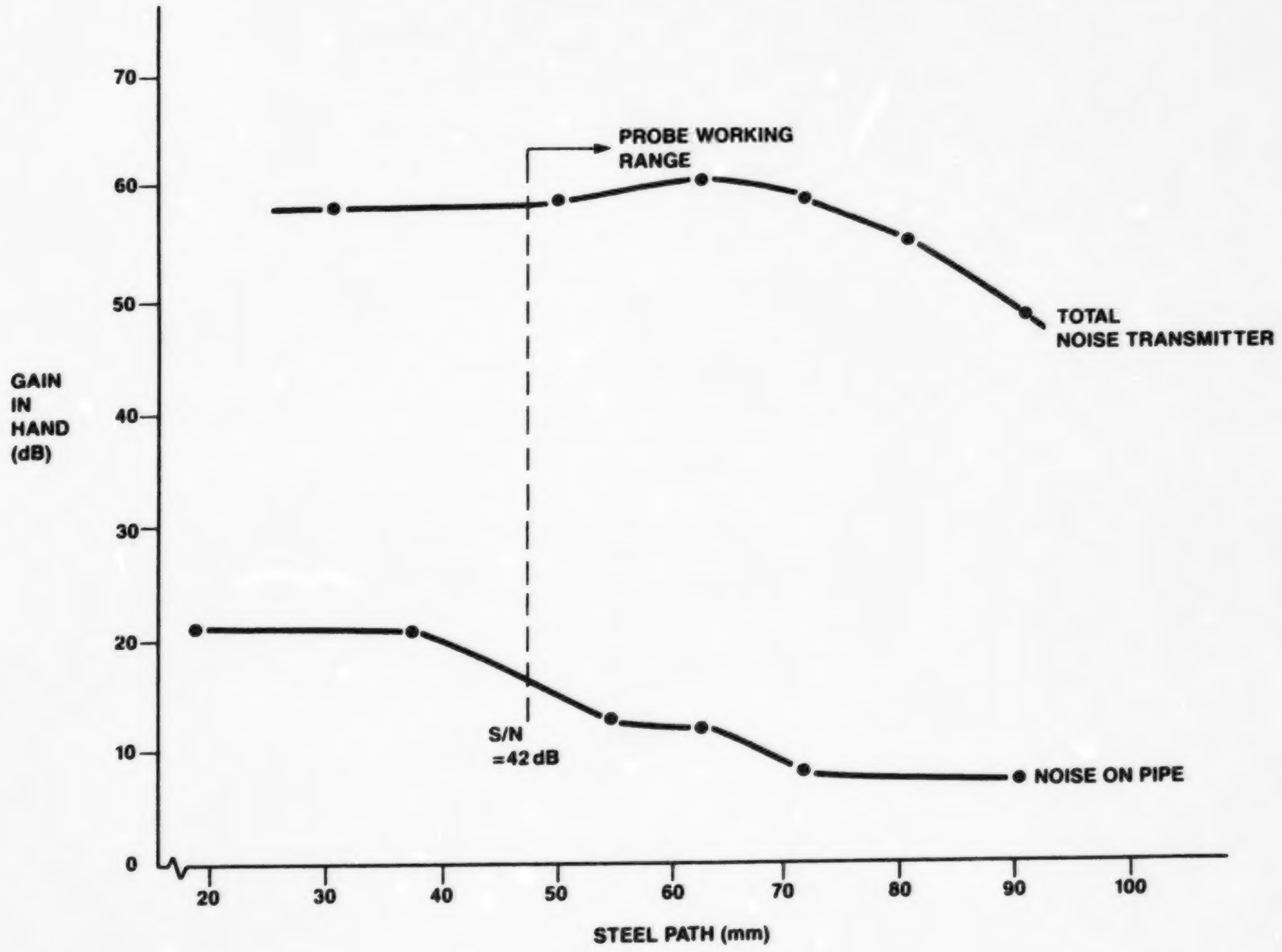

Figure 11: Signal-to-Noise Ratio, Pitch-Catch Transmitter-Receiver RTD 88-111.

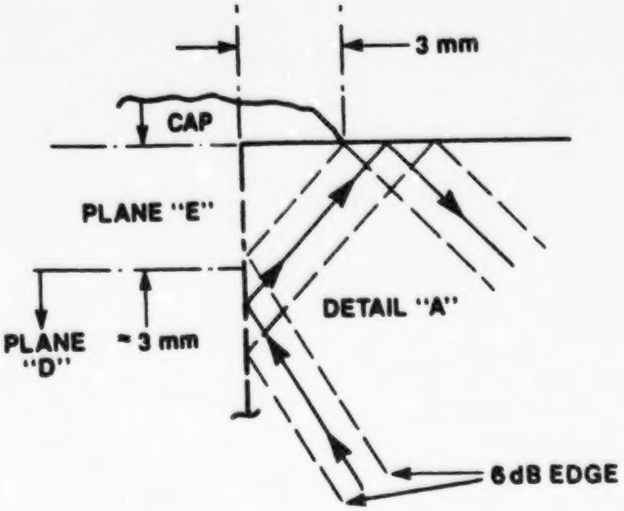
3 mm
CAP
PLANE "E"
PLANE "D"
~3 mm
DETAIL "A"
6dB EDGE

Figure 12: Limitation of the Pitch-Catch Technique Near to the Surface.

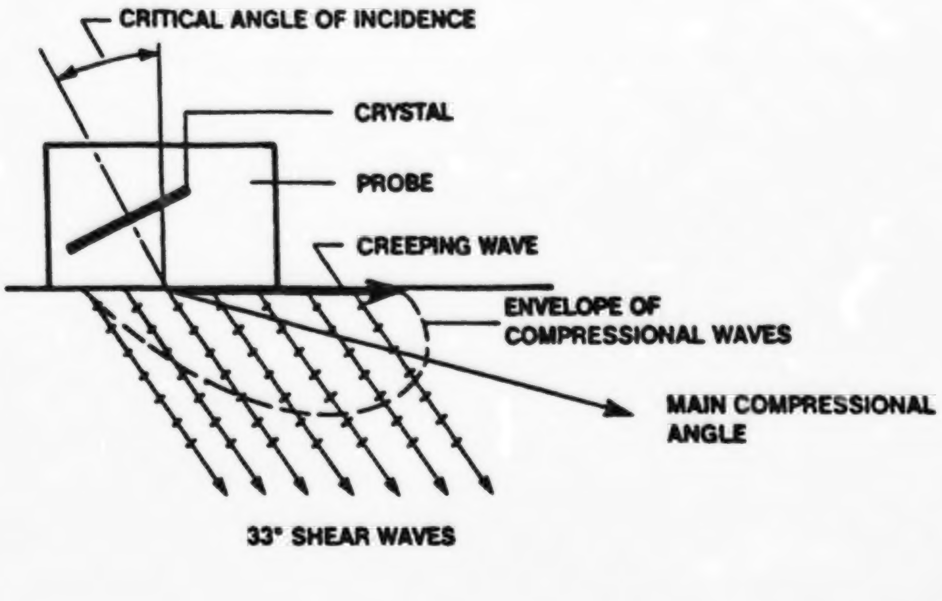
CRITICAL ANGLE OF INCIDENCE
CRYSTAL
PROBE
CREEPING WAVE
ENVELOPE OF COMPRESSIONAL WAVES
MAIN COMPRESSIONAL ANGLE
33° SHEAR WAVES

Figure 13: Creeping Wave.

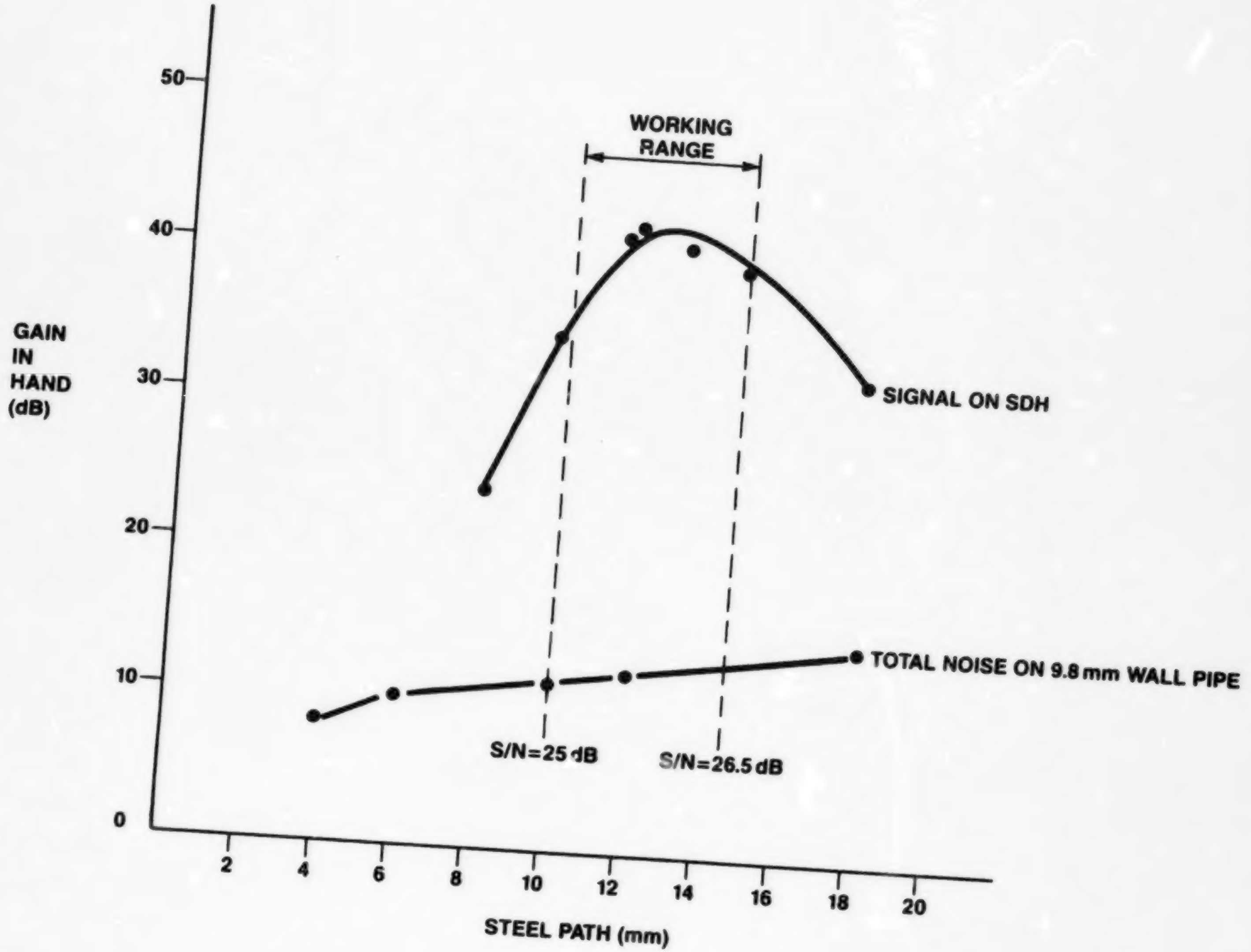

Figure 14: Signal-to-Noise Ratio, Creeping Wave Transducer RTD-BAM 88-110.

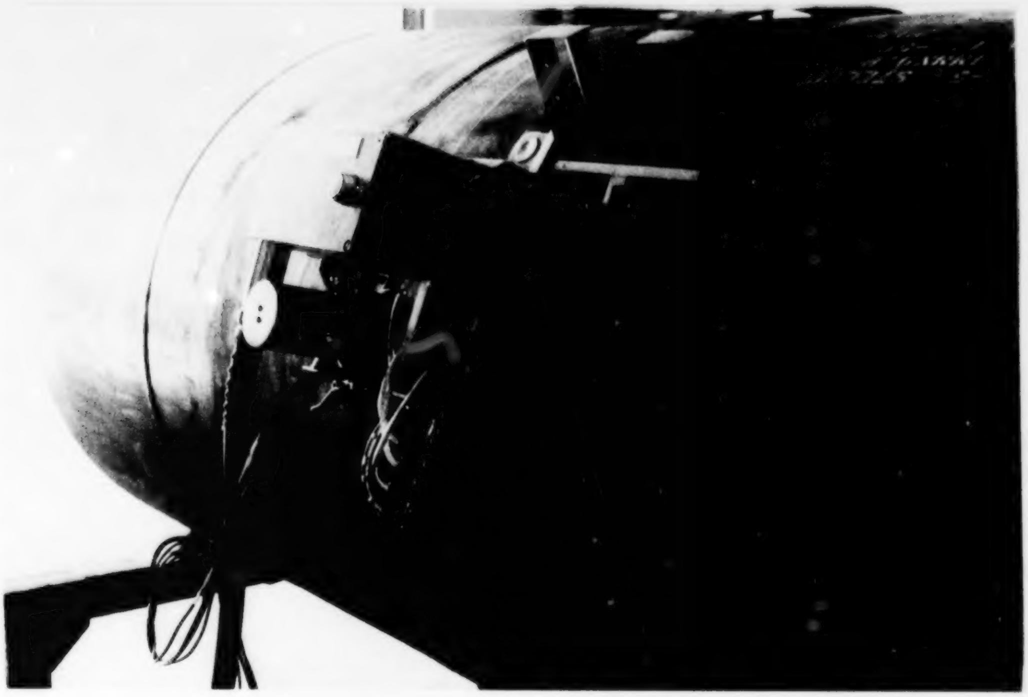

Figure 15: Modified Probe Holder, 4 Transducers 9.8mm wall.

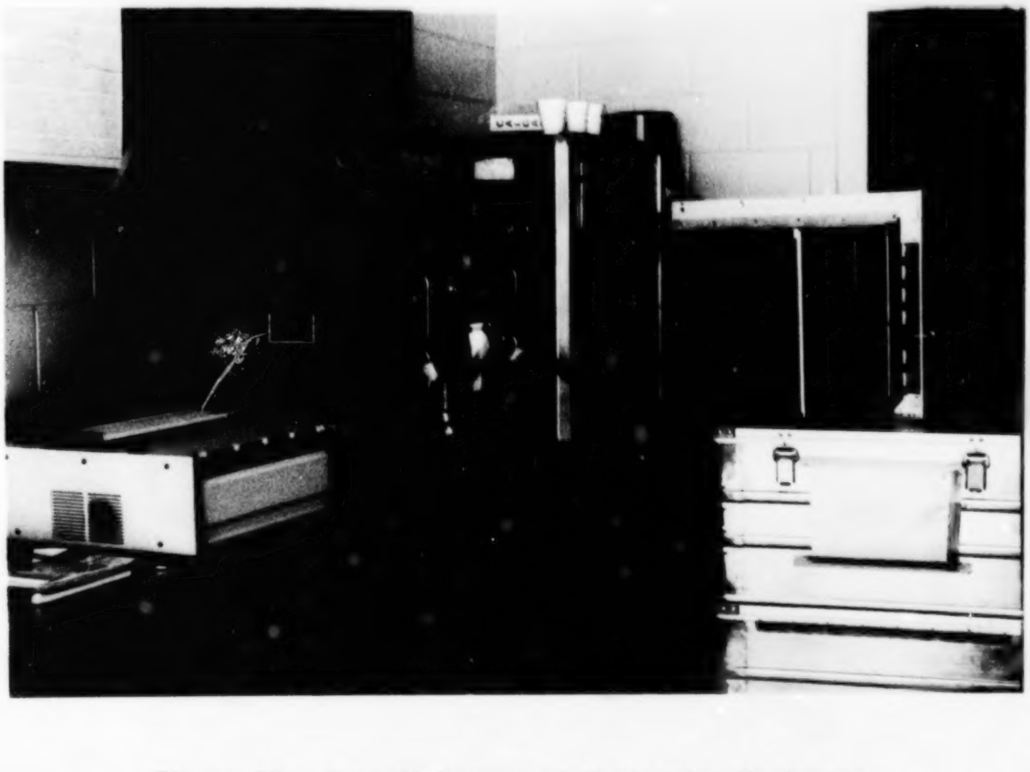

Figure 16: Overall Layout of Monitoring Equipment.

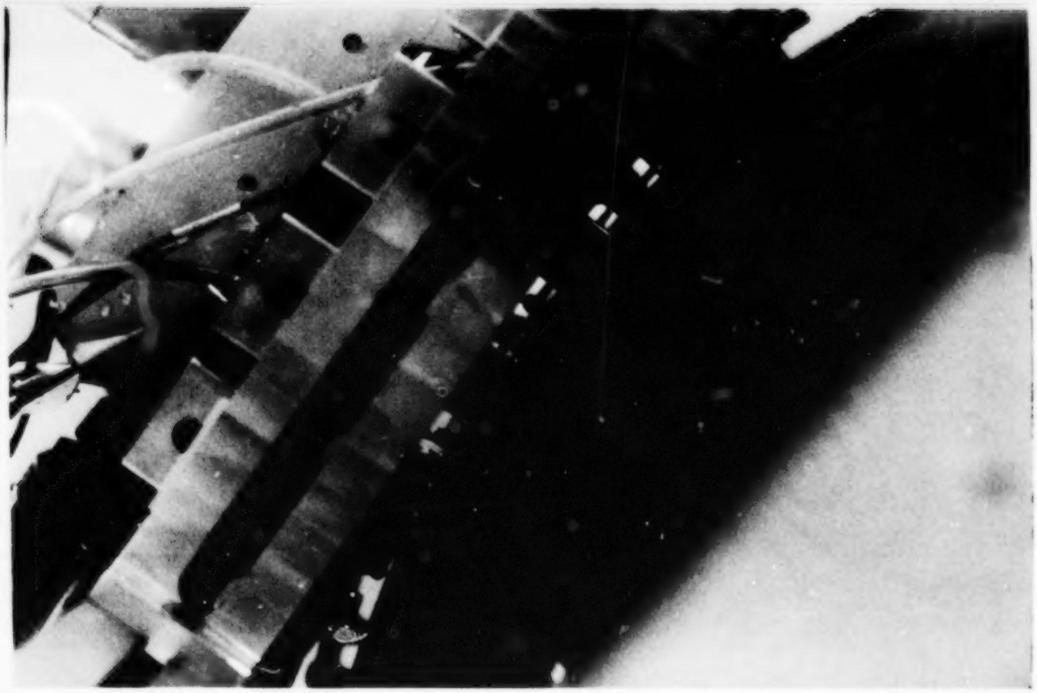

Figure 17: Probes in Contact with Pipe Surface and Couplant System.

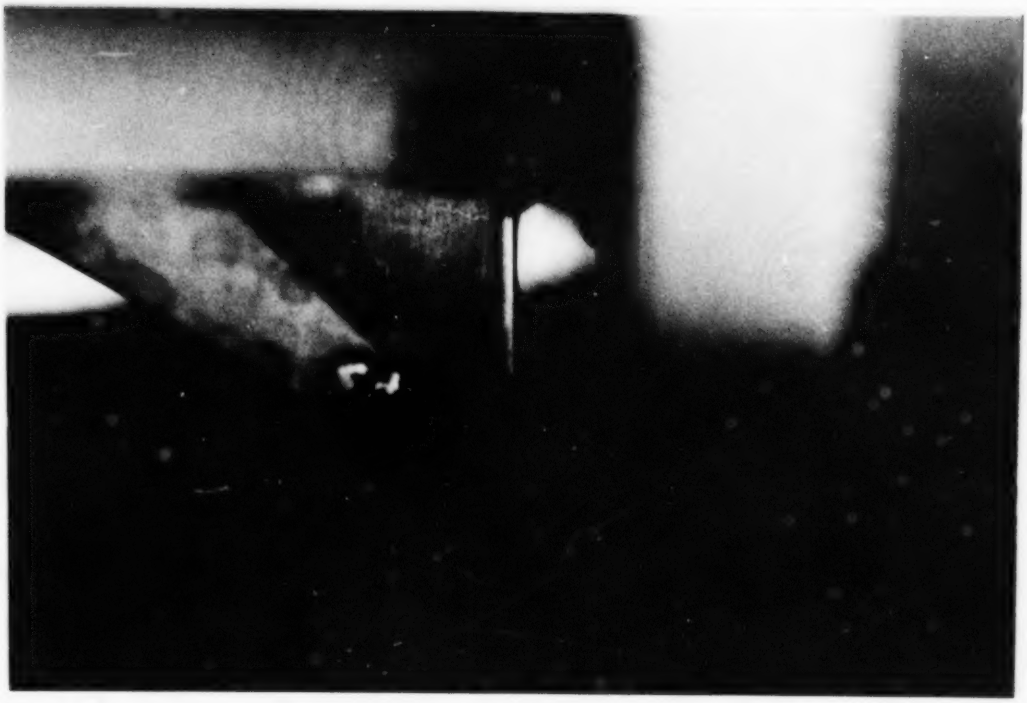

Figure 18: Probe 003 and Cap Interference at Design + 1mm, Excessive Cap Overlap.

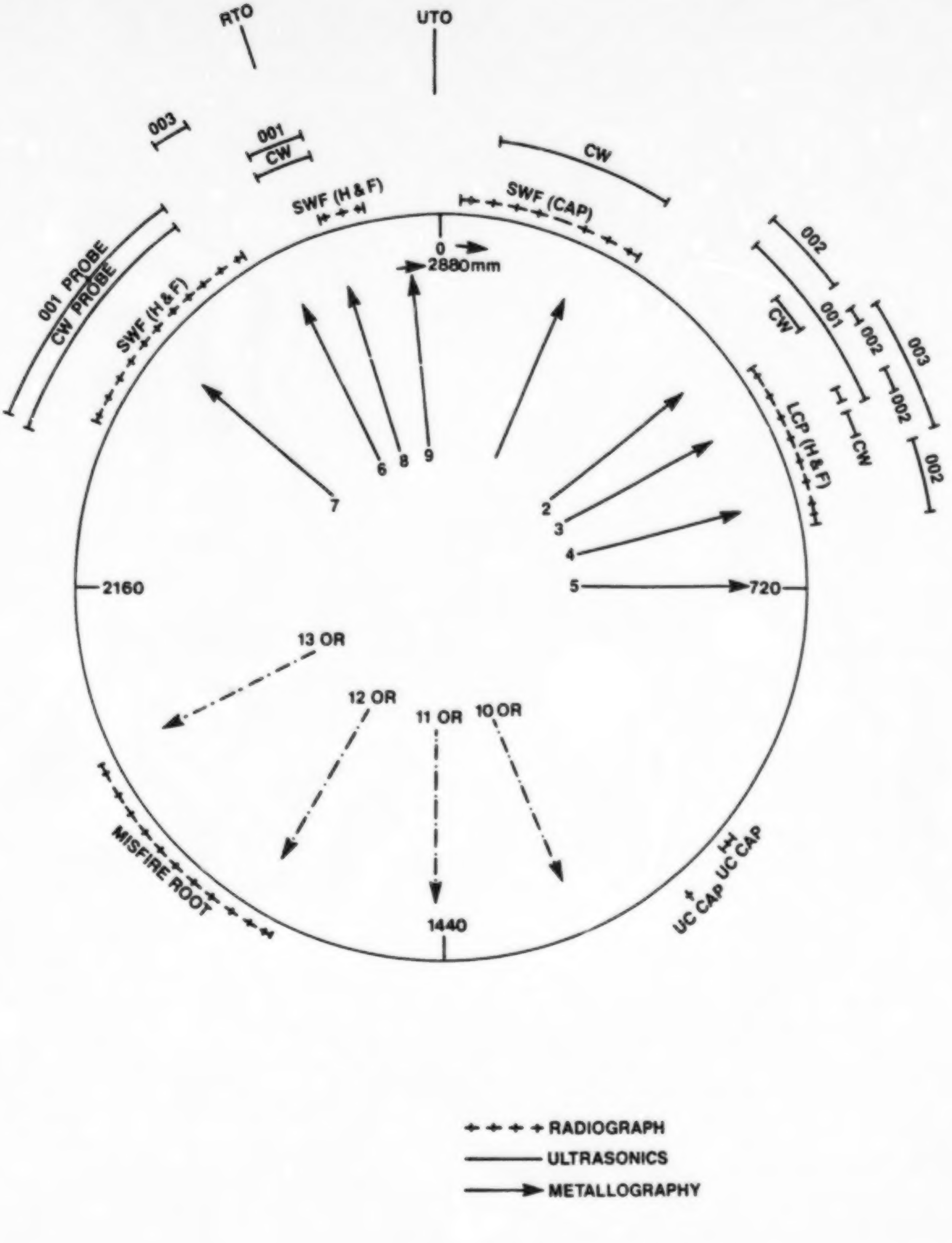
RTO
UTO
003
001
CW
CW
001 PROBE
CW PROBE
SWF (H & F)
SWF (H & F)
SWF (CAP)
002
001
CW
002
003
002
CW
002
LCP (H & F)
0
2880mm
6
8
9
7
2
3
4
5
720
2160
13 OR
12 OR
11 OR
10 OR
1440
MISFIRE ROOT
UC CAP
UC CAP
RADIOGRAPH
ULTRASONICS
METALLOGRAPHY

Figure 19: Ultrasonic and Radiographic Comparisons, 9.8mm Wall, Reference Side.

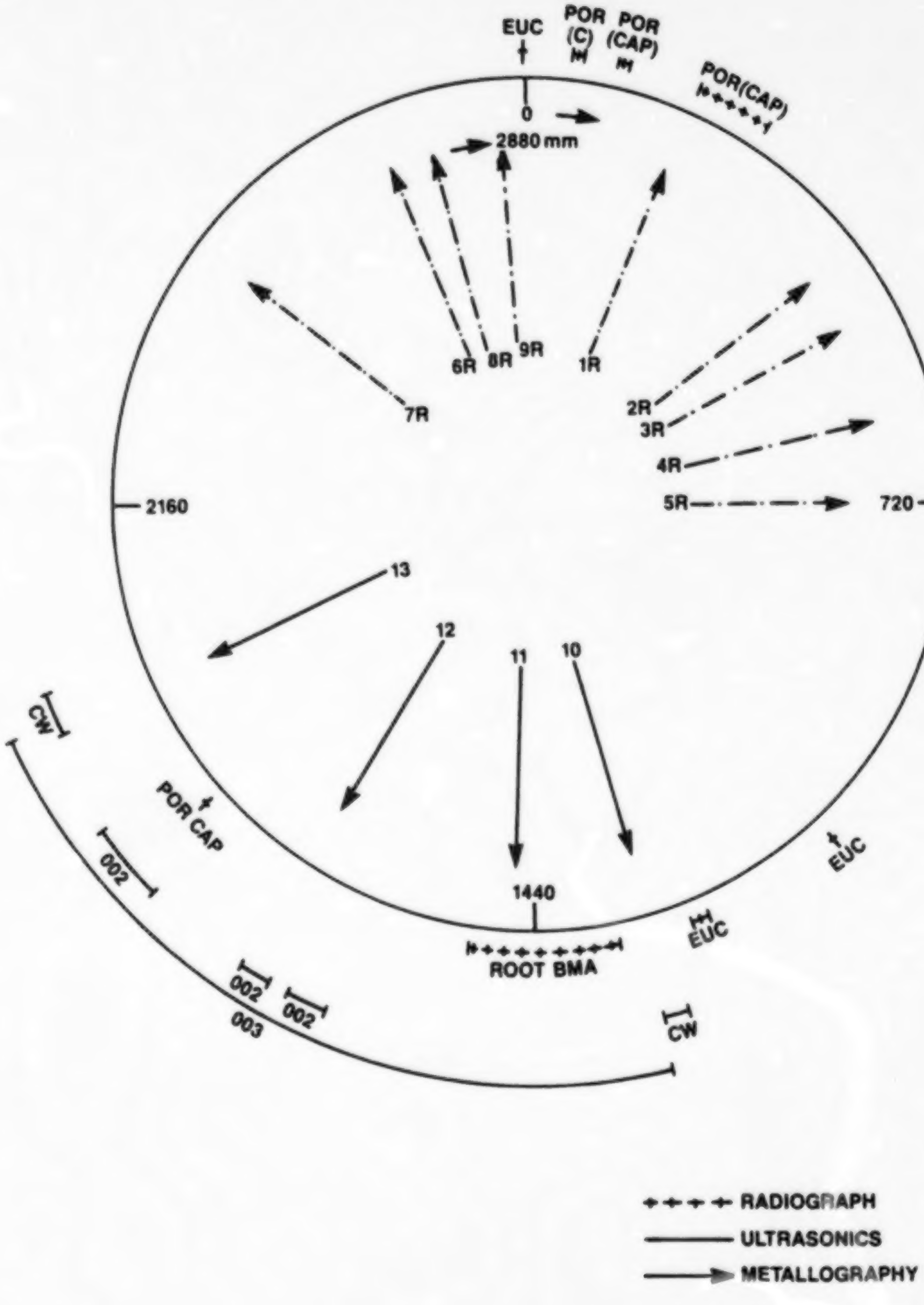
EUC
POR (C)
POR (CAP)
POR(CAP)
0
2880 mm
6R
8R
9R
1R
7R
2R
3R
4R
5R
2160
720
13
12
11
10
CW
POR CAP
002
1440
EUC
EUC
ROOT BMA
002
002
003
CW
RADIOGRAPH
ULTRASONICS
METALLOGRAPHY

Figure 20: Ultrasonic and Radiographic Comparisons, 9.8mm Wall, Opposite Reference Side.

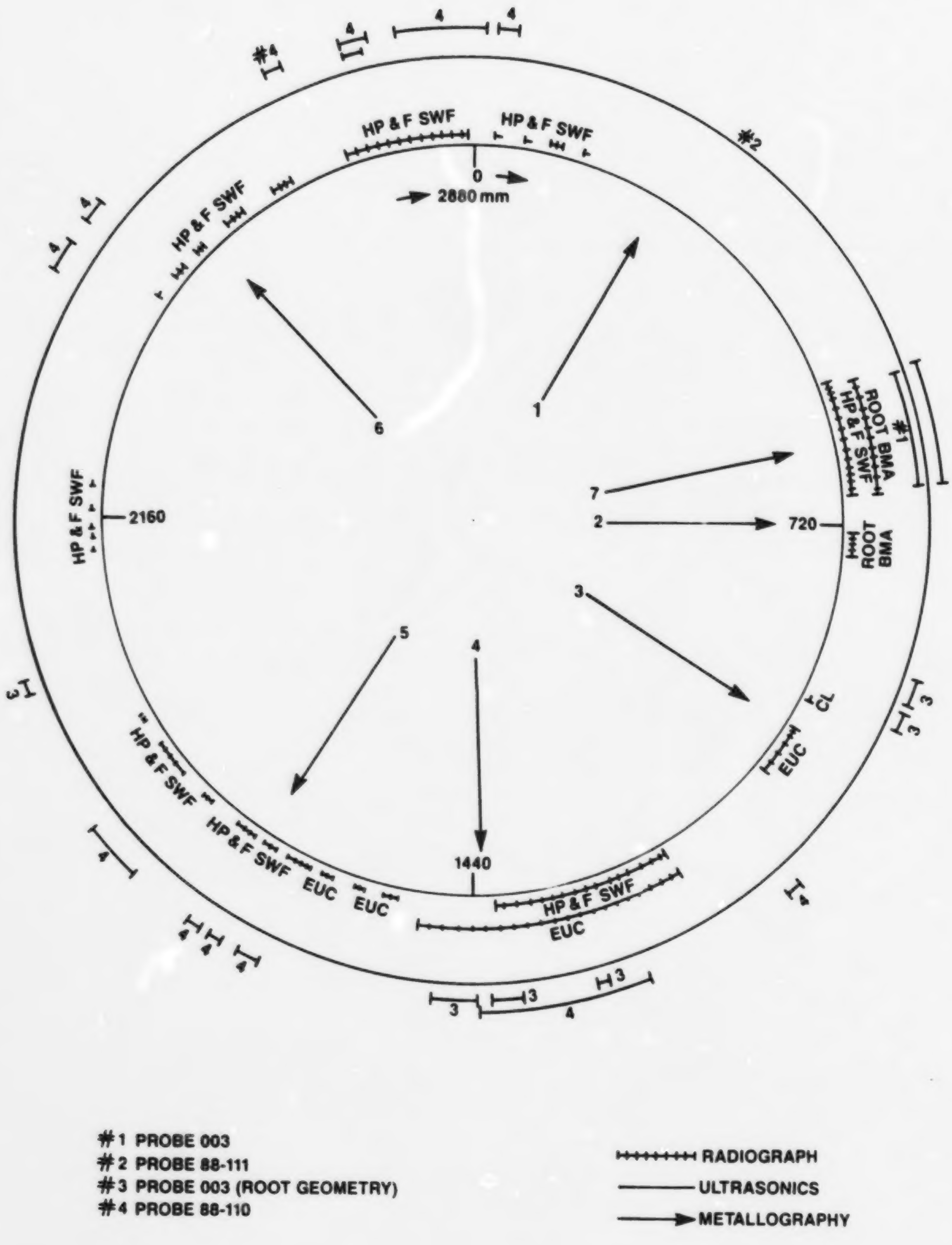
#4
4
4
4
4
4
#2
HP & F SWF
HP & F SWF
0
2880 mm
HP & F SWF
ROOT BMA
HP & F SWF
#1
720
ROOT BMA
2160
HP & F SWF
1
2
3
4
5
6
7
CL
EUC
3
3
3
HP & F SWF
HP & F SWF
EUC
EUC
1440
HP & F SWF
EUC
4
4
4
4
4
3
3
3
4
#1 PROBE 003
#2 PROBE 88-111
#3 PROBE 003 (ROOT GEOMETRY)
#4 PROBE 88-110
RADIOGRAPH
ULTRASONICS
METALLOGRAPHY

Figure 21: Ultrasonic and Radiographic Comparisons, 20.6mm Wall, Reference Side.

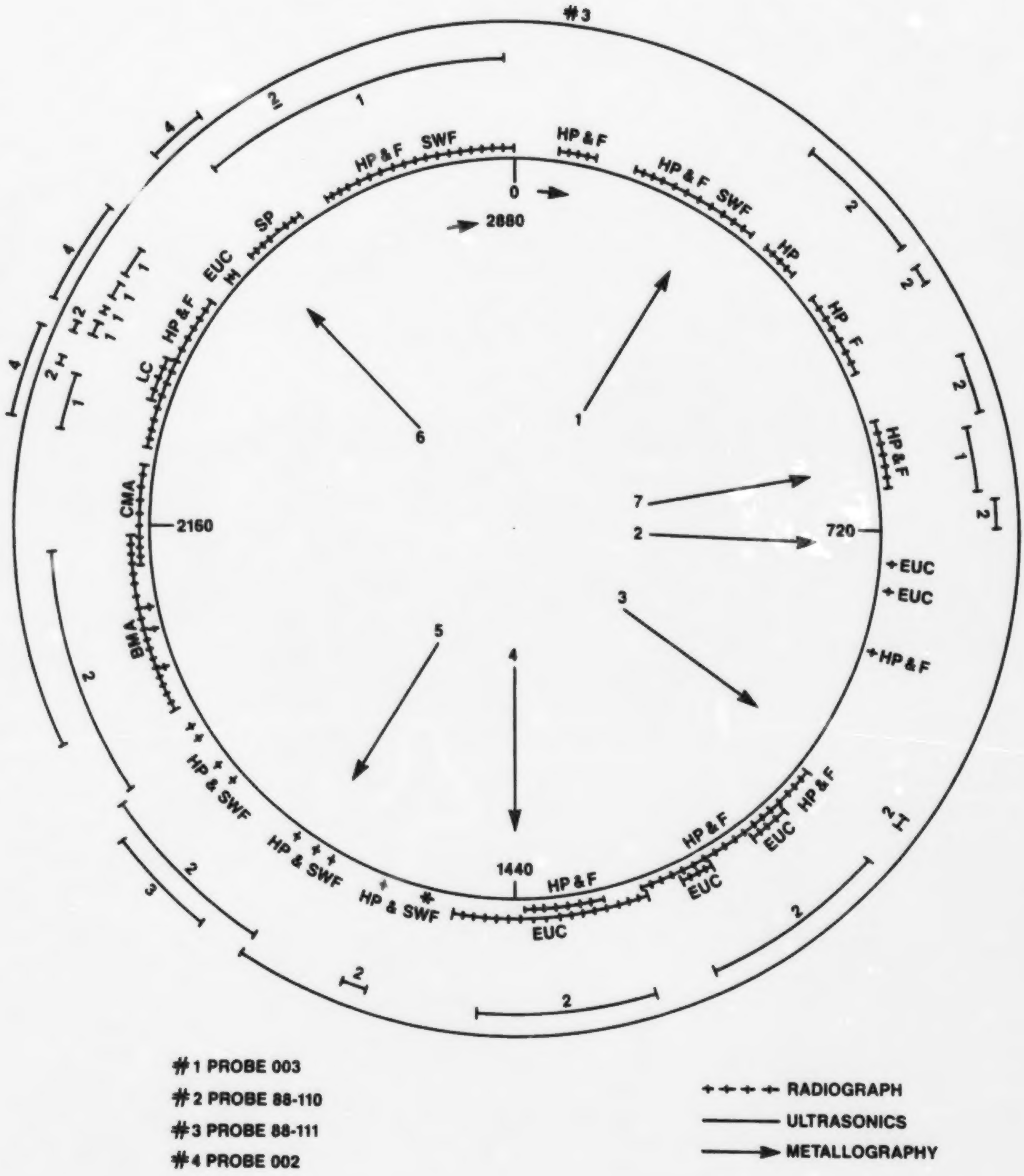
#3
0
2880
720
1440
2160
HP & F
SWF
HP
SP
EUC
LC
CMA
BMA
HP & SWF
1
2
3
4
5
6
7
#1 PROBE 003
#2 PROBE 88-110
#3 PROBE 88-111
#4 PROBE 002
RADIOGRAPH
ULTRASONICS
METALLOGRAPHY

Figure 22: Ultrasonic and Radiographic Comparisons, 20.6mm, Opposite Reference Side.

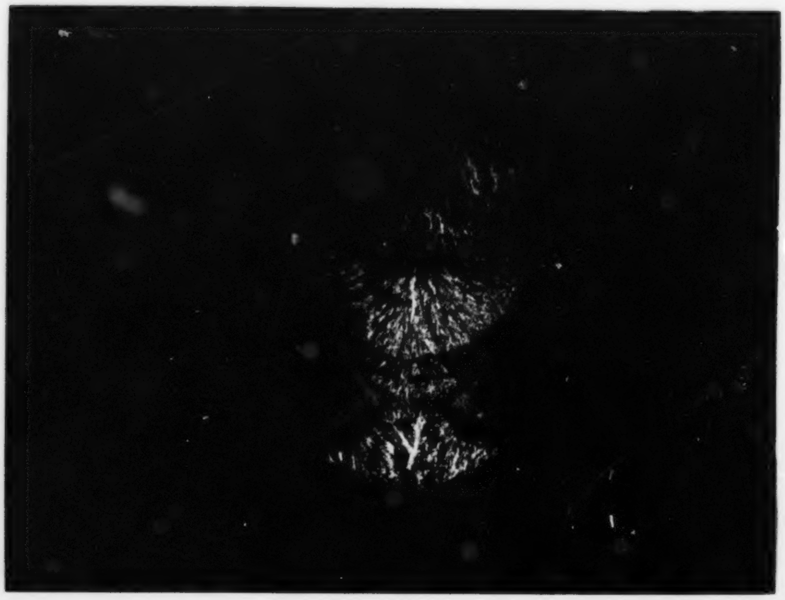

Figure 23: 9.8mm Wall, Section 5, No Defect. X 4

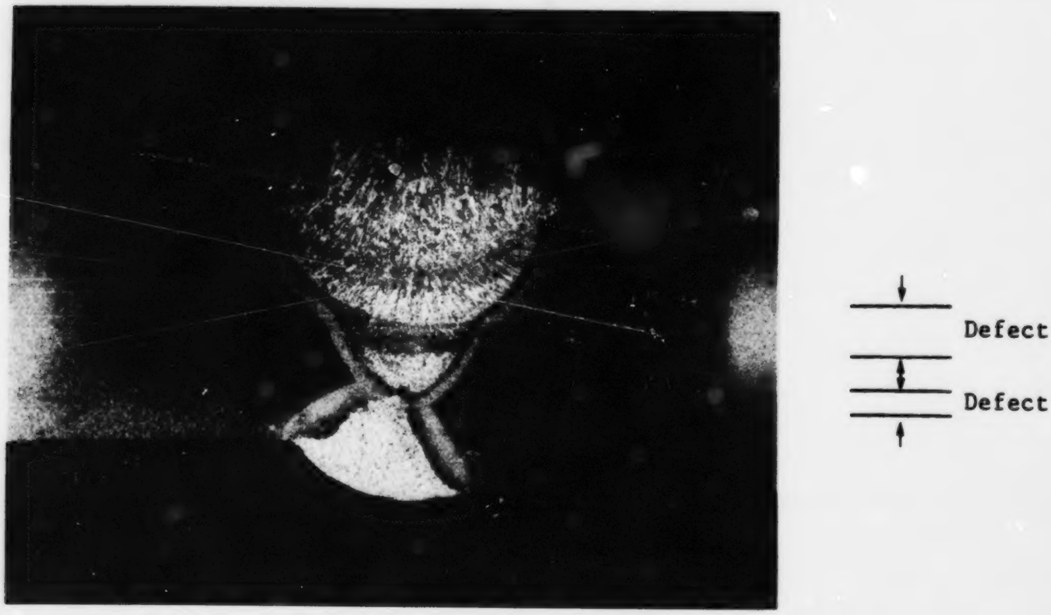
Defect
Defect

Figure 24: 9.8mm Wall, Section 2. Defects Only Found by Ultrasonics. X 4

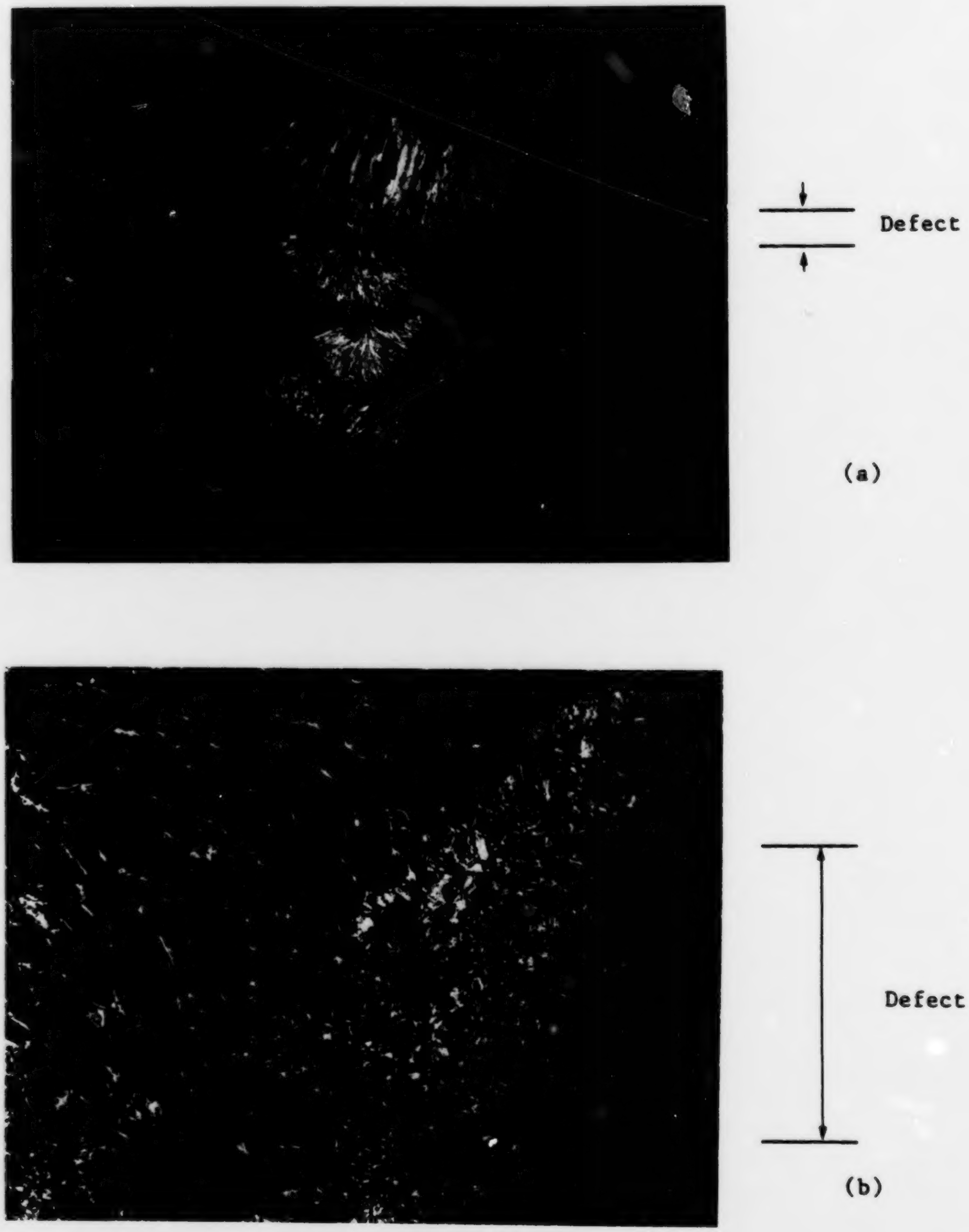
Defect
(a)
Defect
(b)

Figure 25: 9.8mm Wall, Section 13. Defect Under the Cap Only Found by Ultrasonics. (a) X 4 (b) X 50

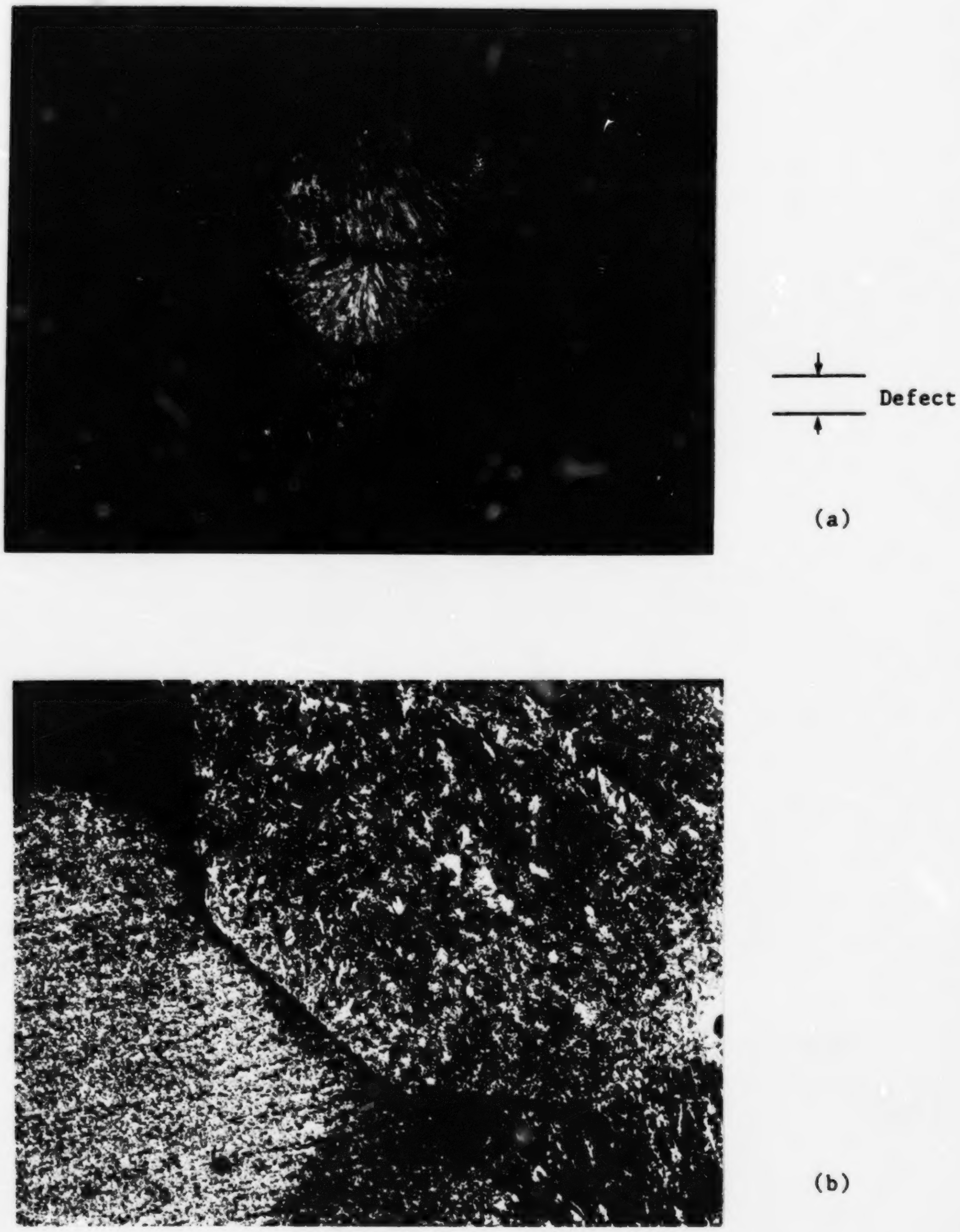

Figure 26: 9.8mm Wall, Section 11, Lack of Root Bead Fusion Found by Ultrasonics and identified only as Bead Misalignment by Radiography. (a) X 4 (b) X 50

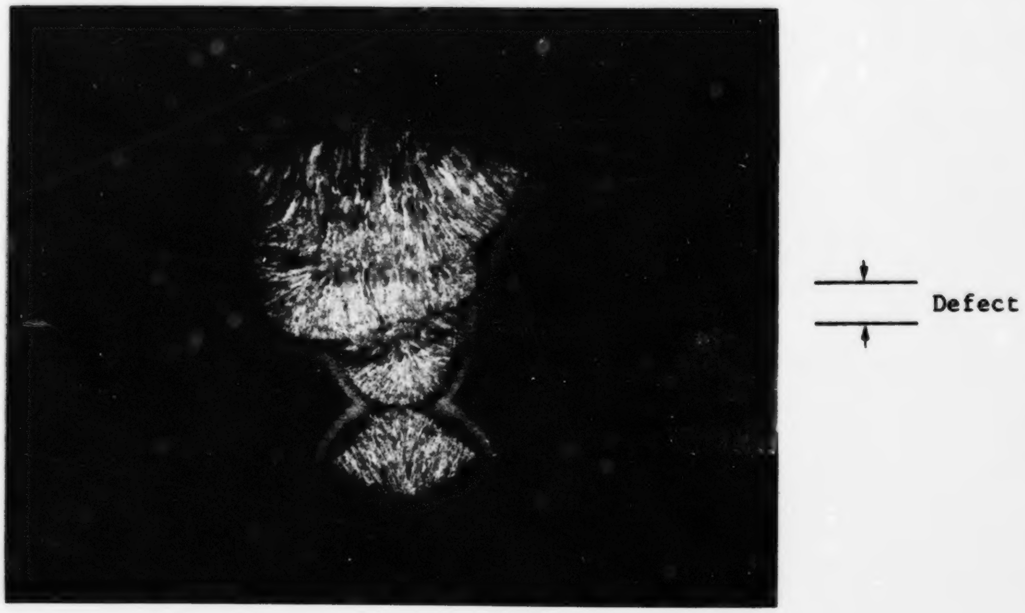

Figure 27: 9.8mm Wall, Section 7, Lack of Sidewall Fusion Detected by the Creeping Wave, and Partial Defect Extending Down the Hot Pass Detected by Probe 001. X 4

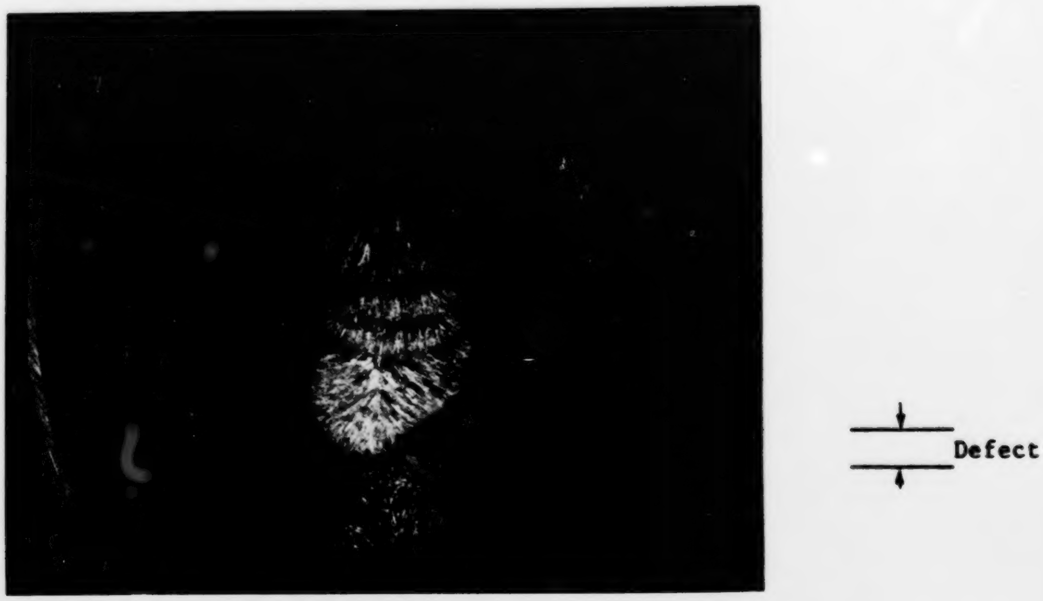

Figure 28: 20.6mm Wall, Section 6, Showing Hot Pass Root Defect Only Found by Radiography. X 3

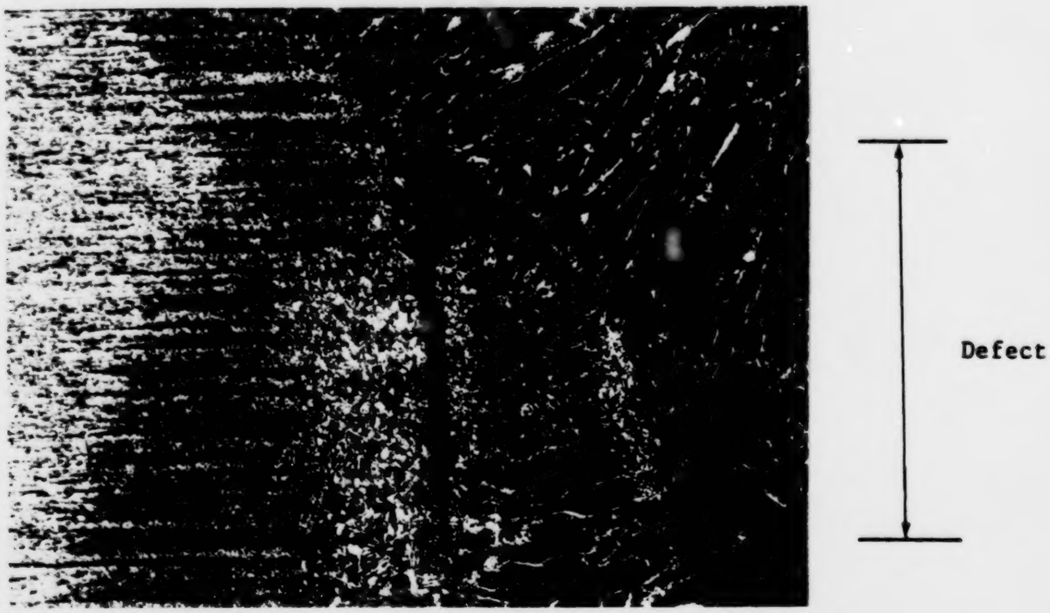

Figure 29: 20.6mm Wall, Section, Lack of Sidewall Fusion Defect Only Found by Ultrasonics. X 50

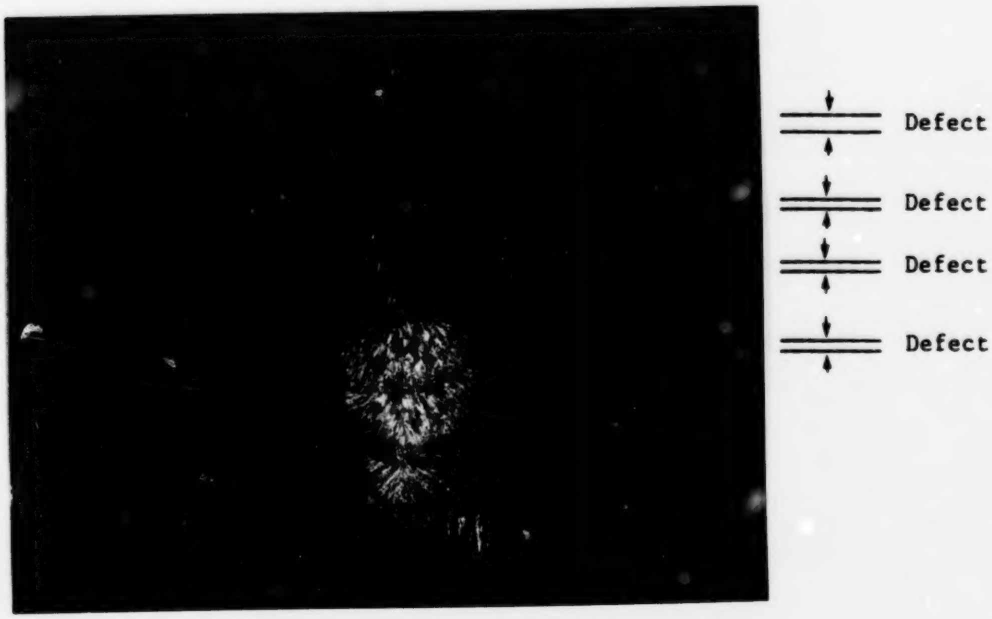
Defect
Defect
Defect
Defect

Figure 30: 20.6mm Wall, Section 4, Lack of Sidewall Fusion and External Under Cut, only the EUC was Reported by Radiography. X 3

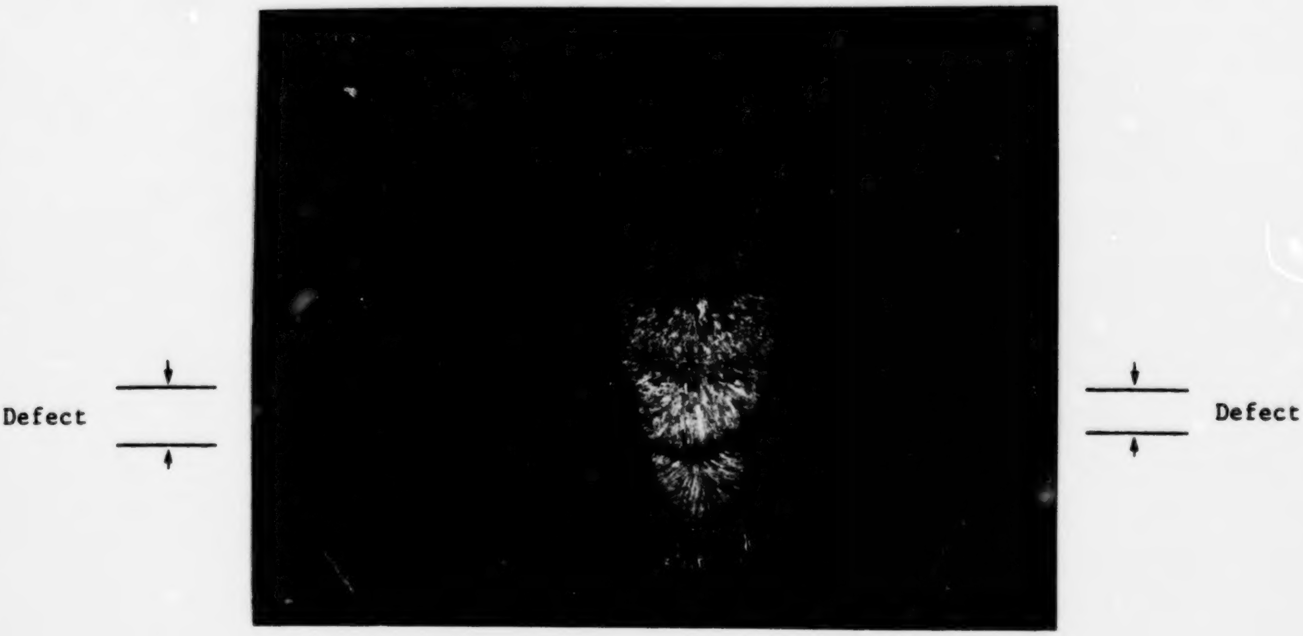
Defect
Defect

Figure 31: 20.6mm Wall, Section 2, Lack of Sidewall Fusion Reported by both and Root Geometry by Ultrasonics. X 3

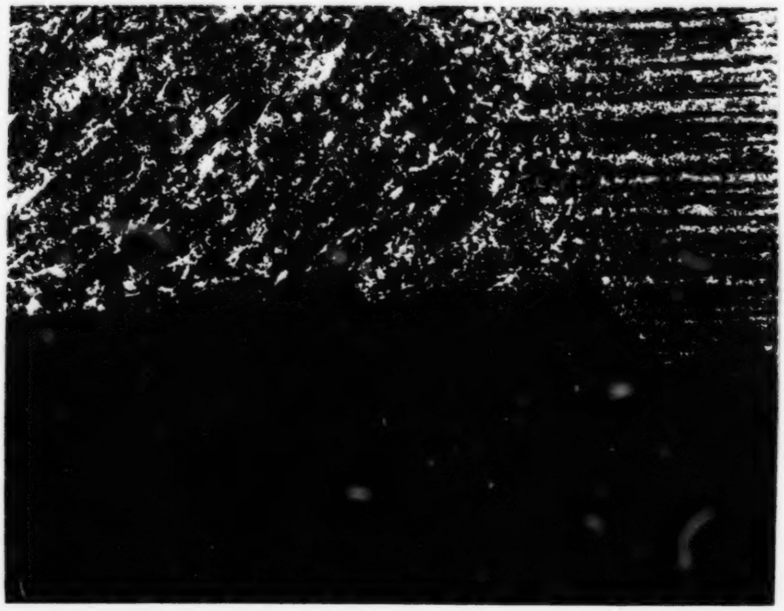

Figure 32: 20.6mm Wall Section 7, Details of the Root Geometry Picked Upon Probe 003, and the Unmelted Portion of the Root Geometry. X 50

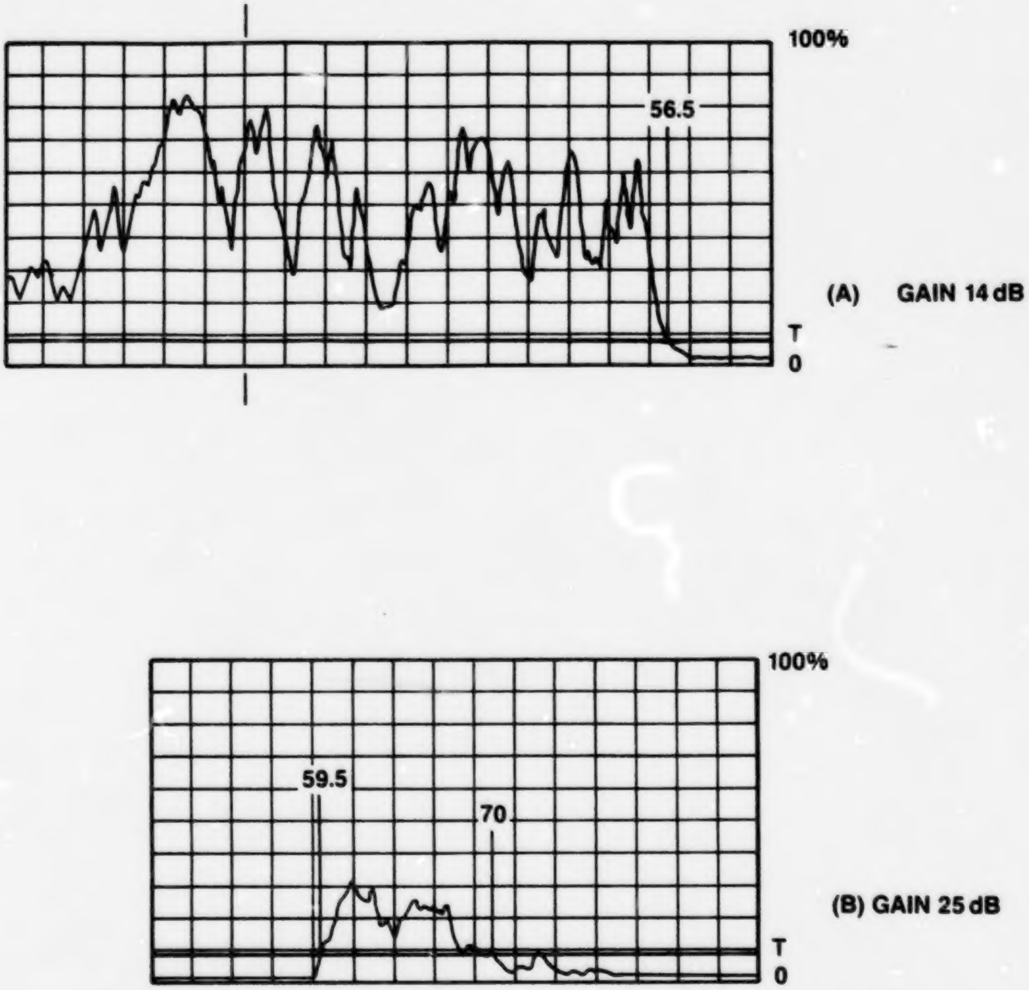

Figure 33: Echo Amplitude Charts for Probe 003 from (a) Lack of Fusion Defect in the 9.8mm Wall, and (b) Unmelted Root Region in the 20.6mm Wall.

APPENDIX 1

Report on Production of Focused Probes for Girth Weld Inspection by The Welding Institute, U.K.

24789/1/88
MARCH 1988

PRODUCTION OF FOCUSED PROBES FOR GIRTH WELD INSPECTION

For: NOVA, An Alberta Corporation

By: J.L. Turner and M.R. Kirby

THE WELDING INSTITUTE
Abington Hall, Abington, Cambridge. CB1 6AL

Telephone 0223 891162 Telex 81183

CONTENTS

		Page No.
1.	INTRODUCTION	1
2.	DESIGN REQUIREMENTS	1
3.	PROBE ASSESSMENT	2
4.	TEST EQUIPMENT	3
6.	CONCLUSIONS	3
7.	REFERENCES	3
	TABLES 1 to 5	
	FIGURES 1 to 8	

24789/1/88
MARCH 1988

PRODUCTION OF FOCUSED PROBES FOR GIRTH WELD INSPECTION

For: NOVA, An Alberta Corporation

By: J.L. Turner and M.R. Kirby

---

1. INTRODUCTION

NOVA Corporation are developing an automated ultrasonic scanning system for the inspection of GMA welds in 36 inch diameter pipes of wall thickness either 9.8 or 20.6mm. A specially adapted version of the RTD Rotoscan system is to be used, driven by a Krautkramer KB 6000 flaw detector. The weld geometry (1) is complex (asymmetric double-V) and specially designed transducers are required to interrogate the separate faces of the weld.

2. DESIGN REQUIREMENTS

NOVA specified that focused ultrasonic transducers were to be used for inspection of the weld root faces in the double-V geometry.

In the case of the lower root face, inclined at 37.5° to the vertical, a 52.5° probe was required with a 6dB beam width (in pulse-echo mode), equal to the inspection plane dimension of 2.5mm.

In the case of the upper root face, of dimension in the 45° plane of 4mm, two 45° probes were specified, each with a 6dB beam width at the inspection plane of 2mm. In this way, the two probes could be used together, with one slightly staggered away from the weld preparation with respect to the other, so that complete coverage of this weld face could be achieved.

It was further required that the same probes be used for each of the two pipe wall thicknesses, which meant that the specified 6dB beam width had to be achieved at two different ranges in each case, as detailed in Table 1. The only way this requirement could be met was by designing the probe so that the weld face in the 9.8mm wall pipe would be intercepted by the converging part of the beam (i.e. before the focal point), while the corresponding face in the 20.6mm wall pipe would be intercepted by the diverging part of the beam (i.e. after the focal point). This meant that, for a given frequency (5MHz), a unique transducer diameter had to be chosen (in so far as this could be achieved in practice from commercially available piezoelectric crystals), and the focusing factor for the transducer had to meet a precisely calculated value. To achieve the latter, careful measurements had to be taken of the ultrasonic velocities of the plastics used for the lens and the delay block, and the required axicon lens angle was calculated using the formula quoted in (2).

Two further design constraints were imposed, firstly, by the small size of the housing into which the transducer had to be fitted (a 25mm square stainless steel housing 1.5mm thick) and secondly, by the requirement that the front of the delay block contact area be no less than 6mm from the edge of the as-machined weld preparation on the outer surface of the pipe. This meant that the emission point had to be as far forward as possible, while at the same time ensuring that the beam cross-section at the perspex/steel interface was cut off to a minimal degree by the front edge of the perspex delay block. In probe designs where the focal point is at the perspex/steel interface, the beam has its minimum cross-section at this point so the emission point can be brought the closest possible distance to the front. However, in the present case, the focal point is in the steel, so that the perspex/steel interface lies within the converging (nearfield) part of the beam.

These constraints meant that the perspex delay block had to be extended through and flush with the front of the steel housing. Even having done this, it was still necessary to move the emission points slightly further back to avoid disruption of the beam profiles and excessive internal noise.

Thus the emission points of the 45° and 52.5° probes were designed to be situated at 6.5mm and 4.75mm from the front of the delay blocks respectively. In the finished probes, these locations were met to within 1.0mm, as determined from the probe beam plots.

3. PROBE ASSESSMENT

The probes were to be tested in accordance with the requirements of NOVA specification SUT-2 (3), which is a modified and supplemented version of the Electrical Supply Industry Standard ESI 98-2 for medium frequency miniature shear wave angle probes. The ESI 98-2 standard was originally intended to apply to unfocused probes designed primarily for manual ultrasonic inspection, but the SUT-2 specification can be applied to the probes described here, albeit with the following provisos:

a) Because the probes are designed for automated inspection purposes, the steel housing completely enshrouds the delay block, with channels for coupling water built into the sides, so that a probe wear allowance cannot be specified in the same way as for transducers designed for manual inspection. It is expected that the wear rate of the protected delay blocks used here will be minimal compared to that of unprotected ones. However, in the event of repair being required, it is anticipated that a specified depth (1mm) of the probe shoe could be machined off without significantly affecting transducer performance, although the functioning of the water channels (1.5mm deep) might be impaired as a result.

b) The SUT-2 specification is applied to the special axicon focused probes on the understanding that these are intended for shorter range use than normal miniature angle probes. Thus overall gain measurements have been carried out on the 25 and 50mm radii of an A4 block (4), as well as on the 100mm radius of an A2 block (4). For the same reasons, the beam profiles and signal curves were obtained using a special block containing 1.0mm diameter side drilled holes at depths of 5.5, 10.5, 15.5, 20.5 and 25.5mm.

c) The SUT-2 specification includes a clause 8.15 (based on ASTM volume 03.03) which states how the focal beam width is to be measured. This is strictly only applicable to immersion or 0° compression wave transducers, and not to probes intended for angle beam inspection. In any case, the present probes are designed to produce specified beam widths at points before and after the focal zone. The focal spot size itself is to a large degree independent of frequency; for example, the 6dB width is easily estimated from $d_F = 1/2\ k_6 D\ (F/N)$ (where $k_6 = 0.51$ and $D = 0.97D_0$). The same is not true, however, of points away from the focal zone; in the far field, for instance, the beam width depends on the beam divergence, which is inversely proportional to frequency. Thus a 10% reduction in frequency (acceptable) leads to a maximum acceptable increase of 10% in beam width at the point of interest, with no additional allowance available for measurement error. This cannot be quoted as better than 25% for each single measurement on a given side drilled hole, although the overall accuracy may be considered to improve after successive measurements over a range of hole depths have been used to draw the full beam plot from which the final beam width dimensions are obtained.

4. TEST EQUIPMENT

A Krautkramer USIP-11 flaw detector (pulse energy 3, filter setting 2 - 8MHz) was used for all the measurements, with the exception of those relating to pulse characteristics operating frequency, cycle spacing and pulse length. For these measurements, a Panametrics 5052 PRX pulser-receiver (minimum pulse damping, pulse energy 4, no filtering) and a Tektronix 7603 cathode ray oscilloscope were used.

5. RESULTS

The three completed probes (Fig.1) each contained 12.7mm diameter PZT-7a crystals of nominal frequency 5MHz. The measured crystal resonant frequencies along with the estimated focusing parameters are given in Table 2.

Table 3, 4 and 5 summarise the data obtained from the three transducers when tested against the SUT-2 specification. The corresponding beam profiles are given in Fig.2, 3 and 4, with the signal/noise curves in Fig.5, 6 and 7. The pulse shapes for the three probes are shown in Fig.8.

6. CONCLUDING REMARKS

The three probes have been manufactured to meet the specific requirements for automated girth weld inspection and meet the specification of NOVA draft standard SUT-2, within the limits defined in Section 3 above.

7. REFERENCES

1 Letter from M Fingerhut to J L Turner dated 27/5/86.

2 Turner J L: 'A new look at ultrasonic focusing devices'. Review of Progress in Quantitative NDE, June 21-16, Williamsburg, Virginia.

3 Fingerhut M: 'Performance specification for medium frequency shear wave angle probes'. NOVA Specification SUT-2, 1987.

4 British Standard: 'Specification for calibration blocks for use in ultrasonic flaw detection'. BS 2704, 1978.

Work reported by

1/3/88
....
J.L. Turner

M. R. Kirby 1-3-88.
....
M.R. Kirby

Table 1 Design requirements

		Reflector Ranges, mm		
Probe No.	Nominal Beam angle, deg	9.8mm W.T. (Range R_1)	20.6mm W.T. (Range R_2)	Required beam widths, mm
001	45	20	35.25	2.0
002	45	20	35.25	2.0
003	52.5	14.5	21.3	2.5

Table 2 Probe characteristics (12.7mm dia PZT-7a crystals of nominal frequency 5MHz)

Probe No.	Crystal frequency, MHz	Focusing factor, N/F	Delay path in perspex, mm	Estimated focal range in steel, mm	Actual focal range in steel, mm*
001	4.996	1.68	15	21.9	23
002	4.900	1.68	15	21.9	22
003	5.147	1.97	15	16.9	17

measured from signal curves (Fig.5, 6 and 7)

Table 3

REPORT SHEET FOR ULTRASONIC PROBE RESULTS (SINGLE CRYSTAL)

Specification Applied: ESI Standard 98-2 for Ultrasonic Probes: Medium Frequency, Miniature Shear Wave, Angle Probes

Probe Manufacturers and Identification: TWI 001

Probe Specification and Dimensions: 5MHz, 12.7 mmϕ, 45°

* Flaw Detector, Cable and Critical Control Settings: Krautkramer USIP-11 (2-8 MHz, Pulse Energy 3)

Electrical Matching: 1.0μH Tuning Inductor

Mechanical Construction (including subjective comments):

Operator and Date: N.J. Farrant ; M.R. Kirby (18-2-88)

Operator's Signature: M. R. Kirby /

Summary of Test

* Panametrics 5052 PRX used for clauses 8.16, 8.17, 8.18, 8.19

Result	Clause	Parameter	Requirement for Single Crystal Angle Probe
5MHz, 12.7ϕ, 45° (TWI 001)	7	Identification	Marked on probe: manufacturer, probe type, beam angle, frequency, crystal size and shape.
1 mm	8.1	Depth of Shoe Probes	The available depth shall be indicated and shall be at least 1 mm.
n/a	8.2	Probe Wear (Used Probes)	Probe face shall be proud of the manufacturer's wear allowance marks.
< 0.05 mm	8.3	Shoe Flatness	Flat within 0.05 mm.
range 25 mm 82 dB " 50 " 80 " " 100 " 76 "	8.4	Overall Gain	At least 50 dB gain in hand.
> 22 dB	8.4.1	Signal to Noise Ratio	Noise shall be at least 20 dB weaker than the signal at the target path.
> 60 dB	8.5	Signal to Electronic Noise	Noise shall be at least 40 dB weaker than the signal at the target path.

Table 3 (contd)

Result	Clause	Parameter	Requirement for Single Crystal Angle Probe
6.25 mm from probe front	8.6	Index Point	Marked index point shall be within 1 mm of measured one.
44.7°	8.7	Beam Angle	For nominal beam angles less than 45° +/- 1.5°, for greater than 45° +/- 2°.
none	8.8	Squint	Not exceeding 1.5° for single crystal probes nor 2° for twin crystal probes.
46dB	8.10	Longitudinal - Angle Beam	At least 35 dB weaker than shear beam. Measured at 100 mm range.
38dB	8.11	Surface Waves	At least 34 dB weaker than shear wave for beam angles below 65°. At least 24 dB weaker for higher angles. Measured at 100 mm range.
>20dB	8.13	Side Lobes	At least 20 dB weaker than the main beam, except angle greater than 64° shall be at least 15 dB weaker than the main beam.
none	8.14	Subsidiary Maxima	Fluctuations in echo amplitude shall not exceed that caused by interference with grass.
Range: Width/mm F 2.0 R_1 2.0 R_2 2.2	8.15	Beam Width (± 25%)	Measured beam width shall be within 10% of design width.
see photo	8.16*	Pulse Shape	Single Peaked: Any secondary peaks in tail of pulse at least 20 dB less than main peak.
≤ 10%	8.17*	Cycle Spacing	Less than +/- 15% variation between each cycle.
4.65 MHz	8.18*	Frequency	Within +/- 10% of the nominal frequency.
1.52 μs	8.19*	Pulse Length	Not exceeding 2.5 microseconds between points on the unrectified pulse at 10% of peak amplitude.

A tick in the "Results" column should be used to indicate compliance with the Standard.

Table 4

REPORT SHEET FOR ULTRASONIC PROBE RESULTS (SINGLE CRYSTAL)

Specification Applied: ESI Standard 98-2 for Ultrasonic Probes: Medium Frequency, Miniature Shear Wave, Angle Probes

Probe Manufacturers and Identification: TWI 002

Probe Specification and Dimensions: 5MHz, 12.7mmø, 45°

*Flaw Detector, Cable and Critical Control Settings: Krautkramer USIP-11 (2-8 MHz, pulse energy 3)

Electrical Matching: 1.0 µH Tuning Inductor

Mechanical Construction (including subjective comments): ____

Operator and Date: N.J Farrant ; M.R. Kirby (18-7-88)

Operator's Signature: M. R. Kirby /

Summary of Test

* Panametrics 5052 PRx used for clauses 8.16, 8.17, 8.18 8.19

Result	Clause	Parameter	Requirement for Single Crystal Angle Probe
5MHz, 12.7ø, 45° (TWI 002)	7	Identification	Marked on probe: manufacturer, probe type, beam angle, frequency, crystal size and shape.
1mm	8.1	Depth of Shoe Probes	The available depth shall be indicated and shall be at least 1 mm.
n/a	8.2	Probe Wear (Used Probes)	Probe face shall be proud of the manufacturer's wear allowance marks.
<0.05 mm	8.3	Shoe Flatness	Flat within 0.05 mm.
range 25mm 86 dB " 50 " 82 " " 100 " 78 "	8.4	Overall Gain	At least 50 dB gain in hand.
>30dB	8.4.1	Signal to Noise Ratio	Noise shall be at least 20 dB weaker than the signal at the target path.
>60dB	8.5	Signal to Electronic Noise	Noise shall be at least 40 dB weaker than the signal at the target path.

Table 4 (contd)

Result	Clause	Parameter	Requirement for Single Crystal Angle Probe
5.5 mm from probe front	8.6	Index Point	Marked index point shall be within 1 mm of measured one.
45.0°	8.7	Beam Angle	For nominal beam angles less than 45° +/- 1.5°, for greater than 45° +/- 2°.
0.5°	8.8	Squint	Not exceeding 1.5° for single crystal probes nor 2° for twin crystal probes.
50dB	8.10	Longitudinal - Angle Beam	At least 35 dB weaker than shear beam. Measured at 100 mm range.
47dB	8.11	Surface Waves	At least 34 dB weaker than shear wave for beam angles below 65°. At least 24 dB weaker for higher angles. Measured at 100 mm range.
>20dB	8.13	Side Lobes	At least 20 dB weaker than the main beam, except angle greater than 64° shall be at least 15 dB weaker than the main beam.
none	8.14	Subsidiary Maxima	Fluctuations in echo amplitude shall not exceed that caused by interference with grass.
Range Width/mm F 2.0 R_1 2.0 R_2 2.1	8.15	Beam Width (±25%)	Measured beam width shall be within 10% of design width.
see plots	8.16*	Pulse Shape	Single Peaked: Any secondary peaks in tail of pulse at least 20 dB less than main peak.
≤ 10%	8.17*	Cycle Spacing	Less than +/- 15% variation between each cycle.
4.60 MHz	8.18*	Frequency	Within +/- 10% of the nominal frequency.
1.60 µs	8.19*	Pulse Length	Not exceeding 2.5 microseconds between points on the unrectified pulse at 10% of peak amplitude.

A tick in the "Results" column should be used to indicate compliance with the Standard.

Table 5

REPORT SHEET FOR ULTRASONIC PROBE RESULTS (SINGLE CRYSTAL)

Specification Applied: ESI Standard 98-2 for Ultrasonic Probes: Medium Frequency, Miniature Shear Wave, Angle Probes

Probe Manufacturers and Identification: TWI 003

Probe Specification and Dimensions: 5MHz, 12.7mm ϕ. 52.5°

* Flaw Detector, Cable and Critical Control Settings: Krautkramer USIP-11 (2-8 MHz, pulse energy 3)

Electrical Matching: 1.0 μH tuning inductor

Mechanical Construction (including subjective comments):

Operator and Date: N J Farrant ; M. R. Kirby (15-2-88)

Operator's Signature: M. R. Kirby / R Farrant

Summary of Test

* Panametrics 5052 PRx used for clauses 8.16, 8.17, 8.18, 8.19

Result	Clause	Parameter	Requirement for Single Crystal Angle Probe
5MHz, 12.7ϕ, 52.5° TWI 003	7	Identification	Marked on probe: manufacturer, probe type, beam angle, frequency, crystal size and shape.
1mm	8.1	Depth of Shoe Probes	The available depth shall be indicated and shall be at least 1 mm.
n/a	8.2	Probe Wear (Used Probes)	Probe face shall be proud of the manufacturer's wear allowance marks.
< 0.05mm	8.3	Shoe Flatness	Flat within 0.05 mm.
range 25mm 86dB " 50 " 81 " " 100 " 78 "	8.4	Overall Gain	At least 50 dB gain in hand.
>38dB	8.4.1	Signal to Noise Ratio	Noise shall be at least 20 dB weaker than the signal at the target path.
>60dB	8.5	Signal to Electronic Noise	Noise shall be at least 40 dB weaker than the signal at the target path.

Table 5 (contd)

Result	Clause	Parameter	Requirement for Single Crystal Angle Probe
5.5 mm from probe front	8.6	Index Point	Marked index point shall be within 1 mm of measured one.
51.2°	8.7	Beam Angle	For nominal beam angles less than 45° +/- 1.5°, for greater than 45° +/- 2°.
none	8.8	Squint	Not exceeding 1.5° for single crystal probes nor 2° for twin crystal probes.
52 dB	8.10	Longitudinal - Angle Beam	At least 35 dB weaker than shear beam. Measured at 100 mm range.
40 dB	8.11	Surface Waves	At least 34 dB weaker than shear wave for beam angles below 65°. At least 24 dB weaker for higher angles. Measured at 100 mm range.
>20 dB	8.13	Side Lobes	At least 20 dB weaker than the main beam, except angle greater than 64° shall be at least 15 dB weaker than the main beam.
none	8.14	Subsidiary Maxima	Fluctuations in echo amplitude shall not exceed that caused by interference with grass.
Range. Width/mm F 2.0 R_1 2.25 R_2 2.5	8.15	Beam Width (± 25%)	Measured beam width shall be within 10% of design width.
see photo	8.16 *	Pulse Shape	Single Peaked: Any secondary peaks in tail of pulse at least 20 dB less than main peak.
≤ 10%	8.17 *	Cycle Spacing	Less than +/- 15% variation between each cycle.
4.73 MHz	8.18 *	Frequency	Within +/- 10% of the nominal frequency.
1.60 μs	8.19 *	Pulse Length	Not exceeding 2.5 microseconds between points on the unrectified pulse at 10% of peak amplitude.

A tick in the "Results" column should be used to indicate compliance with the Standard.

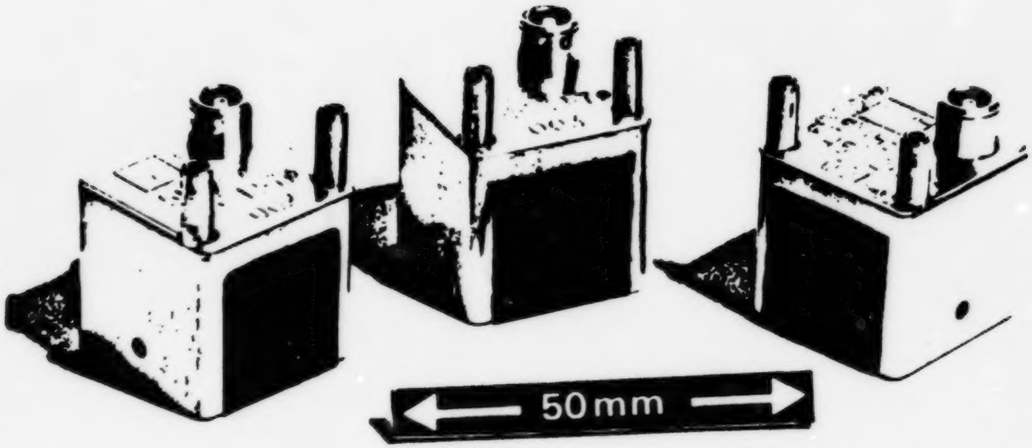

Fig. 1: Photograph of completed transducers

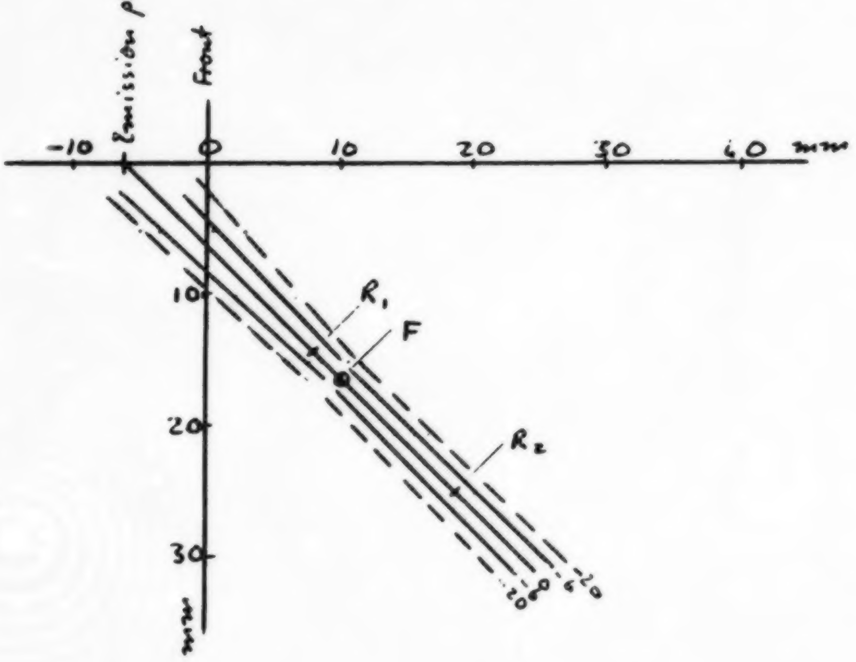
Emission pt.
Front
-10
0
10
20
30
4.0
mm
10
20
30
mm
R₁
F
R₂
-20
-6
0
-6
-20

Scale - 2:1

Index point 6.25 mm from front

Beam Angle = 44.7°

Beam width at F = 2.0 mm

" " " R₁ = 2.0 mm

" " " R₂ = 2.2 mm

Fig.2: Beam Profile for 45° probe 001

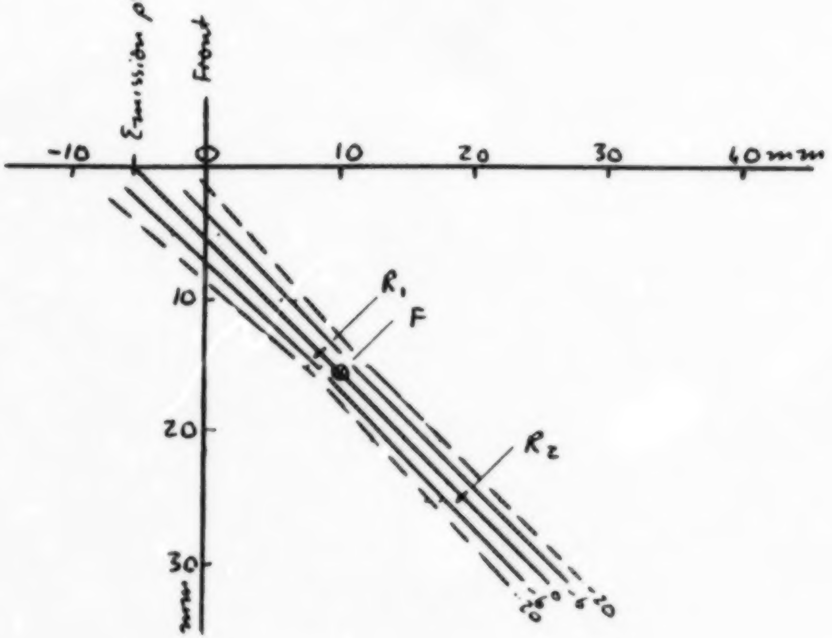
Emission pt.
Front
-10
0
10
20
30
40mm
10
20
30
mm
R1
F
R2
-20
-6
0
-6
-20

Scale - 2:1

Index point 5.5 mm from front

Beam Angle = 45°

Beam width at F = 2.0 mm

" " " R_1 = 2.0 mm

" " " R_2 = 2.1 mm

Fig 3: Beam Profile for 45° probe 002

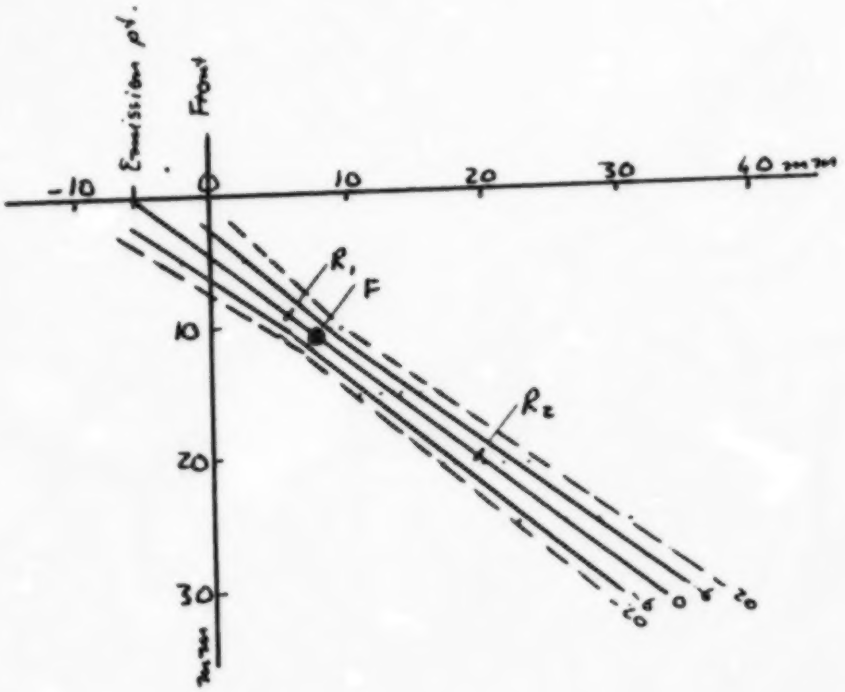
Emission pt.
Front
-10
0
10
20
30
40 mm
10
20
30
mm
R₁
F
R₂
-20
-6
0
6
20

Scale - 2:1

Index point 5.5 mm from front

Beam Angle = 51.2°

Beam width at F = 2.0 mm

" " " R₁ = 2.25 mm

" " " R₂ = 2.5 mm

Fig.4 : Beam Profile for 52.5° probe 005

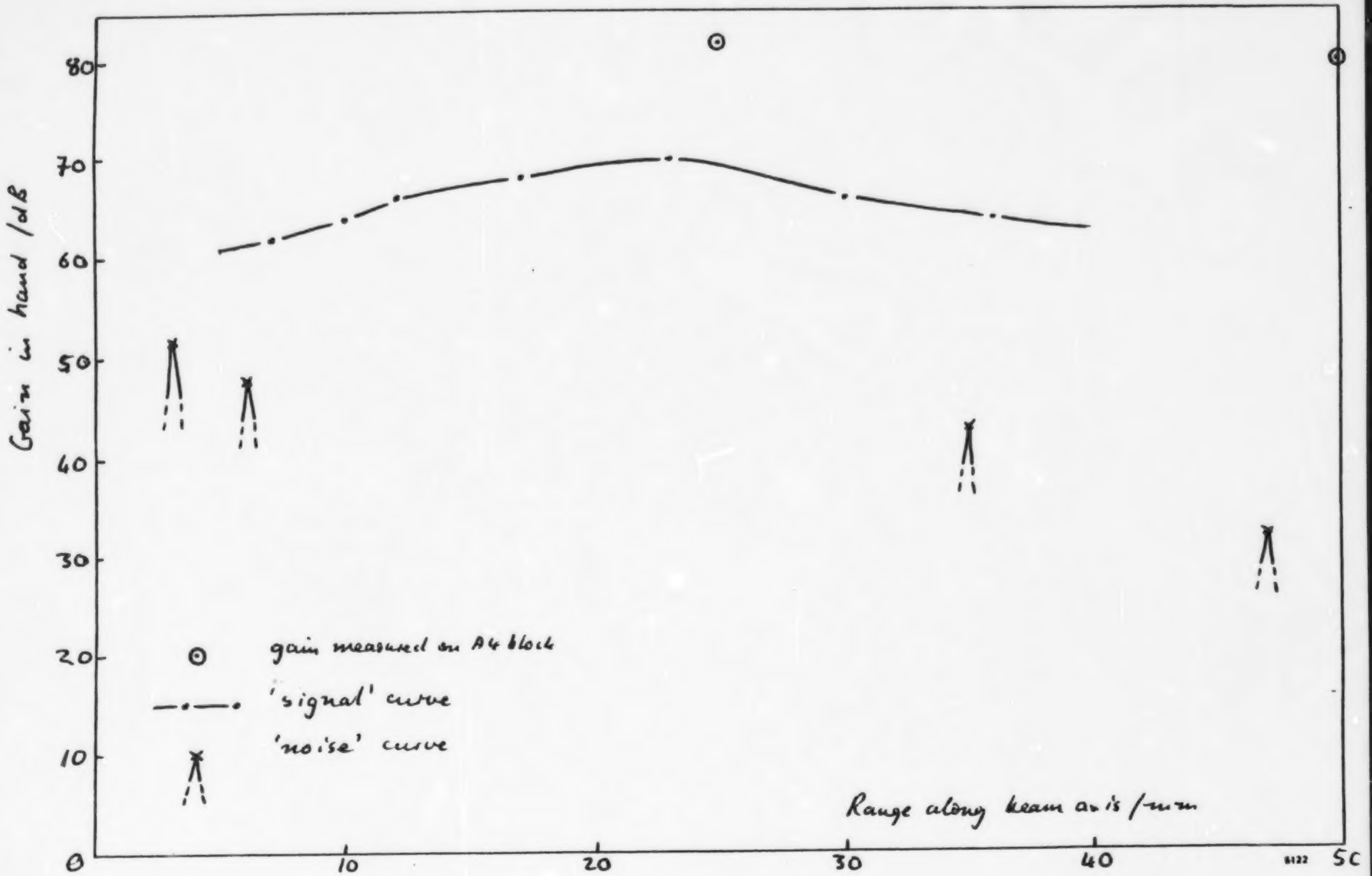

Fig.5: Signal/Noise Curves for 45° probe 001

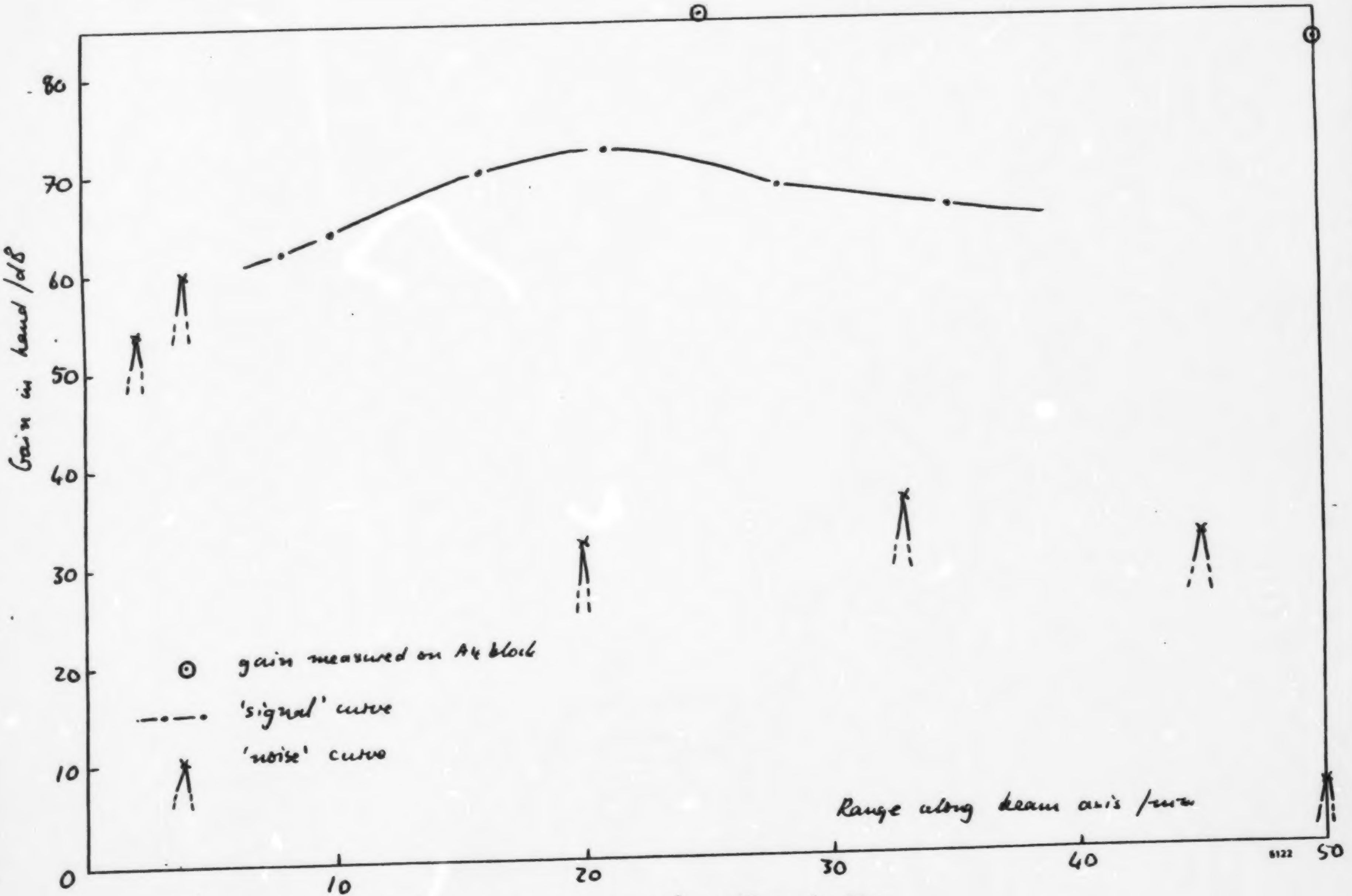

Fig. 6: Signal / Noise Curves for 45° probe 002

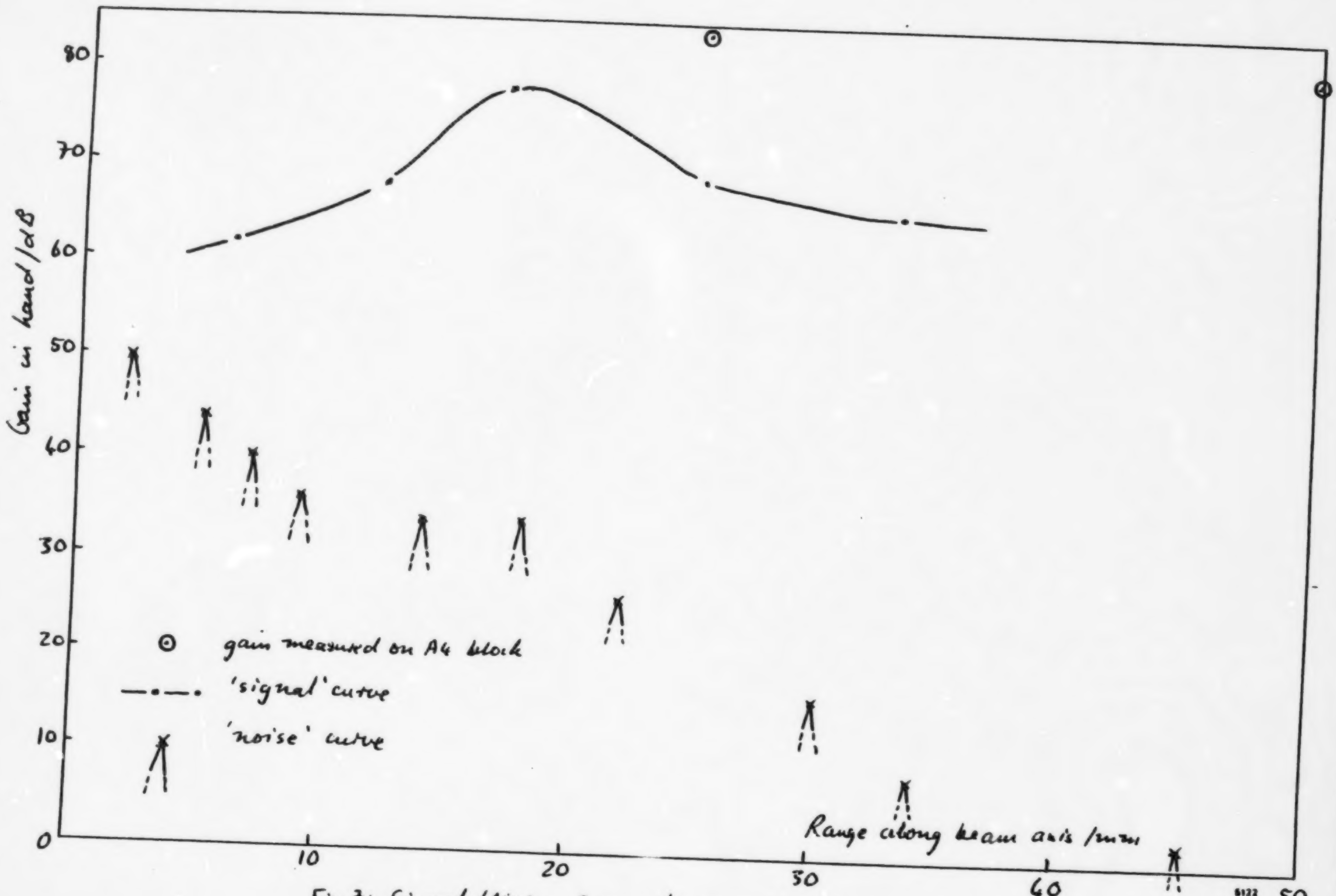

Fig. 7: Signal / Noise Curves for 52.5° probe 003

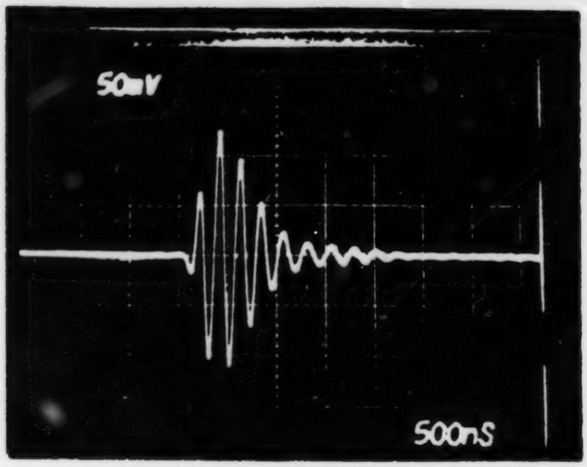

(a) 45° Probe 001

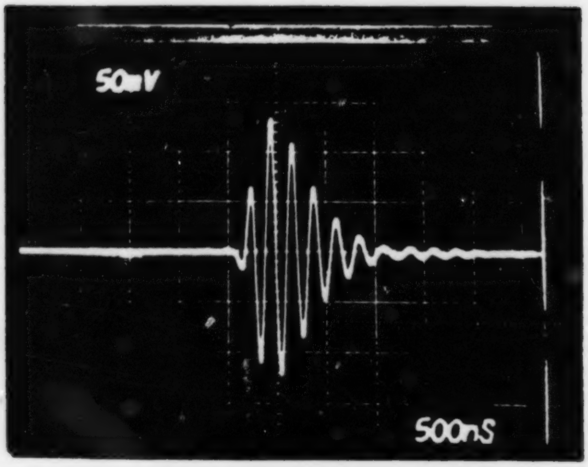

(b) 45° Probe 002

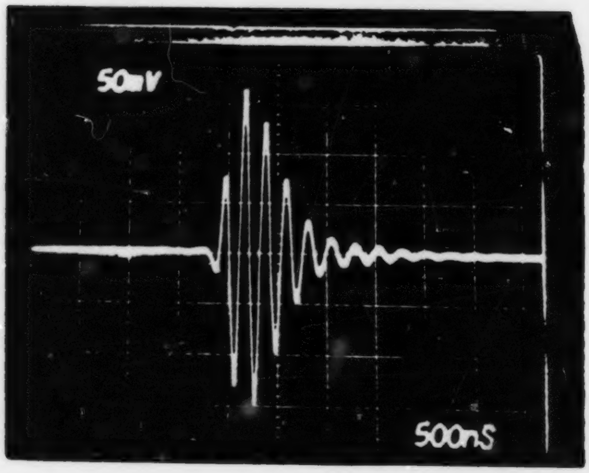

(c) 45° Probe 003

Fig. 8. Photographs of Probe Pulses obtained using Panametrics 5052

APPENDIX 2

Pitch-Catch Probe 88-111

Ultrasonic Beam Plots
Frequency Data Sheets

TEST SET-UP

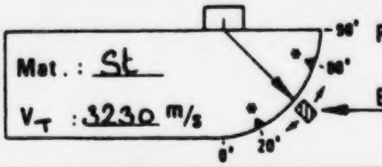

Mat. : St

V_T : 3230 m/s

R = 100 mm.

Eddy Sonic Sensor (ESS)

TRANS-DUCER : RTD
88 - 111
45° T 2.25 - St
ø 10

U.T. FLAW DETECTOR.

Make : Krautkrämer; Type: USIP 11 ; RTD Nr. 8

Tuning

Pulse Str.: 3 Res.: 3

Freq. : 0.5 - 2.5 MHz

Pulse echo sensitivity :

Gain 0 · 4 dB

TRANSDUCER DATA:

Housing:

80 x 40 x 35 (L x W x H)

Conn.: LEMO-00

T.D. Type : ☐ Man. ☒ Mech.

I P : 10 mm on R = 100mm

WD.: 10 mm

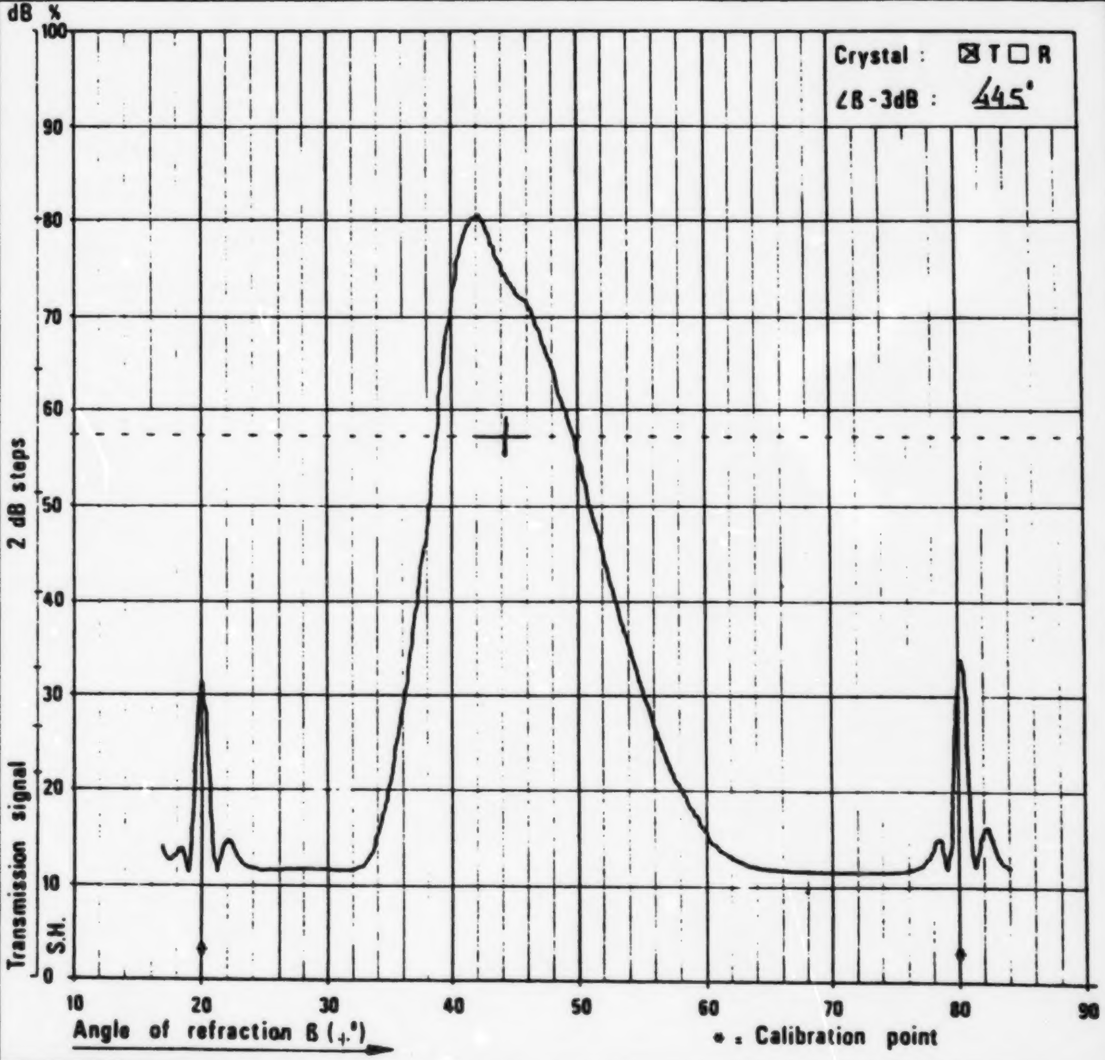

Crystal : ☒ T ☐ R

∠B - 3dB : 445°

Röntgen Technische Dienst b.v.

ULTRASONIC BEAM PLOT

RTD QUALITY SERVICES

D.D 140188

MEASURED BY : J. Vreeken

TEST SET-UP

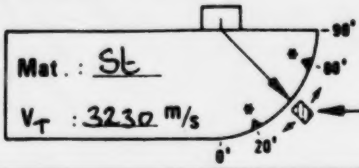

Mat. : St

V_T : 3230 m/s

R = 100 mm.

Eddy Sonic Sensor (ESS)

TRANS-DUCER : RTD
88 - 111
55° R2.25-St
Ø25

TRANSDUCER DATA:

Housing:
80 x 40 x 35 (L x W x H)
Conn.: LEMO-00
T.D. Type: ☐ Man. ☒ Mech.
I P : 50 mm on R = 100 mm
WD.: 20 mm

U.T. FLAW DETECTOR.

Make : Krautkrämer; Type: USIP 11; RTD Nr. 8

Tuning
Pulse Str.: 3 Res.: 3
Freq. : 05 - 25 MHz

Pulse echo sensitivity:
Gain 0 · 0 dB

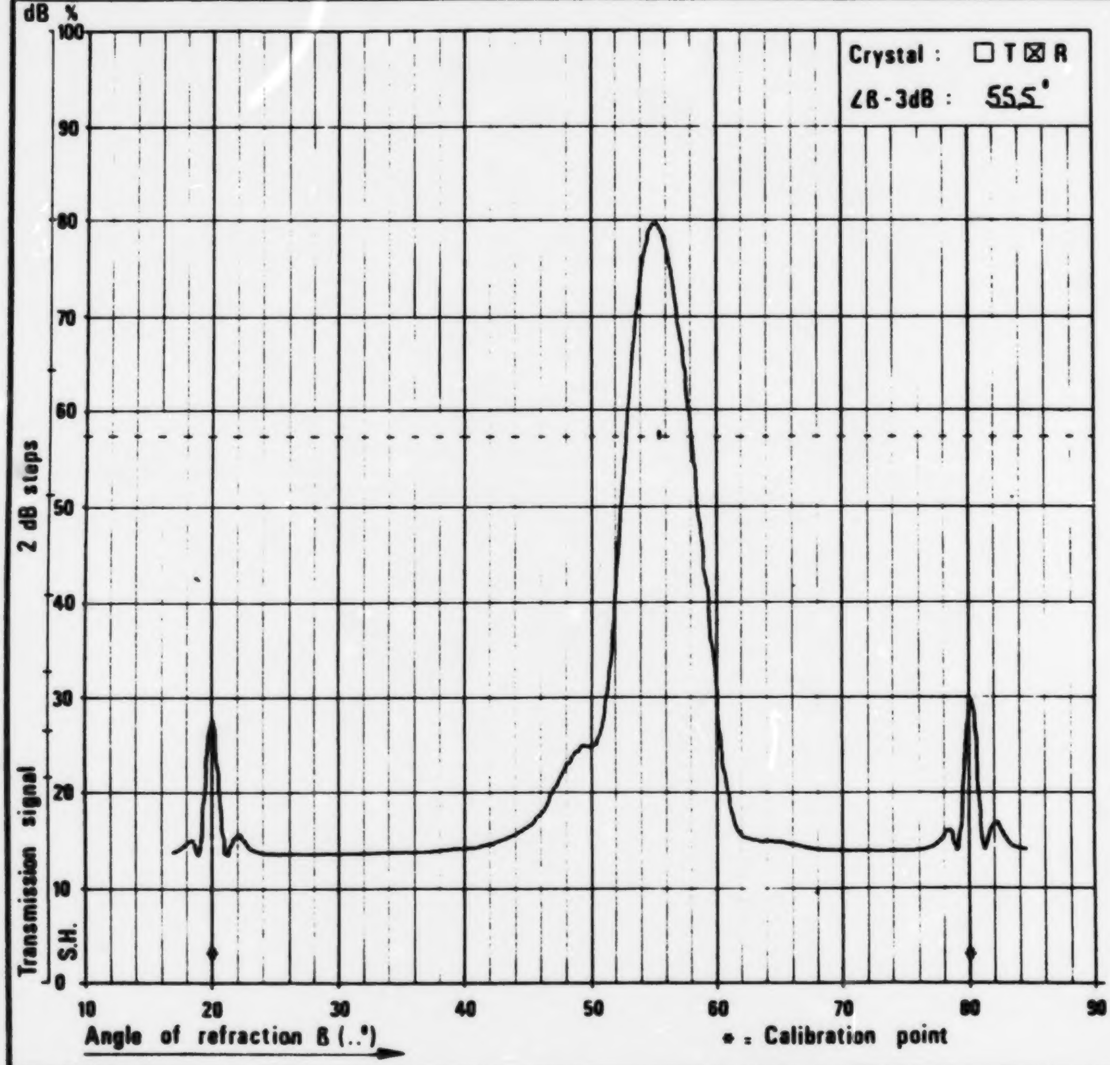

Crystal : ☐ T ☒ R
∠B -3dB : 55.5°

Röntgen Technische Dienst b.v.

RTD QUALITY SERVICES

ULTRASONIC BEAM PLOT

D.D 140188

MEASURED BY: J. Vreeken

EQUIPMENT:
1. Spectrum Analyser
   Marconi Instruments Typ: TF 2370
2. Oscilloscope: KIKUSUI COS 5060
3. Ultrasonic Transducer Analyser:
   Aerotech Laboratories Type: UTA-3

TRANSDUCER: RTD
88-111
4592.25-St
Ø10

T.D. DATA:
Typ: ☐ Man ☒ Mech
Housing: L x W x H
80 x 40 x 35 mm
IP : 10 mm on R 100 mm
WD.: 10 mm
Conn.: LEMO-00
Cable: 2m Coax 50 Ω

Reference Block: RTD
Mat.: Steel
V_l -: 5950 m/s
V_{sh} -: 3230 m/s

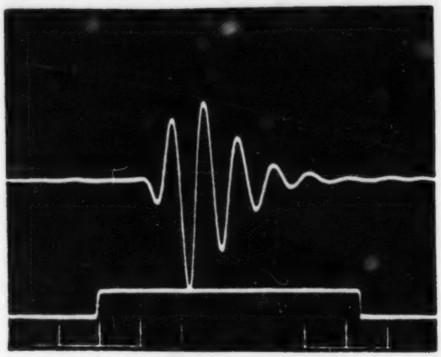

HF Image

$f = \frac{1}{t}$

Time Base: 0.5 µs/Div

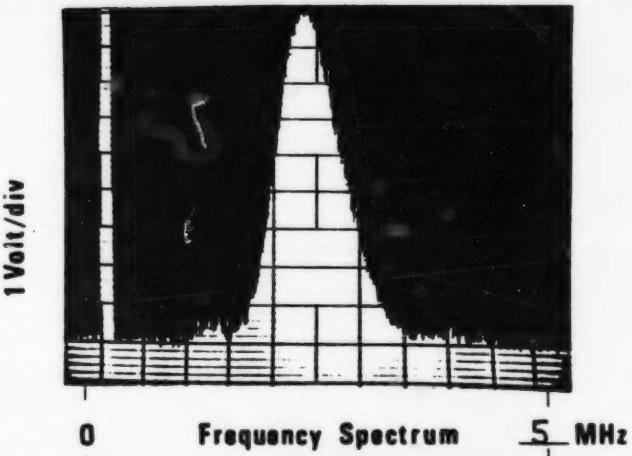

Frequency Spectrum

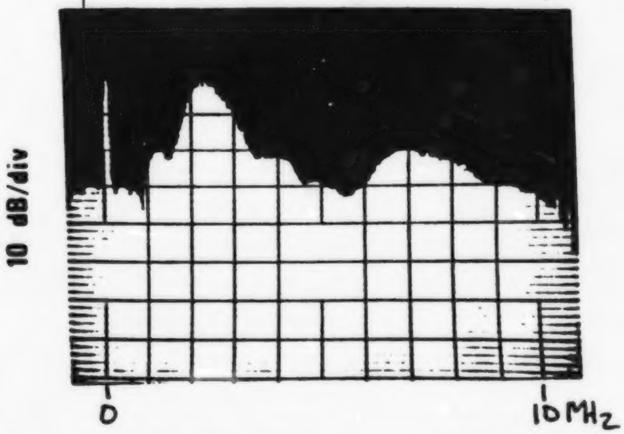

Centre Frequency: 2,38 MHz
Band Width -3dB : 2,08 - 2,70 MHz

☒ Radius Calibration Block

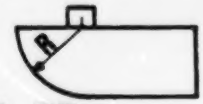

R = 100 mm

☐ Side Drilled Hole

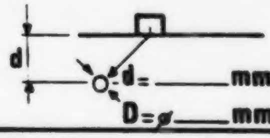

d = ____ mm
D = ø ____ mm

☐ Flat Bottomed Hole

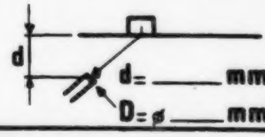

d = ____ mm
D = ø ____ mm

☐ Back Wall

S = ____ mm

☐

Röntgen Technische Dienst b.v.

FREQUENCY SPECTRUM DATA SHEET

Measured by: J Veeken

D.D. 210188

RTD

EQUIPMENT:

1. Spectrum Analyser
   Marconi Instruments Typ: TF 2370
2. Oscilloscope: KIKUSUI COS 5060
3. Ultrasonic Transducer Analyser:
   Aerotech Laboratories Type: UTA-3

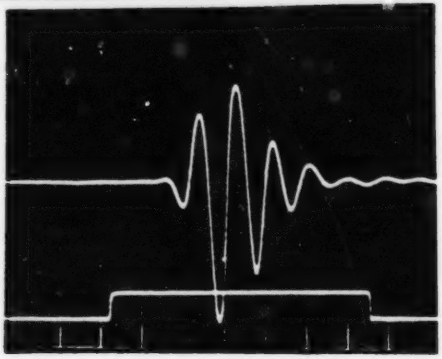

HF Image

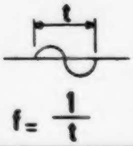

Time Base: ______ μs/Div

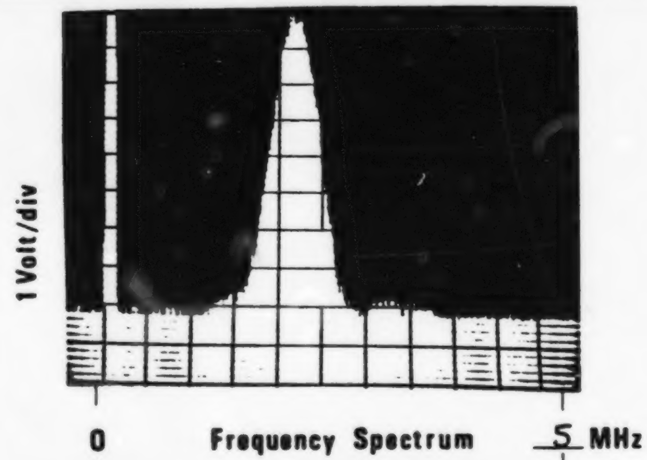

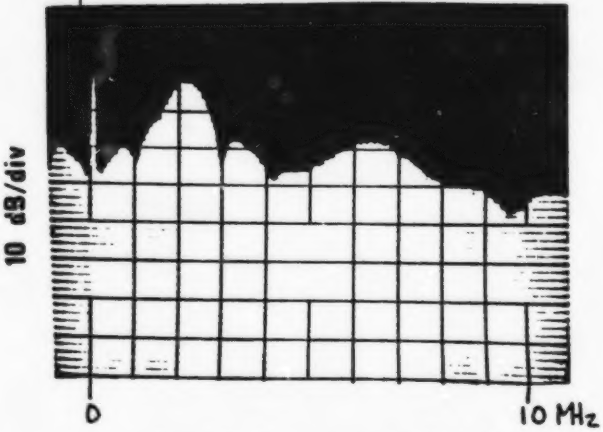

Centre Frequency: 2,20 MHz

Band Width-3dB : 1,92 - 2,46 MHz

TRANS-DUCER : RTD
88-111
55° R2,25-St
⌀25

T.D. DATA:

Typ: ☐ Man ☒ Mech

Housing: L x W x H
80 x 40 x 35 mm

IP : 50 mm on R 100 mm

WD.: 20 mm

Conn.: LEMO.00

Cable: 2m Coax 50 Ω

Reference Block: RTD

Mat.: Steel

V_l -: 5950 m/s

V_{sh} -: 3230 m/s

☒ Radius Calibration Block

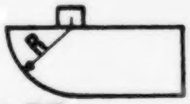

R = 100 mm

☐ Side Drilled Hole

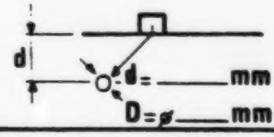

d = ______ mm

D = ⌀ ______ mm

☐ Flat Bottomed Hole

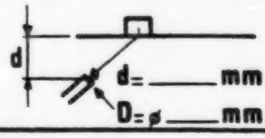

d = ______ mm

D = ⌀ ______ mm

☐ Back Wall

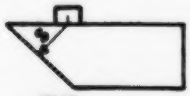

S = ______ mm

☐

Röntgen Technische Dienst b.v.

FREQUENCY SPECTRUM DATA SHEET

Measured by: J. Vreeken

D.D. 210188.

RTD

EQUIPMENT:

1. Spectrum Analyser
   , Typ:
2. Oscilloscope: KIKUSUI COS 5060
3. Ultrasonic Transducer Analyser:
   Aerotech Laboratories Type: UTA-3

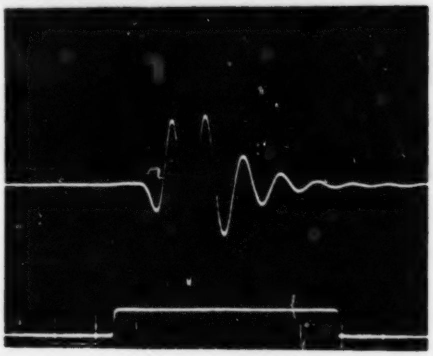

HF Image

$f = \frac{1}{t}$

Time Base: 0,5 µs/Div

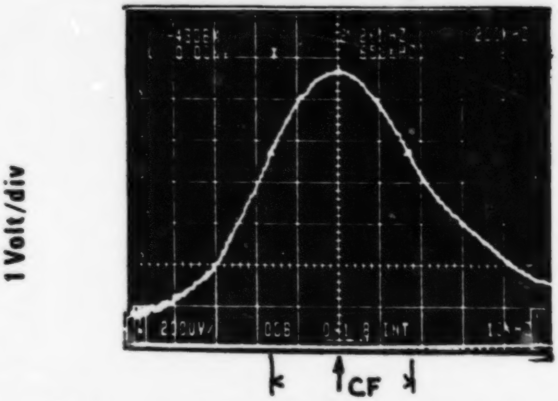

Frequency Spectrum

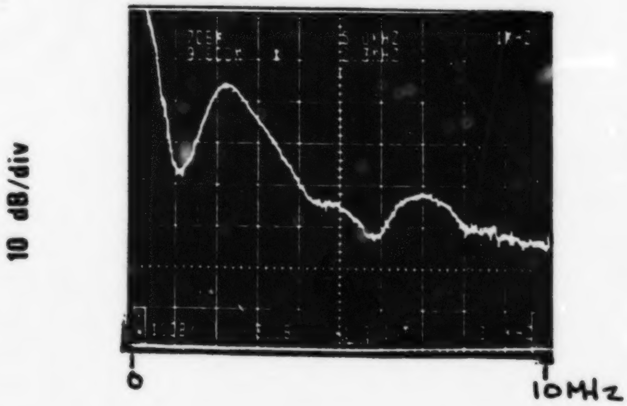

Centre Frequency: 2,26 MHz

Band Width-3dB : 1,94 – 2,60 MHz

TRANSDUCER : RTD
88-111
45°T2,25-SL
ø10

T.D. DATA:

Typ: ☐ Man ☒ Mech

Housing: LxWxH
80 x 40 x 35 mm

IP : 10 mm on R 100 mm

WD.: 10 mm

Conn.: LEMO.00

Cable: 2m Coax 50 Ω

Reference Block: RTD

Mat.: Steel

V_l -: 5950 m/s

V_{sh} -: 3230 m/s

☒ Radius Calibration Block

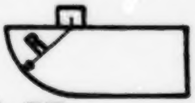

R= 100 mm

☐ Side Drilled Hole

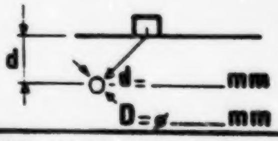

☐ Flat Bottomed Hole

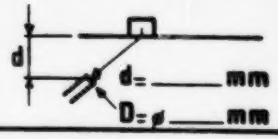

☐ Back Wall

S= ____ mm

☐

Röntgen Technische Dienst b.v.

FREQUENCY SPECTRUM DATA SHEET

Measured by: J. Vreeken

D.D. 140188

RTD

EQUIPMENT:

1. Spectrum Analyser
   Typ:
2. Oscilloscope: KIKUSUI COS 5060
3. Ultrasonic Transducer Analyser:
   Aerotech Laboratories Type: UTA-3

TRANS-DUCER: RTD
88-111
55°R225-St
ø25

T.D. DATA:

Typ: ☐ Man ☒ Mech

Housing: LxWxH
80 x 40 x 35 mm

IP : 50 mm on R 100 mm

WD.: 20 mm

Conn.: LEMO-00

Cable: 2m Coax 50 Ω

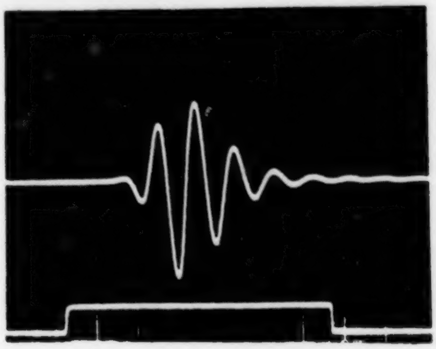

HF Image

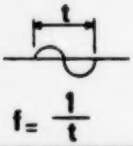

Time Base: 0,5 µs/Div

Reference Block: RTD

Mat.: Steel

V_l -: 5950 m/s

V_{sh} -: 3230 m/s

☒ Radius Calibration Block

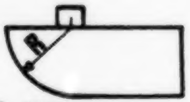

R= 100 mm

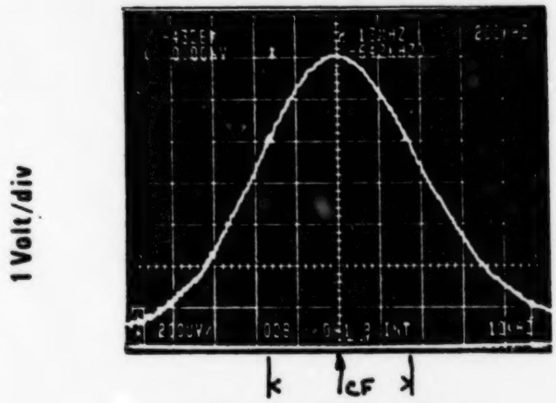

Frequency Spectrum

☐ Side Drilled Hole

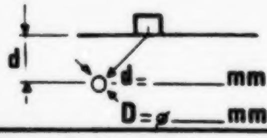

d= mm

D=ø mm

☐ Flat Bottomed Hole

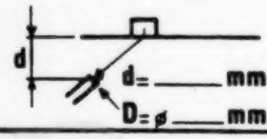

d= mm

D=ø mm

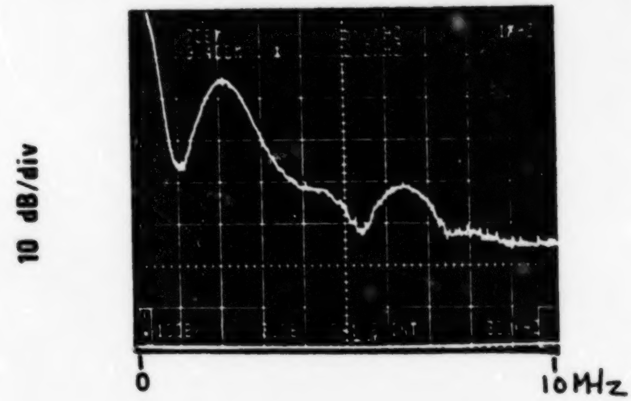

☐ Back Wall

S= mm

☐

Centre Frequency: 2,13 MHz

Band Width-3dB : 1,81 - 2,45 MHz

Röntgen Technische Dienst b.v.

FREQUENCY SPECTRUM DATA SHEET

Measured by:
T. Vreeken

D.D.
140188

APPENDIX 3

Creeping Wave Probe RTD-BAM 88-110

Ultrasonic Beam Plots
Frequency and Focus-Diagram Plots

TEST SET-UP

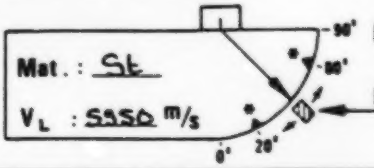

Mat.: St

V_L : 5950 m/s

R = 100 mm.

TRANS-DUCER : RTD-BAM
88-110
TRCr 8-St
2(3,6x10,7)
SA17° FS~15

TRANSDUCER DATA:

Housing:
25 x 25 x 20 (L x W x H)
Conn.: LEMO.00
T.D. Type: ☐ Man. ☒ Mech.
IP : 85 mm on R = 10 mm
WD.: 14,5 mm

U.T. FLAW DETECTOR.

Make : Krautkrämer; Type: USIP 11 ; RTD Nr. 8

Tuning

Pulse Str.: 3 Res.: 3
Freq. : 2 - 8 MHz

Pulse echo sensitivity:
Gain 20 · 12 dB

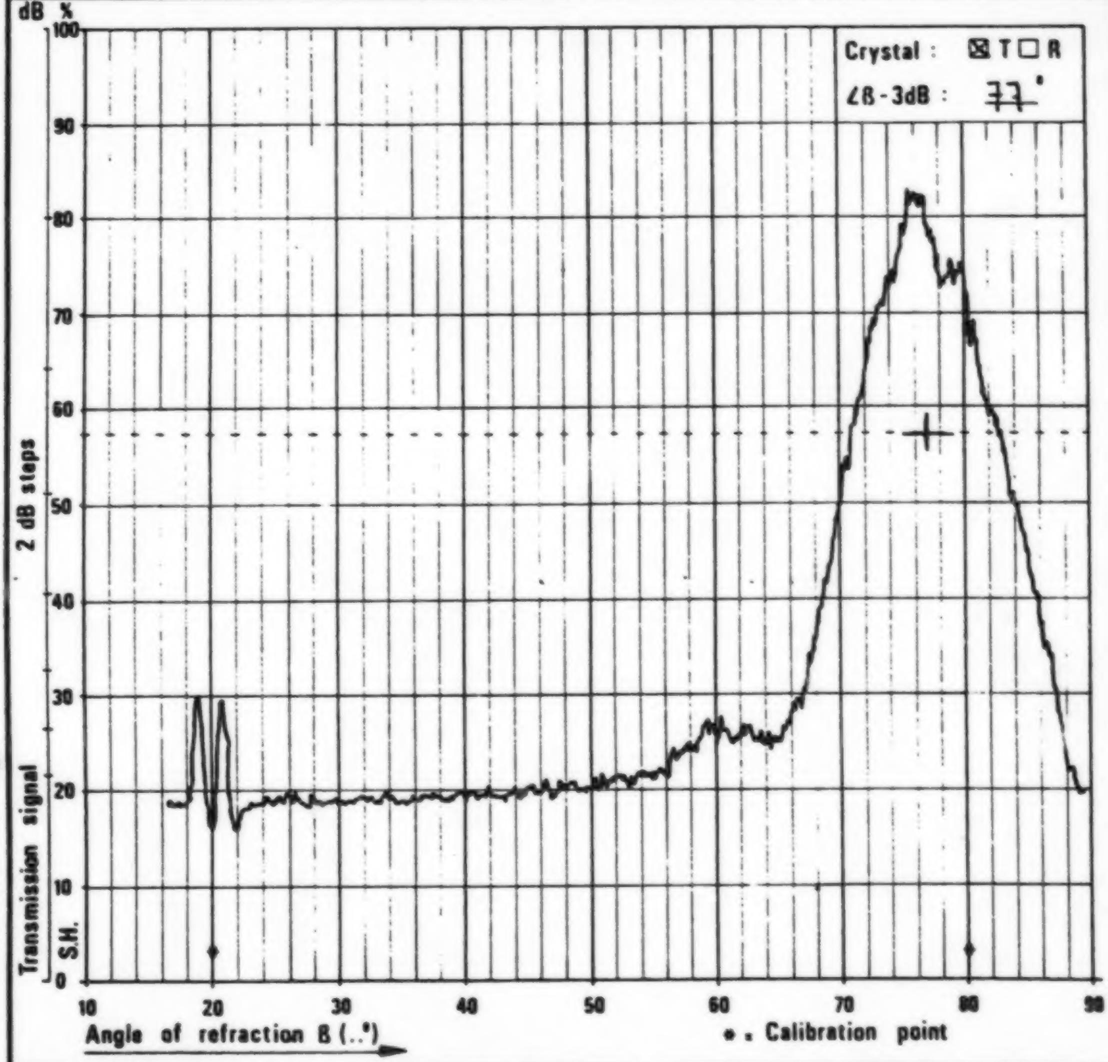

Crystal : ☒ T ☐ R

∠β-3dB : 77°

Röntgen Technische Dienst b.v.

ULTRASONIC BEAM PLOT

D.D 210188

MEASURED BY: J. Vreeken

TEST SET-UP

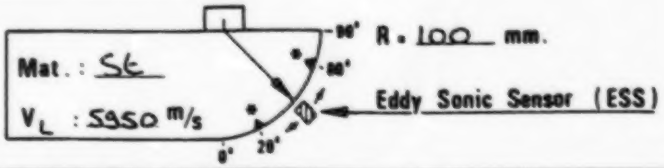

Mat.: St

V_L : 5950 m/s

TRANS-DUCER : RTD-BAM
88-110
TRcc 8-St
2(3,6x 10,7)
SA17° BS~15

TRANSDUCER DATA:

Housing:
25 x 25 x 20 (L x W x H)
Conn.: LEMO-00
T.D. Type: ☐ Man. ☒ Mech.
I P : 8,5 mm on R = 10 mm
WD.: 14,5 mm

U.T. FLAW DETECTOR.

Make : Krautkrämer; Type: USIP 11; RTD Nr. 8

Tuning

Pulse Str.: 3 Res.: 3
Freq. : 2 - 8 MHz

Pulse echo sensitivity:
Gain 20 + 14 dB

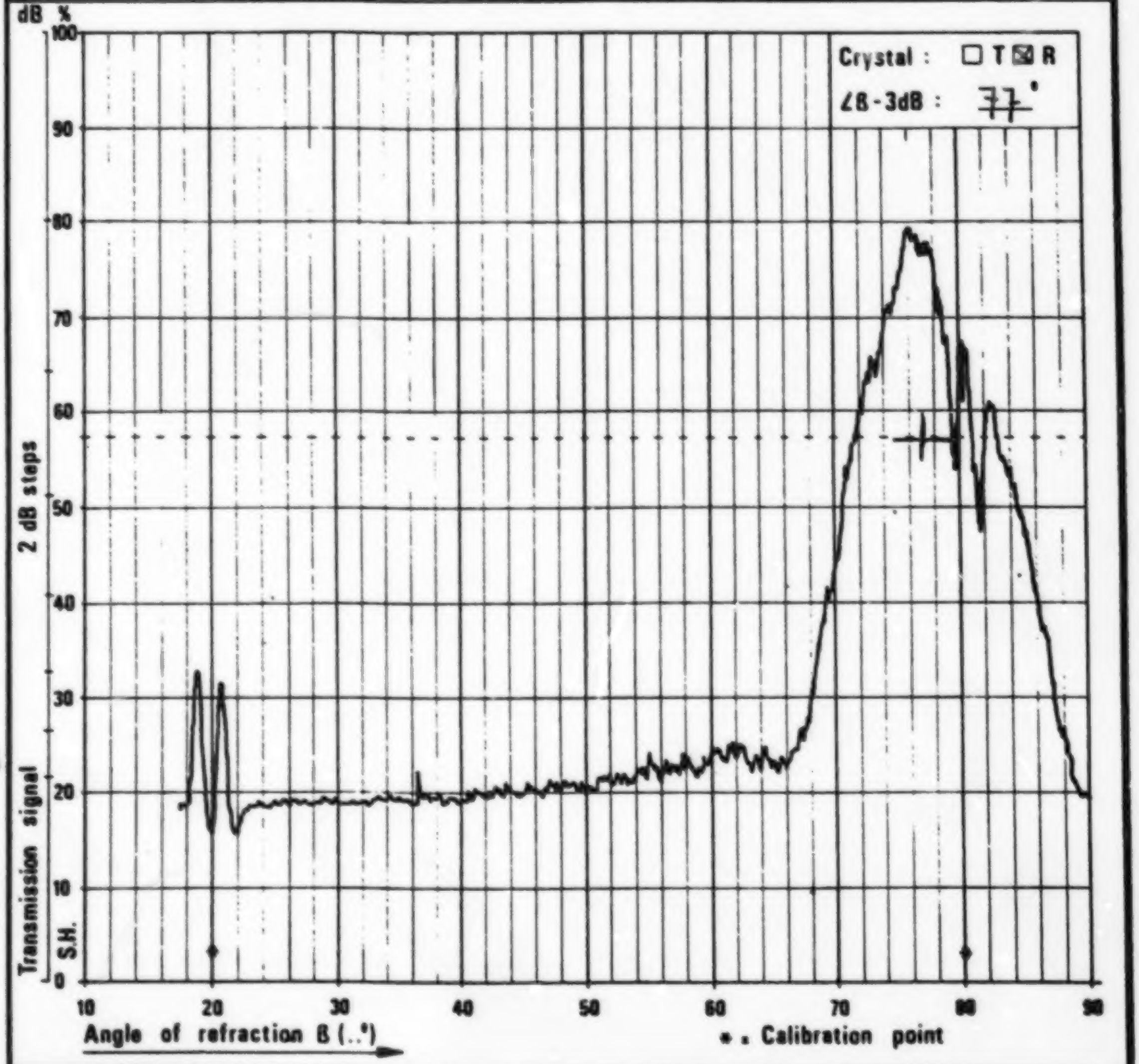

Crystal : ☐ T ☒ R

∠B-3dB : 77°

Röntgen Technische Dienst b.v.

ULTRASONIC BEAM PLOT

RTD QUALITY SERVICES

D.D 210188

MEASURED BY: J. Vreeken

EQUIPMENT:

1. Spectrum Analyser
   Marconi Instruments Typ: TF 2370
2. Oscilloscope: KIKUSUI COS 5060
3. Ultrasonic Transducer Analyser:
   Aerotech Laboratories Type: UTA-3

TRANS-DUCER: RTD-BAM
88-110
TRG 8-SL
2(3.6x10.7)
SA17° FS~15

T.D. DATA:

Typ: ☐ Man ☒ Mech

Housing: L x W x H
25 x 25 x 20 mm

IP : 85 mm on R 10 mm

WD.: 14.5 mm

Conn.: LEMO-00

Cable: 2m Coax 50 Ω

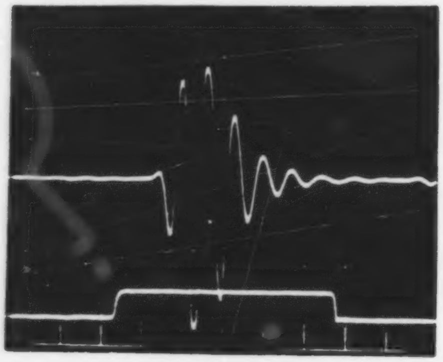

HF Image

$f = \frac{1}{t}$

Time Base: 0,2 µs/Div

Reference Block: R=10

Mat.: Steel

V_l -: 5950 m/s

V_{sh} -: 3230 m/s

☒ Radius Calibration Block

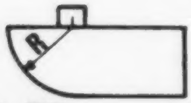

R= 10 mm

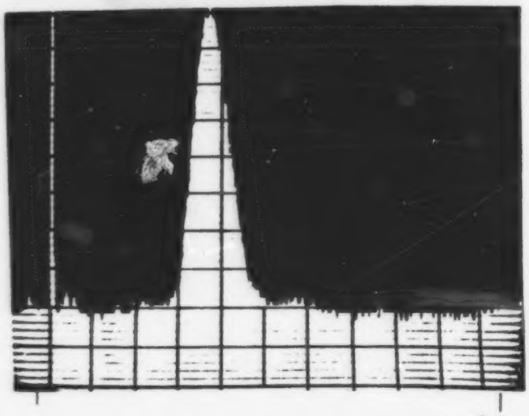

0 Frequency Spectrum 20 MHz

☐ Side Drilled Hole

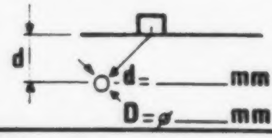

☐ Flat Bottomed Hole

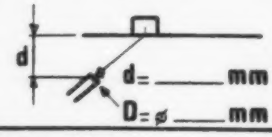

☐ Back Wall

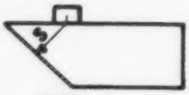

S= ____ mm

☐

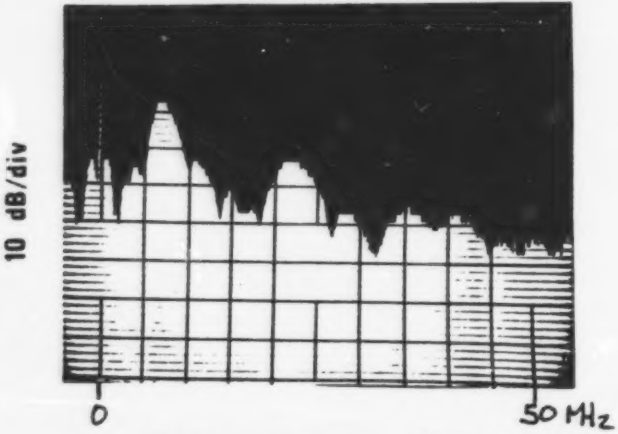

Centre Frequency: 7,5 MHz

Band Width-3dB : 6,8 - 8,2 MHz

Measured by: J. Vreeken

D.D. 210188

Röntgen Technische Dienst b.v.

FREQUENCY SPECTRUM DATA SHEET

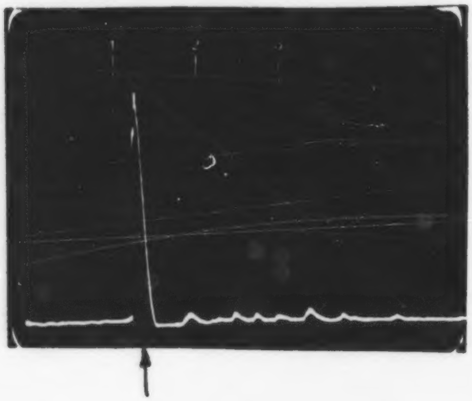

TRANSDUCER : RTD-BAM
88 -110
TRCr 8-St
2(3.6x10.7)
SA17° FS~15

CABLE : 2m Coax 50 Ω

ULTRASONIC EQUIPMENT
TYPE : USIP 11 NR. : 7
MANUFACT. : Krautkrämer
PULSE : 3 RES. : 3
AMPL. : 20+18 dB
FREQ. : 2-8 MHz

CALIBRATION BLOCK : R=10
MAT : Steel
REFERENCE BLOCK : RTD
MAT : Steel
V_L ≈ : 5950 m/s
V_{SH} ≈ : 3230 m/s
∠β_{SH} : 33 °

HOUSING DIM.:
25 x 25 x 20 (l x w x h)
CONTACT SURFACE:
25 x 25 (l x w)
CONNECTOR:
LEMO-00
INDEX: 8,5 AT R: 10

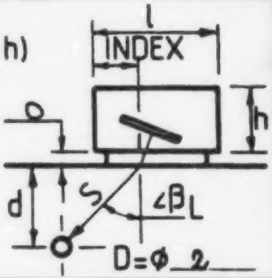

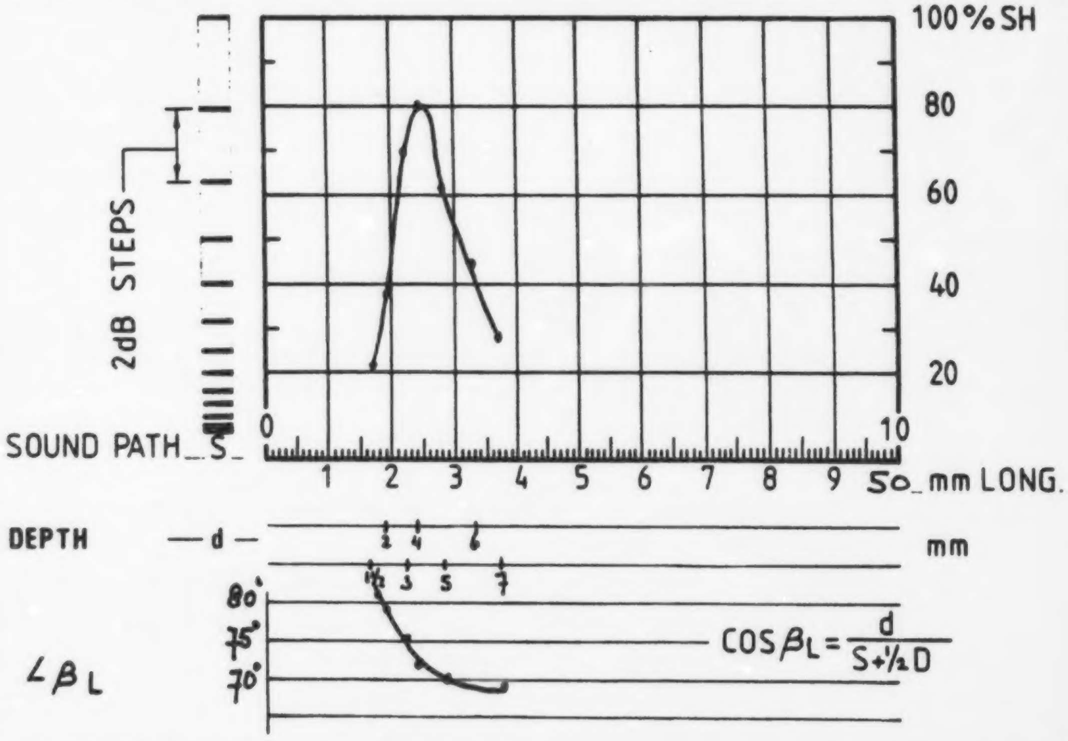

$$\cos\beta_L = \frac{d}{S+\frac{1}{2}D}$$

NJ't H.120181

Röntgen Technische Dienst bv

FOCUS-DIAGRAM

AMPLITUDE= f (SOUND PATH - DEPTH - ANGLE)

D.D. 210180	Schaal	Get. J. Vreeken	Nr.

RTD QUALITY SERVICES

044 - 0630

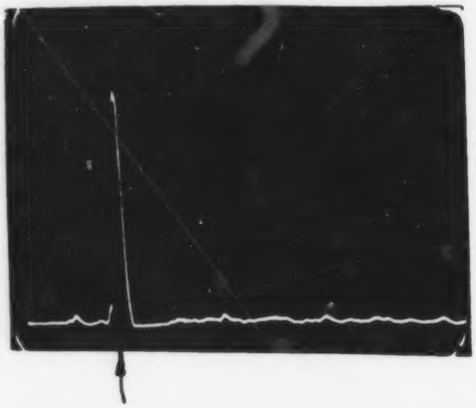

TRANSDUCER: RTD-BAM
88-110
TRCr 8-St
2(3,6x10,7)
SA17 FS~15

CABLE: 2m Coax 50 Ω

ULTRASCNIC EQUIPMENT

TYPE : USIP 11 NR. : 7
MANUFACT: Krautkrämer
PULS : 3 RES.: 3
AMPL.: 40+8 dB
FREQ.: 2-8 MHz

CALIBRATION BLOCK: R.10
MAT: Steel
REFERENCE BLOCK : RTD
MAT: steel
V_L ~: 5950 m/s
V_{SH} ~: 3230 m/s

HOUSING DIM.:
25 x 25 x 20 (l x w x h)
CONTACT SURFACE:
25 x 25 (l x w)
CONNECTOR:
LEMO-00
INDEX: 8,5 AT R: 10 NOTCHDEPTH: 1 mm

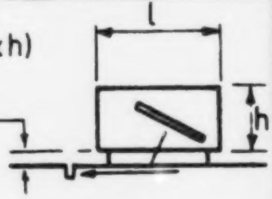

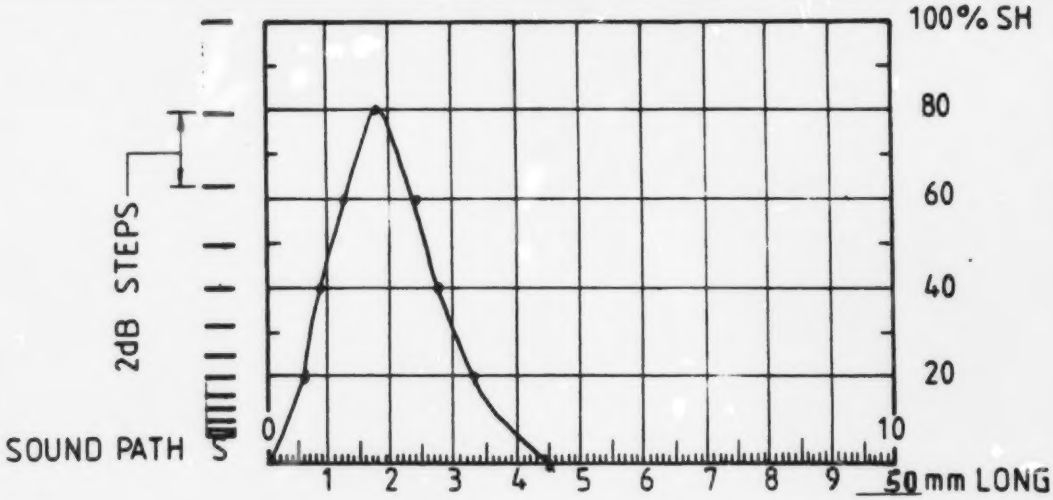

J.Vr. 200781

Röntgen Technische Dienst bv

FOCUS-DIAGRAM CREEPING WAVE PROBE

AMPLITUDE= f (SOUNDPATH)

RTD QUALITY SERVICES

D.D. 210188	Schaal	Get. J. Vreeken	Nr.

APPENDIX 4

Detailed Comparisons Between Radiographic and Ultrasonic Records

RADIOGRAPHIC
RESULTS OS SIDE = REFERENCE
LINE SIDE OF PIPE

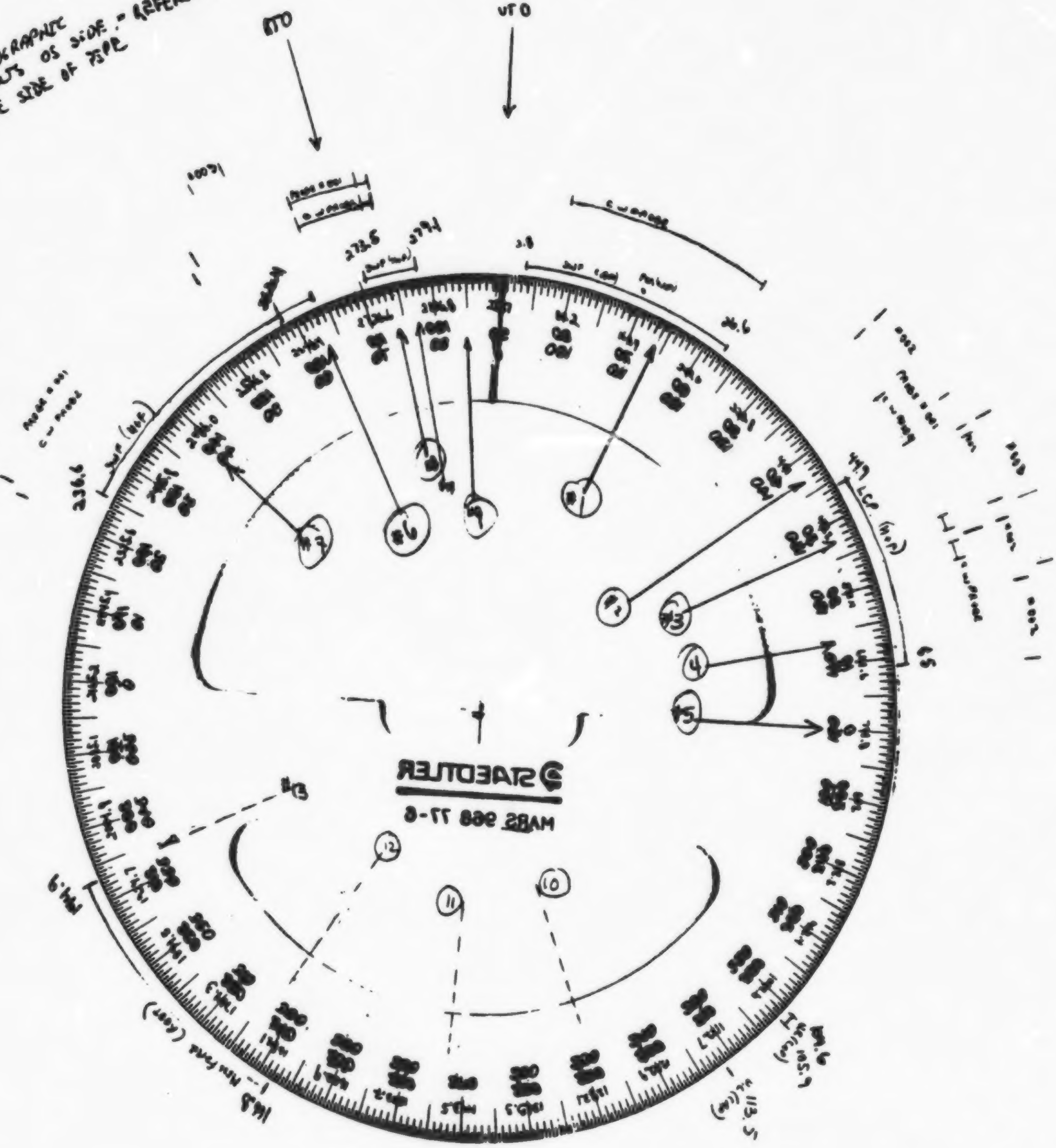
BTO
VTO
273.5
3.8
26.6
236.6
65
144.9
113.5
#1
#2
#3
4
#5
#7
#8
9
10
11
12
#13
STAEDTLER
MARS 968 77-6

Reference Side 9.8mm

RADIOGRAPHIC RESULTS ON SIDE OPPOSITE REFERENCE LINE SIDE OF PIPE.

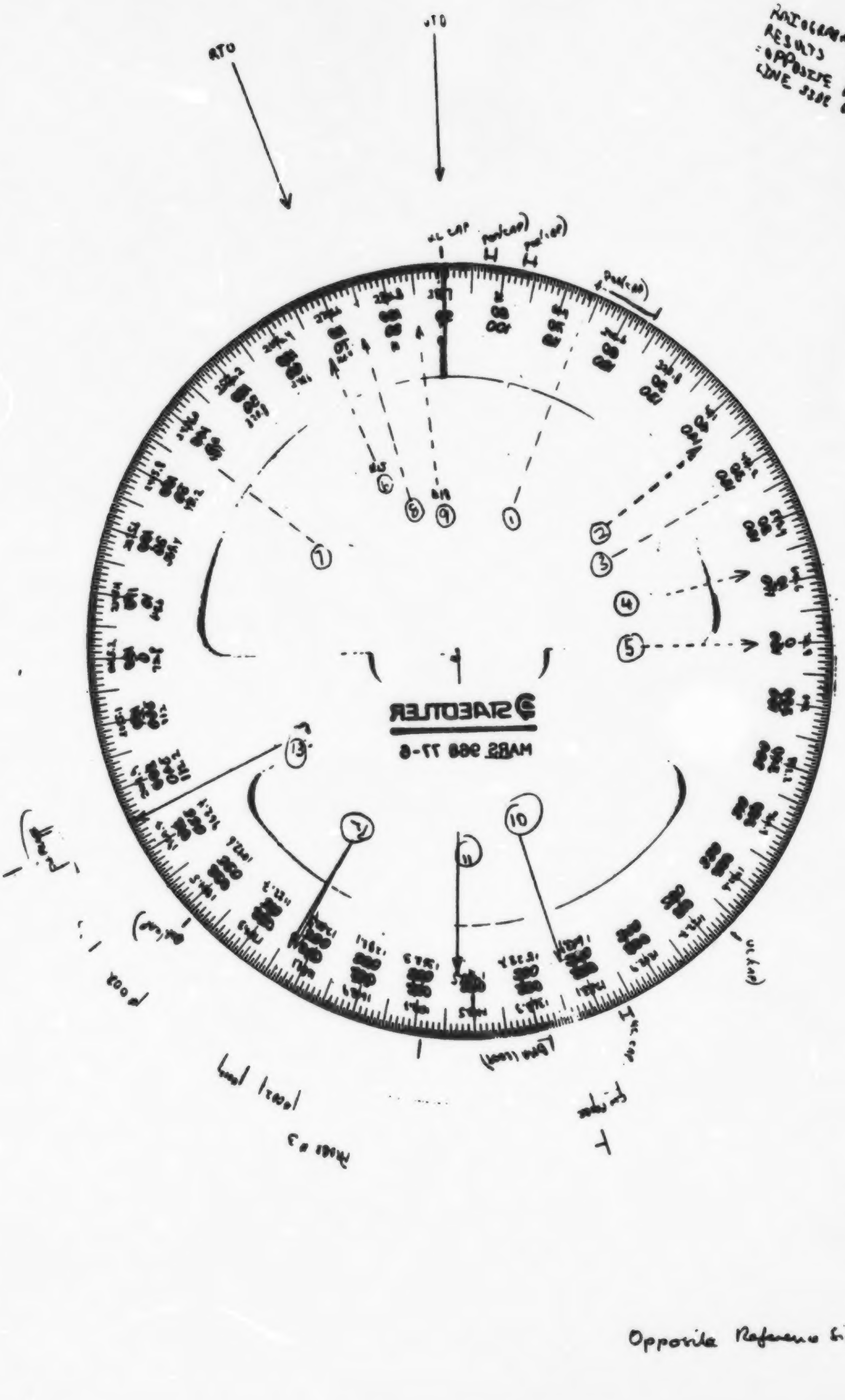
RTO
VTO
STAEDTLER
MARS 968 77-6
1
2
3
4
5
7
8
9
10
11
12
13

Opposite Reference Side 9.8 mm

0.5 20.6mm

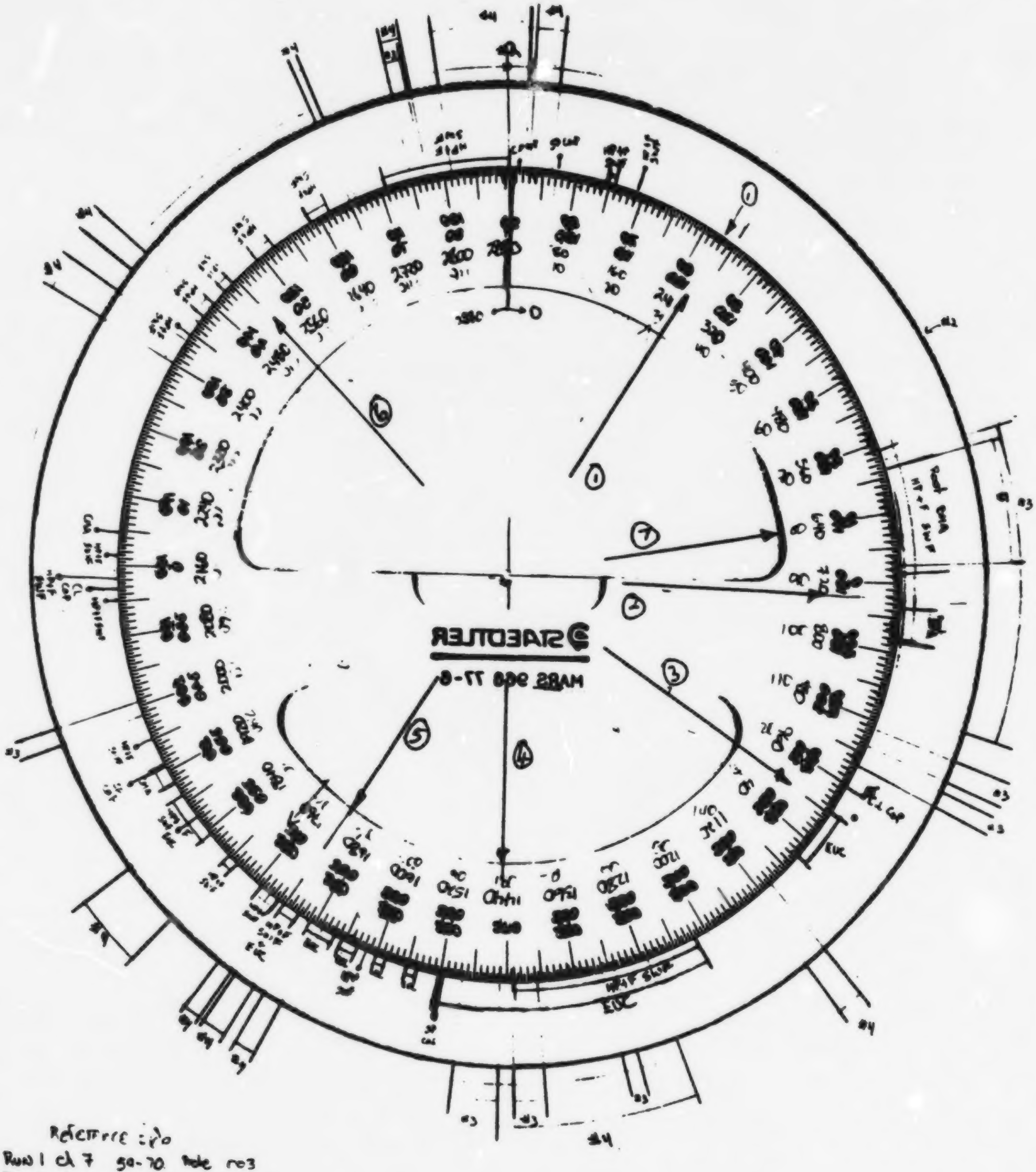

①
②
③
④
⑤
⑥
⑦
STAEDTLER
MARS 968 77-6
#1
#2
#3
#4
EVC
0
2880

Reference info

#1	Run 1 ch 7	50-70	Probe 003
#2	Run 2 ch 3	0-2880	Probe BB-111
#3	Run 2 ch 5	As seen	Probe 003/Rod (300)
#4	Run 3 ch 1	as seen	Probe BB-110

N.S 20.6 mm

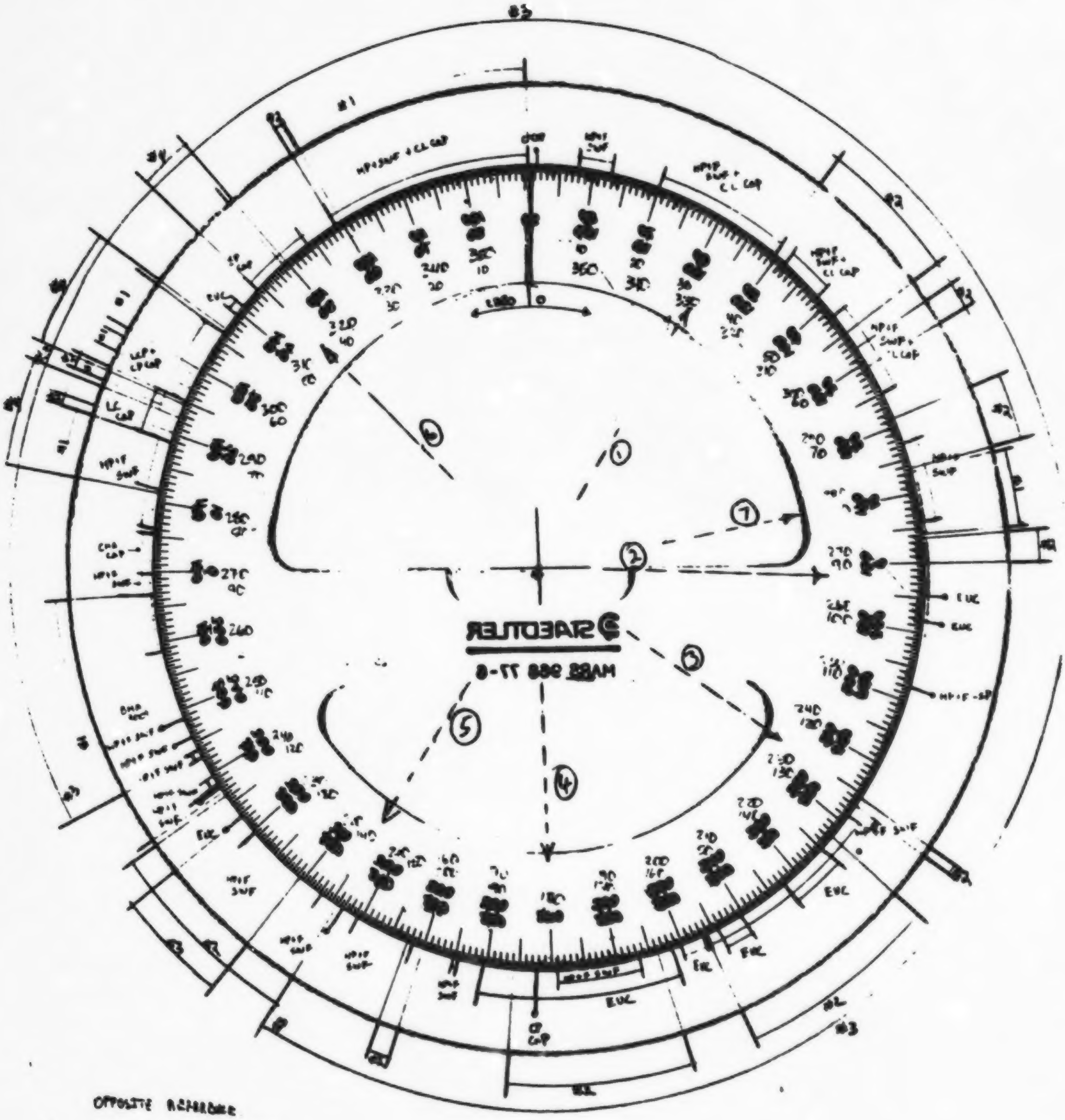
#1
#2
#3
#4
1
2
3
4
5
6
7
STAEDTLER
MARS 988 77-6
HP1F SNP
CL GAP
EVC
LE GAP
CMA GAP
CP GAP
0
90
180
270

OPPOSITE [illegible]

#1 Run 9 ch 7 Probe 003
#2 Run 8 ch 1 Probe SS-110
#3 Run 9 ch 3 Probe SS-111
#4 Run 20 ch 5 Probe 002